

**SYNTHESIS OF NOVEL GLYCOLIPID AGONISTS  
OF THE PROTEIN CD1d**

**by**

**YOEL RUSLAN GARCIA DIAZ**

A thesis submitted to the  
University of Birmingham  
for the degree of  
**DOCTOR OF PHILOSOPHY**

School of Chemistry  
College of Engineering  
and Physical Sciences  
University of Birmingham  
January 2010

UNIVERSITY OF  
BIRMINGHAM

**University of Birmingham Research Archive**

**e-theses repository**

This unpublished thesis/dissertation is copyright of the author and/or third parties. The intellectual property rights of the author or third parties in respect of this work are as defined by The Copyright Designs and Patents Act 1988 or as modified by any successor legislation.

Any use made of information contained in this thesis/dissertation must be in accordance with that legislation and must be properly acknowledged. Further distribution or reproduction in any format is prohibited without the permission of the copyright holder.

## ABSTRACT

Invariant NKT (iNKT) cells are a subset of T lymphocytes that express an invariant  $\alpha\beta$  T cell receptor (TCR) as well as an NK1.1 marker. They play an important role in autoimmune diseases, such as type I diabetes and lupus. In contrast to conventional CD4<sup>+</sup> and CD8<sup>+</sup> T lymphocytes that recognise foreign peptides bound to the major histocompatibility complex (MHC) class I or MHC class II, iNKT cells recognise a range of foreign lipids and glycolipids bound to CD1d proteins.  $\alpha$ -Galactosyl Ceramide ( $\alpha$ GalCer), originally isolated from a marine sponge, is a powerful agonist of CD1d capable of triggering an immune response that results in the proliferation of a range of regulatory cytokines, including IFN- $\gamma$  (Th1), as well as IL-4 (Th2). This mixed cytokine response (*i.e.* Th1 *and* Th2), combined with the “unresponsive state” of iNKT cells after activation with  $\alpha$ GalCer, limits the therapeutic potential of this agonist. To address some of these issues, we have also synthesised an  $\alpha$ GalCer analogue, namely Threitol Ceramide (ThrCer), that exhibits attenuated activity relative to  $\alpha$ GalCer. ThrCer is a truncated analogue of  $\alpha$ GalCer that conserves the stereochemistry of the hydroxyl functions present in  $\alpha$ GalCer and that exhibit a much stronger ether bond under acidic hydrolysis linking the sugar moiety with ceramide than the glycosidic bond in  $\alpha$ GalCer. We have labelled ThrCer with a biotin residue and with a <sup>14</sup>C radiolabel, and our collaborators have used these derivatives to show that ThrCer behaves similarly to  $\alpha$ GalCer in endogenous lipid trafficking and its tissue distribution *in vivo*. We have also made advances towards the stereoselective synthesis of recently discovered natural agonists of iNKT cells from pathogenic origin, namely  $\alpha$ -galactosyl diacylglycerol ( $\alpha$ GalDAG).

To my children Isabella and Tomás Carlo  
and to my parents.

## AKNOWLEDGEMENTS

I thank my supervisors Liam and Del for the opportunity to study and to research that they provided me, and for their professional support through-out, and no less personal. I believe that in the future, away from their tutorship, I will look back to my PhD experiences for inspiration and rigour in my professional career and in science.

I thank Petr for the debates and reflexions on the natural world, and the world not so natural, that we had after hours. I specially thank Justea for being a super friend and reading my thesis.

I thank Carolle for indirect help, moral support, and looking after Tomás Carlo and Isabella while I studied.

Many thanks to all my friends for being just that, my friends.

I thank the University of Birmingham and the School of Chemistry and for funding.

## TABLE OF CONTENTS

ABBREVIATIONS	vi-xi
<b>INTRODUCTION</b>	
I. INTRODUCTION	1
1.1. <i>General Introduction.</i>	1
1.2. <i>The Major Histocompatibility Complex And CD1 Receptors.</i>	3
1.3. <i><math>\alpha</math>-Galactosyl Ceramides Analogues And CD1d-dependent Bioactivity.</i>	10
1.4. <i>Syntheses of <math>\alpha</math>-Galactosyl Ceramides.</i>	16
<b>AIMS AND OBJECTIVES</b>	
II. AIMS AND OBJECTIVES	30
<b>RESULTS AND DISCUSSION</b>	
III. SYNTHESIS OF THREITOL CERAMIDE AND LABELLED ANALOGUES	39
3.1. <i>Synthesis Of Threitol Ceramide.</i>	39
3.2. <i>Synthesis of <math>^{14}\text{C}</math>-Labelled Threitol Ceramide.</i>	51
3.3. <i>Synthesis Of Biotin-Labelled Threitol Ceramide.</i>	54
IV. TOWARDS THE SYNTHESIS OF $\alpha$ -GALACTOSYL DIACYLGLYCEROL	82
4.1. <i>Naturally Occurring CD1d Agonists.</i>	82
4.2. <i>1,2-Cis-Stereoselective Glycosylation Reactions.</i>	86
4.3. <i>Synthesis of <math>\alpha\text{GalDAG}</math>.</i>	100
<b>CONCLUSIONS AND FUTURE WORK</b>	
V. CONCLUSIONS AND FUTURE WORK	110
5.1. <i>Synthesis of Threitol Ceramide And Labelled Analogues Conclusions.</i>	110
5.2. <i>Towards The Synthesis Of <math>\alpha\text{GalDAG}</math> Diacylglycerol Conclusions.</i>	110
5.3. <i>Future Work.</i>	111
<b>EXPERIMENTAL SECTION</b>	
VI. EXPERIMENTAL SECTION	113
<b>REFERENCES</b>	
VII. REFERENCES	155

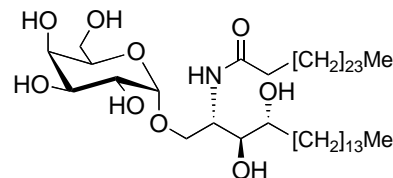
## ABBREVIATIONS

°C Degree Celsius

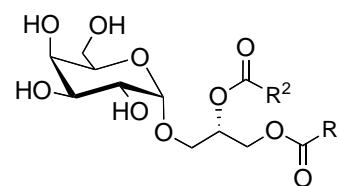
Ac Acetyl



$\alpha$ GalCer  $\alpha$ -Galactosyl ceramide

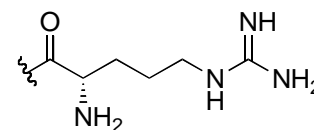


$\alpha$ GalDAG  $\alpha$ -Galactosyl diacylglycerol

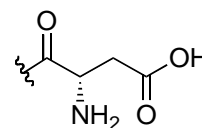


R<sup>1</sup>, R<sup>2</sup>: a range of alkyl chains

Arg Arginine residue

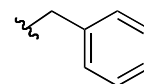


Asp Aspartic acid residue

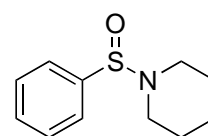


BCR B cell receptor

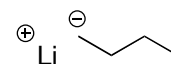
Bn Benzyl



BSP 1-(Benzensulfinyl) piperidine



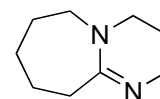
<sup>n</sup>BuLi Butyl lithium

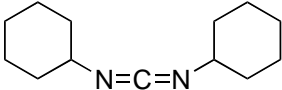
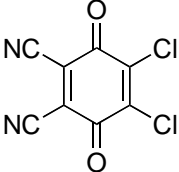
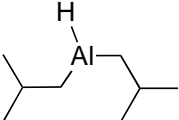
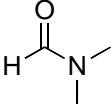
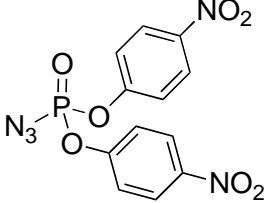
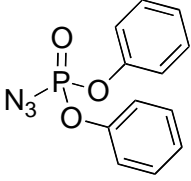
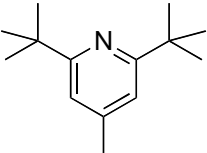
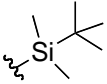
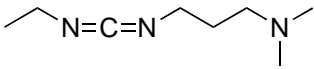
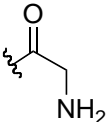


CD Cluster of differentiation

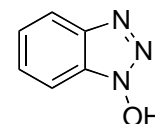
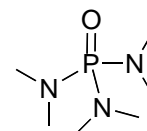
d Day(s)

DBU 1,8-Diazabicyclo[5.4.0]undec-7-ene

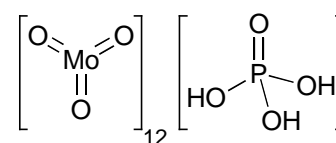


DCC	<i>N,N'</i> -Dicyclohexylcarbodiimide	
DDQ	2,3-Dichloro-5,6-dicyano-1,4-benzoquinone	
DIBALH	Diisobutylaluminium hydride	
DMF	<i>N,N'</i> -Dimethylformamide	
DMSO	Dimethyl sulfoxide	
BNPPA	Bis( <i>p</i> -nitrophenyl)phosphoryl azide	
DPPA	Diphenylphosphoryl azide	
DTBMP	2,6-Di- <i>tert</i> -butyl-4-methyl-pyridine	
TBS	<i>tert</i> -Butyldimethylsilyl	
EDC	<i>N</i> -(3-Dimethylaminopropyl)- <i>N'</i> -ethylcarbodiimide	
Et	Ethyl	
FGI	Functional group interconversion	
Gly	Glycine residue	

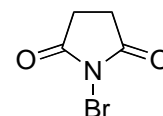
h	hour(s)
HMPA	Hexamethylphosphoramide
HOBt	1-Hydroxybenzotriazole
IFN	Interferon
iGb3	Isoglobotrihexosylceramide
IL	Interleukin
iNKT cell	Invariant natural killer T cell
<i>i</i> Pr	Isopropyl
lit.	Literature
Me	Methyl
MHC	Major histocompatibility complex
min	Minute(s)
MP	<i>p</i> -Methoxyphenyl



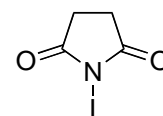
MPA	Molybdophosphoric acid
-----	------------------------



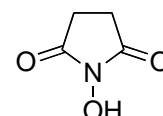
MS	Molecular sieves
NBS	<i>N</i> -Bromosuccinimide

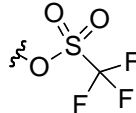
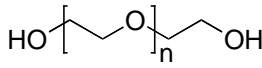
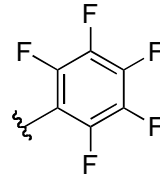
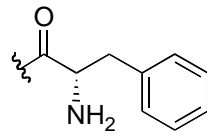
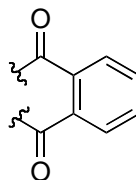
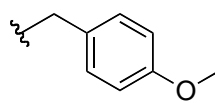
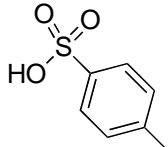
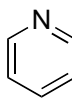


NIS	<i>N</i> -Iodosuccinimide
-----	---------------------------



NHS	<i>N</i> -Hydroxysuccinimide
-----	------------------------------



NMR	Nuclear magnetic resonance	
OTf (TfO)	Trifluoromethanesulfonate (triflate)	
P	Generic protecting group	
PEG	Polyethylene glycol	 M.W. < 20,000 g/mol
PTP	Pentafluorophenyl	
Ph	Phenyl	
pH	pH is defined as minus the decimal logarithm of the hydrogen ion activity	$\text{pH} = -\log_{10} a_{\text{H}}$
Phe	Phenylalanine residue	
Phth	Phthalyl	
PIM <sub>6</sub>	Hexamannosylated phosphatidyl- <i>myo</i> -inositol	
PMB	<i>p</i> -Methoxybenzyl	
pTSA	<i>p</i> -Toluenesulfonic acid	
Py	Pyridine	
quant.	Quantitative yield	

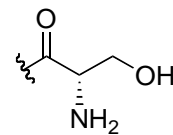
quat. Quaternary carbon

R Generic substituent

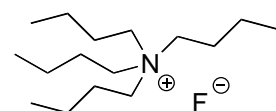
<sup>t</sup>Bu *tert*-Butyl

r.t. Room temperature

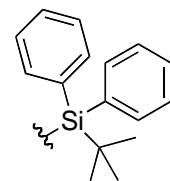
Ser Serine residue



TBAF Tetrabutylammonium fluoride

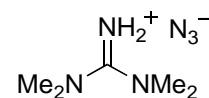


TBDPS *tert*-Butyldiphenylsilyl

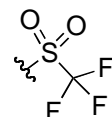


TCR T cell receptor

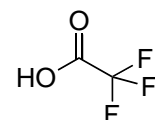
TMGN<sub>3</sub> Tetramethylguanidium azide



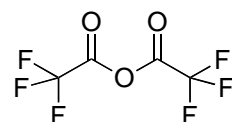
Tf Trifluoromethanesulfonyl (triflyl)



TFA Trifluoroacetic acid



TFAA Trifluoroacetic anhydride

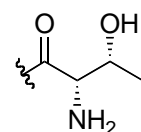


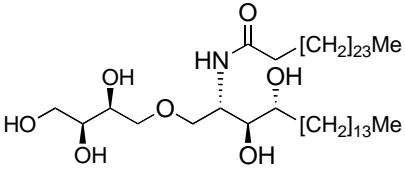
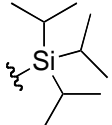
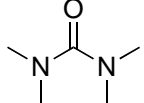
Th T helper

THF Tetrahydrofuran



Thr Threonine residue



ThrCer	Threityl ceramide	
TIPS	Triisopropylsilyl	
TLC	Thin layer chromatography	
TMS	Trimethylsilyl	
TMU	Tetramethylurea	
X	Generic atom	

# **INTRODUCTION**

## I. INTRODUCTION

### 1.1. General Introduction.

Immunology has its origins with the discovery, by Edward Jenner in 1796, that individuals injected with small amounts of cowpox or vaccinia serum develop resistance against smallpox. Edward Jenner called this treatment *vaccination* and is generally considered the father of immunology after the series of ambitious experiments on children in 1796 led to this discovery. Edward Jenner, however, did not know the identity of the agents causing the diseases, and it was not until the nineteenth century that Robert Koch was able to demonstrate that infectious diseases are caused by microorganisms, and that each different invader is capable of infesting the host with a different disease or causing a specific pathological condition. We group these microorganisms today into four different types according to their size, mode of action and constitution: viruses, bacteria, pathogenic fungi, and parasites.<sup>[1]</sup>

Robert Koch's discovery stimulated researchers to investigate each pathogenic microorganism in the hope of developing a vaccine that could be used for the protection against infectious diseases. In the 1880s, Louis Pasteur used this approach in his discovery of a vaccine against cholera for chickens, and a vaccine against rabies for humans. Shortly after, in the 1890s, Emil von Behring and Shibasaburo Kitasato found that the serum of animals immune to diphtheria or tetanus contained specific proteins, today called immunoglobulins and antibodies,

that could give the host short-lived immunity to these diseases. With this discovery, Behrin and Kitasato uncovered the *adaptive* immune response, so called because it develops during the lifetime of the individual as an adaptation to the infection of a pathogen. In most cases, this leads to a lifelong protective immunity to re-infection with the same pathogen.

In contrast to the adaptive immune response, the *innate* immune response, known to us by the work of the great Russian immunologist Eli Metchnikoff, does not require prior exposure to the pathogen. This type of immune response acts through phagocytic cells, which Metchnikoff called macrophages, that are capable of engulfing and digesting the invader.<sup>[1]</sup> The innate and adaptive immune responses compliment each other in the way that if a particular pathogen is not recognised by macrophages and successfully invades the host, an adaptive immune response is raised to protect the host. If this second line of defence is successful, a record of this pathogen and of the specific mechanism of defence is created. If the host is challenged in the future with the same pathogen, a faster and more effective adaptive immune response is raised. The ability to remember a pathogen is the pillar of the adaptive immune response. The innate immune response cannot remember different pathogens because it operates through receptors encoded in the host's genome.<sup>[1]</sup>

For the fight against the wide range of pathogens that an individual would encounter in its lifetime, the immune system circulates molecules throughout the host that are capable of detecting, binding, and presenting foreign molecular fragments to the immune system's receptors. For example, B cells, which secrete immunoglobulins,

with a vast range of antigen specificity. While most immunoglobulins are free to travel through the host independently of the parent B cell, some immunoglobulins are membrane-bound and act as surface receptors for antigens. These cells with membrane-bound immunoglobulins are known as B cell receptors, BCR. An immune response is initiated when an immunoglobulin meets with an antigen which is presented to BCR, which in turn secretes more immunoglobulins of the same antigen specificity, so called antibodies, amplifying the immune response.<sup>[1]</sup> The main function of B cells in the adaptive immune response is to scan the extracellular space for signs of invasion, pathogens or their toxic byproducts, and to then mount a response that is appropriate in size and type against the particular invader.

In contrast to B cells, T cells scan the surfaces of the organism's own cells for signs of infection. They recognise debris products of intracellular infection that are transported to the cell surface and upon recognition of the antigen are then activated to secrete a range of cytokines initiating an immune response. The primary objective of the immune response is to remove the specific invader that caused the infection selectively.

## **1.2. The Major Histocompatibility Complex and CD1 Receptors.**

The Major Histocompatibility Complex, MHC, molecules are a specialised class of cell glycoprotein capable of binding a large array of small foreign peptides, which are produced during a cellular infection. The MHC molecules then present these peptide

antigens to T cells, which often results in the cells being marked for destruction, and the eradication of the infection.<sup>[1, 2]</sup>

The MHC molecules are encoded in a large cluster of genes that were first identified by their potent effects on the immunological response to transplanted tissues. There are two different types of MHC molecules, termed MHC class I and MHC class II, which recognise and present peptides from different parts of the cell. Peptides found in the cytosol are recognised by MHC class I molecules and presented to CD8 T cells, whilst peptides found in intracellular vesicles are recognised by MHC class II molecules and presented to CD4 T cells. In turn, the two different subsets of T cells are activated and each subset initiates an immune response for destroying the pathogen that is resident in the specific cell compartment.

It is suggested that MHC proteins encoded within or near the MHC gene sequence are evolutionary and structurally related. MHC class I-like proteins are encoded outside the MHC. These families of proteins are related to each other and they all have a low level of homology with MHC class I proteins. These homology studies suggested that the three classes of proteins, *i.e.* MHC class I, MHC class II and MHC class I-like proteins, evolved from a common ancestor and that those encoded within or near the MHC may have differentiated as the result of evolutionary diversification. However, it is apparent that different evolutionary roots distinguished the MHC-linked class I-like proteins from its subclass MHC non-linked class I-like proteins.<sup>[2-4]</sup>

A hallmark of MHC molecules is the extreme polymorphism that they exhibit. This is in strong contrast with the family of Cluster of Differentiation 1, CD1, molecules in which there is no evidence for any significant polymorphism. CD1 molecules belong to the MHC class I-like class of proteins and are an enigmatic family of proteins that present *glycolipid* antigens to T cells.

Why has the CD1 family of ancient proteins been conserved? Why do they lack polymorphism? Why do we need them along with the sophisticated MHC? We cannot answer these questions in full at the present time; however a significant amount of research has been done that is providing information about the role of this family of proteins.<sup>[5-9]</sup>

The evolutionary origin of the vast polymorphism in MHC proteins is to ensure that there are MHC proteins available across the entire species able to bind and present a specific peptide antigen for the necessary immune response against a pathogen to ensure the survival of the species. The finding that the protein CD1b is capable of presenting glycolipids found in the pathogen *Mycobacterium tuberculosis* supported theories that CD1 proteins may not need to be polymorphic because they present bacterial lipids to T cells and because lipids are products of complex biosynthetic pathways they evolve much slower than peptides, which means it is less important for CD1 proteins to be polymorphic.<sup>[10]</sup> It was subsequently found that CD1d also binds and presents glycolipids to T cells. One such glycolipid is  $\alpha$ -galactosyl ceramide,  $\alpha$ GalCer, which was isolated from a marine sponge.<sup>[11, 12]</sup>  $\alpha$ GalCer binds to CD1d and the resulting complex had been shown to be a powerful activator of the

immune system leading to the rapid proliferation of interleukin-4, IL-4, and Interferon  $\gamma$ , IFN- $\gamma$ , after activation.<sup>[13]</sup> A study by Porcelli *et al.* identified a subset of natural killer T cells (NKT cells) that expresses an invariant T cell receptor, TCR,  $\alpha$  chain (V $\alpha$ 24-J $\alpha$ 18 in humans and V $\alpha$ 14-J $\alpha$ 18 in mice) that was reactive and specific for the CD1d- $\alpha$ GalCer complex.<sup>[14]</sup>

Another finding, that currently remains unexplained, is the apparent autoreactivity of TCRs with CD1d proteins *in the absence of foreign lipids*.<sup>[15]</sup> It is possible that the TCR recognises CD1d proteins even when they have no antigen bound although *in vivo* it is improbable that CD1d proteins remain with an empty hydrophobic pocket in an environment where lipids, phospholipids and glycolipids are ubiquitous. This has led to the thinking that the TCRs are recognising CD1d proteins with bound *self*-lipids, and the possibility that CD1d proteins may be involved in autoimmune responses, which may lead to autoimmune diseases.<sup>[16]</sup>

CD1 genes in *Homo sapiens* are expressed only in certain cells, most commonly in dendritic cells, DCs. We find CD1A, CD1B, CD1C, CD1D and CD1E in *Homo sapiens*; the number of related genes present in other species varies.<sup>[17]</sup> In mice, for example, only two are found, namely CD1D and CD1E. CD1d proteins are rather different from CD1a, -b and -c proteins, and consequently CD1 proteins have been divided into Type I (CD1a, -b, and -c) and Type II (CD1d).<sup>[18]</sup> CD1e has not been placed in either group yet because so little is known about it. Even though CD1E genes are known, the transcribed CD1e protein was not found until 2000.<sup>[19]</sup> Although

this work did not identify a role for CD1e, it showed that CD1e does not behave like the rest of the CD1 family of proteins. CD1e is not expressed on the surface of the DCs and then internalised like the rest of the family; rather CD1e expressed in DCs does not reach the surface and appears to move from the Golgi to late endosomes, which suggests that this protein may have a very different function. Indeed, recent work showed that CD1e may act as a helper protein for CD1b presentation of PIM<sub>6</sub> (hexamannosylated phosphatidyl-*myo*-inositol) to  $\alpha$ -mannosidase.<sup>[20]</sup>

Structurally, CD1 proteins and MHC class I proteins are only distantly related [Figure 1]. Even though they are both composed of an  $\alpha$  strand, divided into  $\alpha_1$ ,  $\alpha_2$  and  $\alpha_3$  domains, and a smaller  $\beta$  strand, these domains have low homology.<sup>[21, 22]</sup> For example, the  $\alpha_1$  domain of CD1 proteins presents no clear homology with the  $\alpha_1$  domain of MHC class I molecules. Whilst the  $\alpha_2$  domain of CD1 molecules conserves all the cysteines which form the intra-domain through disulfide bonds, the overall homology with class I molecules is still only 25-35%.<sup>[23]</sup> The  $\alpha_3$  domain is more homologous but still quite divergent (45% homology); indeed this domain more closely resembles the  $\beta_2$  domain of MHC class II molecules than it does the  $\alpha_3$  domain of MHC class I molecules, which has led to the suggestion that there was an evolutionary force for CD1 molecules to interact with other proteins (the  $\alpha_1$  and  $\alpha_2$  domains come together to form a cavity where the antigen can bind, the  $\alpha_3$  domain and  $\beta_2$  strand are locked away from the binding events and are quite capable of interacting with other proteins).<sup>[22, 24]</sup>

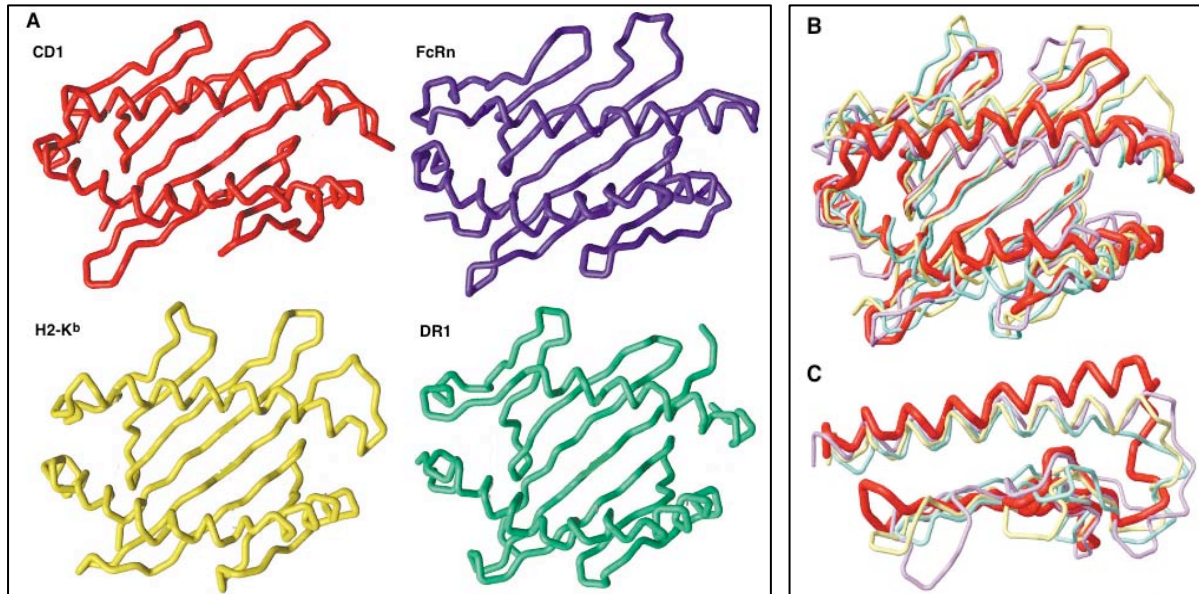
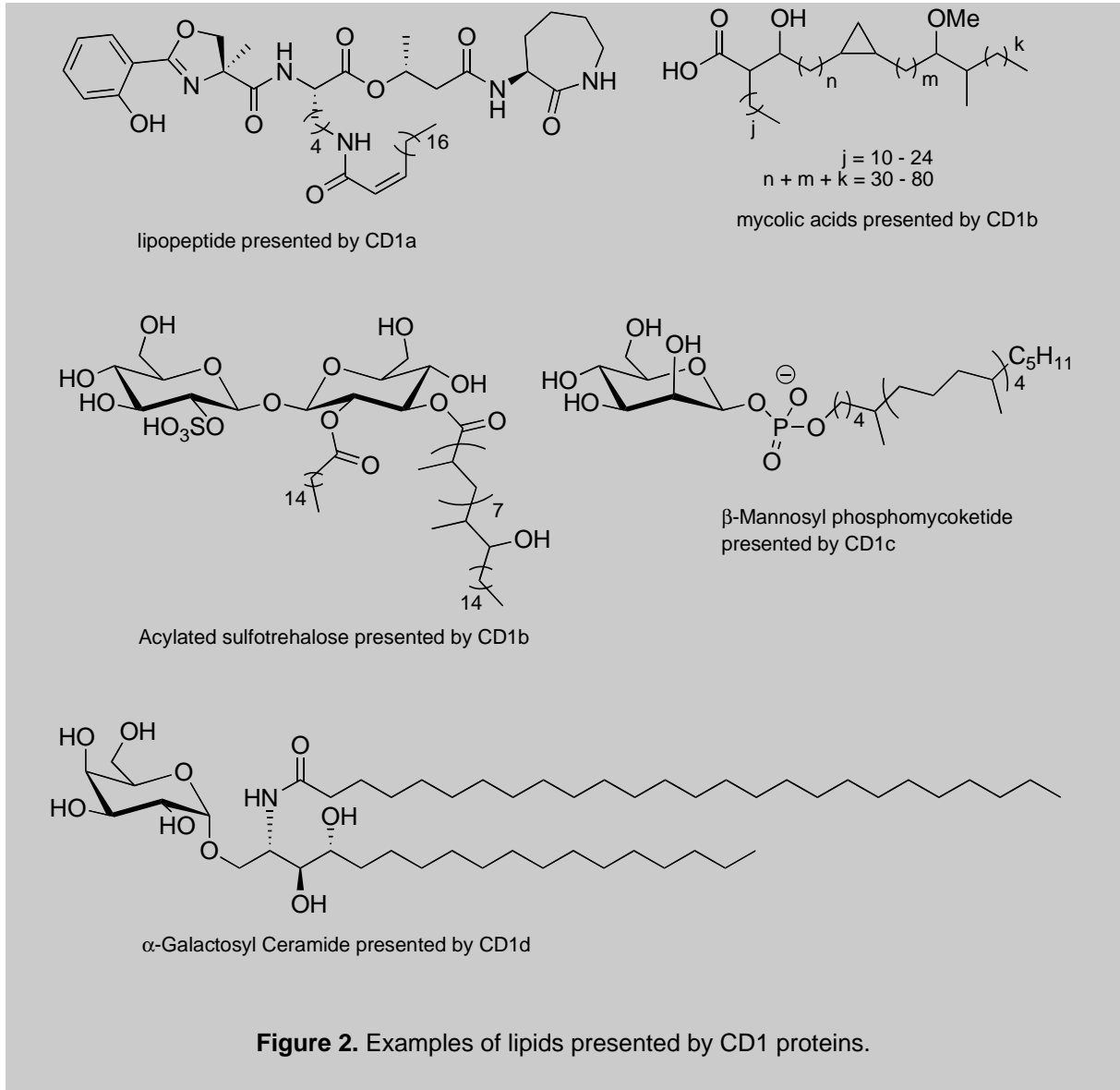


**Figure 1.** Comparison of CD1d protein with one of each class.<sup>[22]</sup> **(A)** Showing similarity between the  $\alpha$  helices of CD1d with FcRn (MHC Class I-like), H2-K (MHC Class I), HLA-DR1 (MHC Class II). **(B)** and **(C)** Showing the four proteins superimposed.

The binding pockets of CD1 proteins are hydrophobic and are specially designed for binding a large array of lipids. For example, CD1d binds di-alkyl glycolipids into two deep hydrophobic pockets, which leaves the polar sugar head group exposed over the binding cleft for interactions with TCRs.<sup>[14]</sup> CD1b molecules have a very deep hydrophobic pocket which can hold lipids as large as 80 carbons in length, such as those found as components of the cell wall in *Mycobacterium tuberculosis*.<sup>[18, 25-27]</sup> The exact nature of these hydrophobic tails translates into protein-antigen binding affinity, which affects the time that the TCR is in contact with the complex (this is important for determining the type of cytokine response). Also, because the ligand occupies these large pockets when bound that would otherwise be empty, it affects the shape of the complex. The ability to recognise a range of endogenous, exogenous and pathogenic lipids and glycolipids, in addition to the large range of

peptides recognised by MHC molecules, undoubtedly provides the immune system with even more powerful tools for patrolling the cellular environment than was appreciated before the discovery of the CD1 family of proteins [Figure 2].



### 1.3. $\alpha$ -Galactosyl Ceramide Analogues And CD1d-dependent Bioactivity.

The glycolipid  $\alpha$ -galactosyl ceramide,  $\alpha$ GalCer, binds with the CD1d protein. The resulting complex is recognised by TCRs located on  $\lambda$ NKT cells and this leads to the development of helper T cells type 1, named a Th1 response, and also to the development of helper T cells type 2, named a Th2 response.<sup>[6, 28]</sup> The rapid response of the immune system by activation of  $\lambda$ NKT cells via CD1d presentation makes this protein of unique importance with potential application in the treatment of cancer, malaria, as well as various autoimmune diseases.<sup>[8]</sup>  $\alpha$ GalCer is the most powerful antigen yet discovered for CD1d in terms of the immune response it precipitates. However since this response is both pro-inflammatory *and* regulatory,  $\alpha$ GalCer is an unlikely drug. The majority of recent research efforts for understanding these activation events and for developing possible therapeutic agents have been based on  $\alpha$ GalCer analogues.

The crystal structure of the CD1d- $\alpha$ GalCer complex has been described [Figure 3].<sup>[29]</sup> It was found, as expected, that the hydrophobic tails of  $\alpha$ GalCer are buried into the two hydrophobic pockets, designated A' and C'. The acyl chain, 26 carbon atoms in length, fits optimally into pocket A' while the phytosphingosine, 18 carbon atoms in length, occupies the smaller pocket C'.

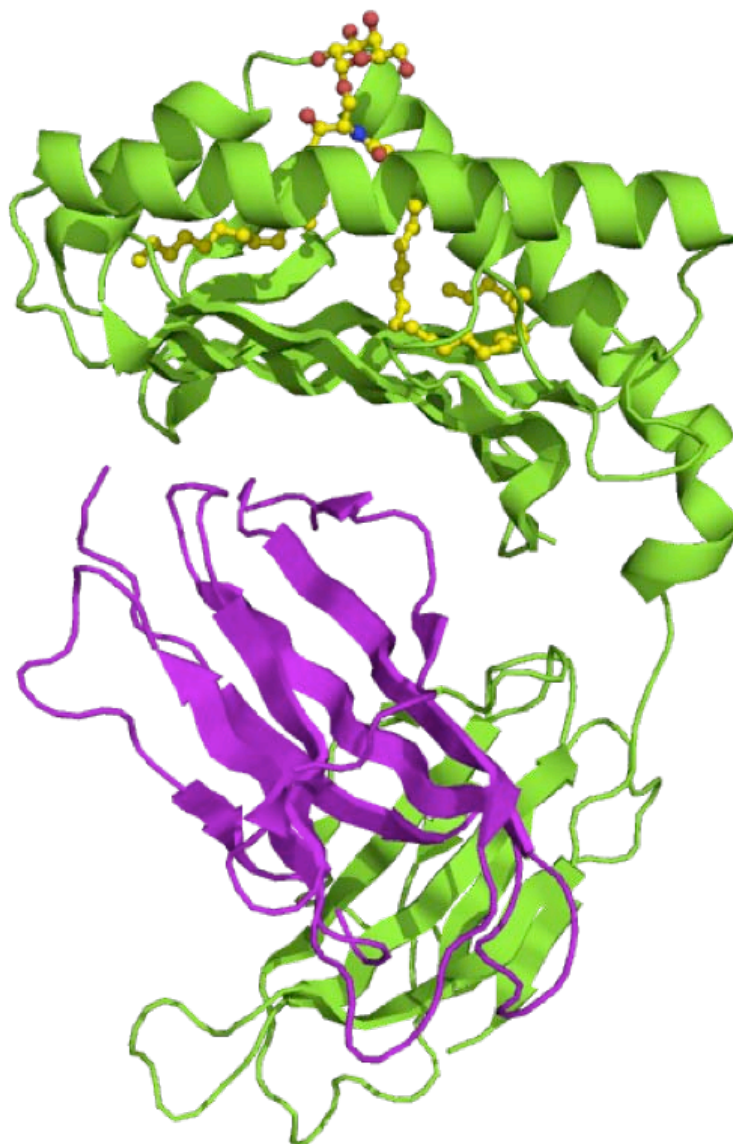


**Figure 3.** The X-ray crystal structure of the CD1d- $\alpha$ GalCer complex.<sup>[29]</sup>

The optimum length of the two hydrophobic tails of  $\alpha$ GalCer 1 for binding to CD1d explains the selectivity of CD1d for ligands possessing relatively short hydrophobic chains, 12 to 26 carbon atoms in length [Figure 4]. Mammalian glycosphingolipids and ceramide phospholipids have a maximum length of 24 carbon atoms in the acyl chains, and for glycosphingolipids, the sphingosine is usually 20 carbon atoms in length.<sup>[15]</sup> In the X-ray crystal structure study,<sup>[29]</sup> the authors suggested that ligands

with hydrophobic tails longer than those of  $\alpha$ GalCer will not fit into the CD1d groove correctly and will not, therefore, be optimally supported by the hydrophobic interactions with the amino acid residues in the pocket. Likewise, ligands with shorter chains might still bind to CD1d but with reduced binding affinity.

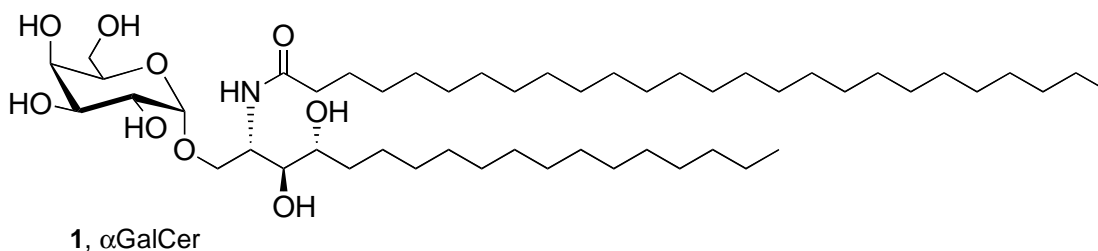


**Figure 4.**  $\alpha$ -Galactosyl ceramide.

$\alpha$ GalCer also tolerates substitution on the sugar moiety allowing for the identification of active galactosyl sulfatides<sup>[30]</sup> and a variety of polyglycolipids as CD1d antigens.<sup>[31]</sup> This diversity in tolerated substitutions on the sugar moiety is not matched with diversity in activity. In fact, the activity of most sugar-substituted analogues of  $\alpha$ GalCer is similar in type to the parent compound. A more diverse immune response is found when the lipid tail of the molecule is modified, which provided us with a strategy for tuning the immune response; however, in most cases the immune response is still mixed, *i.e.* regulatory and pro-inflammatory, which continues to restrict the therapeutic applications of such analogues. For example, it has been demonstrated that the effect of reducing the lipid chain length in the phytosphingosine component is to increase the amount of IL-4 (regulatory response) *versus* IFN- $\gamma$  (pro-inflammatory response) being produced.<sup>[32]</sup>

Although it has been demonstrated that  $\alpha$ GalCer is an effective and very powerful activator of the immune system, it has also been found that after a single activation event with  $\alpha$ GalCer,  $\mathcal{N}$ KT cells display a long period of anergy during which  $\mathcal{N}$ KT cells population diminish to nearly undetectable levels and are unresponsive when pulsed with further doses of  $\alpha$ GalCer.<sup>[33]</sup> It was postulated that anergy is the result of a too powerful activation, which induces a process in which the  $\mathcal{N}$ KT cells deepen their surface receptors to avoid further activation. This lack of reactivity lapses over two weeks after a single stimulation; it is a major problem for the possible therapeutic applications of  $\alpha$ GalCer and must also be taken in consideration when designing new  $\alpha$ GalCer analogues for activation of  $\mathcal{N}$ KT cells, *i.e.* analogues which are less powerful activators of  $\mathcal{N}$ KT cells and which induce shorter anergy periods are preferable for therapeutic applications.

The hydrophobic tails of  $\alpha$ GalCer are an obvious target for the fabrication of new analogues. Many modifications in these parts of  $\alpha$ GalCer can change the nature of the hydrophobic interactions with the binding pockets of CD1d [Figure 5]. For example, Miyamoto *et al.* synthesised a truncated analogue of  $\alpha$ GalCer with 24 carbon atoms in length as the acyl chain and a phytosphingosine with nine carbon atoms in length, compound **2**.<sup>[32]</sup> Like  $\alpha$ GalCer, this compound, which they named OCH, was also found to stimulate  $\mathcal{N}$ KT cells by way of CD1d and induced an immune response with a Th2 bias. In a separate study, Oki *et al.* synthesised various analogues of  $\alpha$ GalCer possessing different sphingosine lengths and demonstrated that the production of IFN- $\gamma$  is more susceptible to the length of the phytosphingosine

base than is the production of IL-4.<sup>[34]</sup> The authors postulated that the shorter sphingosine length destabilises the CD1d- $\alpha$ GalCer complex because of a reduction in the ligand's overall hydrophobicity, which therefore reduces the time that the complex is in contact with the TCR. This observation led to the conclusion that a longer exposure to the TCR is required to induce higher levels of IFN- $\gamma$ .

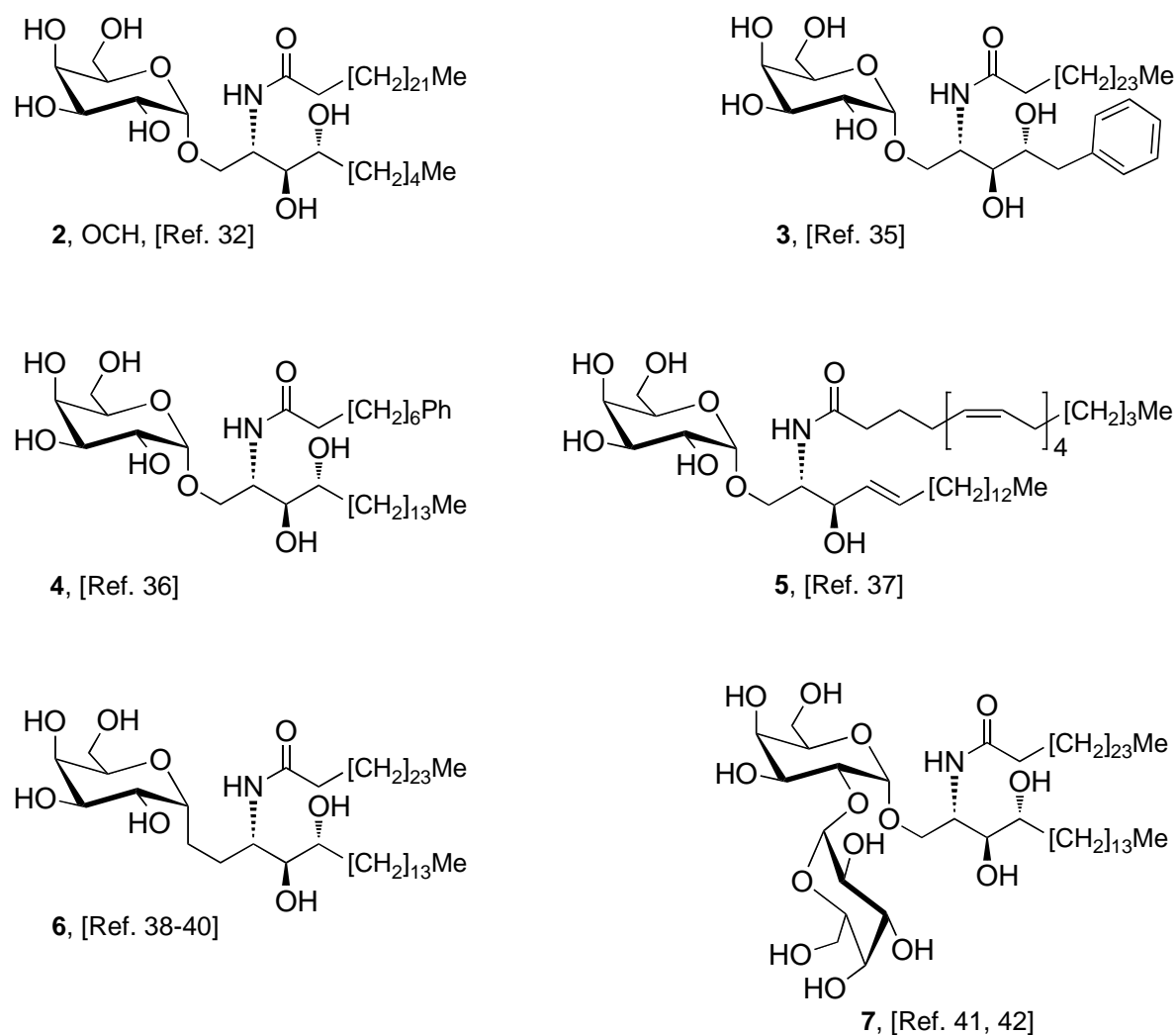


**Figure 5.** Examples of synthetic  $\alpha$ GalCer analogues.

Toba *et al.* explored other modifications on the phytosphingosine and compared these new analogues to OCH. They found that in compound **3** [Figure 5], while this

molecules still features a short sphingosine chain, the hydrophobicity has been increased with respect to OCH by introducing a phenyl substituent. As a result, **3** is capable of inducing larger amounts of IL-4 and IFN- $\gamma$  than OCH.<sup>[35]</sup> The response displayed by **3** is still a Th2 bias in the cytokine response although this is less pronounced than that observed with OCH.

In another study, which focused on the effects of varying the hydrophobicity of the acyl chain, it was found that aromaticity in this part of the molecule can also influence the cytokine profile of the immune response. For example, compound **4** was found to be optimal for inducing a higher production of IFN- $\gamma$  *in vitro* and was also capable of producing abundantly a range of cytokines typical of a Th1 immune response *in vivo*.<sup>[36]</sup> Interestingly, in another report, compound **5**, which contains an arachidonic acid acyl chain, was found to favour a Th2 response.<sup>[37]</sup> The pattern emerging for the acyl chain seems to point to short aromatic substitutions favouring the preferential production of Th1 cytokines while heavily unsaturated acyl chains favour the production of Th2 cytokines [Figure 5].

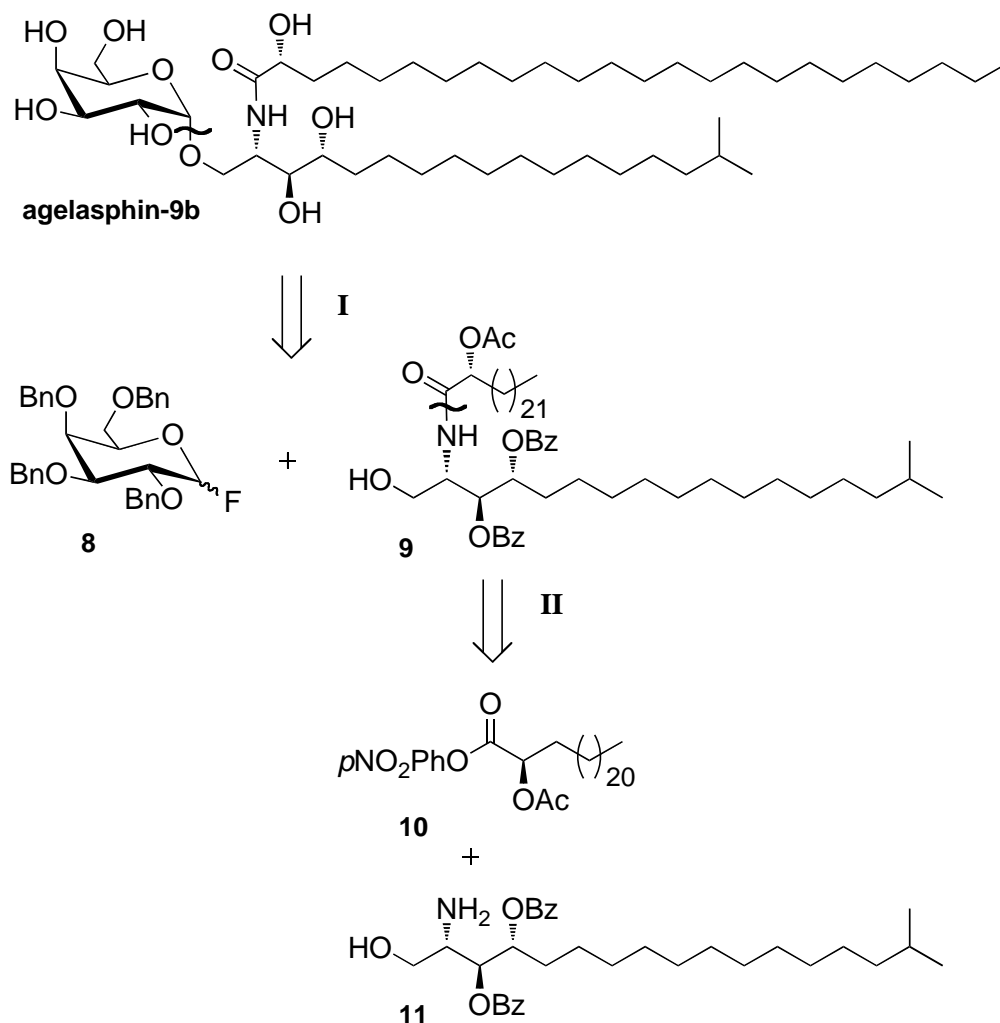
The C-glycosyl analogue of  $\alpha$ GalCer, compound **6**, is another glycolipid which was found to produce a Th1-biased immune response. In this analogue, the hydrolytically labile glycosidic bond of  $\alpha$ GalCer is replaced with a much stronger carbon-carbon bond.<sup>[38-40]</sup> Consequently this compound is expected to survive a wider range of conditions for a longer time than is  $\alpha$ GalCer, which can therefore increase the time that CD1d can present this  $\alpha$ GalCer analogue to the TCR. This is another example

where the analogue suspected of increasing presentation time induces a Th1-biased immune response.

The disaccharide **7** was used as a probe to demonstrate that although some disaccharides can be presented for recognition to TCRs without lysosomal processing, this example required removal of the second galactose moiety before it can be recognised by TCRs [Figure 5].<sup>[41, 42]</sup> This constitutes an example of a carbohydrate antigen processing mechanism and an ability for *i*NKT cells to recognise smaller fragments of complex glycolipids.

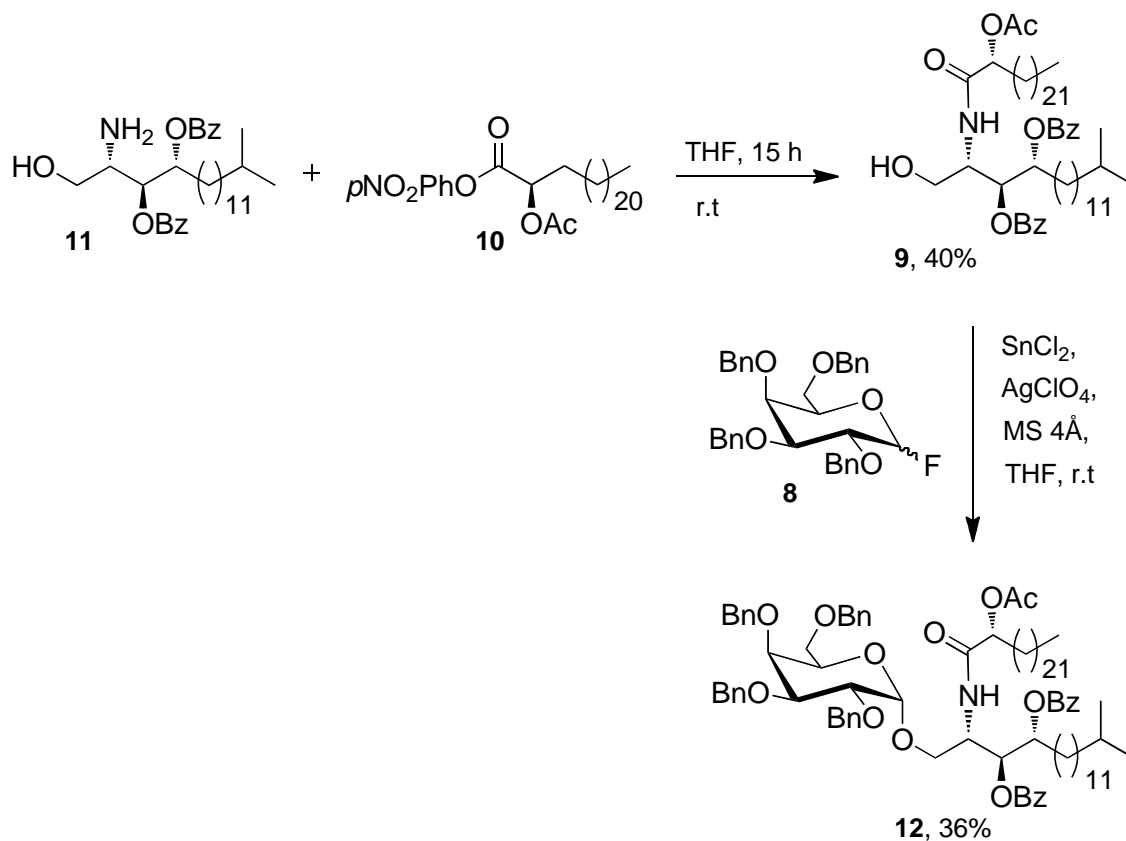
#### 1.4. Syntheses of $\alpha$ -Galactosyl Ceramides.

$\alpha$ -Galactosyl ceramides were first found in the natural world by Natori *et al.* who isolated them from the marine sponge *Agelas mauritianus*.<sup>[43]</sup> A range of glycosphingolipids were isolated, with most possessing an  $\alpha$ -galactosyl ceramide structures that were acylated with an alpha hydroxy fatty acid of 26 and 24 carbons in length. In another paper published simultaneously, Natori *et al.* presented the synthesis of **agelasphin-9b** to confirm the absolute and relative stereochemistry of the isolated sphingolipid.<sup>[44]</sup> The key retrosynthetic steps are outlined below [Scheme 1].



**Scheme 1.** Retrosynthesis of  $\alpha$ -galactosyl ceramide **agelasphin-9b**.

The retrosynthetic analysis identified the glycosidic bond as the first disconnection revealing a suitably protected ceramide moiety **9** as the acceptor and perbenzylated galactosyl fluoride **8** as the sugar donor. The amide bond in the ceramide acceptor was further disconnected and the synthetic equivalents were identified as the *p*-nitrophenylester **10** and the corresponding suitably protected phytosphingosine **11**. This retrosynthetic analysis benefits from a late-stage glycosylation step, requiring only two further deprotection steps to reach the synthetic target.



**Scheme 2.** Key stereoselective glycosylation yields **agelasphin-9b**'s precursor **12**.

In the forward synthesis [Scheme 2] the amine **11** was reacted with the *p*-nitrophenylester **10** in THF to provide the target amide in 40% yield. Natori *et al.* did not offer an explanation for the moderate yield of this reaction; however, it is possible that a side-reaction involving intramolecular migration of a benzoate group on to the neighbouring amine might be responsible for the low yield of product **9**. In spite of the low yield, Natori *et al.* were able to proceed to the glycosylation step with the perbenzylated galactosyl fluoride sugar donor **8**. The use of perbenzylated glycosyl fluoride **8** as a sugar donor in a glycosylation reaction was first reported by Mukaiyama *et al.*<sup>[45]</sup> Activation of the donor with  $\text{SnCl}_2/\text{AgClO}_4$  provided the  $\alpha$ -glycoside preferentially: a range of alcohol acceptors including sterically hindered

alcohol acceptors like 2,3,6-tri-O-benzyl- $\alpha$ -D-glucopyranoside, cholesterol and 3 $\beta$ -cholestanol, all afforded favourable  $\alpha$ : $\beta$  ratios of the glycoside products in high yields. However, Natori *et al.* did not obtain a high yield in the glycosylation reaction involving donor **8** with the ceramide acceptor **9**. Although they did not comment on the reaction efficiency, we can hypothesise that intramolecular H-bonding between the amide and the free hydroxyl renders the acceptor a poorer nucleophile and may account for the low efficiency of this reaction [Figure 6].

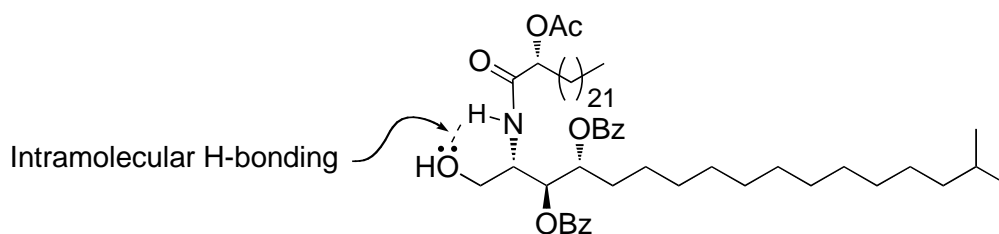
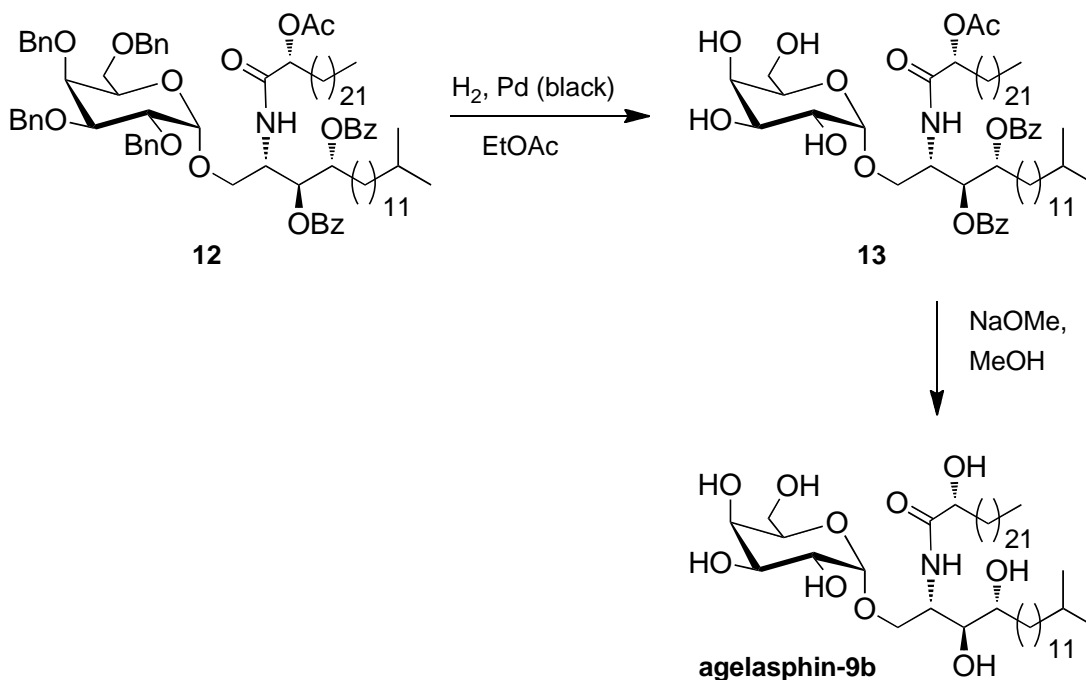


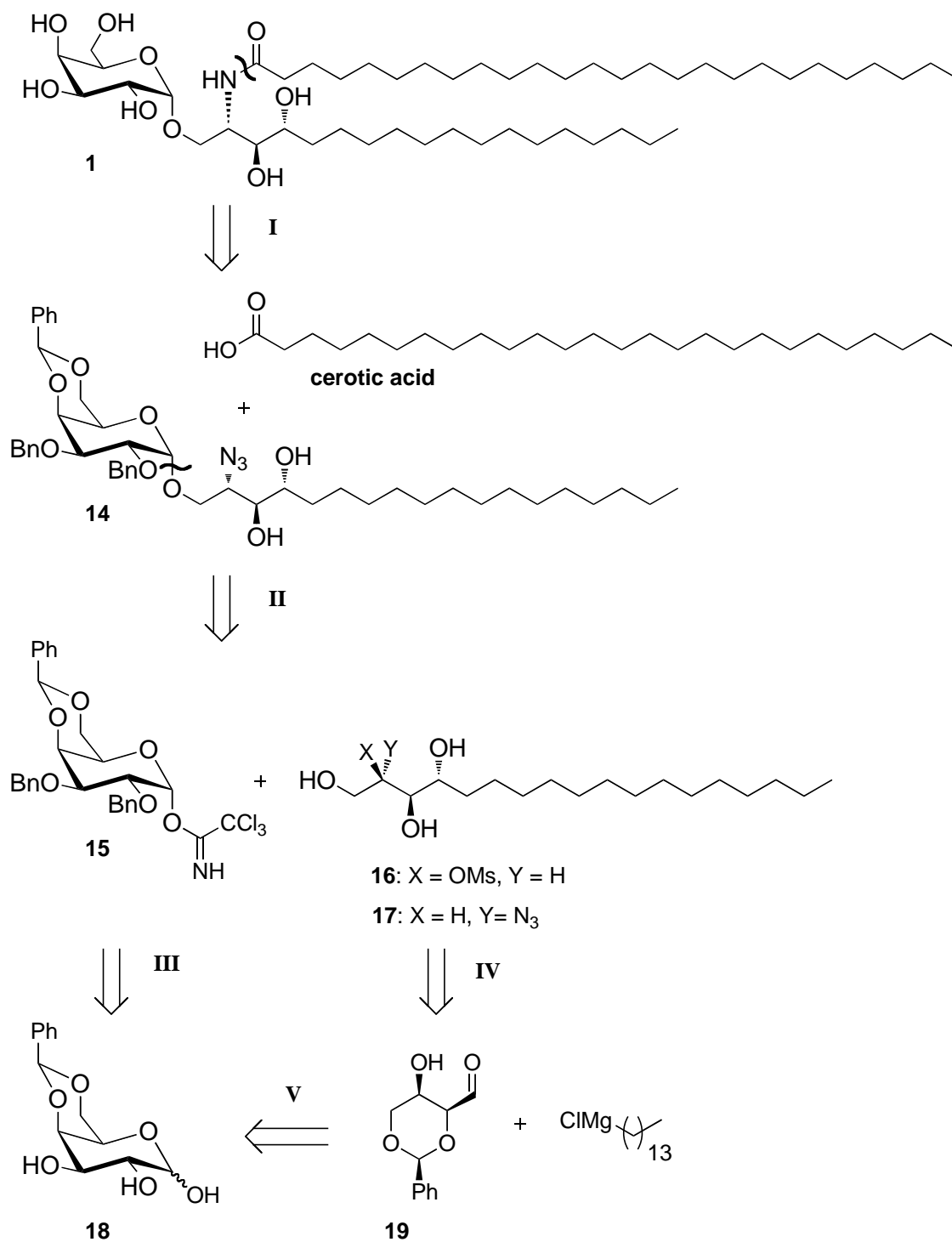
**Figure 6.** Intramolecular H-bonding in ceramides.

Nevertheless, Natori *et al.* obtained the desired glycoside product **12** as a single anomer and recovered 40% of the unreacted acceptor **9**. The product **12** was then subjected to hydrogenolysis with H<sub>2</sub> and Pd (black) as catalyst for the deprotection of the benzyl groups, affording **13**, followed by removal of the two type of ester protecting groups under basic conditions to afford the target **agelasphin-9b** [Scheme 3]. Although Natori *et al.* did not report the yields of these final two deprotection steps, it is reasonable to assume that both steps were efficient and given that the sugar donor **8** is relatively easily accessible, this is an attractive first stereoselective route to  $\alpha$ -galactosyl ceramides.



**Scheme 3.** Chemoselective deprotection sequence yields **agelasphin-9b**.

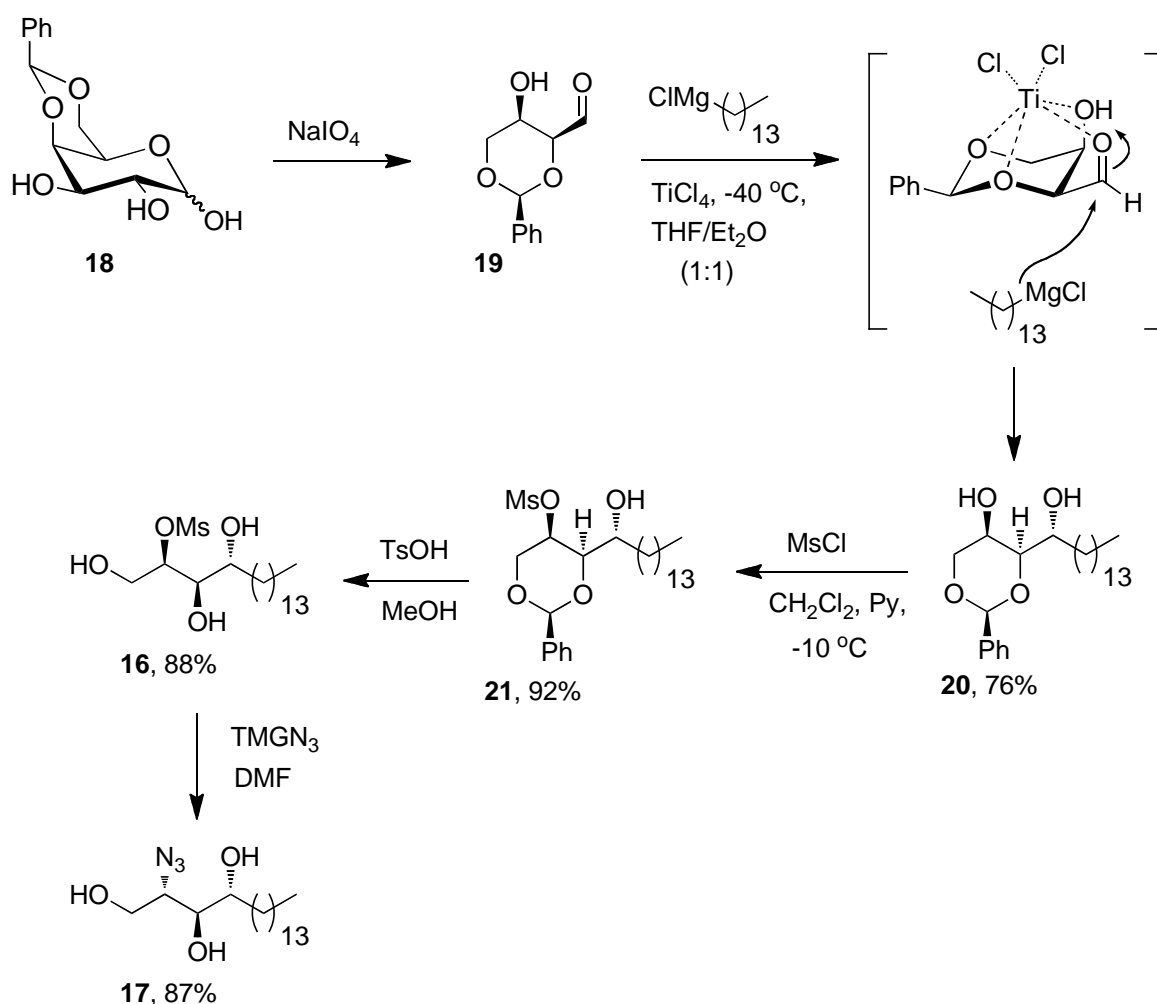
In another approach to these molecules, Figueroa-Perez *et al.* chose to install the fatty acid after the glycosidation step, which would allow them to explore a range of different acceptors [Scheme 4].<sup>[46]</sup> Specially, they had in mind two different triols **16** and **17** as acceptors. Triol **16** possesses a methanesulfonate leaving group that could be displaced in an  $\text{S}_{\text{N}}2$  reaction with a nucleophilic source of nitrogen (*i.e.* azide) to yield the required intermediate **14** after glycosidation with the donor **15** [Scheme 4]. Alternatively, triol **17** which carries the  $\text{N}_3$  already would yield **14** directly after the glycosidation step. Figueroa-Perez *et al.* identified synthetic routes from a common galactose derivative **18** from which both the sugar donor *and* the acceptor triols would be synthesised.



**Scheme 4.** Schmidt retrosynthetic analysis of  $\alpha$ GalCer.

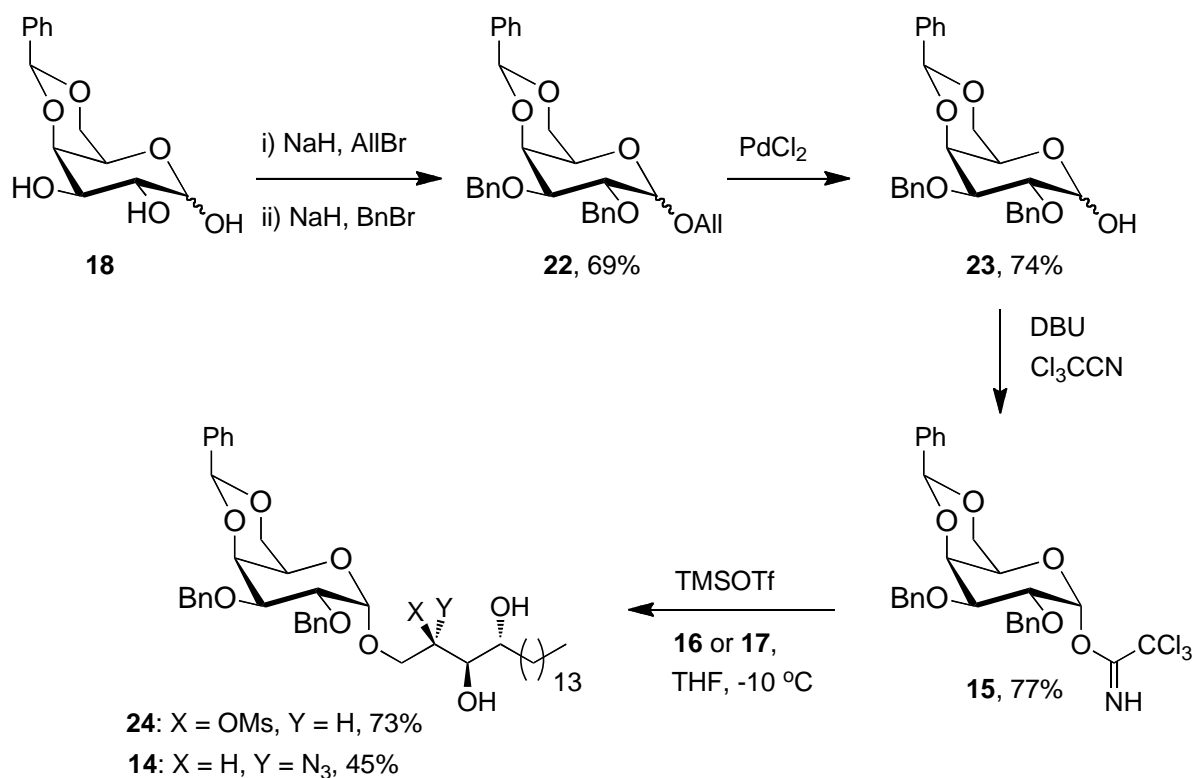
The triols **16** and **17** were prepared from the galactose derivative **18** in five and six steps, respectively. Aldehyde **19** was obtained by oxidative cleavage of **18** with NaIO<sub>4</sub>

[Scheme 5]. The addition of alkyl Grignard reagents to aldehyde **19** had been studied previously,<sup>[47]</sup> where it had been observed that in the presence of the chelating Lewis acid  $\text{TiCl}_4$ , only the required diastereoisomer is obtained in high yield. It was then possible to install the methanesulfonate leaving group chemoselectively in the less hindered alcohol in diol **20**. The acetal in the product **21** was then selectively hydrolysed in acidic methanol [Scheme 5]. The triol **16** was then converted in to triol **17** by a displacement reaction of the methanesulfonate with tetramethylguanidinium azide,  $\text{TMGN}_3$ , in DMF [Scheme 5].



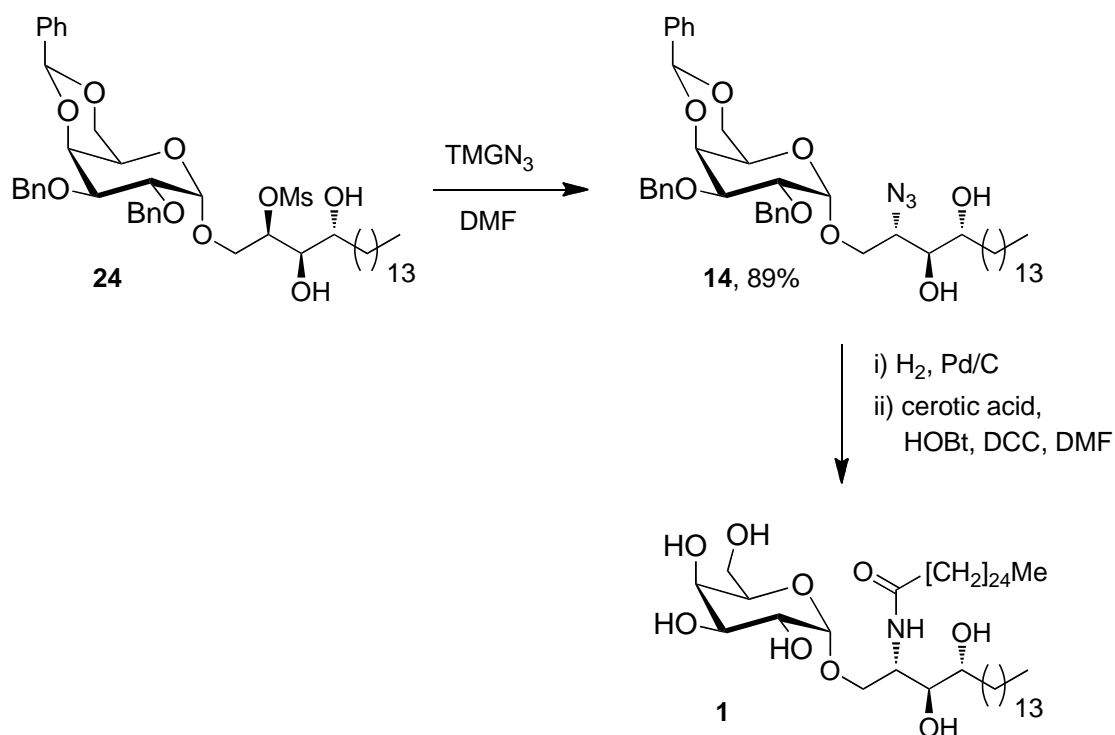
**Scheme 5.** Synthesis of azido-phytosphingosine **17**.

The sugar donor **15** was also prepared from the triol galactose derivative **18** [Scheme 6]. Triol **18** was first treated with one equivalent of NaH and allyl bromide, which preferentially reacted with the hemiacetal alcohol to provide an allyl glycoside, which was subsequently treated with two further equivalents of NaH and benzyl bromide to yield the fully protected sugar **22** [Scheme 6]. The allyl group was chemoselectively deprotected with PdCl<sub>2</sub> and the resulting hemiacetal **23** was converted into the trichloroacetimidate sugar donor **15** on reaction with DBU and trichloroacetonitrile [Scheme 6]. The key glycosylation was carried out at -10 °C in THF with both acceptor triols **16** and **17**. The desired glycoside products **24** and **14** were obtained by the chemoselective reaction of the primary alcohol in the presence of two secondary alcohols with the activated donor [Scheme 6]. Figueroa-Perez *et al.* found that the glycosidation with acceptor triol **16** afforded product **24** in high yield, while with acceptor triol **17** the glycosidation afforded a mixture of products from which the desired glycoside **14** could be isolated in low yield.



**Scheme 6.** Stereoselective synthesis of glycoside **24** and **14**.

The methanesulfonate leaving group in glycoside **24** was then displaced with inversion of configuration with TMGN<sub>3</sub> in DMF to afford **14** in high yield [Scheme 7]. The benzyl protecting groups, the benzylidene and the azide were hydrogenolysed with H<sub>2</sub> in the presence of catalytic amount of Pd/C and the fully deprotected amide was acylated with cerotic acid by reaction with *N,N'*-dicyclohexylcarbodiimide, DCC, and employing hydroxybenzotriazole, HOBt, as a nucleophilic catalyst, to afford  $\alpha$ GalCer **1**.

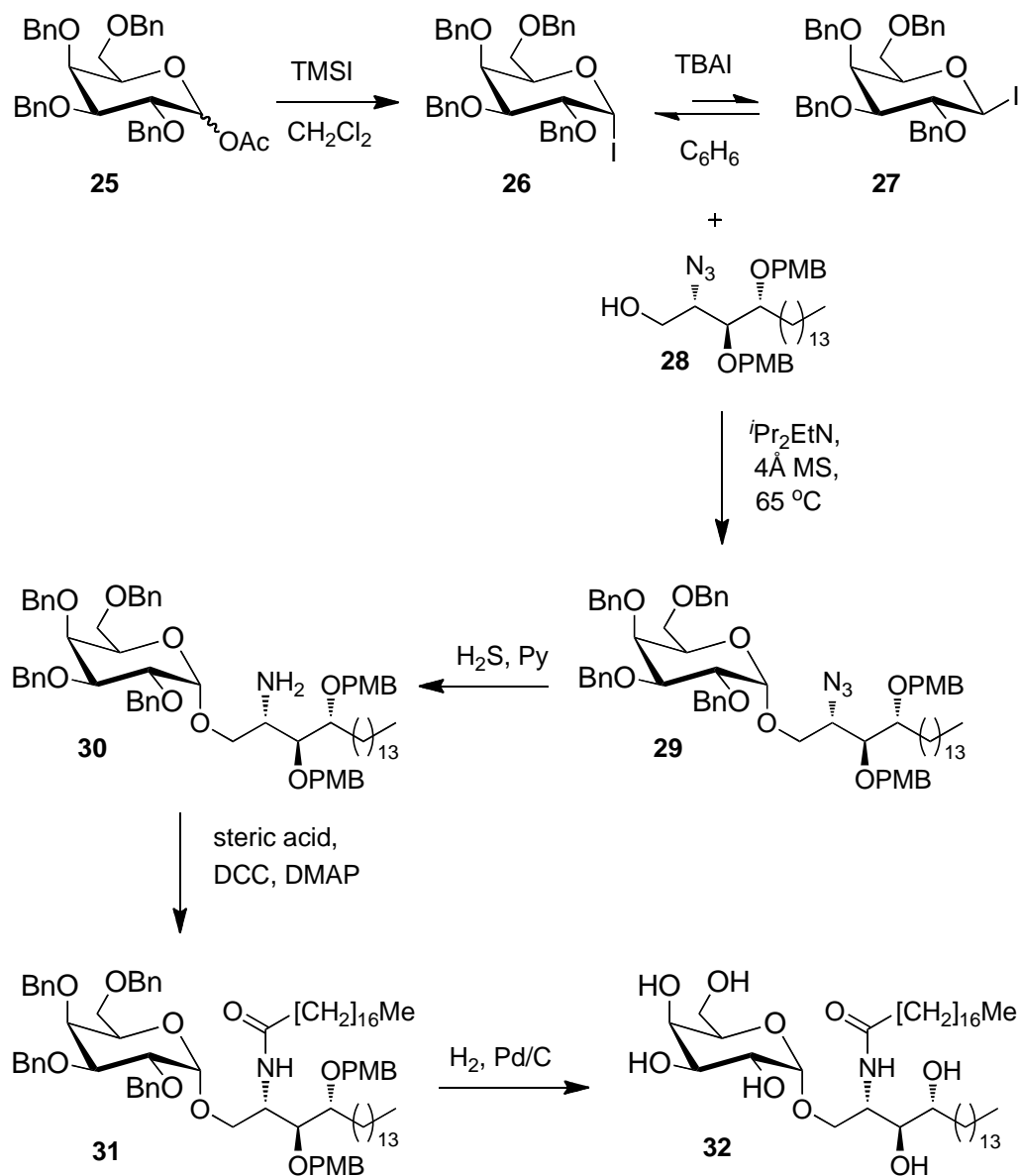


**Scheme 7.** Synthesis of  $\alpha$ -GalCer **1** from **24**.

In another example of  $\alpha$ -galactosyl ceramides synthesis, Gervay-Hague and co-workers have employed a perbenzylated galactosyl iodide as the sugar donor [Scheme 8].<sup>[48]</sup> The highly reactive, and prone to hydrolysis, sugar donor **26** was prepared *in situ* from **25** by treatment with trimethylsilyl iodide, TMSI. The resulting  $\alpha$ -galactosyl donor **26** was then treated with an excess of tetrabutylammonium iodide, TBAI, to establish an equilibrium with a small amount of the more reactive  $\beta$ -galactosyl donor **27**, which reacts with the acceptor alcohol **28** in an  $\text{S}_{\text{N}}2$  fashion to yield exclusively the  $\alpha$ -galactoside product **29** in high yield. The azide was then reduced to the amine **30** with hydrogen sulfide and pyridine, which was subsequently acylated to afford amide **31**. Finally, hydrogenolysis of the benzyl and *p*-

methoxybenzyl protecting groups present in **31** yielded  $\alpha$ -galactosyl ceramide **32**

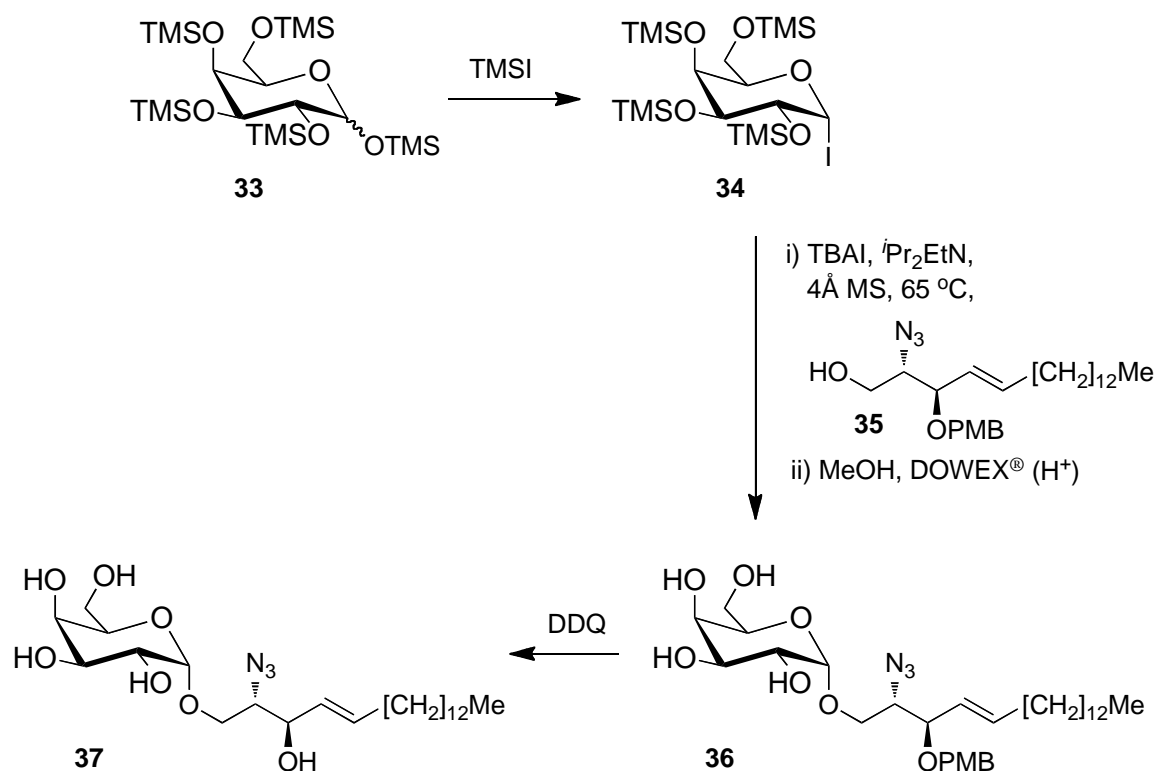
[Scheme 8].



**Scheme 8.** Stereoselective synthesis of  $\alpha$ -galactosyl ceramide **32**.

Although Gervay-Hague and co-workers successfully synthesised  $\alpha$ -galactosyl ceramide employing perbenzylated galactosyl iodide, the method was limited to the synthesis of saturated ceramides since they relied on the global deprotection of the

benzyl and *p*-methoxybenzyl groups by hydrogenolysis, which is incompatible with ceramides possessing unsaturation. Gervay-Hague and co-workers addressed this issue in the same publication.<sup>[48]</sup> They discovered that the persilylated galactose **33** can be converted quantitatively into the persilylated galactosyl iodide **34** by reaction with TMSI, and that this reacts smoothly under the conditions established previously for perbenzylated galactosyl iodide with acceptor **35** and with complete selectivity for the  $\alpha$ -anomer yielding galactoside **36** [Scheme 9].



**Scheme 9.** Gervay-Hague's stereoselective  $\alpha$ -galactosylation.

Although all methods for the synthesis of  $\alpha$ -galactosyl ceramides described here are similar, crucially they differ in the glycosylation conditions employed to achieve stereoselectivity and the stage when to install the fatty acid, before or after the glycosylation step. Gervay-Hague's method that employs the persilylated galactosyl

iodide as sugar donor yielding the deprotected sugar directly after acidic treatment is considered the most attractive method. It is not only a short stereoselective route to  $\alpha$ -galactosyl ceramides in which the reactive sugar donor is quantitatively made *in situ* from trivially accessible persilylated galactose but also permits to carry unsaturations in the sphingosine base which is forbidden in other methods when the deprotection strategies rely on hydrogenolysis [Scheme 9].

## **AIMS AND OBJECTIVES**

## II. AIMS AND OBJECTIVES

From a synthetic view point,  $\alpha$ GalCer presents us with a number of challenges. Although the molecule possesses various stereogenic centres, these can mostly be bought in from natural sources, namely galactose and phytosphingosine, which are available commercially as single enantiomers. However, the  $\alpha$ -galactosidic bond is a relatively difficult bond to make stereoselectively and this aspect of the synthesis in particular needs careful planning. The alcohols need to be appropriately protected before the fragments can be put together. These protecting groups then need to be removed at a later stage, which further extends the length of the synthesis and increases likelihood of encountering problematic steps.

It should also be noted that the glycosidic bond in  $\alpha$ GalCer can be relatively easily degraded in a biological environment, not only by the possible presence of  $\alpha$ -galactosidases but also by hydrolysis in the acidic cellular media where  $\alpha$ GalCer may be delivered.

In a recent study it was discovered that replacing the galactosyl polar-head group with a truncated galactose moiety addressed some of the problems associated with  $\alpha$ GalCer, including the long period of anergy after a single activation and the propensity to induce  $\lambda$ NKT cell-dependent lysis of DCs.<sup>[49]</sup> The analogues were arabinitol ceramide, AraCer, threitol ceramide, ThrCer, and glycerol ceramide, GlyCer [Figure 7].

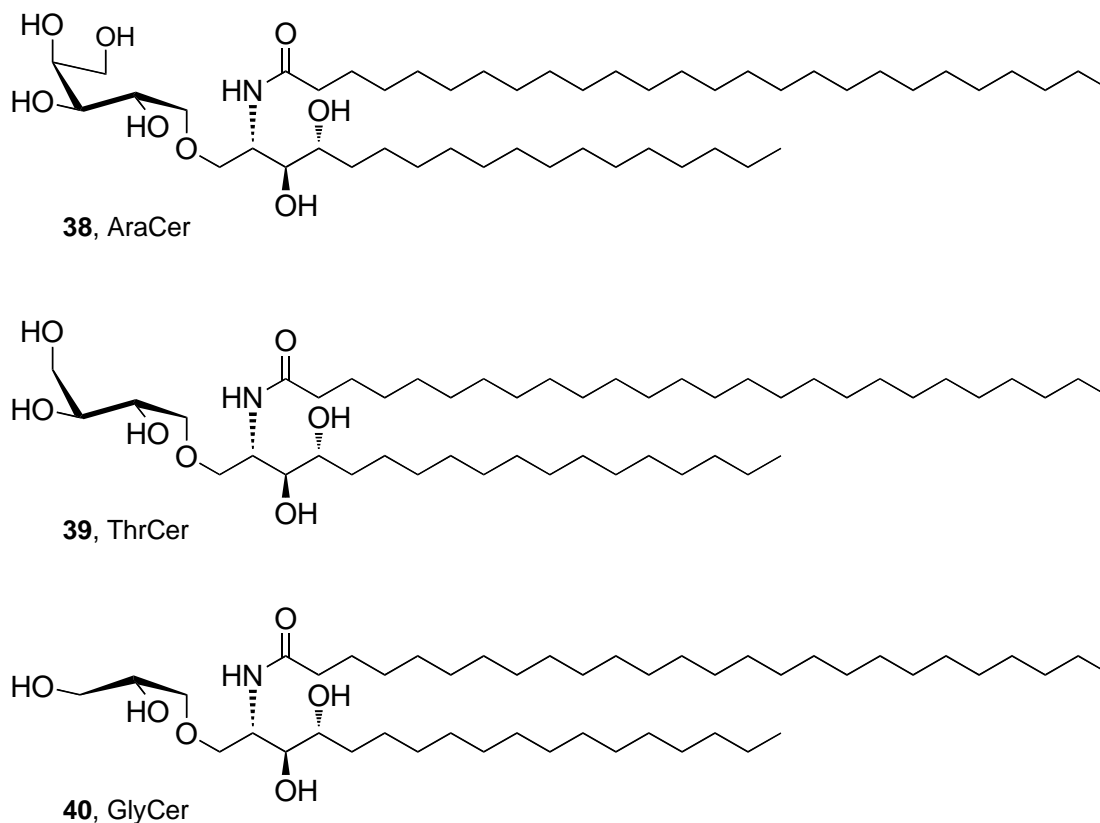


**Figure 7.** Truncated derivatives of  $\alpha$ GalCer.

Although GlyCer and AraCer analogues stimulate  $\mathbb{N}$ KT cells with varying success it was found that ThrCer was an accomplished analogue of  $\alpha$ GalCer. ThrCer stimulates  $\mathbb{N}$ KT cells and induces the secretion of IFN $\gamma$  and IL-4 with a similar profile over time as  $\alpha$ GalCer activation, but only half the amount of cytokines are produced. As a consequence, it was also found that  $\mathbb{N}$ KT cells recovered from anergy 14 days after a single activation with ThrCer, whereas no stimulus was found after the same time when  $\mathbb{N}$ KT cells were activated with  $\alpha$ GalCer. The three analogues were also assayed for their ability to control tumor growth and of the three, only ThrCer was able to suppress tumor growth after 14 days. Structurally, ThrCer is a truncated

version of  $\alpha$ GalCer where the C(5) and C(6) atoms have been excised from the hexose sugar [Figure 8].

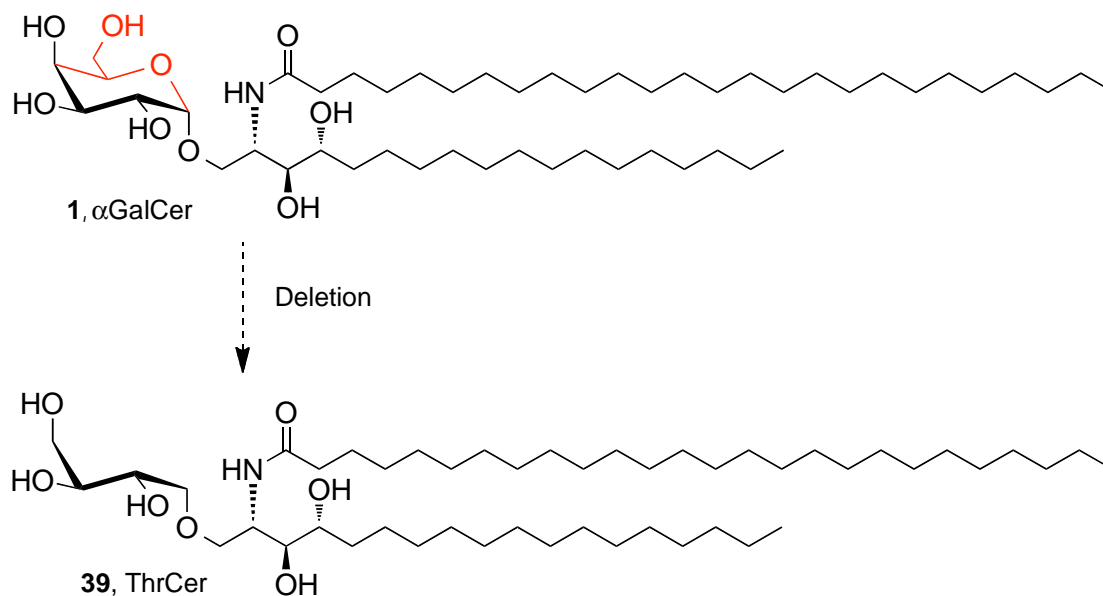


**Figure 8.** ThrCer is a truncated analogue of  $\alpha$ GalCer.

This modification was proposed by analysis of the X-ray crystal structure of the CD1d- $\alpha$ GalCer-TCR complex,<sup>[50]</sup> which pointed to the OH groups on C(2), C(3) and C(4) being essential for the recognition of the CD1d- $\alpha$ GalCer complex by TCRs through H-bonding [Figure 9]. Since the hydroxyl at C(6) was not observed to participate in H-bonding with either CD1d or with the TCR, this suggested that its deletion may not be detrimental for TCR recognition of the CD1d- $\alpha$ GalCer complex, which proved to be the case.

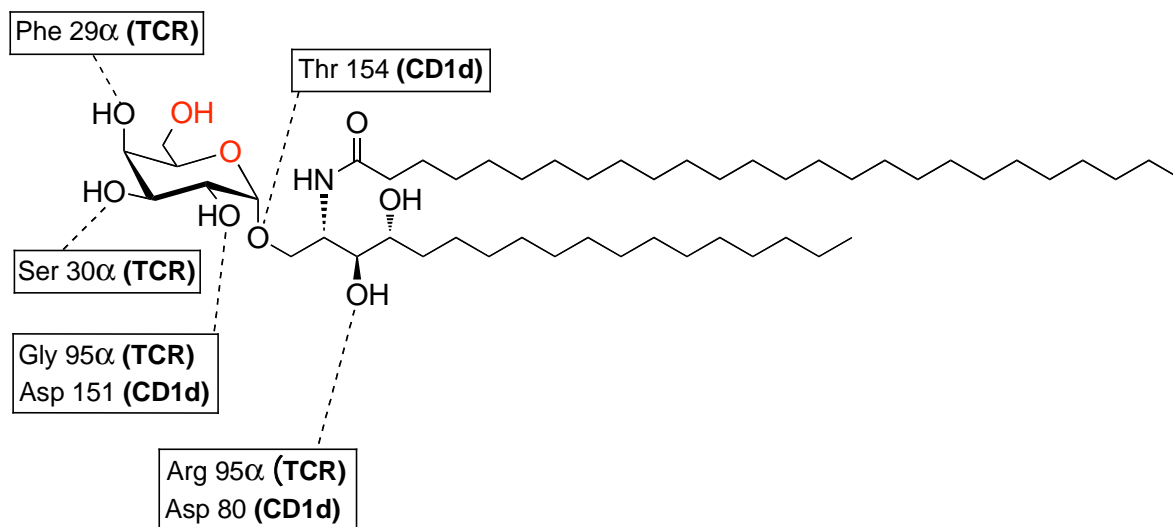
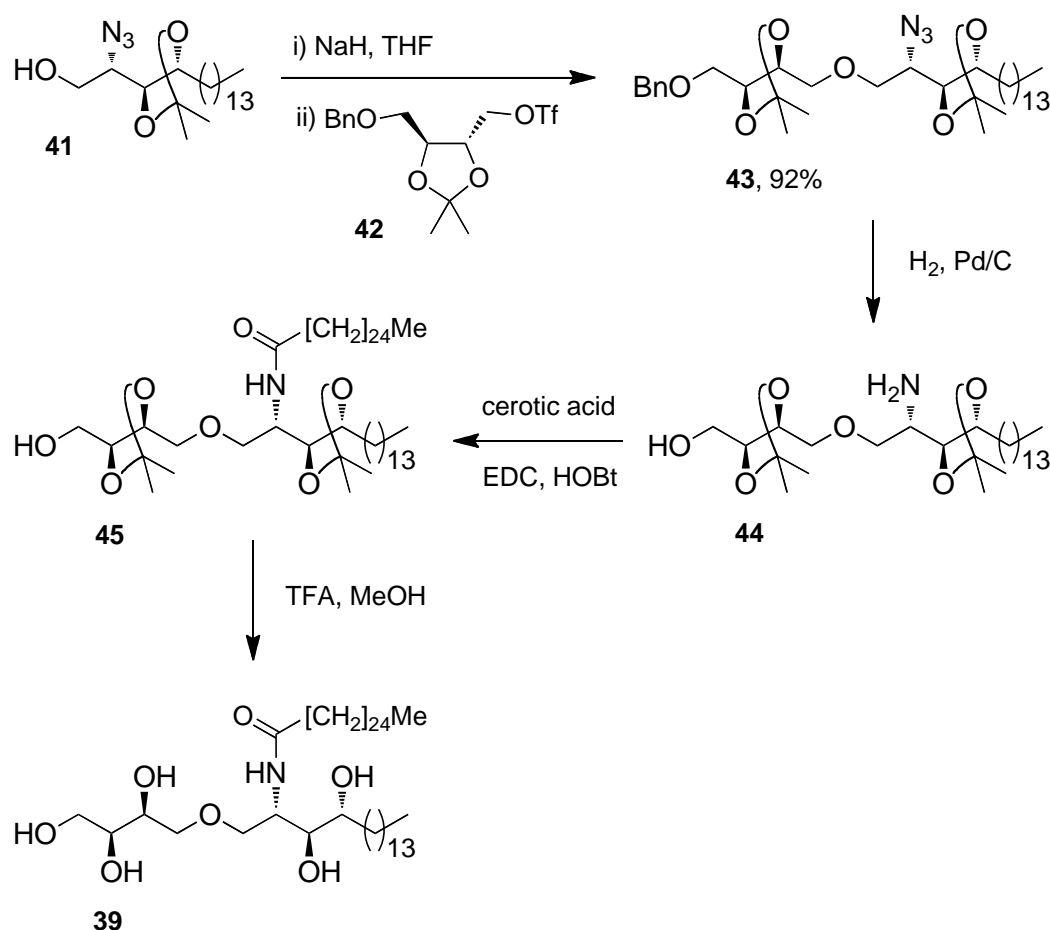


**Figure 9.** Important H-bonding interactions for recognition were revealed in studies of the X-ray crystal structure of CD1d- $\alpha$ GalCer complex and of CD1d- $\alpha$ GalCer-TCR complex. The primary hydroxyl of galactose and the anomeric oxygen (highlighted in red) are not involved in H-bonding interactions with neither the TCR or CD1d.

ThrCer also possesses the advantage over  $\alpha$ GalCer, that the polar head group is bound to the ceramide base via an ether bond, which is more stable towards acidic hydrolysis and biodegradation than the glycosidic bond of  $\alpha$ GalCer. This increased stability should extend the time that ThrCer persists in the cell compartments, increasing the chances of it being loaded on to CD1d for presentation. The ether bond not only confers increased stability to ThrCer but also makes the molecule an easier synthetic target, removing the requirements for exercising a difficult  $\alpha$ -stereoselective glycosylation.

Schmidt and co-workers synthesised ThrCer from commercially available building blocks.<sup>[51]</sup> The key steps of their synthesis are outlined below [Scheme 10]. The key etherification was performed by treating the phytosphingosine derivative alcohol **41**

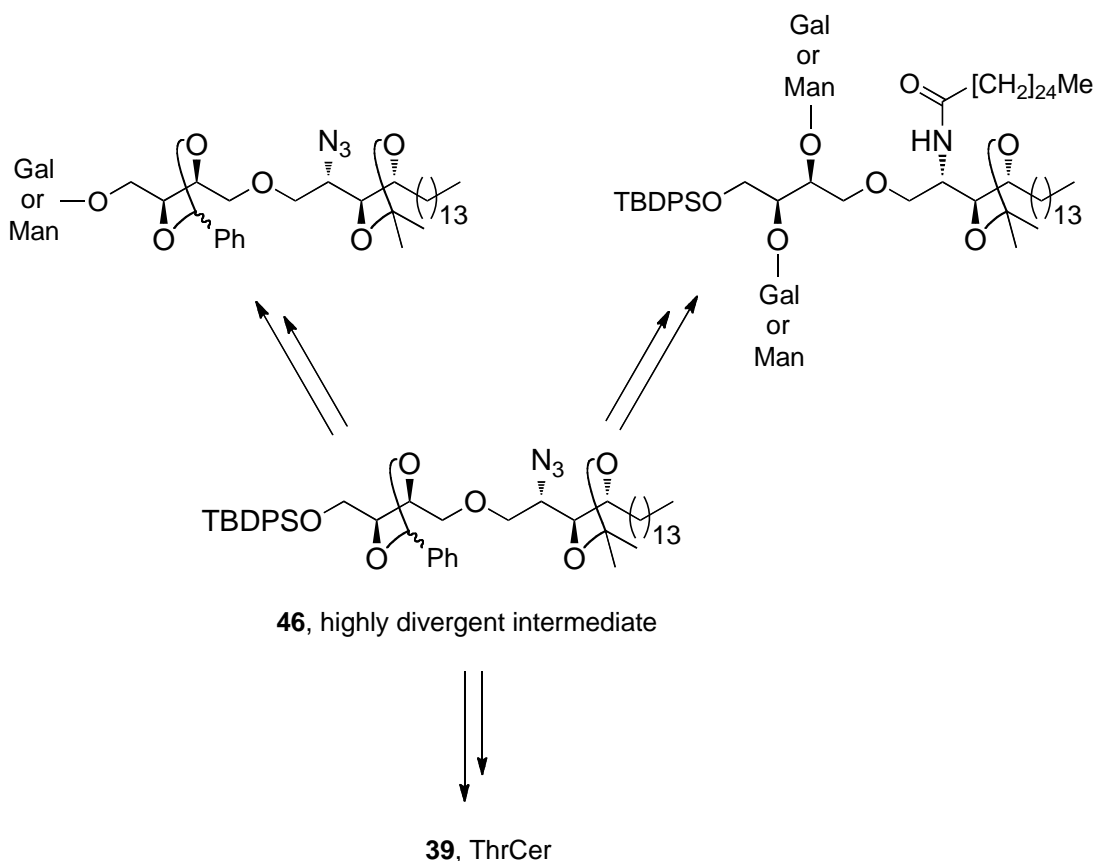
with NaH and reacting the resulting alkoxide with a suitably protected threitol derivative, triflate **42**. Under these conditions, Schmidt and co-workers reported that no elimination byproducts were formed and the ether product **43** was obtained in very high yield. Simultaneous deprotection of the benzyl ethers protection and the azide under hydrogenation conditions yielded **44**, which was chemoselectively acylated to provide amide **45**. The isopropylidenes were then removed by treatment with TFA in MeOH to provide the target ThrCer **39** [Scheme 10].



**Scheme 10.** Schmidt's synthesis of ThrCer.

In our lab we wanted to develop a more general and divergent synthetic route to ThrCer **39** exploiting protecting groups that could be removed orthogonally and allow

selective access to the different hydroxyl groups for diversification. In particular, we were interested in accessing selectively the internal diol in the threitol moiety for further elaboration (for example for glycosidation with a suitable galactosyl or mannosyl donor), which in Schmidt and co-workers' synthesis is protected with an isopropylidene analogously to the internal diol of the phytosphingosine. Consequently, hydrolysis of one isopropylidene in **43** will necessary result in the hydrolysis of the other isopropylidene [Scheme 10]. We identified the intermediate **46** as our key divergent intermediate [Scheme 11]. The intermediate **46** carries a benzylidene protecting group in the threitol moiety that can be reductively opened with DIBAL-H or removed by hydrogenolysis to reveal the internal diol in the threitol moiety which can be subsequently glycosylated [Scheme 11]. The silyl protecting group can also be selectively removed with a fluoride source like tetrabutylammonium fluoride, TBAF, and the resulting alcohol can then also be glycosylated, scheme 11, giving access to other glycosylated ThrCer derivatives. These are important modifications of ThrCer with speculative bioactivity of interest to our collaborators and us and we were interested to access them at later time.



**Scheme 11.** Highly divergent intermediate **46** offer access to ThrCer derivatives.

Furthermore, we required that our synthetic route would also allow us to install the fatty acid as the last step, which would facilitate a proposed synthesis of  $^{14}\text{C}$  radio-labelled ThrCer by minimising the number of synthetic steps we would need to perform on radio-labelled material. For this reason we identified **47** as the key late-stage precursor of ThrCer [Figure 10].

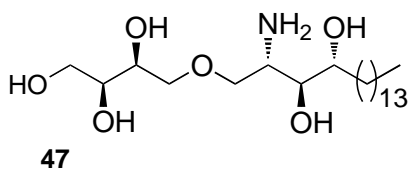


**Figure 10.** Key late-stage ThrCer precursor.

In another vein,  $\alpha$ -galactosyl diacylglycerols,  $\alpha$ GalDAGs, of pathogenic origins are natural glycolipids and were recently shown to be agonists of CD1d that are capable of inducing cytokine production in both mouse  $\mathcal{N}$ KT cells and human  $\mathcal{N}$ KT cells.<sup>[52]</sup> Initial studies have shown that their activity is closely related to the structure of the acyl chains. Our research group, in collaboration with Prof. Michael Brenner's group at the Brigham and Women's Hospital in Boston at Harvard University, wanted to develop a reliable and scalable selective synthesis of  $\alpha$ GalDAG that would allow the synthesis of a range of  $\alpha$ GalDAG analogues to study their potential as therapeutic agents.

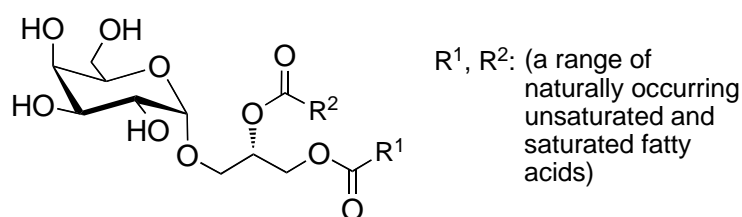


**Figure 11.**  $\alpha$ -Galactosyl diacylglycerol,  $\alpha$ GalDAG, from pathogenic origin can activate  $\mathcal{N}$ KT cells.

◆ **Aims and objectives:**

1. Novel and divergent synthesis of ThrCer.
2. Synthesis of biotin- and <sup>14</sup>C-labelled ThrCer.
3. Stereoselective synthesis of  $\alpha$ GalDAG.

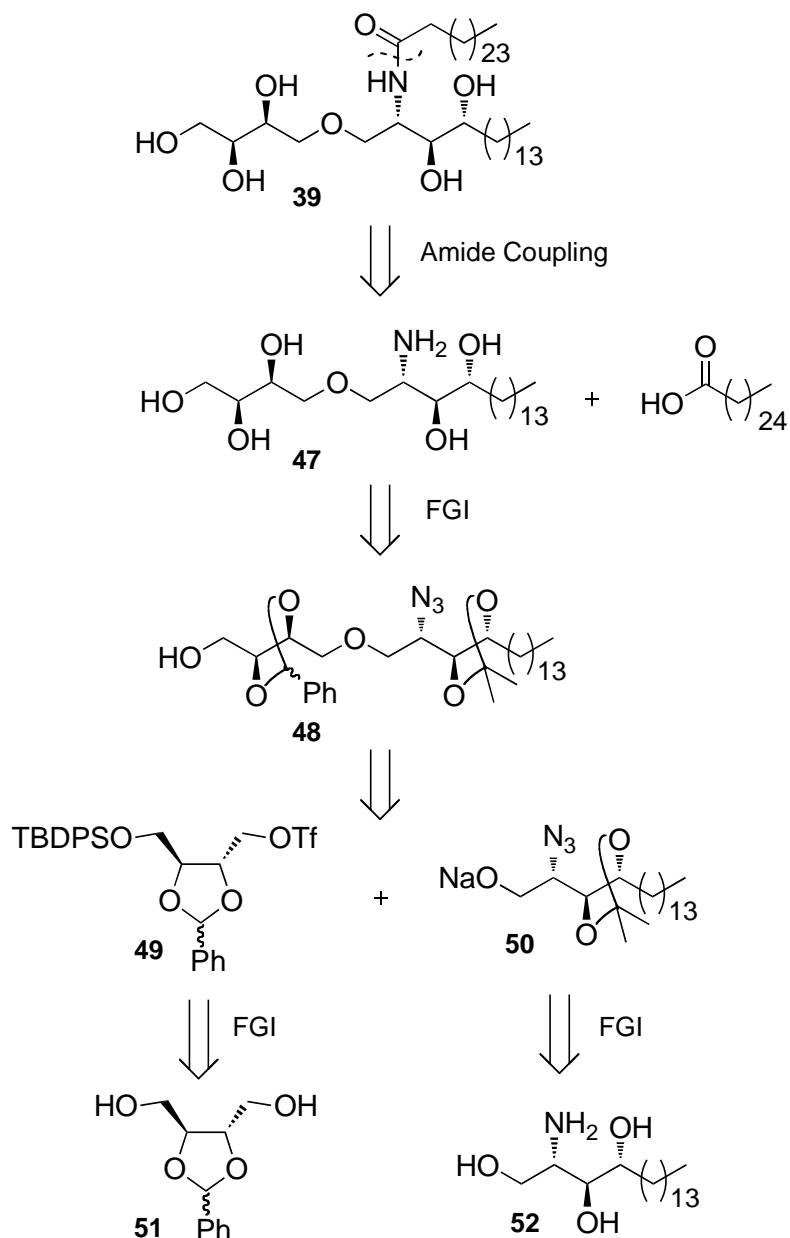
## **RESULTS AND DISCUSSION**

### III. SYNTHESIS OF THREITOL CERAMIDE AND LABELLED ANALOGUES

#### 3.1. Synthesis Of Threitol Ceramide.

The retrosynthesis of ThrCer **39** is outlined in scheme 12. In our analysis we identified two commercially available starting materials, diol **51** and phytosphingosine **52**, that could be converted into two reactive partners, **49** and **50**, uniting these two fragments via an etherification. The ether **48** could be taken through to amine **47** in two steps; thus acidic hydrolysis of the acetal and ketal groups would reveal the pentaol, leaving the azide which can be reduced under hydrogenolysis conditions. The amide coupling that follows could be easily achieved on activation of cerotic acid with a carbodiimide coupling reagent or other activated carboxylic acid derivative to provide the target ThrCer **39**.

Synthesis of Threitol Ceramide and Labelled Analogues



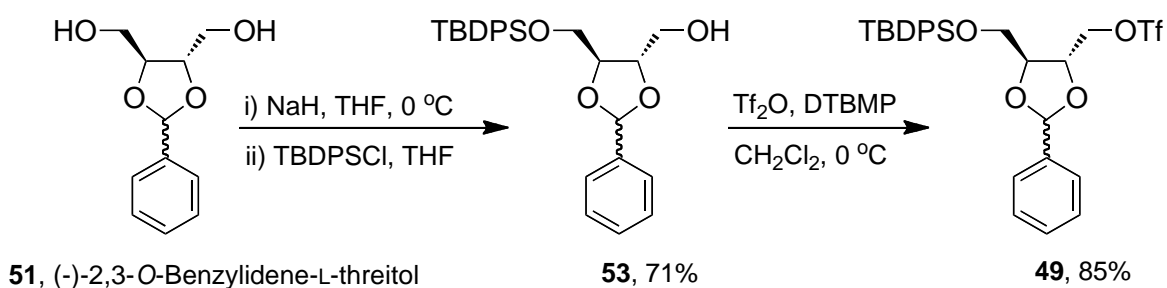
**Scheme 12.** Retrosynthetic analysis of ThrCer **39**.

The starting protected threitol moiety **51** carries the benzylidene acetal as a protecting group for the internal 1,2-diol. This protecting group introduces an additional stereocentre, which means that all asymmetric derivatives of **51** carrying this protecting group will be obtained as a mixture of diastereoisomers. Although this choice of protecting group would add complexity to the characterisation of the

intermediate products, it would also add a degree of flexibility to the synthesis as this protecting group can be removed by hydrogenolysis and by acidic hydrolysis.<sup>[53]</sup> We chose a bulky TBDPS ether group to protect one of the remaining primary alcohols [Scheme 13], foreseeing the basic, and nucleophilic, conditions of the ether bond synthesis that lay ahead. Unhindered silyl ethers are susceptible to nucleophilic attack and therefore are generally not stable in the presence of an alkoxide;<sup>[54]</sup> however, bulky silyl ether protecting groups like TBDPS and TIPS are much more stable to these reaction conditions. The silyl group protecting this terminal OH is also an orthogonal protection that would allow us to elaborate through this end at a later stage should this be necessary, for example if we wanted to glycosylate ThrCer through the primary alcohol. The pseudo C<sub>2</sub>-symmetry in **51** means that a simple mono-protection of the diol was all that was needed to get us through to compound **53** which was achieved following the Schmidt approach with the sodium alkoxide and the TBDPS chloride in THF [Scheme 13].<sup>[51]</sup> The diastereoisomeric of silyl ethers mixture was confirmed by the presence of two singlets at 1.07 and 1.09 ppm in the <sup>1</sup>H NMR spectrum, each the nine protons of the *tert*-butyl group in the 1:1 mixture of diastereoisomers of **53**.

We chose to convert alcohol **53** into an electrophile for the subsequent etherification [Scheme 13]. Of course, we could make the alkoxide from this alcohol and the electrophile on the phytosphingosine fragment and would return to this choice if the proposed etherification failed. Alcohol **53** can be converted into an array of suitable electrophiles. Alkyl bromides and alkyl iodides are often employed in ether bond formation reactions.<sup>[55]</sup> Alkyl bromides can be conveniently prepared directly from

alcohols by reaction with  $\text{Ph}_3\text{P}$  and  $\text{CBr}_4$ , while alkyl iodides are more efficiently made in two steps often involving conversion of the alcohol into a tosylate leaving group,<sup>[56]</sup> followed by subsequent displacement with a source of iodide, usually  $\text{NaI}$  in acetone. Sulfonates, like tosylates and mesylates, are easily prepared from alcohols in one step, and are themselves also commonly employed as leaving groups in nucleophilic substitution reactions, including etherifications.<sup>[57-59]</sup>



**Scheme 13.** Synthesis of orthogonally protected triflate **49**.

In this ether synthesis, we chose to convert our alcohol into a sulfonate, scheme 13, in line with the literature and taking in consideration that triflates are very good alkyl electrophiles,<sup>[51]</sup> owing their high electrophilicity to three strongly electron-withdrawing fluoro substituents. The  $\text{p}K_{\text{a}}$  of triflic acid is estimated to be around -14 in water making it one of the strongest acids commonly used in organic chemistry.<sup>[60]</sup> Such a low  $\text{p}K_{\text{a}}$  tells us that the conjugate base need not be in contact with a counter ion and can exist as a separate solvated entity; this is what defines a good leaving group. A potential disadvantage of alkyl triflates though, is that they can decompose rapidly before they can be used in a following displacement reaction. The decomposition pathway usually involves elimination reactions that yield the alkene, or rupture of the

C-OTf bond, which leaves behind a highly reactive cation that decomposes in undetermined reactions.

Alkyl triflates are usually prepared from the corresponding alcohol by reaction with triflic anhydride in the presence of an excess of pyridine which functions as an acid scavenger.<sup>[61]</sup> In our synthesis of triflate **53**, we found that although TLC analysis showed that the triflate formed readily, it rapidly decomposed when pyridine was used as the acid scavenger. We thought that the pyridine was perhaps causing the decomposition of our alkyl triflate. Pyridine can act as a nucleophile, and; in some cases, pyridine is strong enough a base to induce elimination of the triflate;<sup>[62]</sup> both of these reaction pathways would lead to the decomposition of the alkyl triflate. In line with Schmidt and co-workers report,<sup>[51]</sup> we then employed a hindered pyridine base, DTBMP, and TLC analysis showed that the triflate was formed quantitatively and instantaneously after the dropwise addition of triflic anhydride to a solution of the alcohol in CH<sub>2</sub>Cl<sub>2</sub> [Scheme 13]. Considering its instability, the alkyl triflate **53** was used directly without purification in the key etherification reaction. Attempts to purify this triflate by flash column chromatography resulted in considerable losses of material and low overall yields although Schmidt and co-workers had reported good overall yields in their approach that includes a purification of a similar triflate by flash column chromatography [Scheme 13].<sup>[51]</sup>

The nucleophilic reacting partner for the etherification was prepared from commercially available phytosphingosine, which was first converted quantitatively to



example, Boc, Cbz and Fmoc carbamates are all commonly employed as protecting groups for amines.<sup>[65]</sup> However, carbamate protecting groups can be easily deprotonated with a strong base like NaH, which we required for the formation of the alkoxide **50** for our etherification. Although the alkoxide is expected to be a better nucleophile than the carbamate anion on steric and  $pK_a$  grounds,\* the use of a carbamate protecting group could render the etherification more difficult and afford lower yields due to competing *N*-alkylation and elimination reactions. The azide also gives us the opportunity to carry out a stepwise deprotection of the ether **46**. Protecting group orthogonality was not a requirement for the synthesis of ThrCer but it might be an advantage at later stage were we might need to prepare more complex substrates. We also compared the azide to the phthalimide as another protection strategy for amines; although the latter can also be orthogonally deprotected under nucleophilic conditions, there were no literature examples for the protection and deprotection sequence of the phytosphingosine with phthalimide but there were many examples of azide protection being used effectively on phytosphingosine substrates.<sup>[46, 48, 66]</sup> The protection of the amine in phytosphingosine **52** as an azide under Wong's conditions provided **54** in very high yield and was readily confirmed by the appearance of a peak at  $2108\text{ cm}^{-1}$  in the IR spectrum of the product **54**, corresponding to the characteristic azide stretch. The product was also confirmed by MS [Scheme 14].

The next step required the selective protection of the two secondary alcohols in **54** to leave the primary alcohol ready for etherification. The choice of protecting groups

---

\*The primary alcohol should be less sterically hindered than the carbamate; the  $pK_a$  of a primary alcohol is estimated around 16 while that for a carbamate *NH* is estimated around 12.

should allow easy deprotection and because we would already have an acetal in the threitol fragment, another acetal or ketal would conveniently minimise the number of deprotection steps and therefore seemed to be a sensible first choice.

The selective protection of 1,2-diols when 1,3-diol protection is also possible, as in our case, is usually achieved by employing a ketal protecting group, commonly an acetonide. Selective protection is possible because of the relative thermodynamic stability of the possible ring products. Acetal and ketal formation is a reversible process that can lead to high levels of selectivity in favour of the thermodynamic product. Protection of a 1,3-diol with an acetal generates a six-membered ring dioxane product. In this case, acetals derived from aldehydes such as benzylidenes are more thermodynamically stable than the corresponding 1,2-diol acetals, which generate a five-membered dioxolane ring, because the acetal substituent can be placed in an equatorial position in the six-membered ring thereby minimising 1,3-diaxial interactions. When the protection is performed with a ketone, however, the resulting five-membered ring ketal is more stable because the 1,3-*trans* diaxial interactions present in the six-membered ring products resulting from 1,3-diols, are destabilising.

When we attempted to selectively protect the 1,2-diol in triol **54** in acetone containing a sub-stoichiometric amount (10 mol%) of pTSA, we obtained a mixture of products. <sup>1</sup>H NMR analysis revealed that the desired 1,3-dioxolane was the major compound in a ratio of 4:1 with the minor 1,3-dioxane product as evidenced in the <sup>13</sup>C NMR spectrum showing a CH<sub>2</sub> peak at 25 ppm corresponding to the two methyl

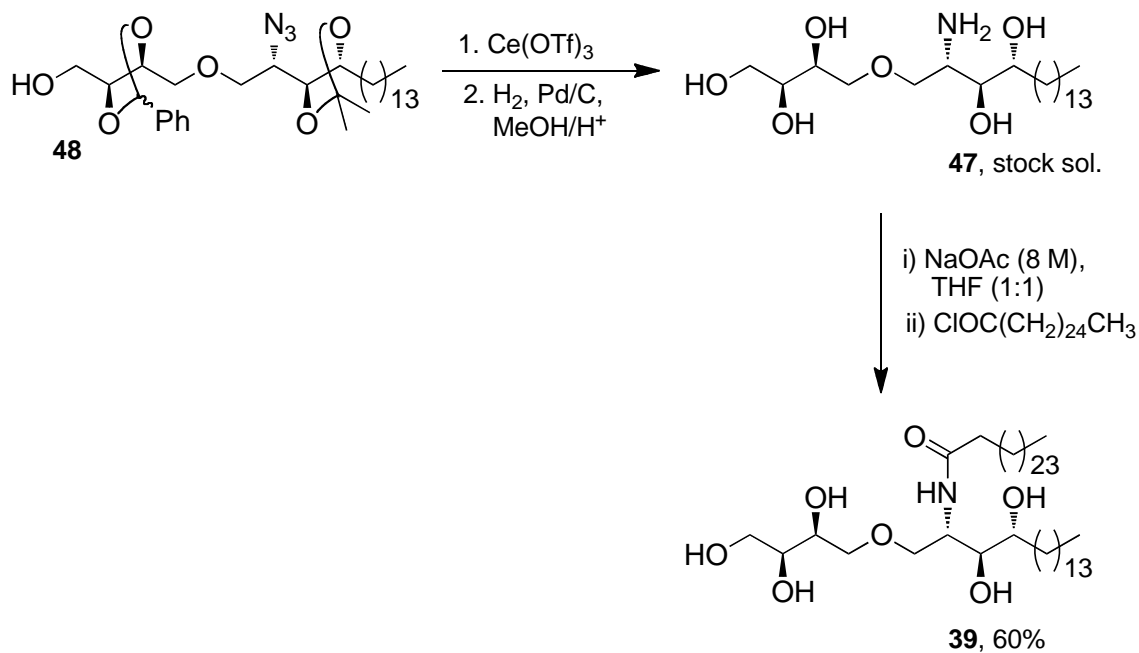
substituents of the ring. The purification of the desired major product from this mixture was achieved by column chromatography only on small scale (100 mg).

An improved and scalable method was to treat the triol with sub-stoichiometric amounts (5 mol%) of Sc(OTf)<sub>3</sub> in a 1:1 mixture of acetone/2,2-dimethoxypropane [Scheme 14].<sup>[67]</sup> This method afforded a mixture of acetals **55** and **56**. Pure **56** was then obtained by selectively hydrolysing the more labile acyclic acetal in **55** under mild acidic conditions. The desired protection pattern in the product **56** was confirmed by analysis of the <sup>13</sup>C NMR spectrum that showed the isopropylidene methyl groups as two resonances at 25.5 ppm and 28.0 ppm, which is characteristic of a five-membered ring isopropylidene protected anti-1,2-diol [Scheme 14].

With the two suitably protected reacting partners in hand, the etherification proceeded smoothly on treating the sodium alkoxide **50** with triflate **49** at 0 °C in line with the Schmidt synthesis [Scheme 15].<sup>[51]</sup> The product **46** was confirmed by obtaining accurate mass spectral and spectroscopic data, which provided evidence for the benzylidene acetal showing two singlets in the <sup>1</sup>H NMR spectrum at 5.95 and 6.00 ppm, and in the <sup>13</sup>C NMR spectrum two resonances at 25.6 and 25.7 ppm plus another two at 28.1 and 28.2 ppm, corresponding to the two methyl groups of the isopropylidene 1,2-diol protecting group. The ether **46** was then desilylated using TBAF as a fluoride source [Scheme 15]. The resulting alcohol **48** is an important intermediate that can be used, for example, as a suitably protected acceptor in future studies where ThrCer may need to be glycosylated. The alcohol **48** was confirmed



## Synthesis of Threitol Ceramide and Labelled Analogues



**Scheme 16.** Synthesis of ThrCer from fully deprotected amine **39**.

The hydrogenolysis of the crude azido-pentaol resulting from the acetal hydrolysis using Pd/C in acidic MeOH was monitored by TLC. The reaction progressed over four hours by which time TLC analysis showed that all the starting azide had been consumed [Scheme 16]. After filtering off the charcoal and evaporating the volatiles under reduced pressure, a solution of the crude amine **47** was prepared in THF (0.1 M, based on starting azide **48** and assuming 100% conversion for the deprotection sequence) and used in the next step without purification.

Acyl chlorides are commonly prepared by reacting the corresponding carboxylic acid with an excess of oxalyl chloride in  $\text{CH}_2\text{Cl}_2$  at  $0^\circ\text{C}$  employing DMF as a nucleophilic catalyst.<sup>[69, 70]</sup> However, we had in mind to transfer this methodology to the synthesis of  $^{14}\text{C}$ -labelled ThrCer and were doubtful this approach, which introduces DMF, would be amenable to the very small scales that we would be employing for the synthesis of

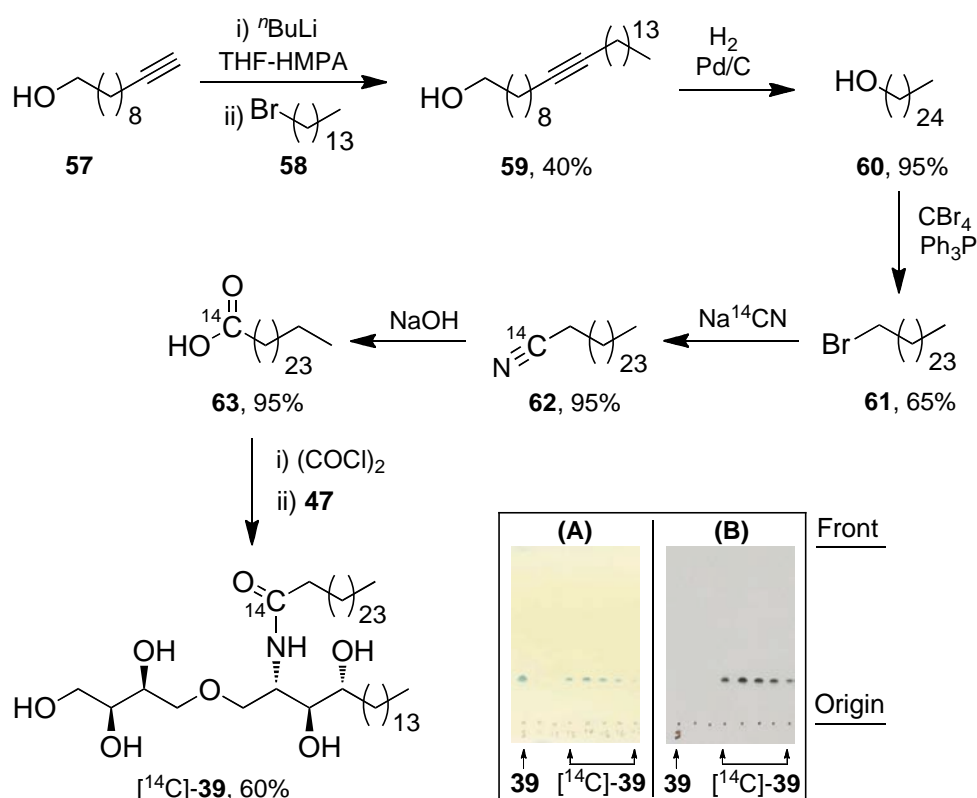
<sup>14</sup>C-labelled ThrCer. We, therefore, adopted what we considered would be a more reliable methodology in which cerotic acid was heated in a solution of oxalyl chloride at 70 °C for two hours after which time the reaction mixture was brought to r. t. and the volatiles were evaporated under reduced pressure to provide the acyl chloride which was used immediately in the amidation reaction with amine **47**. In this way the target ThrCer **39** was obtained in good yield after purification by silica gel chromatography [Scheme 16]. The product **39** was confirmed by HRMS. Key spectroscopic signals included the amide carbonyl stretch in the IR spectrum at 1634 cm<sup>-1</sup> and in the <sup>1</sup>H NMR spectrum the N-H resonance was observed as a multiplet ranging from 6.93 to 6.96 ppm.

This synthesis route provided ThrCer in 10 steps from commercially available material. The material was supplied to our collaborators (Prof. V. Cerundolo's research group at Oxford University) to use in immunological assays. Importantly for us, the synthesis gave us invaluable experience with coupling amine **47** with the acid chloride of cerotic acid which we hoped would be directly transferable to synthesis of <sup>14</sup>C-labelled ThrCer.

### 3.2. Synthesis Of $^{14}\text{C}$ -Labelled Threitol Ceramide.

We next turned our attention to a radiolabelled analogue of ThrCer **39**. Mindful of the need to minimise any manipulations involving radioactive compounds, we chose to incorporate a  $^{14}\text{C}$  label into the fatty acid, which would be introduced at a late stage in the synthesis. Moreover, in our synthesis of non-radiolabelled ThrCer **39** [Scheme 16], we had already shown that the acylation of amine **47** could be performed in excellent yield even on the small scales that we would be employing in the synthesis of its radiolabelled analogue.  $\text{Na}^{14}\text{CN}$  was identified as a convenient source of  $^{14}\text{C}$ ; thus, we envisaged nucleophilic displacement of a suitable alkyl halide would provide a straightforward method for generating an alkyl nitrile and hence the carboxylic acid upon hydrolysis.

## Synthesis of Threitol Ceramide and Labelled Analogues



**Scheme 17.** Synthesis of  $^{14}\text{C}$ -labelled ThrCer. (A) TLC of **39** and **[ $^{14}\text{C}$ ]-39** developed with phosphomolybdic acid stain. (B) Radiogram of (A) before it was stained.

The required  $\text{C}_{25}$ -chain alkyl halide **61** was assembled by coupling undecynol **57** with alkyl bromide **58** [Scheme 17]. Use of two equivalents of base to deprotonate both the alcohol and terminal alkyne in **57**, and HMPA as the solvent in the nucleophilic substitution, allowed the reaction to proceed without protection of the primary alcohol. The product **59** was confirmed by HRMS and in the  $^{13}\text{C}$  NMR spectrum the two quaternary resonances corresponding to the internal alkyne were observed at 80.2 and 80.3 ppm. Subsequent hydrogenation of the alkyne in the substitution product **59** provided alcohol **60**, which was transformed into bromide **61** by treatment with  $\text{CBr}_4/\text{PPh}_3$ . One-carbon homologation proceeded efficiently on heating a solution of bromide **61** with  $\text{Na}^{14}\text{CN}$  in DMSO at  $85\text{ }^\circ\text{C}$  to provide nitrile **62**. Finally, base-

mediated hydrolysis of nitrile provided  $^{14}\text{C}$ -labelled acid **63** in quantitative yield [Scheme 17].<sup>[71]</sup> Following our established procedure for acylation, acid **63** was converted into the corresponding acid chloride, by treatment with oxalyl chloride, and then reacted with amine **47** to provide Thr[ $^{14}\text{C}$ ]Cer [ $^{14}\text{C}$ ]-**39** [Scheme 17]. All radioactive products were characterised by TLC analysis against non-radiolabelled products that were prepared separately and had been previously characterised, and by taking TLC radiograms of the TLC plates [Scheme 17].

Our approach to the synthesis of Thr[ $^{14}\text{C}$ ]Cer proved to be a very efficient process that required minimal radiolabel manipulation. We have also shown that radiogram analysis of TLCs of both, fully characterised non-radiolabelled and newly synthesised radiolabelled compounds, can be used effectively to monitor reactions involving radioactive compounds with minimal health risk. In this manner, we have synthesised 18 mg of [ $^{14}\text{C}$ ]-**39**.

Our collaborators, Prof. V. Cerundolo and co-workers at Oxford University, have used the radio-labelled ThrCer, [ $^{14}\text{C}$ ]-**39**, to establish a direct correlation between the amount of IFN $\gamma$  secreted by  $\text{NKT}$  cells and the lipid uptake of professional antigen presenting cells DCs [Figure 12]. IFN $\gamma$  ELISA was performed on the supernatant taken from 100,000 [ $^{14}\text{C}$ ]-**39** pulsed DCs cultured overnight with 50,000  $\text{NKT}$  cells. Counts per minutes, cpm, were measured for 500,000 DCs pulsed with varying concentrations of [ $^{14}\text{C}$ ]-**39** for 36 hours [Figure 12].

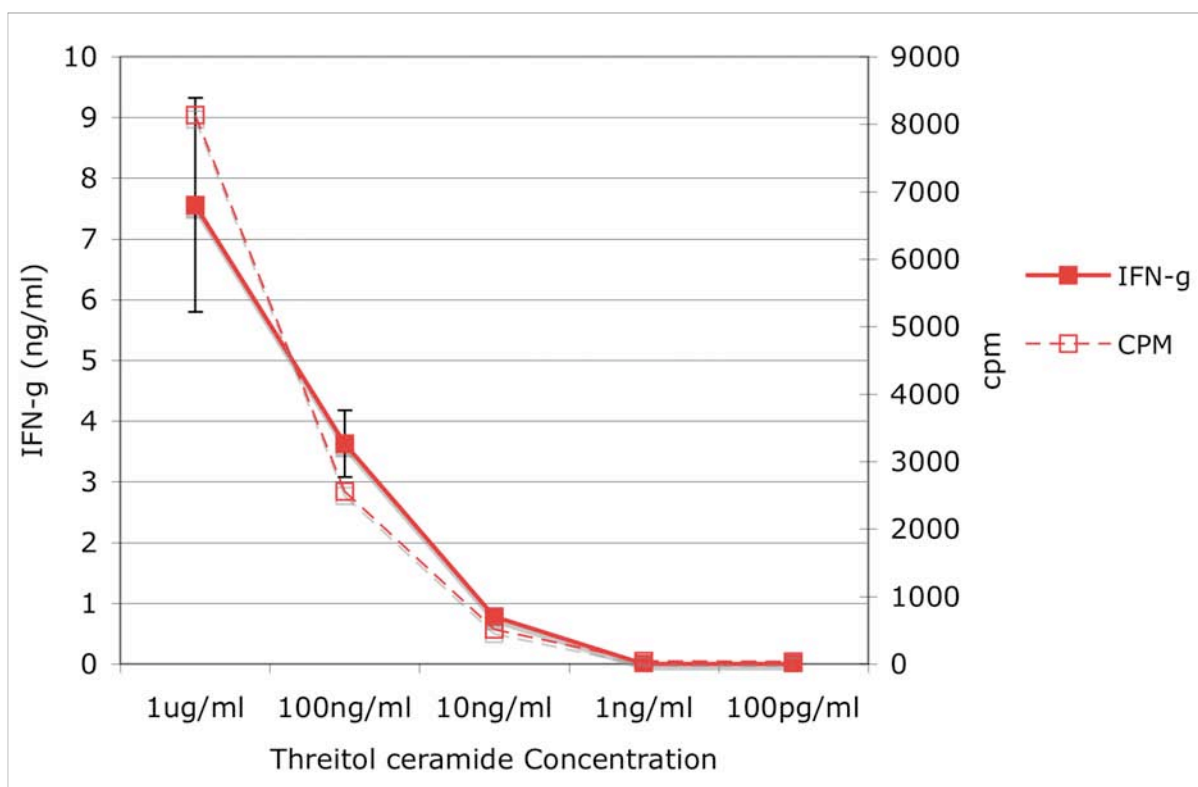


**Figure 12.** Comparison of IFN $\gamma$  assay and lipid uptake of DCs pulsed with [ $^{14}$ C]-39.

### 3.3. Synthesis Of Biotin-Labelled Threitol Ceramide.

The label of choice in this instance was biotin [Figure 13]. Streptavidin is a tetrameric protein of 5.3 kDa which has very high affinity for biotin in aqueous systems, the affinity constant is estimated to be  $K_a \sim 10^{15} \text{ M}^{-1}$ .<sup>[72-74]</sup> The protein is capable of binding one biotin ligand per monomer. Streptavidin-biotin complexes, where streptavidin has been labelled with a fluorescent tag, are easily detectable; however, the biotin moiety has to be available for binding with streptavidin to function as a label and this requires that biotin is attached via a spacer.

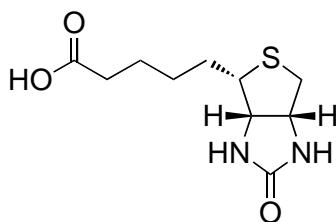


**Figure 13.** Biotin.

The fucosylation process by which fucose is incorporated into glycoproteins on the surface of neurones is suspected to play an important role in learning and memory processes in the brain. The bioconjugate **64** was used as chemical probe for imaging hippocampal neurones *in vitro* and *in vivo* which demonstrated the presence of Fuc- $\alpha$ (1-2)Gal lectins in neurones and neurites [Figure 14].<sup>[75]</sup> In this example the biotin moiety was linked to the disaccharide with a diethylene spacer. Spacing the biotin from the disaccharide can help the recognition of the biotin by streptavidin and the recognition of the disaccharide by the lectin receptors.

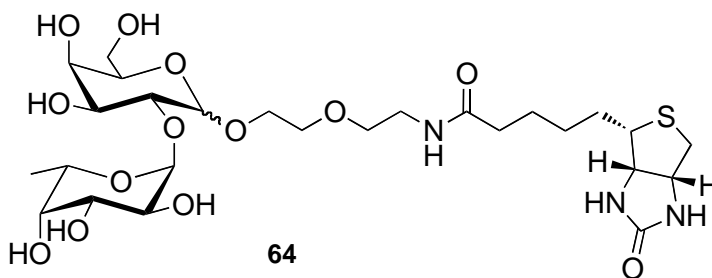
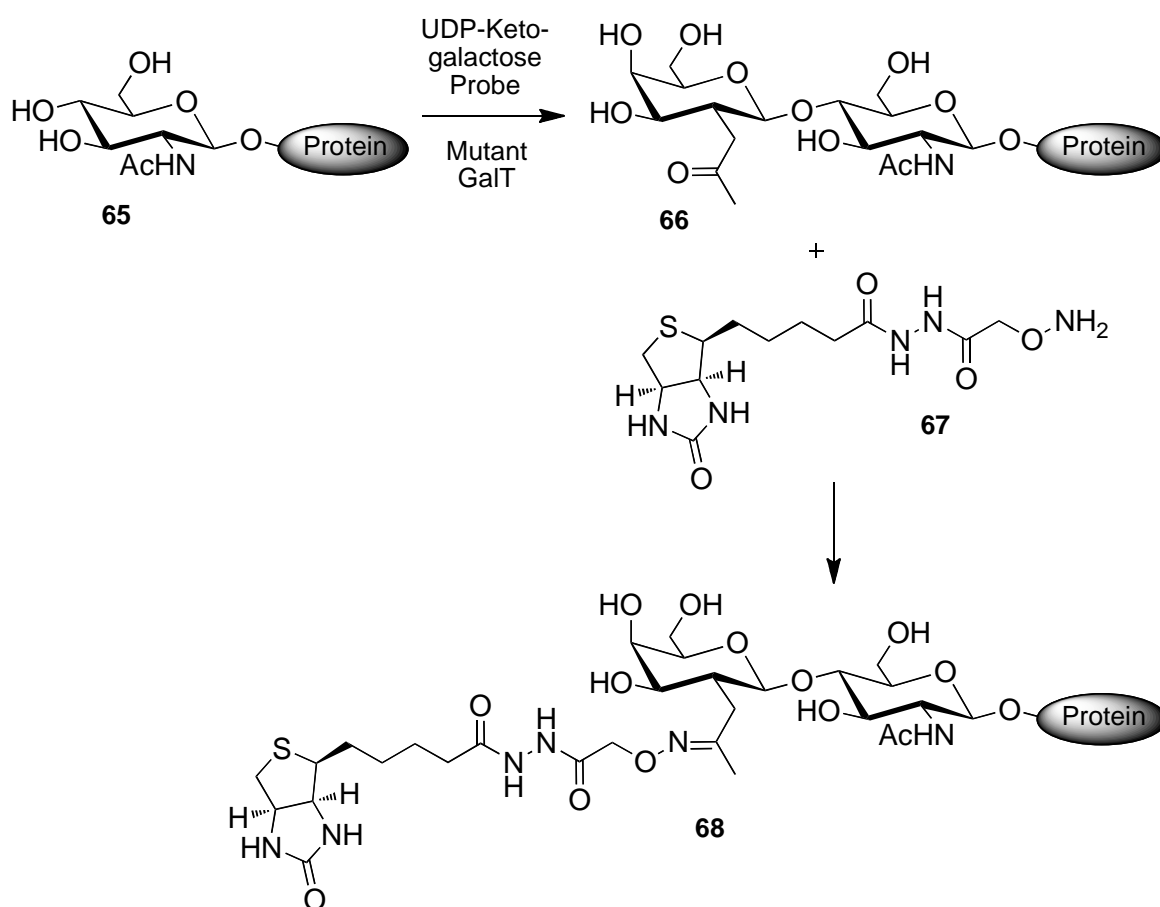


**Figure 14.** Fuc- $\alpha$ (1-2)Gal biotin bioconjugate.

Biotin tags are also used to allow rapid purification of selective species from complex mixtures by biotin-streptavidin affinity chromatography. For example, to study O-GluNAc-modified glycoproteins and their functional roles, an *in situ* chemoselective biotinylation was developed to facilitate the isolation and purification of the modified

proteins in tissue samples. Tai *et al.* effected an enzymatic modification to **65** with a galactose transferase mutant that was known to tolerate modification at C2 of galactose [Scheme 18]. The crude mixture of **66** and other glycoproteins were then treated with an excess of the highly nucleophilic biotin derivative **67** which reacted chemoselectively with the ketone **66**. The resulting bioconjugate **68** was then purified by biotin-streptavidin affinity chromatography [Scheme 18].



**Scheme 18.** *In situ* determination by biotinylation of *N*-acetylglucosamine glycoproteins.

$\alpha$ GalCer has also been labelled with biotin utilising the primary alcohol on the galactose moiety which was identified as a suitable position for elaboration [Figure 15].<sup>[76]</sup> Zhou and co-workers demonstrated that this position tolerates the introduction

of small molecules including biotin and other fluorescent probes having only a small detrimental impact on the activity of the resulting bioconjugate. Although the discovery that **69** activates *NKT* cells constituted an important finding, this information is not useful for us since we have already deleted this position in the sugar head group of our new glycolipid, ThrCer, which leaves just three alcohols for interacting with the TCR. We thought that if we attach the biotin label from one of these alcohols in a similar manner as Zhou *et al.*, we would likely disturb the interactions with the TCR and risk changing the nature of the biological response in comparison to that of the parent compound, ThrCer **39**.

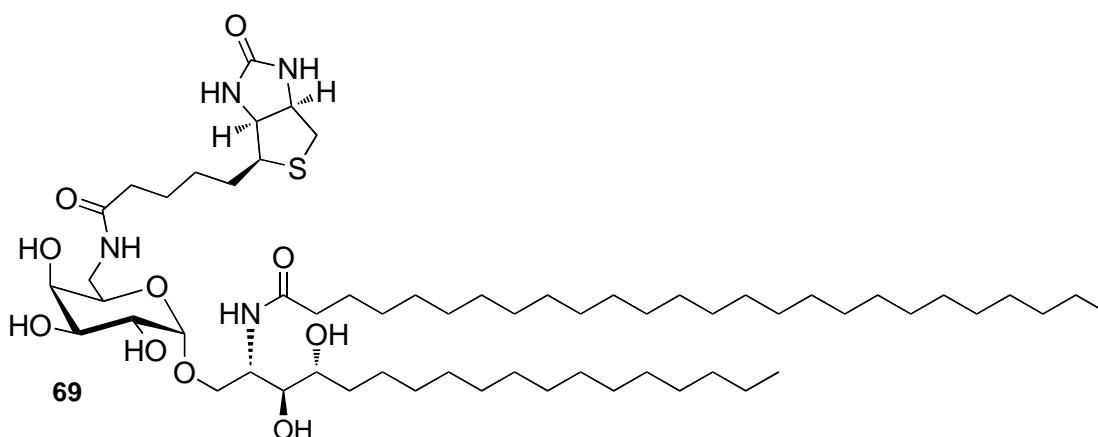


**Figure 15.**  $\alpha$ GalCer biotin bioconjugate.

The challenge for us was to identify a site in ThrCer from which the biotin moiety could be attached that would allow its recognition by streptavidin after the CD1d/ThrCer binding event. At the same time, it would also be critical for the labelled ThrCer derivative to retain an activity that resembles that of ThrCer. The location of the label would therefore be crucial for the success of this project. From a synthetic point of view we thought that late-stage installation of the label would be beneficial.

This strategy would allow us to diversify this part of the molecule which might need tuning, *i.e.* type of linkage, length of the linkage, different label. With this in mind we wanted to evaluate the possibility of installing the label on the acyl chain, although at the outset we did not know how this would impact on the biological activity of the labelled glycolipid compound.

It is synthetically convenient to introduce modifications that take advantage of existing substituents. For example, the functionalisation of alcohols, or amines, can be achieved relatively easy; moreover, these modifications do not often introduce new stereocentres which can add to the complexity of the analogues. In comparison, modifications that introduce new functionality or substituents are often harder targets to synthesise. If a new stereocentre is formed with the modification, then it is also important to consider a stereoselective synthetic approach that can give access to all the stereoisomers. Although such an approach can be more synthetically demanding, it would allow us to evaluate the stereoisomers separately in biological assays and to compare their biological activity.

With these factors in mind, we focused our attention on introducing an additional substituent which we could then elaborate and link through to the label. It was identified in the X-ray crystal structure of the CD1d- $\alpha$ GalCer complex that at least one of the alcohols in the phytosphingosine base is involved in H-bonding with CD1d and TCR residues.<sup>[29]</sup> Mindful that H-bonds between CD1d and ThrCer are important elements that hold together the quaternary structure of the protein-ligand complex, which is likely to be important for its recognition by the TCR, we turned our attention

to the acyl chain. In the X-ray crystal structure of the CD1d- $\alpha$ GalCer complex,<sup>[29]</sup> we observed that the  $\alpha$  and  $\beta$  carbons in the acyl chain are not buried in the hydrophobic pocket [Figure 16]. This led us to postulate that we might be able to install the label at one of these positions and will not affect the CD1d/lipid binding event or the recognition of the CD1d-lipid complex by the TCR as these positions are relatively distant from the alcohols that are believed to be responsible for activation (assuming ThrCer behaves analogously to  $\alpha$ GalCer). Also, aided by a hydrophilic spacer, a label linked from one of these positions should extend away from the complex and be available for recognition by streptavidin [Figure 16].

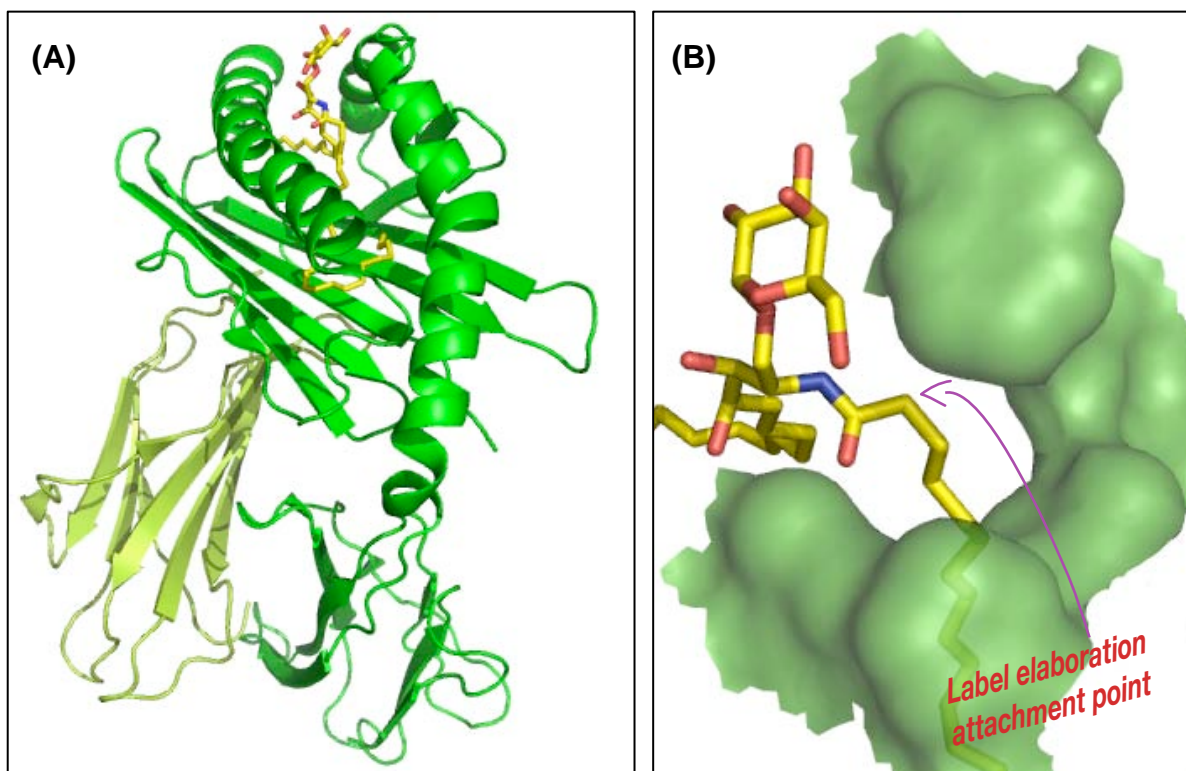


**Figure 16.** (A) Cartoon representation of X-ray crystal structure of CD1d- $\alpha$ GalCer complex. (B) Space-filled close up of X-ray crystal structure of CD1d- $\alpha$ GalCer complex showing sphingosine base burial pocket.

The nature of the substitution that we might introduce needed careful consideration. An  $\alpha$ -hydroxyl function would offer two common possibilities for elaboration, via an ester or an ether linkage. The ester, while relatively easy to make, is not always stable in biological assays as it can be easily hydrolysed by the action of esterases. An ether, on the other hand, is far less labile and usually survives biological assays *in vitro* and *in vivo*; however, it represents a more challenging bond to make at such a late stage in the synthesis. Ether syntheses usually require the preparation of an alkoxide at one of the reactive partners, and a good leaving group in the other reactive partner. While the hope in an ether synthesis is that the alkoxide behaves as a nucleophile and displaces the leaving group in the electrophile, it can also behave as base or react with a different electrophilic centres elsewhere in the molecule.

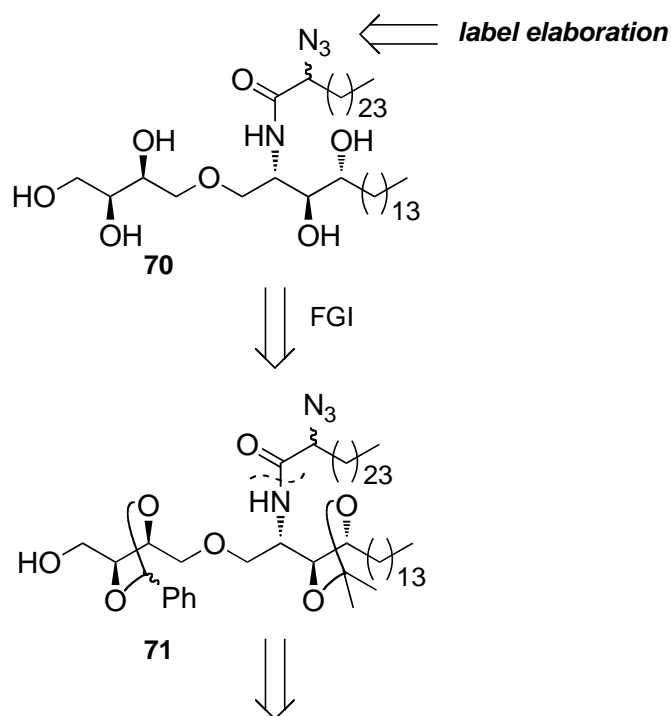
We turned our attention to introducing an  $\alpha$ -azido function next to the amide in ThrCer as this would open up a range of possible attachment strategies. An azide offers the possibility to elaborate further as a substituted amine, or through another amide bond, after reduction of the azide to the primary amine. Amines are usually very stable in biological assays; they are also good nucleophiles and as bases, are readily protonated in weakly acidic media.<sup>†</sup> Amines often participate in H-bonding interactions with the protein; they are good H-bonding donors and acceptors<sup>‡</sup> and their interactions with CD1d residues might affect the quaternary structure of CD1d which could have implications on the factors that determine the immune response. More significantly, under physiological conditions an amine would be protonated, and

---

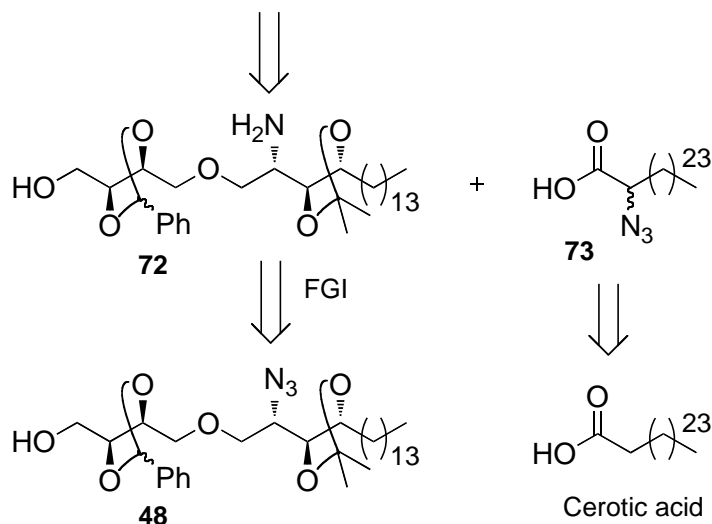
<sup>†</sup> Typical  $pK_a$ s for protonated amines range between 10 and 12 units.

<sup>‡</sup> Tertiary amines cannot participate in H-bonding as H-donors but they are good H-acceptors.

it would introduce undesirable charge in the vicinity of this hydrophobic site. For these reasons we discounted the possibility of using an amine in the linker. On the other hand, amide bonds are found commonly in biological systems and are less susceptible to non-enzymatic hydrolysis than esters. Amide bonds are also relatively easy to make and this fitted well with our strategy which leaves this bond synthesis for a late stage elaboration [Scheme 19' and 19'']. The azido functionality will provide orthogonal protection for the amide bond coupling with amine **72**. More importantly, the azido intermediate **70** can be used directly in azide-alkyne [3+2] cycloaddition reactions to provide a 1,2,3-triazole [Scheme 19' and 19'']. We, therefore, focused on the synthesis of this key intermediate **70**; the retrosynthesis is outlined below [Scheme 19' and 19''].



**Scheme 19'**. Retrosynthetic analysis of key intermediate azide **70**.

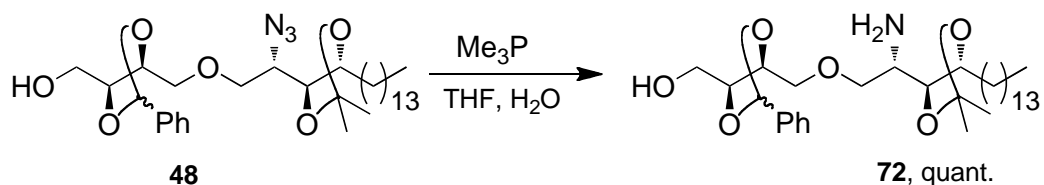


**Scheme 19''.** Retrosynthetic analysis of key intermediate azide **70**.

We have already described the synthesis of the azide **48** starting from phytosphingosine and 2,3-*O*-benzylidene-protected threitol [Scheme 15]. This time though, we focused first on the azide reduction in **48** rather than deprotecting the alcohols. Hydrogenation of alkyl azides to alkyl amines is a common and very effective method to achieve this deprotection and the crude product usually requires minimal purification; however, the reduction conditions are likely to induce hydrogenolysis of the benzylidene acetal as well, and wary of the solubility problems that are associated with amphiphilic lipids, we turned to another more selective method. The Staudinger reaction is another common method for reducing an azide to an amine. In this reaction, a phosphine, usually  $\text{Ph}_3\text{P}$ , reacts with the azide function to form an imino phosphorane with the liberation of nitrogen gas. The imino phosphorane can be broken down with water, freeing the amine and producing a phosphine oxide as a by-product. Although there are examples in the literature where the imino phosphorane is stable at room temperature in aqueous media, in which

case refluxing conditions are required to successfully free the amine, the reaction conditions are nevertheless very mild, *i.e.* chemoselective for the azide, and usually produce the amine in yields in excess of 90%.

However, the purification of the amine product can be problematic and separating it from the phosphine oxide by-product can be time-consuming and compromise the yield of the reaction. Trimethylphosphine has also been shown to efficiently reduce azides to amines.<sup>[64]</sup> This small trialkyl phosphine has the disadvantage that it is easily oxidised by air; triphenylphosphine, on the contrary, is very stable under aerobic conditions; however, trimethylphosphine oxide is a solid with a high vapour pressure and can be removed from the product mixture under reduced pressure.<sup>[77]</sup> The reduction of **48** with trimethylphosphine yielded the requisite amine **72**, which was used in the next step without purification [Scheme 20].



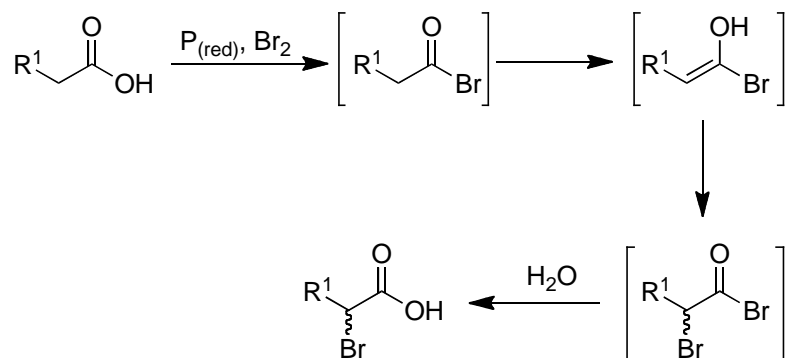
**Scheme 20.** Staudinger reduction of azide **48** provided amine **72**.

We needed to synthesise the  $\alpha$ -azido acid **73** for our next coupling reaction [Scheme 19' and 19'']. The Strecker reaction is a method in which an aldehyde is reacted with  $\text{HCN}^{\S}$  in an aqueous ammonium hydroxide solution and yields an  $\alpha$ -amino nitrile product which can be hydrolysed to the corresponding  $\alpha$ -amino carboxylic acid. This

<sup>\S</sup>  $\text{HCN}$  is generated *in situ* by the reaction of  $\text{NaCN}$  and  $\text{NH}_4\text{Cl}$ .

important reaction has received considerable attention over the years. Strecker-like reactions with imines continue to be developed and in this field we find catalytic and stereoselective processes for the synthesis of  $\alpha$ -amino nitriles; which, after nitrile hydrolysis, we can potentially convert into the desired  $\alpha$ -azido carboxylic acid by an azido transfer reaction in a similar manner to that described for the synthesis of **52**. However, this approach to our  $\alpha$ -azido acid target requires several additional steps and add a considerable amount of labour and expense to the synthesis.

Although we considered preparing the desired  $\alpha$ -azido carboxylic acid in an enantioselective fashion, it was more convenient in the first instance, to synthesise  $\alpha$ -azido acid as a racemate although this consequently means that the target product will be obtained as a mixture of diastereoisomers. Moreover, we have no way of knowing in advance how the biology of these two target diastereoisomers will differ from each other. After a discussion with our collaborators, we agreed to provide the target biotin-labelled compound as a mixture of diastereoisomers in the first instance. Taking this into account and mindful of the tendency of cerotic acid derivatives to present us with solubility problems, we turned our attention to the Hell-Volhard-Zelinsky reaction [Scheme 21].<sup>[78-80]</sup>



**Scheme 21.** Proposed mechanism for the Hell-Volhard-Zelinsky reaction.

Studies into the mechanism of this reaction suggest that the reaction proceeds via the haloenol which reacts with a bromonium ion source in the reaction mixture;<sup>[81, 82]</sup> the most common source of bromonium ion is  $\text{Br}_2$  but NBS can also be employed. The resulting  $\alpha$ -bromo acid bromide can then be converted into the corresponding  $\alpha$ -bromo carboxylic acid by hydrolysis of the intermediate acid bromide.

The Hell-Volhard-Zelinsky procedure gave us the requisite  $\alpha$ -bromo cerotic acid **74** [Scheme 22].<sup>[83, 84]</sup> The product was recrystallised from hexanes and used without further purification in the following step. With this compound in hand, our attention turned to the displacement reaction. We found a few examples of  $\alpha$ -bromo carbonyl displacement reactions by an azido nucleophile although no examples where this carbonyl is a free carboxylic acid. We were aware that we could convert the carboxylic acid to the corresponding methyl ester and effect the  $\alpha$ -bromo displacement in line with previous literature work but we were more interested in exploring the possibility of performing the displacement on the free carboxylic acid. We had in mind to minimise the need for aqueous work-up and silica column

purification because in our experience of working with this class of long chain fatty acids, an aqueous work-up complicates the extraction and purification steps due to very low solubility of the products and their tendency to form emulsions.

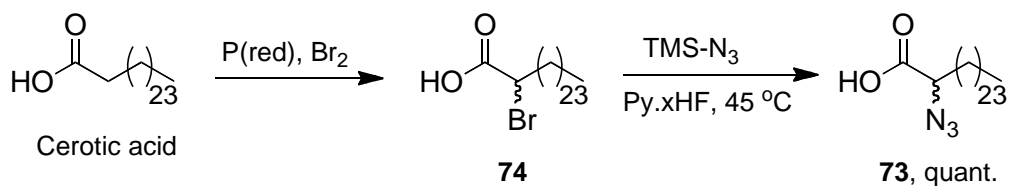
We thought that to succeed in displacing the  $\alpha$ -bromide without protecting the carboxylic acid we needed to compare the nucleophile's  $pK_a$  with that for the carboxylic acid. All nucleophiles can behave as bases and our fears were that if the free carboxylic acid is deprotonated under the reaction conditions by the nucleophile, it will not only render the nucleophile less nucleophilic, but the  $\alpha$ -bromo carboxylate is also a worse electrophile. The  $pK_a$  of hydrazoic acid has been measured at 4.6 in water.<sup>[85]</sup> The  $pK_a$  of a carboxylic acid is also around 5 which led us to think that in a reaction mixture there might be an acid-base equilibrium of the azide salt and the carboxylic acid with hydrazoic acid and the carboxylate from which the reaction might proceed. Initially we explored employing  $\text{NaN}_3$  as a nucleophilic source of azide in DMF to displace the bromide. In spite of following literature precedent for this transformation<sup>[86, 87]</sup> the reaction did not proceed to products and only the starting bromide was recovered after heating the reaction mixture to 70 °C for twelve hours. We then considered  $\text{TMSN}_3$  as the source of nucleophilic azide. As a notable advantage, the reaction could be performed in low boiling point solvents such as THF or  $\text{CH}_2\text{Cl}_2$  and the by-products, as well as the excess of the reagent, are also likely to be volatile for easier work-up.

The reaction of  $\text{TMSN}_3$  with  $\alpha$ -bromo cerotic acid in THF did not yield products at r.t. nor at 70 °C, even when an excess of reagent was employed and the mixture was

stirred for a week at 70 °C. The reaction was monitored by mass spectrometric analysis of the crude mixture. We postulated that the reaction needed activation of the TMSN<sub>3</sub>. Cesium fluoride can act as a fluoride source and in combination with TMSN<sub>3</sub> would catalyse the bromide displacement.<sup>[88, 89]</sup> The fluoride anion has a high affinity silicon forming one of the strongest covalent single bonds known;<sup>[90]</sup> the Si-F bond energy averages at 582 kJ mol<sup>-1</sup>. We were pleased to see the formation of the desired product **73** when one equivalent of CsF was employed in the reaction but even after three days and with an excess of CsF, the reaction did not go to completion. As the product **73** and starting bromide were inseparable on silica, we chose to develop the reaction further to ensure complete consumption of starting material which would facilitate purification.

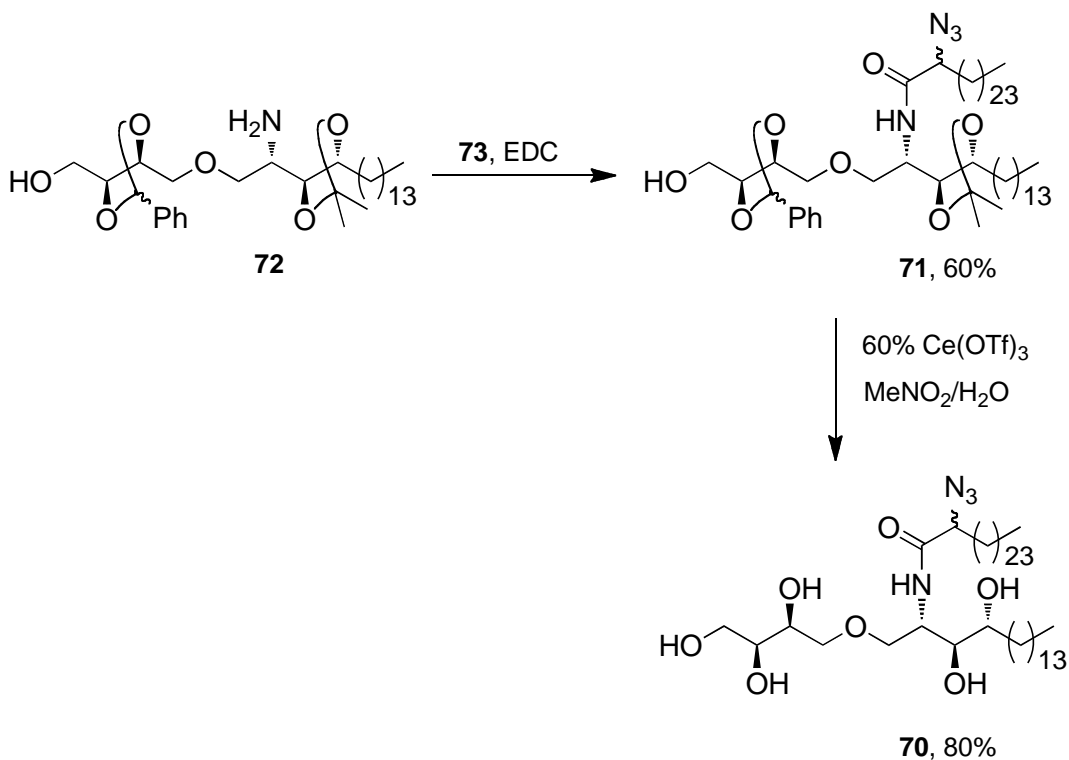
We thought that the low solubility of the CsF salt in THF was the cause of our problems. HF, another mild source of fluoride, can also be employed for targeting silyl groups, which in this case would encourage the formation of HN<sub>3</sub> *in situ* that we hoped would act as a mild source of nucleophilic azide. Using the Py.xHF complex in place of CsF over twelve hours in THF at 45 °C, we now saw complete conversion of the starting material to the desired azide product **73** when 1.5 of equivalents Py.xHF (70 wt. % in pyridine) were employed as the promoter [Scheme 22]. This was a satisfying result because no aqueous work up was required and the product was isolated by simple evaporation of the volatiles. Electrospray mass spectral analysis showed only one peak corresponding to the product and TLC analysis showed only traces of impurities. This material was used in the next step without further purification.

Synthesis of Threitol Ceramide and Labelled Analogues



**Scheme 22.** Synthesis of the requisite  $\alpha$ -azido cerotic acid.

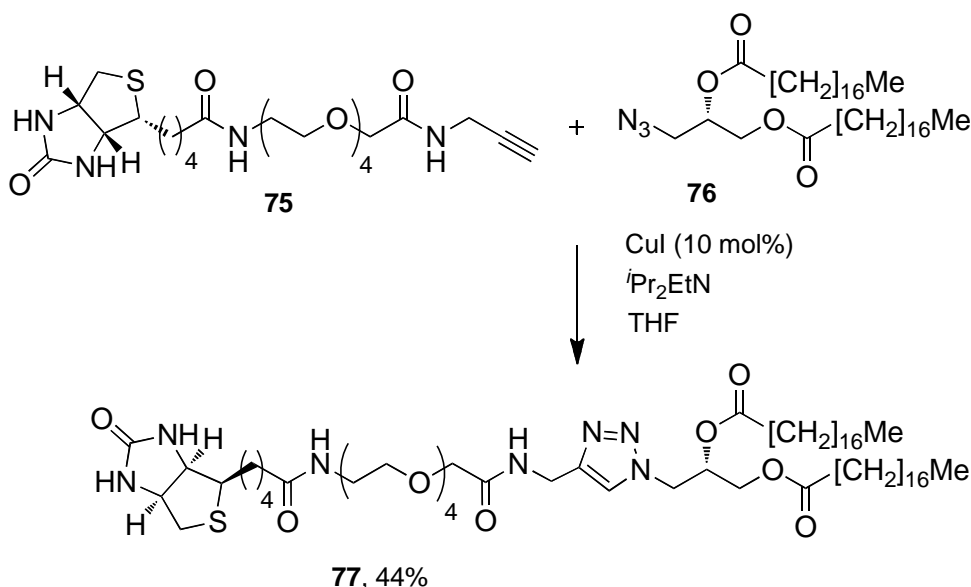
We were encouraged by this result and with the  $\alpha$ -azido carboxylic acid in hand we focused on the coupling reaction ahead. Activation of the carboxylic acid **73** was achieved *in situ* with EDC, and reaction proceeded with excellent chemoselectivity for the amine over the alcohols, providing amide **71** as a 1:1:1:1 mixture of four diastereoisomers [Scheme 23]. The global deprotection of the acetal and ketal in **71** was achieved in one step employing 60%  $\text{Ce}(\text{OTf})_3$  as Lewis acid and provided our target **70** as a 1:1 mixture of two diastereoisomers [Scheme 23].



**Scheme 23.** Synthesis of key azido intermediate **70**.

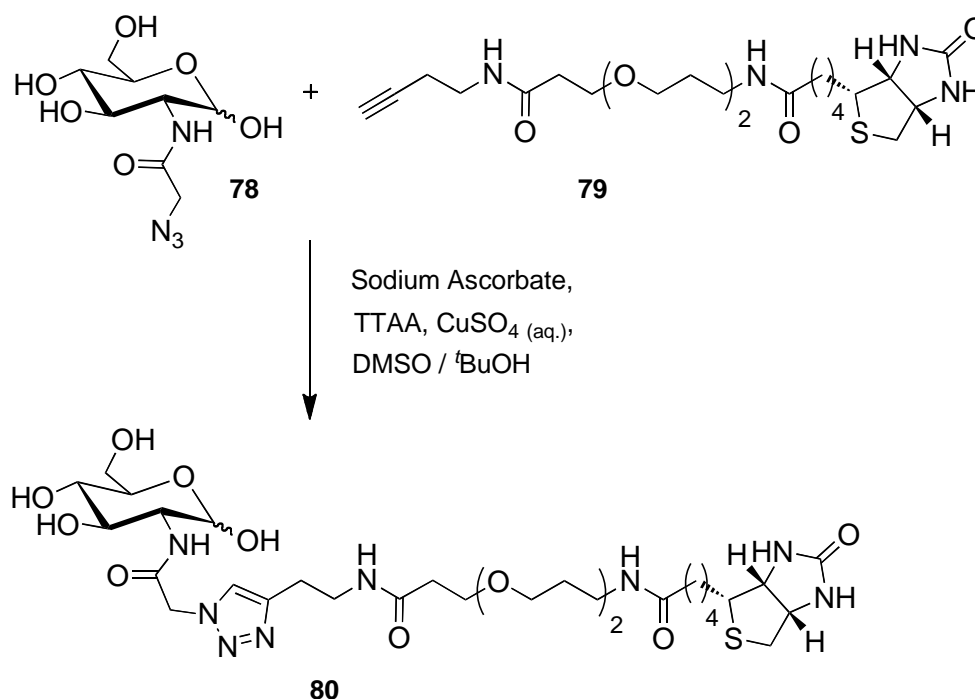
At this stage we had successfully synthesised key azido-intermediate **70**. In our retrosynthetic analysis of **70** we discussed the possibilities that an  $\alpha$ -azido substituent offers for further elaboration. We chose to proceed, in the first instance, with the [2+3] copper-catalysed cycloaddition of the azide **70** with a terminal alkyne to incorporate the label.

1,2,3-Triazole derivatives have been used successfully in biotinylation reactions. For example, in a high-throughput study of protein-membrane interactions Losey *et al.* coupled the diacylglycerol azide derivative **76** with biotin alkyne derivative **75** in the presence of catalytic amount of CuI to yield the biotin conjugate **77** in moderate yield [Scheme 24].<sup>[91]</sup> Under these conditions and in an organic solvent like THF, the Cu(I)-catalysed alkyne-azide cycloaddition required an amine base like Hünig's base to deprotonate the alkyne after complexation with the Cu(I) ion to facilitate the formation of the Cu-acetylide which has been shown to be the first step of the catalytic cycle.<sup>[92]</sup>



**Scheme 24.** [3+2] Cycloaddition biotinylation using CuI as catalyst.

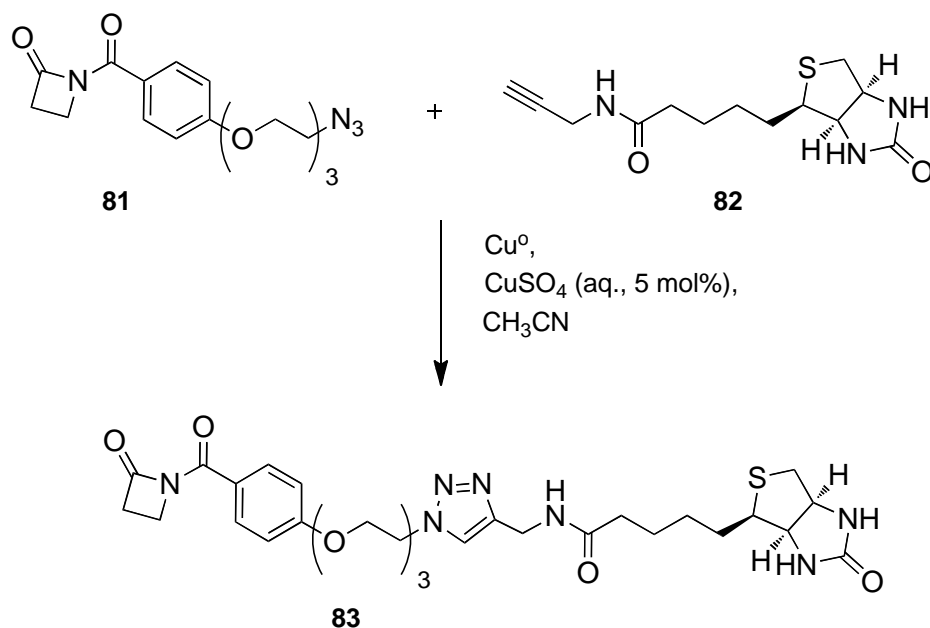
In another example, the biotin alkyne derivative **79** was coupled with a fully deprotected *N*-acetyl-D-glucosamine azide derivative **78** that afforded the glycoconjugate **80** [Scheme 25].<sup>[93]</sup> The reaction conditions employed sodium ascorbate as reductant for reducing Cu(II) to Cu(I) *in situ* and tris(triazolyl)amine as a ligand for copper. These conditions are advantageous in that the prone-to-oxidation Cu(I) ions required in the reaction are generated *in situ* in small amounts and that it was observed that this ligand accelerated the reaction.<sup>[94]</sup>



**Scheme 25.** Cu<sup>II</sup> salts can be employed as pre-catalysts.

In a modelling study of chemical programming of monoclonal aldolase antibody, the  $\beta$ -lactam **81** was conjugated to the biotin moiety **82** by click chemistry ligation employing copper wire as catalyst in acetonitrile [Scheme 26].<sup>[95]</sup> In this process the copper metal is oxidised to Cu(I) by oxygen (perhaps the CuSO<sub>4</sub> can also behave as an oxidant getting reduced to Cu(I) to a small extent).<sup>[96, 97]</sup>

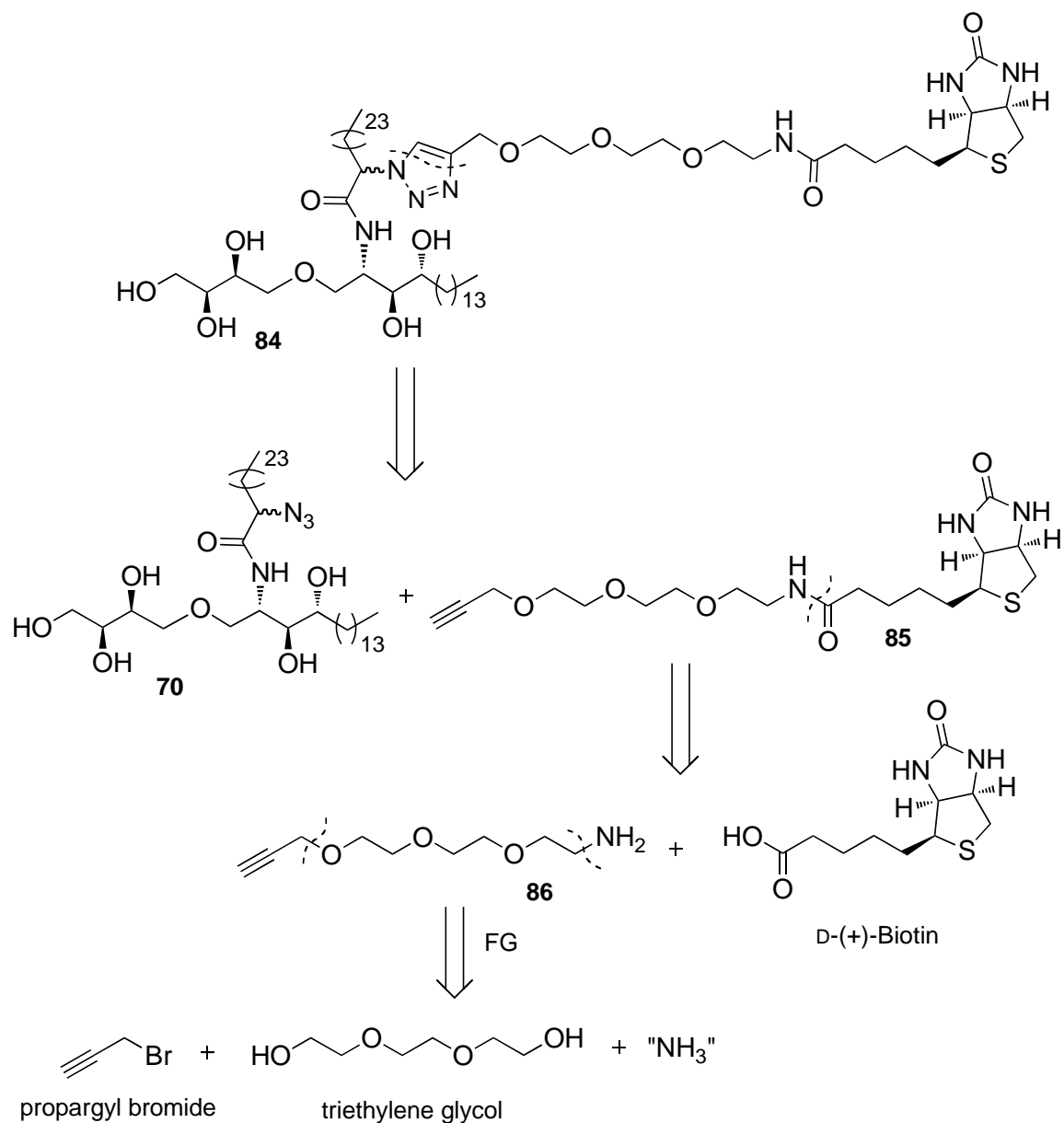
## Synthesis of Threitol Ceramide and Labelled Analogues



**Scheme 26.** Copper metal can also serve as pre-catalyst.

This strategy is attractive, not only because of the shorter synthesis, but also because it is more convergent which has the potential for a higher yielding synthesis. Polyethylene glycol, PEG, linkers are commercially available in different lengths and are biocompatible. They are also soluble in a range of solvents including water. A PEG spacer should improve the hydrophilicity of the label making it available for recognition in aqueous assays. With the position to attach the label identified we developed a retrosynthetic strategy for assembling the labelled ThrCer target **84** [Scheme 27].

## Synthesis of Threitol Ceramide and Labelled Analogues



**Scheme 27.** Retrosynthetic analysis of biotin-ThrCer **84**.

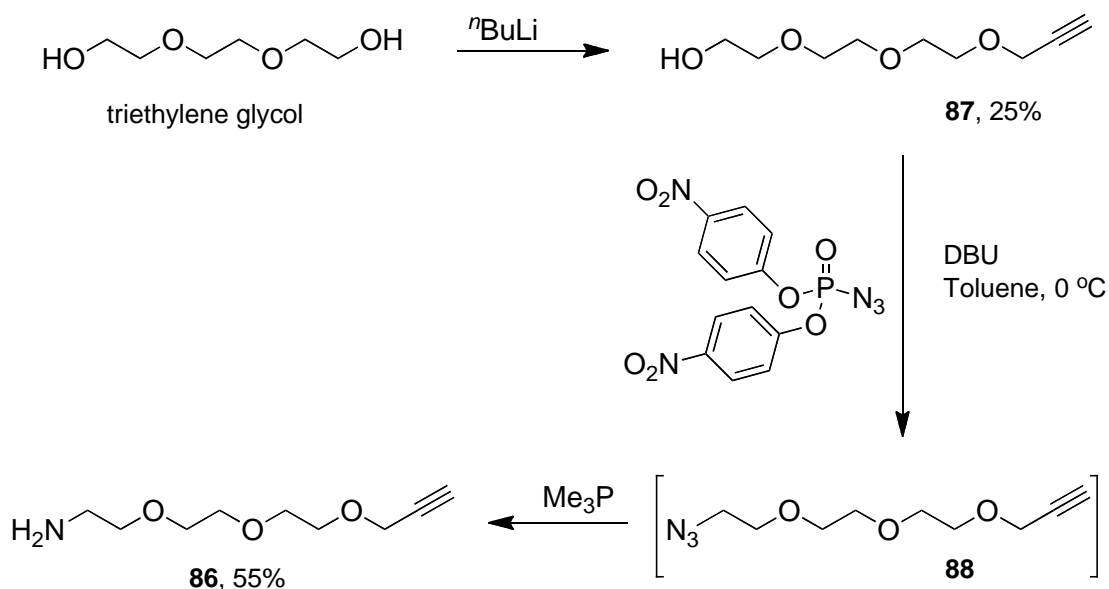
The biotin moiety is normally linked to a substrate by way of an amide bond, taking advantage of the carboxylic acid already present in the molecule; however, cleavage of this amide bond by the endogenous enzyme biotinidase can be a problem in biological and whole-cell assays. Structural modifications of biotin can enhance the stability of this amide bond, but these often result in a decrease in streptavidin

affinity. A compromise between stability and affinity is generally reached by introducing a small (but larger than methyl, for example ethyl)  $\alpha$ -amide substituent.<sup>[98]</sup> We decided not to make any of these modifications to the biotinamide moiety as this topic is still being developed in the literature and we wanted to take full advantage of the biotinamide-streptavidin complex having one of the largest non-covalent affinities known in water ( $K_a \sim 2.5 \cdot 10^{15} \text{ M}^{-1}$ ), which would maximise the chances of the label being detected while bound to our ThrCer substrate.

We started the synthesis of the alkyne **85** by mono-alkylating triethylene glycol [Scheme 28]. Alkyne **87** was prepared employing one equivalent of *n*BuLi in THF at 0 °C for one hour to provide the corresponding lithium alkoxide followed by dropwise addition of propargyl bromide at this temperature. After work up, the desired alkyne product was obtained in 25% yield. A small amount of dialkylated product was also formed. Although the starting material was conveniently washed away in the aqueous phase, TLC analysis indicated that a considerable amount of unreacted starting material accounted for the remaining mass balance. The alkoxide was also prepared using NaH (in DMF and in THF) and, KH (in THF); however, the method employing the lithium alkoxide afforded the best yields [Scheme 28].

Azidation of **87** was achieved in good yield by converting the alcohol into a leaving group *in situ* with bis(*p*-nitrophenyl)-phosphoryl azide, BNPPA. which was readily prepared by nitration of commercially available diphenylphosphoryl azide, DPPA. The reagent DPPA can be used in combination with DBU for the conversion of allylic alcohols into allylic azides.<sup>[99]</sup> However, this phosphoryl reagent is not sufficiently

electrophilic to react in the same way with simple alkyl alcohols. Fortunately it has been demonstrated that nitration of DPPA affords BNPPA, which smoothly reacts with alkyl alcohols to provide the corresponding alkyl azide in one step.<sup>[100]</sup> Undoubtedly it is the presence of the two powerful electron-withdrawing nitro groups, which increases considerably the electrophilicity of this phosphoryl azide. In the preparation of BNPPA, the product can be isolated from the reaction mixture by simple recrystallisation and can be stored (-20 °C) which make this reagent amenable to use.



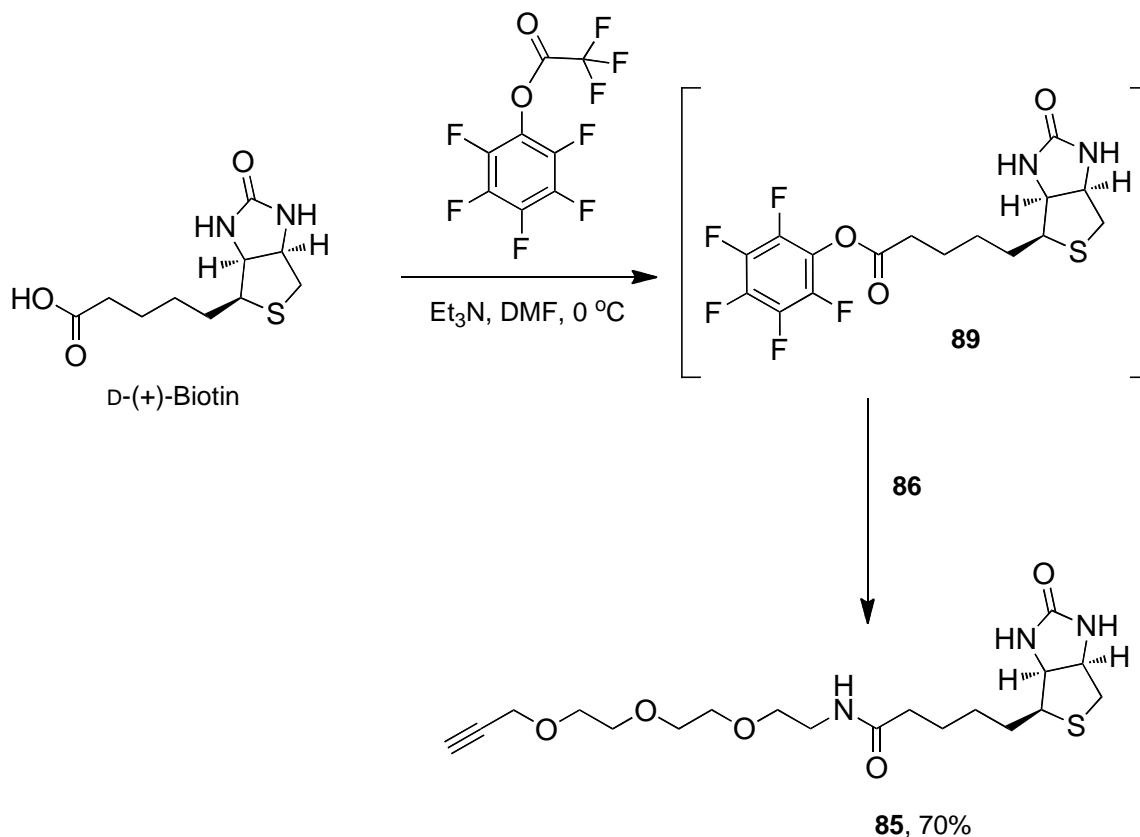
**Scheme 28.** Synthesis of the requisite amine **86**.

A mixture of 1.1 equivalents of BNPPA and the alcohol substrate **87** in toluene was treated at 0 °C with 1.1 equivalents of DBU and rapidly stirred for twelve hours [Scheme 28]. After this time, TLC analysis showed that the reaction was complete as evidenced by the disappearance of the starting alcohol and the formation of a higher running new spot. The work-up proved to be highly problematic as *p*-nitrophenoxide appeared to be generated from the by-product salt. Several base washes with a

saturated solution of  $\text{NaHCO}_3$  failed to separate the phenol from the organic extracts. A portion of the solution was also washed with  $\text{Na}_2\text{CO}_3$  solution, which appeared to wash away all of the *p*-nitrophenol in the first instance, but when the organic phase was concentrated, more coloured material was generated, implying the continued presence of *p*-nitrophenol. In spite of this, the organic fraction was concentrated under reduced pressure and the residue was submitted to column chromatography affording the desired azide **88**, which was still contaminated with approximately 5% of *p*-nitrophenol. Azide **88** was reduced to the corresponding amine with trimethylphosphine in THF. After complete consumption of the starting material, the volatiles were evaporated under high vacuum. The crude amine **86** was washed with 1.0 M HCl solution and the resulting ammonium salt was then back-extracted with  $\text{CH}_2\text{Cl}_2$  after neutralising the aqueous phase with a 2.0 M NaOH solution.

In the following step we coupled D-(+)-biotin with amine **86** [Scheme 29]. D-(+)-Biotin is insoluble in most organic solvents, which complicated this step. Carbodiimide activation of biotin is generally performed at high temperature to overcome the poor solubility of the carboxylic acid and these methods usually employ nucleophilic catalysts, such as *N*-hydroxybenzotriazole, HOBt, which is commonly used in peptide coupling reactions. We wanted to steer away from these methods, wary that our amide product would be soluble in water and difficult to extract from the aqueous phase in the work-up step. It is possible to obtain commercially the *N*-hydroxysuccinimide, NHS, biotin ester, which reacts readily with amines to afford the corresponding biotin amides in high yields; however, this activated ester is relatively expensive. Another activated ester capable of reacting with amines is the

pentafluorophenyl ester, PFP,<sup>[101, 102]</sup> which is readily prepared *in situ* from the free carboxylic acid and we elected to investigate this reagent for our amidation.<sup>[103]</sup>

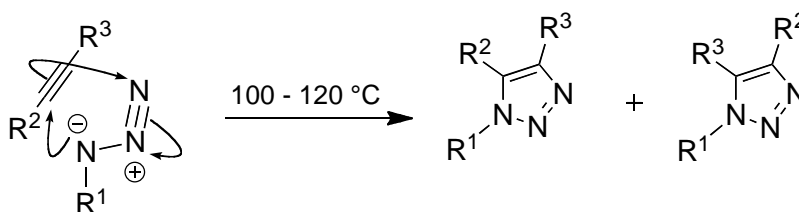


**Scheme 29.** Synthesis of the requisite alkyne **85**.

Pentafluorophenol trifluoroacetate was synthesised in one step by treatment of pentafluorophenol with TFAA in the absence of solvent at r.t. for twelve hours and then purified by distillation. D-(+)-Biotin was then suspended in DMF (0.1 M) and treated with three equivalents of  $\text{Et}_3\text{N}$  at  $0\text{ }^\circ\text{C}$  and stirred at this temperature until the solution became clear (20 minutes). After this time, one equivalent of pentafluorophenol trifluoroacetate was added dropwise at  $0\text{ }^\circ\text{C}$ . The mixture turned pink. The resulting solution was stirred for four hours after which time a white solid had precipitated and TLC showed a complete consumption of the starting acid and

the formation of ester **89** [Scheme 29]. The amine **86** was added at this point as a solution in DMF at 0 °C. TLC analysis showed that the reaction proceeded rapidly. After four hours the DMF and pentafluorophenol were evaporated under reduced pressure. The residue was purified by column chromatography (CHCl<sub>3</sub> / MeOH, 9:1) to afford 70% of the desired product plus 20% of the biotin pentafluorophenyl ester [Scheme 29]. At this stage we had both requisite fragments for the key click chemistry coupling reaction.

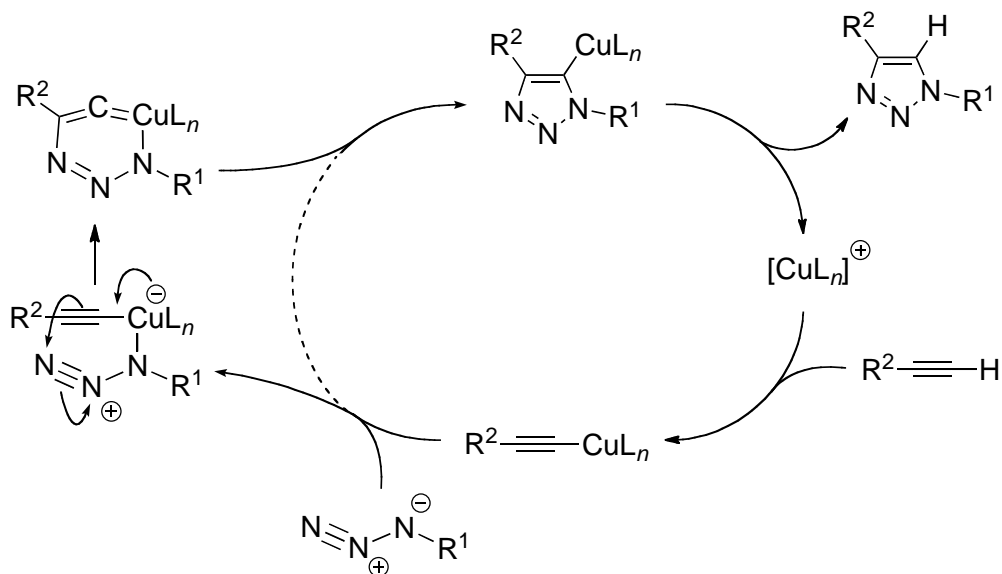
The azide-alkyne [3+2] cycloaddition reaction was first studied by Huisgen in the 1980s under thermal conditions, along with other 1,3-cycloaddition reactions.<sup>[104]</sup> Under thermal conditions, the alkyl azide only reacts with electron-deficient alkynes, and only at elevated temperature; moreover, the products are generally produced as a 1:1 mixture of regioisomers [Scheme 30].



**Scheme 30.** Azide-alkyne [3+2] cycloaddition under thermal conditions.

In the 1990s, various efforts to control the regioselectivity were published that widened the scope of this reaction;<sup>[105-107]</sup> however, it was not until 2002 that a reliable, mild and regioselective method was found. This was described, in two almost simultaneous reports by Tornøe *et al.*<sup>[108]</sup> and Rostovtsev *et al.*<sup>[109]</sup> These groups showed that Cu(I) ions effectively catalyse the 1,3-dipolar-cycloaddition.

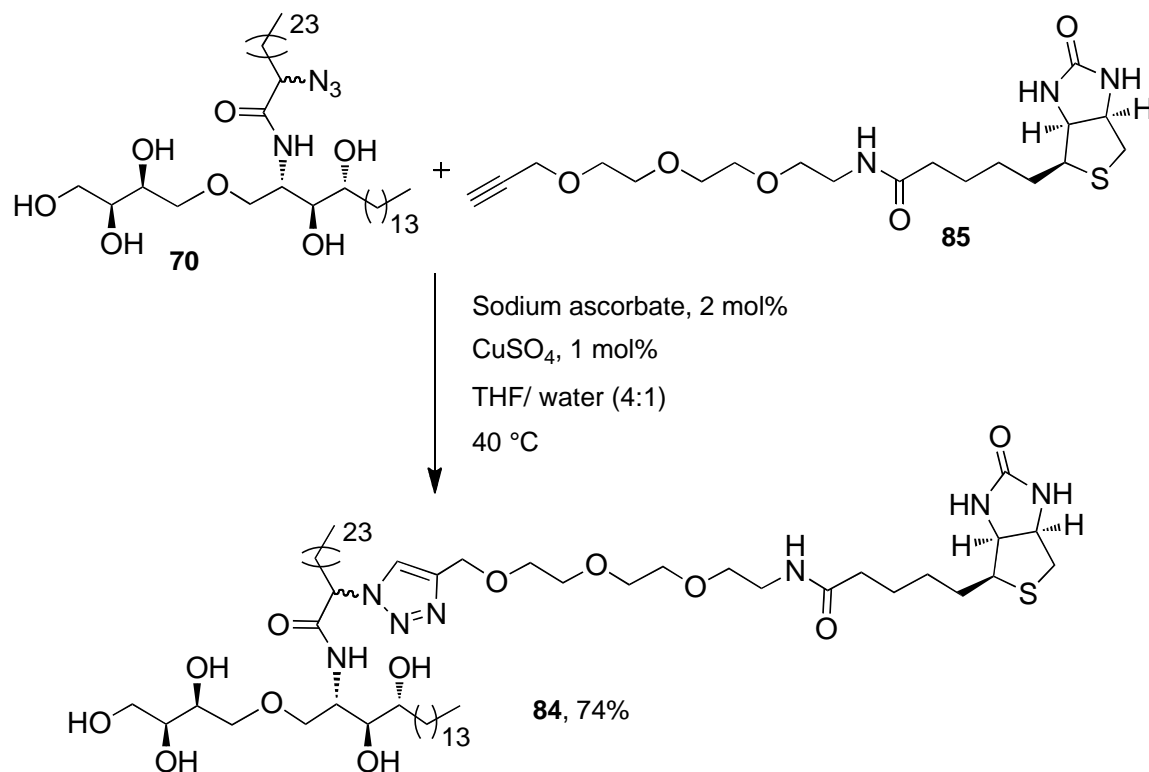
Under these new conditions the reaction constitutes the best example of click chemistry: it affords very high yields of product, the process is compatible with a wide range of solvents including water, it is a highly regioselective and thermodynamically favoured process driven by the formation of an aromatic compound [Scheme 31].



**Scheme 31.** Proposed mechanism for the azide-alkyne [3+2] cycloaddition catalysed by Cu(I).

Synthetically, the Cu(I)-catalysed azide-alkyne “click” is operationally simple and yields a single regioisomer which not only simplifies the characterisation and purification steps but also means that it is simpler to interpret the biological results from assays involving a single regioisomer than from assays with a mixture of regioisomers. In this light, we proceeded with a variant of the Cu(I)-catalysed azide-alkyne “click” in which the Cu(I) ions are generated *in situ* from Cu(II) by the action of sodium ascorbate [Scheme 32].<sup>[110]</sup>

## Synthesis of Threitol Ceramide and Labelled Analogues



**Scheme 32.** Synthesis of the target biotin-labelled ThrCer **84**.

The reaction was performed at 40 °C to maintain the mixture of starting materials and reagents in solution. TLC analysis showed complete consumption of the starting alkyne **85** and azide **70** after twelve hours. The triazole product **84** was precipitated from the reaction mixture by adding water at r.t., and then purified by silica gel column chromatography. We were delighted to have come to the end of a synthesis that afforded 11 mg of biotin-labelled ThrCer **84** [Scheme 32].

The biotinylated ThrCer was tested by MD Vincenzo Cerundolo *et al.* at Oxford University for its ability to stimulate the secretion of IFN $\gamma$  and the results were compared with the parent compound. Figure 17 shows that **84** is capable of inducing an immune response that is similar in magnitude to that of ThrCer confirming our

original hypothesis that incorporating the biotin label with a PEG linked to the fatty acid chain would not affect the bioactivity of the glycolipid.

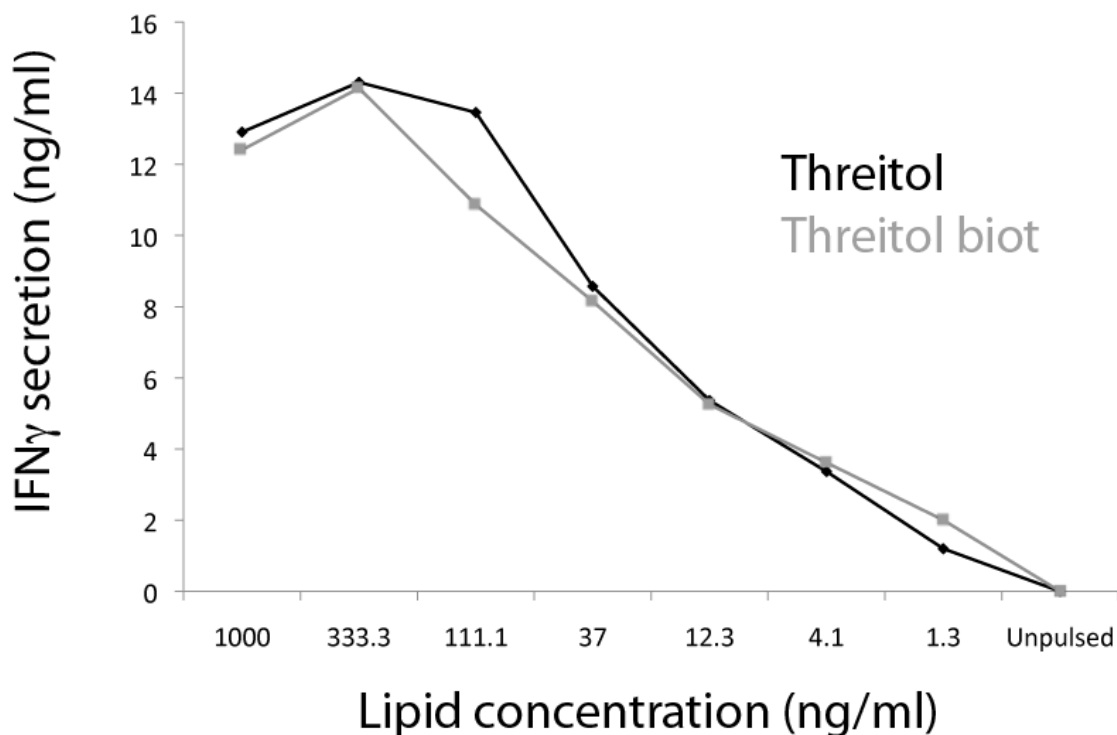


**Figure 17.** Biotinylated threitol ceramide activates human  $\alpha$ NKT cells in vitro. The human  $\alpha$ NKT line PP1 was incubated with C1R CD1d cells pulsed with threitol ceramide (black squares) or biotinylated threitol ceramide (gray diamonds). IFN $\gamma$  secretion was analyzed after 36h by ELISA.

Cerundolo *et al.* also tested for the ability of CD1d to load and externalise the labelled ThrCer **84**. Figure 18 shows staining of antigen presenting cells, APCs, with a biotin-specific reagent—fluorescent streptavidin, fluorescent biotin antibody and with fluorescent soluble  $\alpha$ NKT TCR—on the cell surface confirming that **84** is being externalised for presentation. Panel c) demonstrates that the modified lipid **84** is recognised by  $\alpha$ NKT cell TCRs. Panel d) shows a double staining with biotin antibody and with soluble  $\alpha$ NKT TCRs demonstrating that the increase in fluorescence is linear

and lipid concentration dependent, suggesting that the soluble iNKT TCRs recognise **84** as well as the biotin antibody recognises the biotin label.

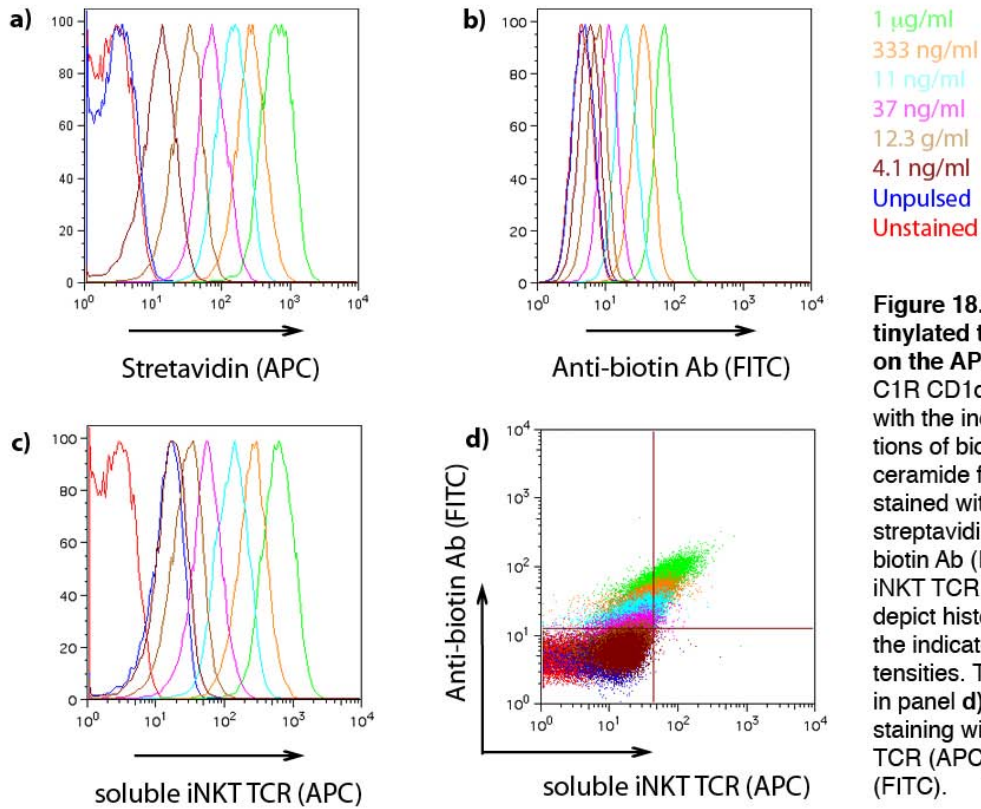


**Figure 18. Detection of Biotinylated threitol ceramide on the APC's cell surface.** C1R CD1d cells were pulsed with the indicated concentrations of biotinylated threitol ceramide for 16h, then stained with **a)** fluorescent streptavidin (APC), **b)** anti-biotin Ab (FITC), **c)** the soluble iNKT TCR (APC). **a)**, **b)** and **c)** depict histogram overlays of the indicated fluorescence intensities. The dot plot shown in panel **d)** depicts a double staining with the soluble iNKT TCR (APC) and anti-biotin Ab (FITC).

## IV. TOWARDS THE SYNTHESIS OF $\alpha$ -GALACTOSYL DIACYLGLYCEROL

### 4.1. Naturally Occurring CD1d Agonists.

Several CD1d agonists have been discovered,<sup>[111]</sup> and to date, the most studied of these is  $\alpha$ GalCer.<sup>[112]</sup> However,  $\alpha$ GalCer is neither an endogenous nor an exogenous lipid;  $\alpha$ GalCer has not been found to be a lipid component of any of the pathogens studied. Thus in search of the natural antigen for CD1d, attention has turned to other glycolipids of mammalian and pathogenic origins.<sup>[113, 114]</sup> One such glycolipid is isoglobotrihexosylceramide **90**, iGb3, which was postulated by Mattner *et al.* to be the natural endogenous antigen for CD1d and responsible for the survival of  $\mathbb{N}$ KT cells in the thymus in mice [Figure 19].<sup>[115, 116]</sup> iGb3 is a trisaccharide ceramide lipid that features a 26 carbon-atom acyl chain, in analogy with that found in  $\alpha$ GalCer. The glucose reducing sugar of this trisaccharide, is glycosylated through a  $\beta$  glycosidic bond to the ceramide base, which is in contrast with the galactose moiety of  $\alpha$ GalCer which presents an  $\alpha$  glycosidic linkage to the ceramide base [Figure 19].

However, the conclusion that iGb3 is solely responsible for the selection of  $\mathbb{N}$ KT cells has been contested by Speak *et al.*<sup>[117]</sup> They showed that the experiments leading to the proposal of the principal role for iGb3 being the natural antigen for CD1d could have led to a condition called lysosomal storage disease in which glycolipids are not processed as efficiently as normal in the lysosome. Speak *et al.* claimed that it was lysosomal storage, and not the absence of iGb3, that caused

$\lambda$ NKT cells not to be selected for survival, from which the principal role of iGb3 was originally inferred.<sup>[115]</sup> The contestants argued that lipid accumulation in the lysosome causes non-specific lipid loading into the hydrophobic pockets of CD1d, which diminishes the chances for an unidentified natural ligand successfully binding with CD1d. However, there are no questions over the fact that iGb3 is an agonist of CD1d and an unidentified role for this glycolipid in CD1d-mediated activation of  $\lambda$ NKT cells cannot be ruled out.

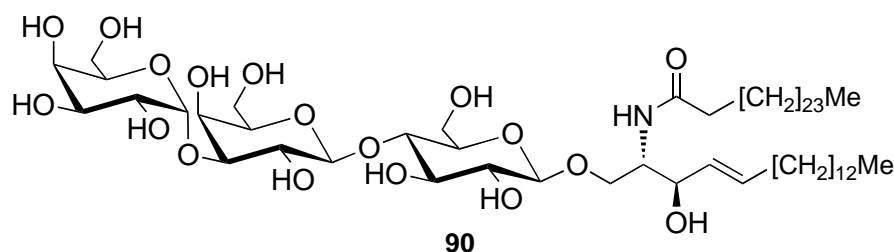


**Figure 19.** Isoglobotrihexosylceramide, iGb3.

$\alpha$ -Galacturonic acid ceramide **91** and  $\beta$ -glucuronic acid ceramide **92** are glycolipids that have also been found to activate  $\lambda$ NKT cells [Figure 20]. These glycolipids have been isolated from *Sphingomonas* and constitute the first direct evidence that glycolipids isolated from pathogenic bacteria bind to CD1d and are recognised by  $\lambda$ NKT cell TCRs resulting in an immune response against the invader.<sup>[30, 118]</sup>

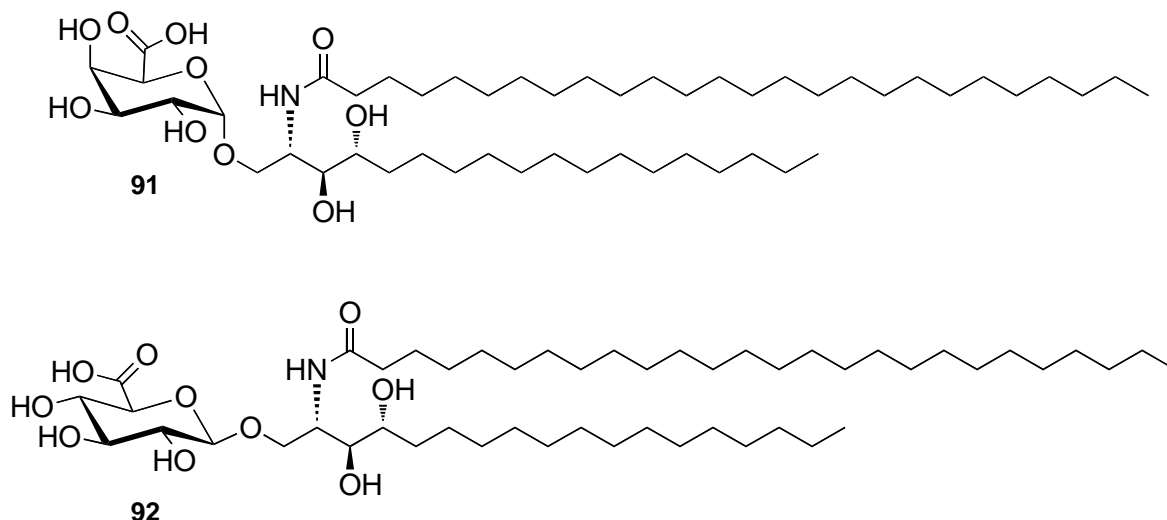


**Figure 20.** Glycosceramides from pathogenic origin are agonists of  $\lambda$ NKT cells.

In another study, non-sphingolipids were isolated from *Borrelia burgdorferi*, the causal agent of Lyme disease, and it was demonstrated that these agents were also agonists of CD1d.<sup>[52]</sup> These glycolipids are composed of a galactose polar head group that is  $\alpha$ -glycosylated to a diacyl-*syn*-glycerol moiety [Figure 21]. In their study, Kinjo *et al.* identified a range of acyl chains on the glycerol fragment but it was not possible to distinguish their exact location *i.e.* which acyl chain was on which alcohol. Thus, they synthesised a range of these glycolipids featuring a combination of the acyl chains from the repertoire that had been found in the wild.

The results very nicely demonstrated the intricate relationship between the activity of the antigen and its structure. For example, compound **BbGL-IIc** and **BbGL-IIf** are acylated with different fatty acids: **BbGL-IIc** features an oleic acid on *syn*-1 glycerol and a palmitic acid on *syn*-2, while **BbGL-IIf** features a linoleic acid on *syn*-1 glycerol and an oleic acid on *syn*-2 [Figure 21]. These two  $\alpha$ -galactosyl diacylglycerol

derivatives exhibit very different biological activity. **BbGL-IIc** performed as an antigen for CD1d and was the best of those compounds tested with mouse  $\lambda$ NKT cells, although interestingly this glycolipid failed to induce high levels of cytokine secretion when it was tested with human  $\lambda$ NKT cells. In sharp contrast, **BbGL-IIf**, which did not activate mouse  $\lambda$ NKT cells, induced the highest production of cytokines of those compounds tested when evaluated with human  $\lambda$ NKT cells. In addition, when the compounds were very similar structurally the activity was similar too; one example is the regioisomers **BbGL-IIId** and **BbGL-IIIf**, which both underperformed in mouse  $\lambda$ NKT cells while in assays with human  $\lambda$ NKT cells they both induced the production of large amounts of cytokines. These results are a cautious reminder that mouse models are not always useful for predicting the bioactivity of structurally similar analogues in humans.

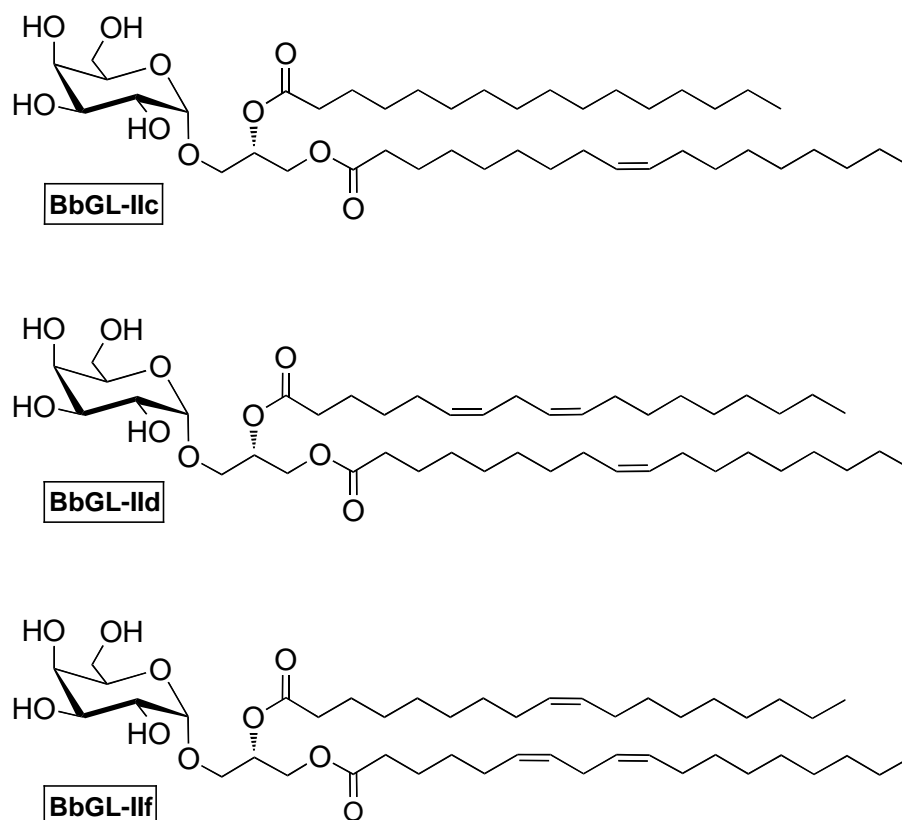


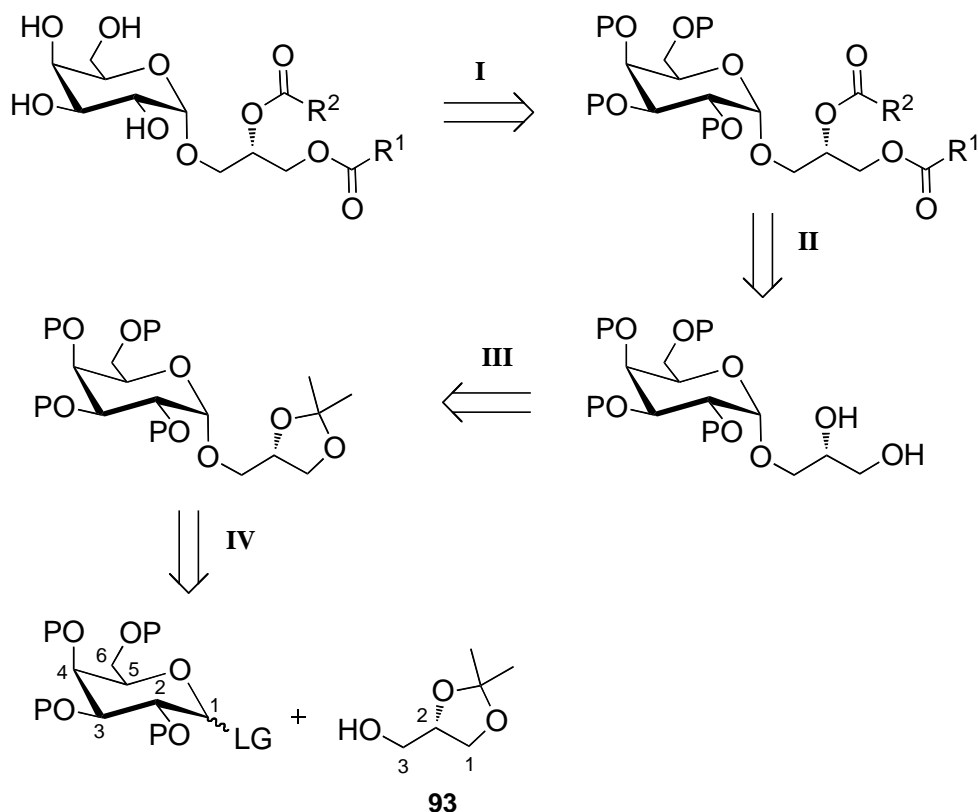
**Figure 21.** Examples of  $\alpha$ GalDAG agonists of NKT cells.

Our research group has established a collaborative project with Prof. Michael Brenner's research group at Harvard University Hospital to investigate further the role of these glycolipids in CD1d-mediated immunity and to consider analogues with non-natural acyl substitution on the glycerol fragment for the discovery of new bioactivity. We therefore wanted to develop a general and flexible synthesis of  $\alpha$ GalDAG.

#### 4.2. 1,2-*Cis*-Stereoselective Glycosylation Reactions.

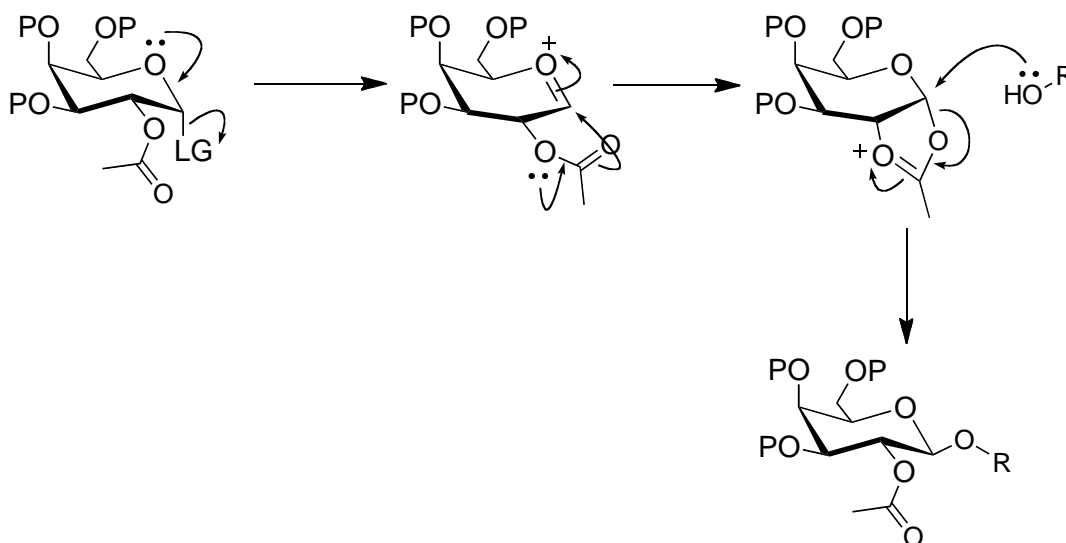
In our retrosynthetic analysis of  $\alpha$ GalDAG we chose to install the fatty acids at a late stage of the synthesis [Scheme 33]. This is a good strategy that would allow us to

introduce diversity into this part of the molecule from a common precursor. It also allows us to consider a range of protected sugar donors for the key glycosylation step which might be important to maximise the  $\alpha$ -stereoselectivity in this reaction.



**Scheme 33.** Retrosynthesis of  $\alpha$ GalDAG.

We considered a range of protecting groups for our galactosyl donor. For example, employing acetate-protected sugar donors was dismissed, as the chemoselective removal of acetates in the presence of other acyl groups is difficult. In addition, it would be important for the donor not to have an acetate protecting group at C(2), as this type of protecting group can participate in the glycosylation step directing the selectivity  $\beta$  in sugars like glucose and galactose (1,2-*trans*-diequatorial), and in sugars like mannose  $\alpha$ (1,2-*trans*-diaxial) [Scheme 34].

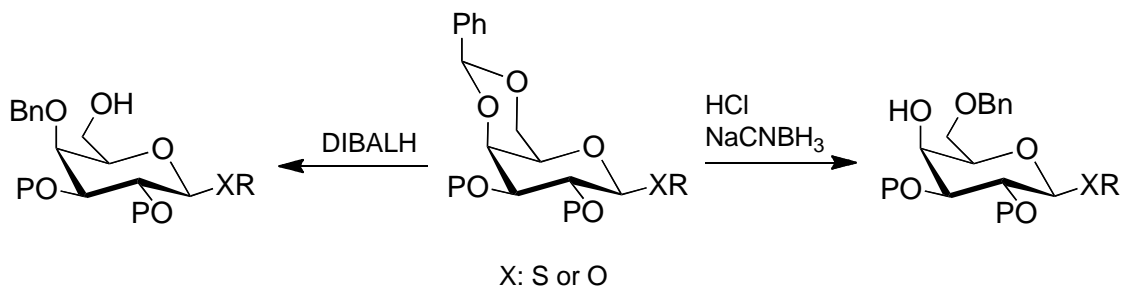


**Scheme 34.** Neighbouring group participation favours 1,2-*trans* products.

Benzyl ethers are commonly used electron-rich protecting groups for sugar donors in glycosylation reactions. Sugar donors protected with benzyl ethers are sometimes called “armed donors” because of their increased reactivity and ease of activation. Glycosylation reactions involving armed donors usually proceed under mild conditions and often at low temperatures.<sup>[119-121]</sup> In contrast, sugar donors protected with electron-withdrawing groups (these donors are called “disarmed donors”) generally require harsher conditions for activation.<sup>[120, 121]</sup> Benzyl ether protecting groups do not participate in the glycosylation step and do influence the stereochemical outcome of the reaction in the way that esters do.<sup>[122, 123]</sup>

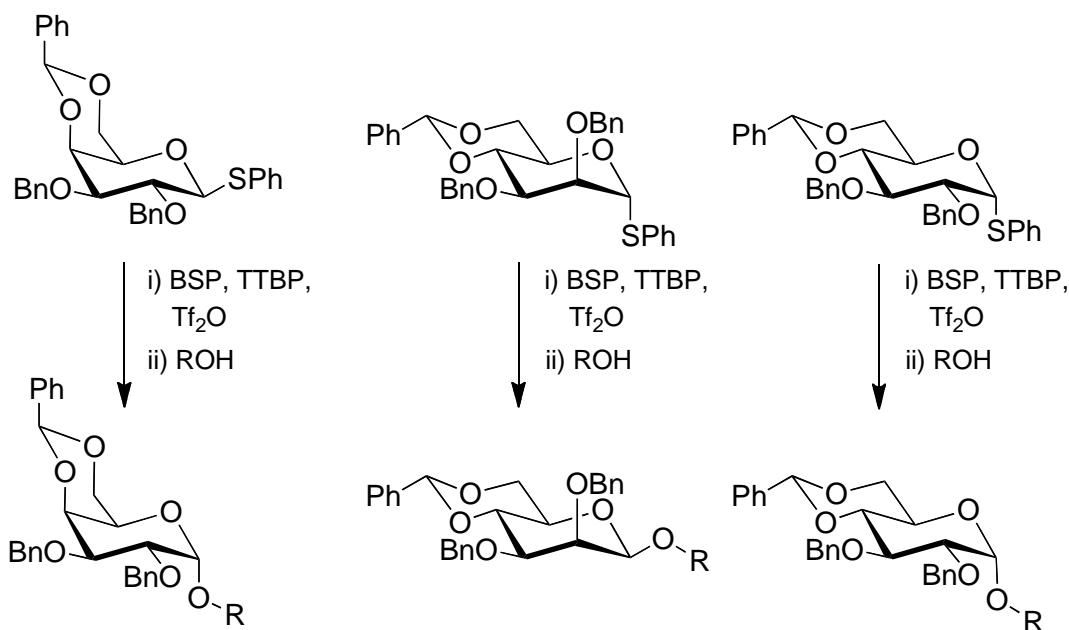
The benzylidene acetal is another common protecting group for simultaneously protecting the C(4)OH and C(6)OH in sugar donors. This versatile protecting group attracts attention because it can be removed under both acidic hydrolytic conditions, and by hydrogenolysis. It has also attracted attention because it can be reductively

opened providing a free C(6)OH or C(4)OH depending on the reducing agent that is employed [Scheme 35].<sup>[124-128]</sup>



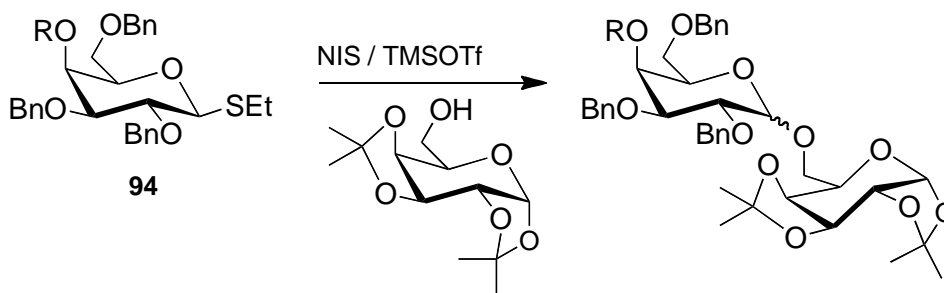
**Scheme 35.** Reductive opening of the benzylidene acetal.

Recent studies have shown that the presence of a 4,6-benzylidene acetal affects the reactivity of the donor and can also influence the stereochemical outcome of some glycosylation reactions.<sup>[129-131]</sup> The acetal is electron-rich in nature which should favour an increase in reactivity of the donor, but it also exerts a torsional effect that disfavors the formation of free ions. Crich *et al.* has studied the influence of this acetal protecting group on the stereochemical outcome of several glycosylation reactions and has demonstrated that a 4,6-benzylidene acetal can be used as an effective 1,2-*cis*-directing protecting group [Scheme 36].



**Scheme 36.** The 4,6-benzylidene protecting group favours 1,2-*cis* products.

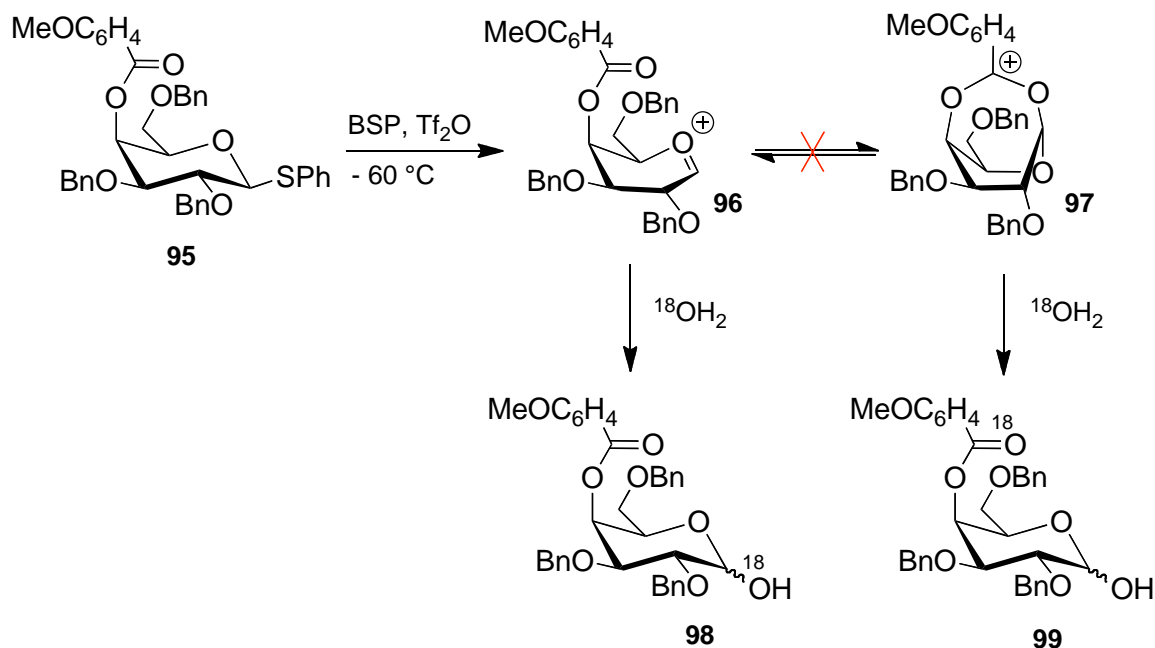
We were interested in identifying a galactosyl donor that affords high levels of 1,2-*cis*-selectivity and that requires minimal protecting group manipulation steps after the glycosylation reaction. Boon *et al.*<sup>[132]</sup> reported that donor **94** provides, under optimised conditions, very high levels of selectivity in favour of the  $\alpha$ -anomer [Scheme 37]. The high levels of selectivity were thought to be due to the remote aryl ester group participating in the reaction. This example provides one of the most supportive pieces of evidence in the literature for the participation of remote groups in glycosylation reactions. The data in this report evidenced a shift in mechanism between alkyl ester and aryl ester protecting groups. However, the situation is complicated by the high selectivity obtained with the pivalate ester protecting group, pointing to steric factors also being important in determining the selectivity of the reaction [Scheme 37].



entry	R	anomeric ratio ( $\alpha$ : $\beta$ )
1	acetyl	7.2:1
2	4-nitrobenzoyl	14:1
3	benzoyl	17:1
4	4-methylbenzoyl	18:1
5	4-methoxybenzoyl	33:1
6	pivaloyl	16:1

**Scheme 37.** Remote ester protecting group favours 1,2-*cis* selectivity.

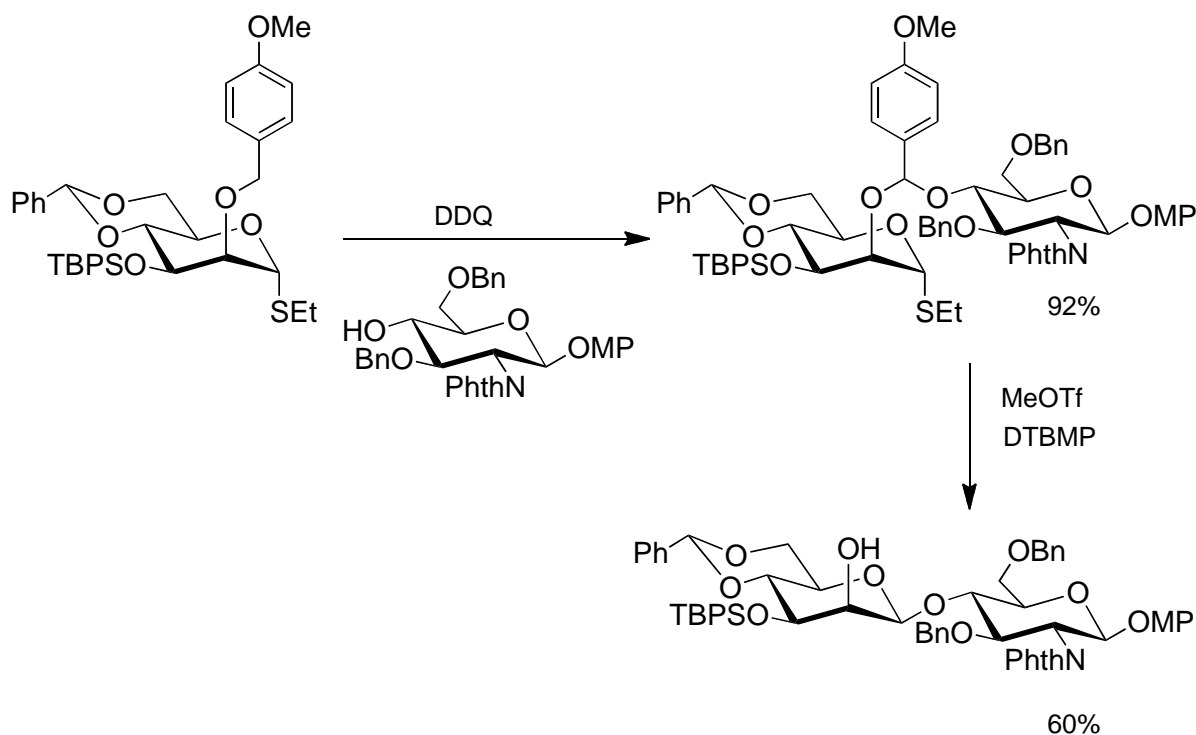
In a recent study, Crich and co-workers investigated the role of the remote ester at C(4) in governing the high levels of  $\alpha$ -stereoselectivity obtained for this type of donor [Scheme 38].<sup>[133]</sup> They found that if they quench the promoted donor **94** at low temperature using  $^{18}\text{O}$ -labelled water, the  $^{18}\text{O}$ -label was only incorporated in the hemiacetal oxygen, compound **98**, and not in the ester, compound **99**, as it would be expected if **96** is in equilibrium with **97** [Scheme 38]. This study raised questions about the origins of the  $\alpha$ -stereoselectivity for this donor and while it does not provide us with answers, it tells us that the proposal that this remote axial ester can participate in a similar fashion as that of an ester at C(2) is unlikely and that perhaps, it is a balanced combination of steric and stereoelectronic factors that determine the stereochemical outcome for this reaction.<sup>[133]</sup>



**Scheme 38.** Remote ester protecting groups do not participate in the glycosylation.

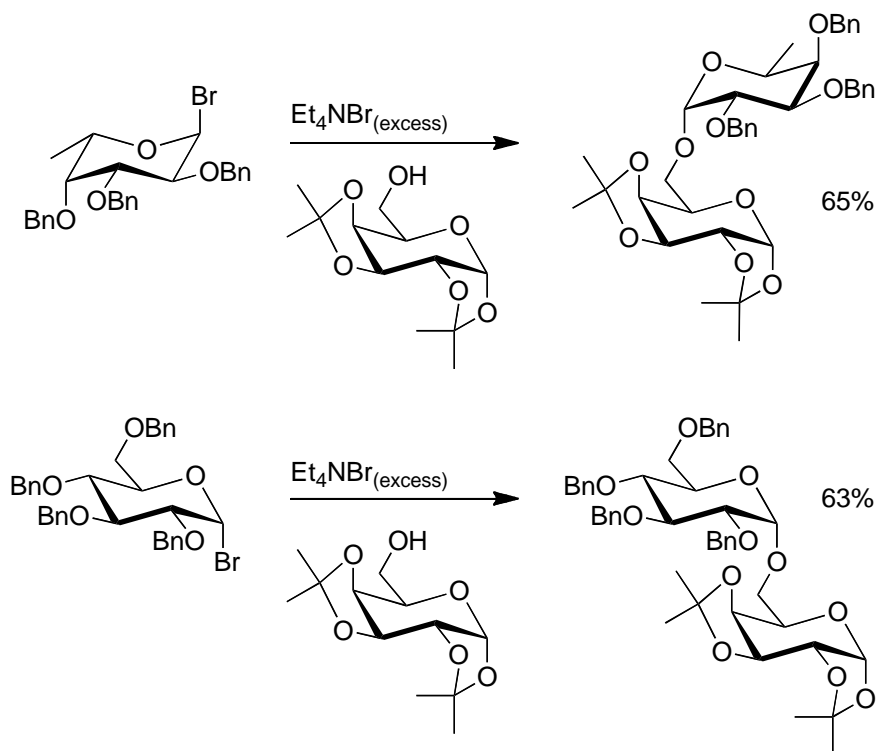
In another example of 1,2-*cis*-stereoselective glycosylation, the donor and the acceptor are brought together through a tether linking via the C(2)OH of the donor and the nucleophilic alcohol of the acceptor [Scheme 39]. This type of pre-assembly determines the face to which the acceptor is delivered upon activation of the anomeric centre in the donor. In a pioneering example from Bols,<sup>[134, 135]</sup> the acceptor is positioned on the  $\alpha$ -face of the donor via a silylene tether. Upon activation of the thioglycoside, the silyl ether attacks the electrophilic anomeric centre with complete stereoselectivity for the  $\alpha$ -face. This approach to 1,2-*cis*-stereoselective glycosylation has been applied to other sugars like mannose with equal success.<sup>[136]</sup>





**Scheme 40.** Acetal tether facilitates intramolecular aglycon delivery.

It is also possible to achieve high levels of stereo 1,2-*cis* stereoselectivity in the absence of directing protecting groups or pre-assembly of the donor and acceptor. Lemieux reported that 2,3,4,6-tetrabenzylgalactosyl bromide reacts in the presence of an excess of bromide ions with a series of acceptors with complete  $\alpha$  selectivity [Scheme 41].<sup>[123]</sup> Primary alcohol acceptors afforded 60 to 65% of the  $\alpha$ -anomer while secondary alcohols afforded only moderate yields ranging from 40 to 45% of the  $\alpha$ -anomer. The remaining mass balance was accounted to be hydrolysed and unreacted donor. Notably, the  $\beta$ -anomer was not found among the products for this reaction.

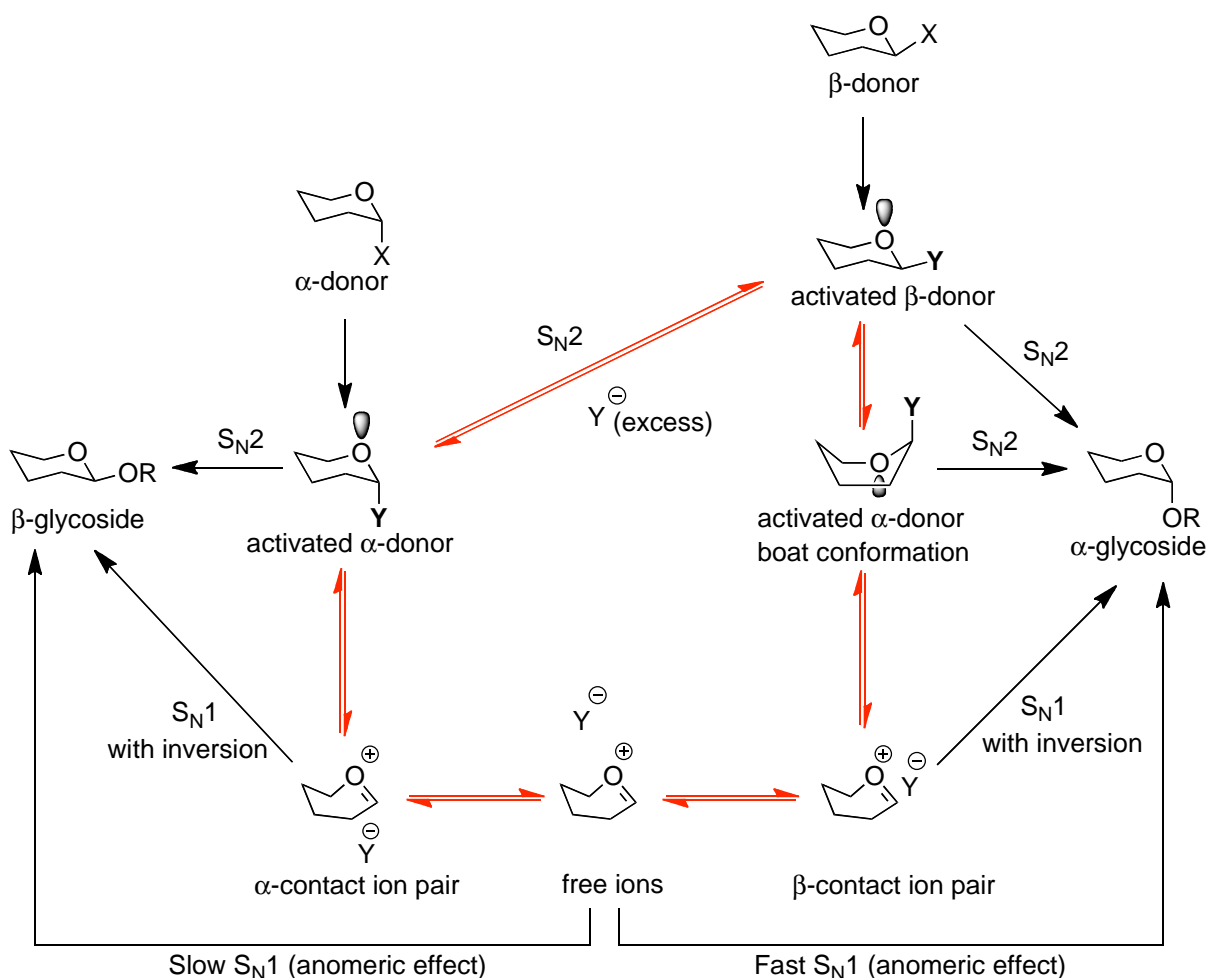


**Scheme 41.** Armed glycosyl bromide donors favour 1,2-*cis* products.

Lemieux's findings can be explained if we consider that under the reaction conditions and in the presence of an excess of bromide ions, the  $\alpha$ -glycosyl bromide equilibrates with a small amount of the more reactive  $\beta$ -anomer, which reacts with the acceptor in an  $\text{S}_{\text{N}}2$  fashion to give the  $\alpha$  product [Scheme 42]. This  $\alpha$ -halide can also dissociate to give  $\alpha$ -contact ion pairs and if these react with the acceptor, they will also give  $\beta$ -products. If  $\alpha$ -contact ion pairs are in equilibrium with free ions the latter react rapidly with the acceptor and also favour the  $\alpha$  products. The preference for the free ions to afford  $\alpha$ -products is a consequence of the anomeric effect that stabilises the  $\alpha$ -anomer via *endo*- and *exo*-orbital overlap while the  $\beta$ -anomer is stabilised only by *exo*-orbital overlap. This higher thermodynamic stability of the  $\alpha$ -anomer over the  $\beta$ - implies that the transition state leading to the formation of the  $\beta$ -anomer is higher

in energy than that of the transition state leading to the formation of the  $\alpha$ -anomer.

Consequently, the  $\alpha$ -anomer will form faster from free ions than would the  $\beta$ -anomer.

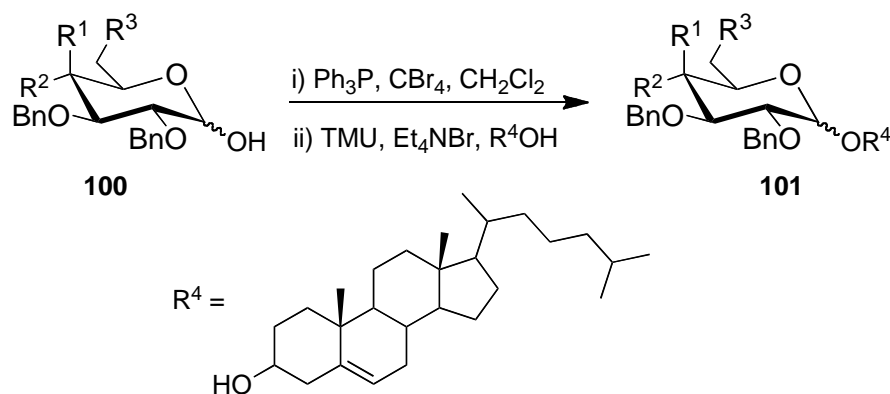


**Scheme 42.** Equilibrium of the activated donor in the absence of participating protecting groups.

The specific mechanistic path of a glycosidation reaction is highly dependent on the reaction conditions, the steric and stereoelectronic attributes of the donor and acceptor. Let's consider an  $\alpha$  or  $\beta$ -donor that is activated or promoted under the reaction conditions [Scheme 42]. For a glycosyl bromide or glycosyl iodide, this might simply be achieved by dissolving the donor and an excess of the halide salt with the acceptor. The equilibrium highlighted in red will be quickly established, and favours

the more stable species, namely the  $\alpha$ -halide by virtue of the anomeric effect. However, while this activated  $\alpha$ -donor is generally capable of reacting with the acceptor in an  $S_N2$  fashion, if an equilibrium with a more reactive species is established, i.e.  $\beta$ -bromide, the acceptor will react preferentially with this more reactive species and this can lead to high levels of stereoselectivity.

However, this type of reaction has the drawback of having to prepare a highly hydrolytically unstable donor, i.e. the armed-glycosyl bromide. In a recent publication, Shingu *et al.* showed that armed-hemiacetal benzylated galactose **100** can be employed as an alternative sugar donor to provide the glycoside product **101** with excellent levels of stereoselectivity in favour of the  $\alpha$ -anomer [Scheme 43].<sup>[140]</sup>

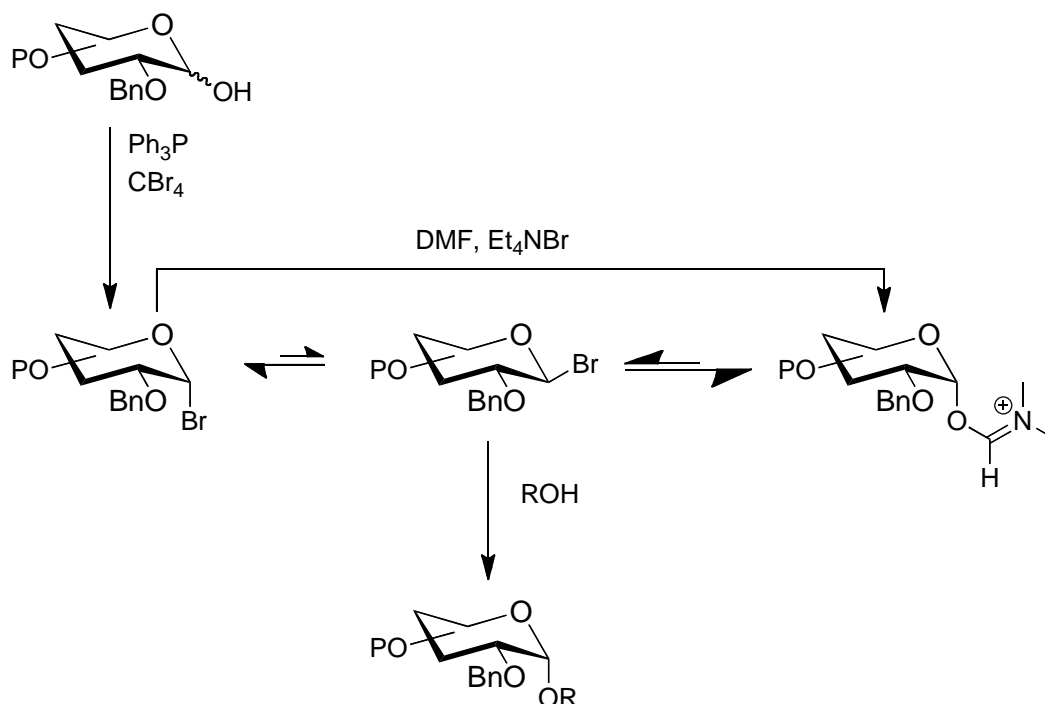


entry	R <sup>1</sup>	R <sup>2</sup>	R <sup>3</sup>	anomeric ratio ( $\alpha$ : $\beta$ )
1	H	OBn	OAc	> 99 : 1
2	H	OBn	OBn	90 : 10
3	OBn	H	OAc	> 99 : 1
4	OBn	H	OBn	88 : 12
5	OBn	H	-	86 : 14

**Scheme 43.** Armed glycosyl bromide donor prepared *in situ*.

In this remarkable discovery, the hemiacetal **100** is first converted to the corresponding glycosyl bromide. The excess reagent required for carrying out this conversion does not interfere detrimentally with the glycosylation reaction that follows *in situ*. These reaction conditions have the obvious advantage of not requiring to isolate the highly unstable perbenzylated galactosyl bromide.

In a separate study, Shingu *et al.* discovered that this glycosylation also occurs when DMF is employed as the solvent in the absence of TMU with similar results as in  $\text{CH}_2\text{Cl}_2$  in the presence of an excess of TMU.<sup>[141]</sup>  $^1\text{H}$  NMR spectra recorded at low temperatures of the glycosyl bromide in DMF indicated that an  $\alpha$ -glycosyl species corresponding to the DMF adduct was the major component [Scheme 44]. The authors postulated that in the presence of excess bromide ions the  $\alpha$ -glycosyl-TMU adduct can form the more reactive  $\beta$ -glycosyl bromide easier than the  $\alpha$ -glycosyl bromide can, and therefore TMU acts as a facilitator in this glycosylation.



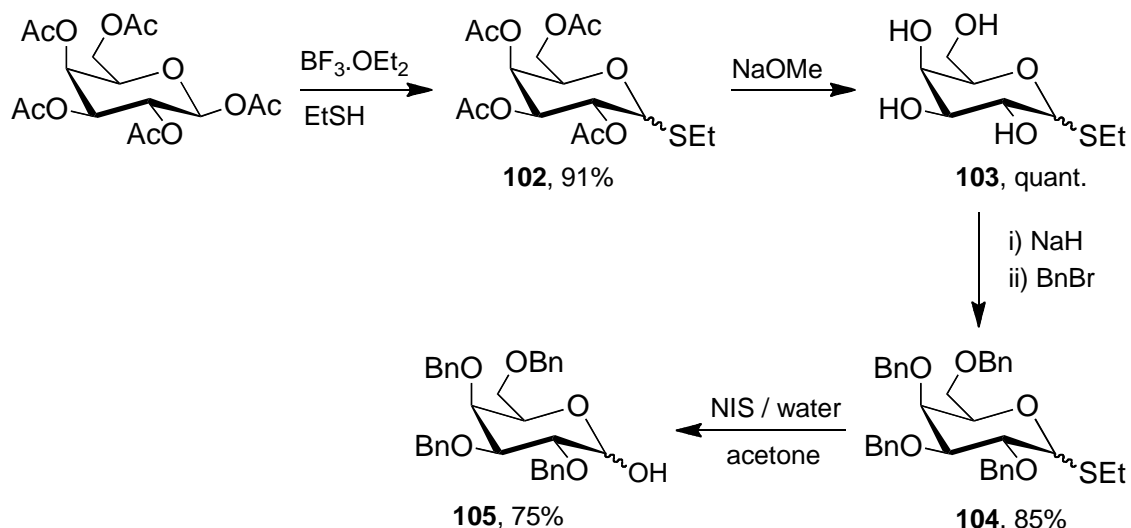
**Scheme 44.** DMF  $\alpha$ -adduct is an intermediate of the glycosylation reaction.

We have summarised the most prominent examples in the literature of directed 1,2-*cis* stereoselective glycosylation reactions and discussed the various factors governing their stereochemical outcome. Consequently, we selected the benzylated galactosyl bromide for our glycosylation with the 1,2-isopropylidene glycerol based on the rationale that this hydrolytically unstable donor can be prepared *in situ* and that the glycosylation affords high levels of selectivity in favour of the desired 1,2-*cis*-product. The benzyl protecting group can be conveniently removed by hydrogenolysis after the glycosylation step and the alcohols can be re-protected with a protecting group that is orthogonal with the acetal present in the glycerol *and* with the ester to allow chemoselective removal; in our first approach we chose to explore the use of chloroacetate protecting groups which are usually removed under very mild basic conditions ( $\text{Et}_3\text{N}$ /water mixture) or using a mild nucleophile (an example

would be urea). Under these conditions the ester functionality in the glycerol would be expected to remain intact.

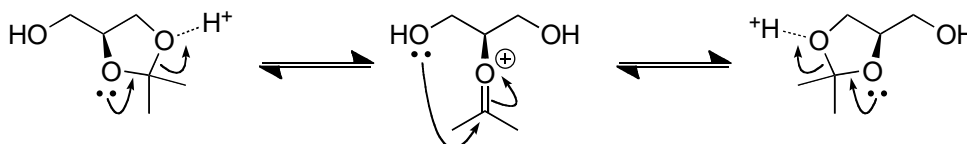
#### 4.3. Synthesis Of $\alpha$ GalDAG.

The synthesis of the required 2,3,4,5-benzyl-galactose was achieved starting from commercially available  $\beta$ -galactose pentaacetate, which, on activation with  $\text{BF}_3 \cdot \text{OEt}_2$  at 0 °C in the presence of EtSH afforded thioglycoside **102** in excellent yield as a 1:1 mixture of anomers [Scheme 30].<sup>[142]</sup> The acetate groups were then removed with a sub-stoichiometric amount of NaOMe in MeOH to afford the fully deprotected thioglycoside **103** after work-up. The work-up consisted of neutralising the reaction mixture with an acidic Dowex ion exchange resin which exchanges the Na cations in the reaction mixture with an equivalent amount of protons. Proceeding in this way, and once the resin was removed by filtration and the methanol evaporated under reduced pressure, the fully deprotected thioglycoside **103** was collected as a white foam without the need for further purification.<sup>[142]</sup> The very polar tetra-ol **103** was then protected with benzyl ethers to provide the thioglycoside **104**, which was then chemoselectively hydrolysed with *N*-iodosuccinimide in an acetone/water mixture (10:1) to yield the hemiacetal **104** as our sugar donor precursor as a 1:1 mixture of diastereoisomers.<sup>[143, 144]</sup> The product was characterised by HMRS, and the 1:1 ratio of diastereoisomers was evidenced in the  $^1\text{H}$  NMR and in the  $^{13}\text{C}$  NMR spectra; the diastereomeric OH proton signals appeared in the  $^1\text{H}$  NMR spectrum at 2.93 and 3.15 ppm and they integrated as 0.5 H indicative of a 1:1 diastereomeric ratio. The IR spectrum showed the OH stretch as further evidence of the acetal hydrolysis.



**Scheme 45.** Synthesis of 2,3,4,6-tetrabenzyl-D-galactose **105**.

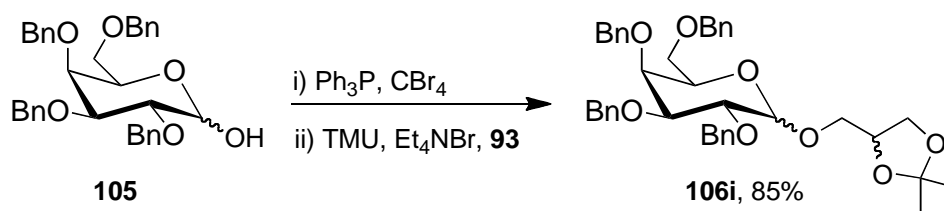
With **104** in hand, we were ready to proceed to the glycosylation step. Shingu *et al.* reported that these glycosylation conditions scrambled the stereochemistry of the acceptor **93**. Such epimerisation presumably comes from an acid-catalysed acetal migration [Scheme 46].



**Scheme 46.** Acid catalysed isopropylidene migration.

Initially, we performed the reaction under the reported conditions [Scheme 47].<sup>[140]</sup> The hemiacetal **104** was treated with  $\text{Ph}_3\text{P}$  and  $\text{CBr}_4$  at r.t. for four hours. TMU,  $\text{Et}_4\text{NBr}$  and the acceptor **93** were then added sequentially. TLC analysis showed that the reaction was complete after 24 hours as evidenced by the disappearance of the starting material. The NMR spectra of the crude reaction mixture were too complex to be interpreted accurately and it was necessary to purify the product before further

analysis. We found, as evidenced by the chemical shift of the anomeric carbon in the  $^{13}\text{C}$  NMR spectrum of the mixture of purified products, that the glycosylation favoured the  $\alpha$ -anomer (approximately 10:1 of  $\alpha$ : $\beta$  ratio);\*\* however, as found by Shingu *et al.* the stereocentre of the glycerol had also been scrambled under the reaction conditions providing the  $\alpha$ -galactoside **106i** as a 1:1 mixture of the two epimers [Scheme 47].<sup>[140]</sup> We reasoned, based on the assumption that this glycosylation is irreversible, that since acetal migration was not possible after the glycosylation has taken place, the migration must be fast in comparison with the glycosylation rate; thus all of the enantiomerically pure acceptor must be converted into a racemic mixture prior to reacting with the donor to afford the observed 1:1 mixture of the epimers.

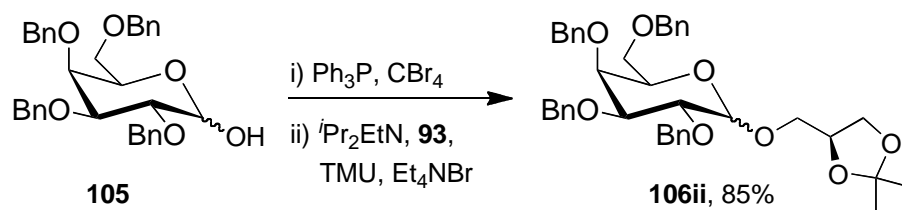


**Scheme 47.** The glycosylation conditions induce epimerisation of the acceptor **93**.

We postulated that the acetal migration that was racemising the glycerol acceptor **93** could be controlled if we employed an acid scavenger during the glycosylation; however, we did not know what effect employing a base would have on the stereoselectivity or rate of glycosylation. We were therefore delighted to observe that acetal migration was completely suppressed when an excess of  $i\text{Pr}_2\text{EtN}$  was employed as a sterically hindered base. We were also pleased to observe that the

\*\* The anomeric carbon in **52i** resonates at 98 ppm in the  $^{13}\text{C}$  NMR spectrum for the  $\alpha$ -anomer and at 104 ppm for the  $\beta$ -anomer.

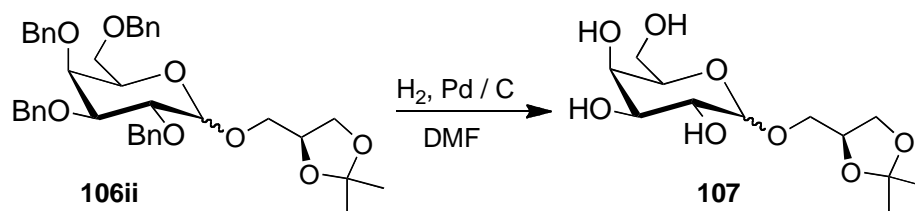
base did not show any adverse effects on the stereoselectivity or rate of the reaction and the glycoside **106ii** product was obtained in high yield as an inseparable mixture of  $\alpha$ - and  $\beta$ -products in about 10:1 favouring the desired  $\alpha$ -glycoside product [Scheme 48]. We were unable to measure an accurate ratio of the two products due to substantial peak overlap in the  $^1\text{H}$  NMR spectrum of the crude mixture and on the purified mixture of  $\alpha$ - and  $\beta$ -products and consequently, a rough estimate was obtained from the  $^{13}\text{C}$  NMR spectrum of the crude reaction mixture. The product was confirmed by HRMS and the characteristic  $\alpha$ -anomeric proton in the  $^1\text{H}$  NMR spectrum at 4.99 ppm integrating as one H. The  $^{13}\text{C}$  NMR spectrum showed the characteristic  $\alpha$ -anomeric carbon environment at 98 ppm as further diagnostic data.



**Scheme 48.** Hünig's base prevents epimerisation of **93**.

We were encouraged by these results and stereoselectivity, and although the  $\alpha$ - and  $\beta$ -isomers were inseparable by standard chromatography, we were confident that we could accomplish their separation at a later stage in the synthesis. Mindful that the acyl chains on the target  $\alpha$ GalDAGs feature unsaturation that is incompatible with the hydrogenolysis of benzyl ether protecting groups, we planned a protecting group exchange before the acylation steps. We therefore took the  $\alpha$ - and  $\beta$ -mixture of anomers forward to the debenzoylation step. Hydrogenolysis of the benzyl ethers in

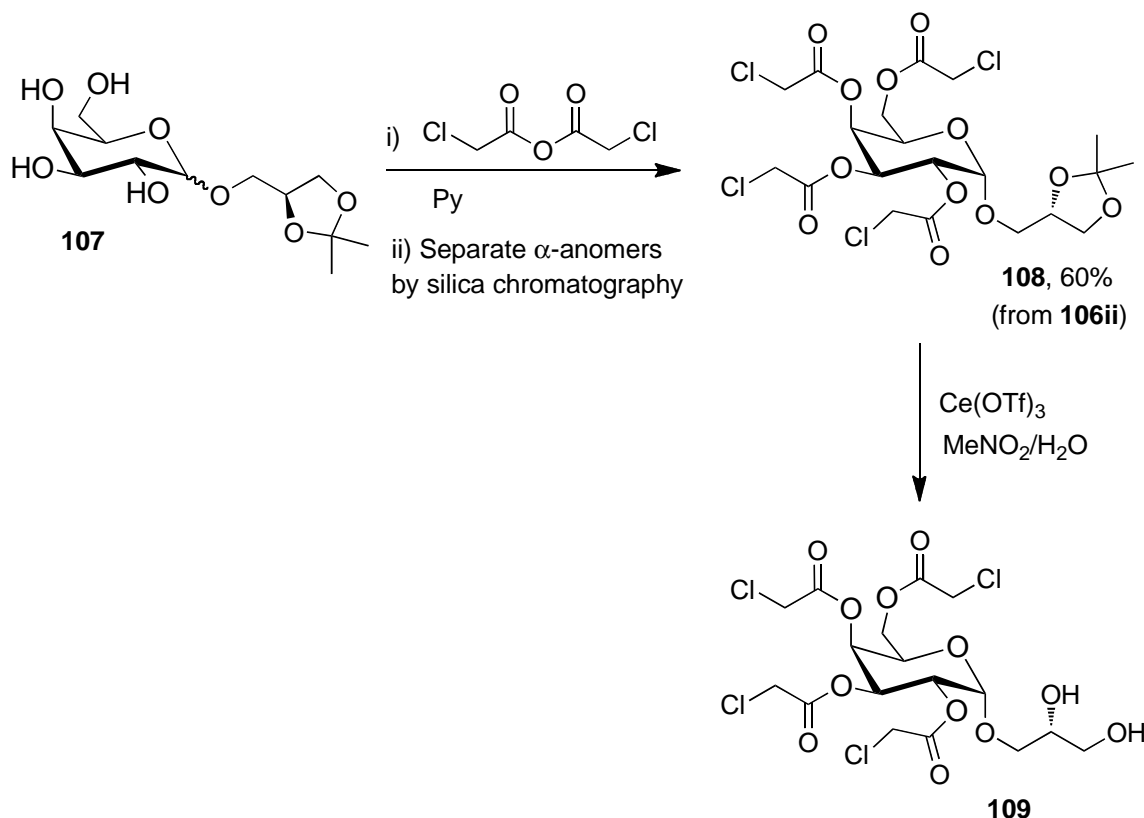
**106ii** in MeOH or EtOH/THF or THF using either Pd/C or Pd(OH)<sub>2</sub>/C under an atmosphere of H<sub>2</sub> provided the fully debenzylated product but unfortunately the isopropylidene group on the glycerol fragment was also removed under these reaction conditions. The deprotection of the acetal is likely to be promoted by the generation of a small amount of acid under the hydrogenolysis conditions although we were unable to determine its specific identity. We were pleased to see that employing DMF as a solvent in the hydrogenolysis provided the debenzylated product **107**, and this time only a small amount of acetal removal was observed by TLC analysis. We were unable to find any precedent for this observation; however, we propose that DMF acts as a weak base for the adventitious acid generated in this reaction, thereby suppressing the acetal hydrolysis.



**Scheme 49.** Debenzylation in DMF suppressed acetal deprotection.

The protecting groups chosen to re-protect the alcohols in **107** needed to be orthogonal to the acetal, and to the esters that would be present in the final product. We therefore protected the tetra-ol **107** with chloroacetates which can be removed selectively under very mildly basic conditions allowing us to retain other ester functionalities, including those in our  $\alpha$ GalDAG targets. The chloroacetate protection was achieved in pyridine with chloroacetic anhydride as the acylating agent.<sup>[145]</sup> Pleasingly, the two chloroacetyl-protected anomers had sufficiently different  $R_f$  on

silica gel to allow the small amount of  $\beta$ -anomer to be separated from the desired  $\alpha$ -anomer **108** by standard silica gel chromatography [Scheme 50]. The product was confirmed by HRMS and the  $^1\text{H}$  NMR spectrum showed the anomeric proton at 5.27 ppm with a coupling constant of 3.7 Hz.

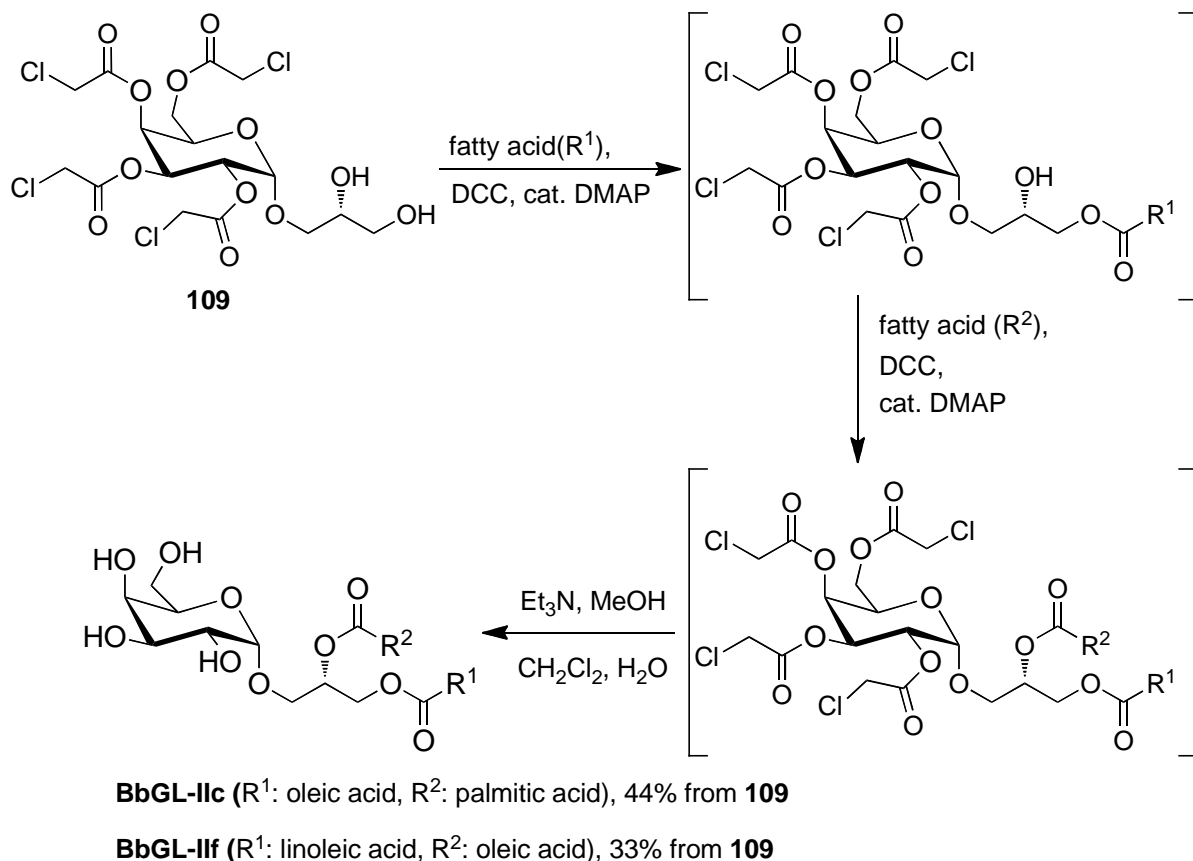


**Scheme 50.** Synthesis of the key diol **109**.

The diol **109** was readily obtained after  $\text{Ce}(\text{OTf})_3$ -mediated hydrolysis of the acetal in  $\text{MeNO}_2$  saturated with water [Scheme 50]. We anticipated that selective acylation of the primary alcohol in **109** could be achieved in the presence of a DCC coupling reagent on steric grounds employing one molar equivalent of the corresponding fatty acid. However, we were also aware of the migratory aptitude of esters on 1,2-glycerol diols.<sup>[146, 147]</sup> Diacyl glycerols in Nature are found as mixtures of 1,2-diacyl and 1,3-diacyl glycerols and the ratio usually favours the more thermodynamically stable,

namely the 1,3-diacyl glycerol.<sup>[148]</sup> When we performed the mono acylation of **109** with oleic acid in the presence of DCC we obtained a mixture that largely favoured the acylation of the primary alcohol albeit in poor yield (35-40%) [Scheme 51]. We determined by analysis of the <sup>1</sup>H NMR spectra of the crude products, a ratio of 15:1 of primary acylation against acylation of the secondary alcohol in **109**, the later possesses a characteristic shift downfield of the CH proton in the glycerol appearing 5.2 ppm as a multiplet. The mass balance included diacyl glycerol and unidentified by-products, as well as approximately 10% of starting diol **109**. The low yield was even worse for the second acylation. The mass recovery as the diacylglycerol after the second acylation was approximately 30%. We hypothesised that some of the chloroacetate protecting groups may be removed under the acylation conditions (DCC coupling generates a urea by-product that may be sufficiently nucleophilic to attack the chloroacetate protecting groups) and this position could subsequently be acylated under the esterification conditions. We could not confirm our hypothesis and several attempts proceeding promptly after quick flash chromatography to avoid long exposure of the products to silica gel that might induce chloroacetate removal or acyl migration we obtained the products in moderate yield over the two steps.

Towards the Synthesis of  $\alpha$ -Galactosyl Diacylglycerol



**Scheme 51.** Synthesis of  $\alpha$ GalDAG targets from diol **109**.

**BbGL-IIc** was purified successfully by flash column chromatography and was supplied to our collaborators in Harvard University for further testing and assays with  $\lambda$ NKT cells. We have not obtained the results from these bioassays.

However, **BbGL-IIf** could not be totally purified by flash column chromatography. Figure 22 shows  $^1\text{H}$  NMR spectra of **BbGL-IIf** after standard flash column chromatography purification (spectrum in blue) and after re-purification (spectrum in red). The black rectangles enclose the more significant impurities signals in the  $^1\text{H}$  NMR spectrum before and after re-purification. We weren't able to identify this

impurity and an attempt to purify the product further by HPLC proved unsuccessful due to the low UV absorption which hindered the detection of **BbGL-IIf**.

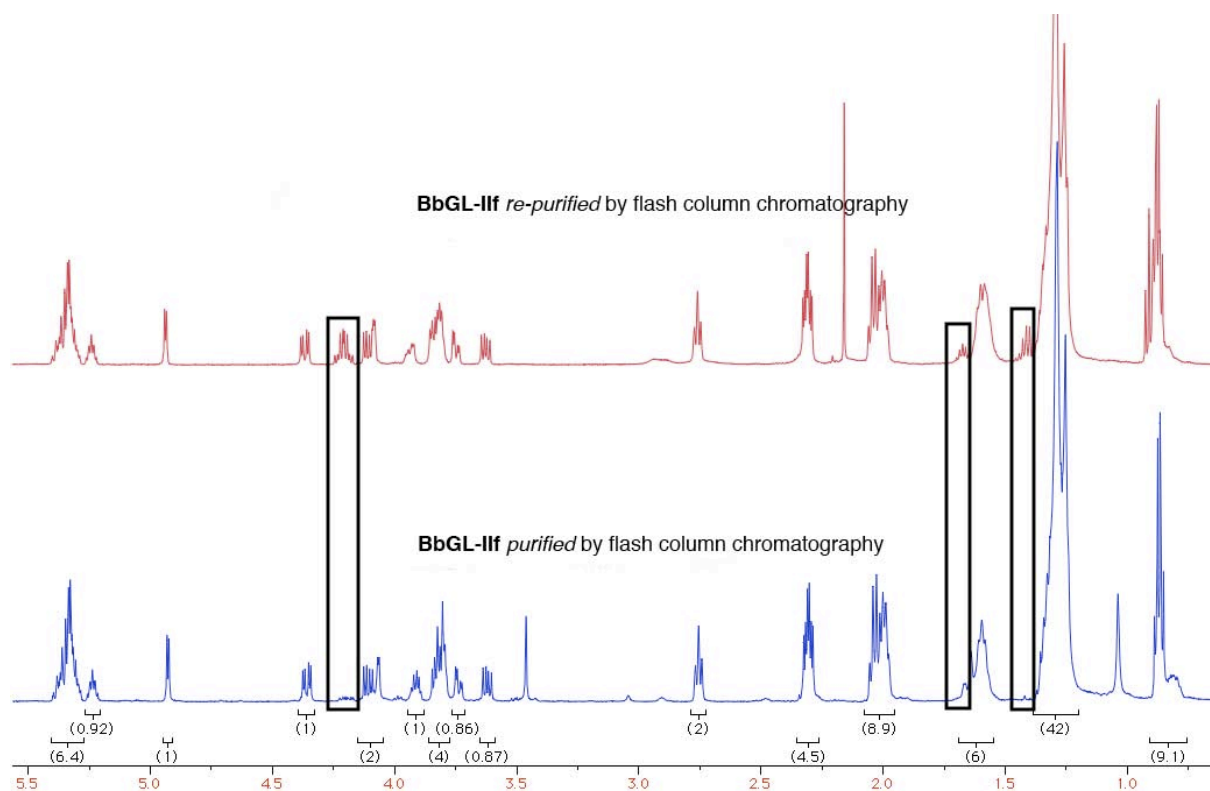


**Figure 22.** <sup>1</sup>H NMR spectrum of BbGL-IIf after standard purification by silica gel flash column chromatography (blue spectrum) and re-purification (red spectrum).

## **CONCLUSIONS AND FUTURE WORK**

## V. CONCLUSIONS AND FUTURE WORK

### 5.1. Synthesis Of Threitol Ceramide And Labelled Analogues Conclusions.

We have developed a novel synthesis of ThrCer, and have successfully introduced a  $^{14}\text{C}$  label to facilitate immunological studies in mice which are focusing on understanding the intracellular trafficking and uptake of this novel glycolipid. We have also designed and synthesised the novel glycolipid biotin-ThrCer **84**. Preliminary immunological assays have shown that this conjugate exhibits a very similar CD1d-mediated immunoresponse to the unlabelled ThrCer, which makes it a valuable chemical tool for studying *in vitro* and *in vivo* tissue distribution of this glycolipid in mice and in humans.

### 5.2. Towards The Synthesis Of $\alpha$ -Galactosyl Diacylglycerol Conclusions.

We have developed a stereoselective synthesis of diol **109**, which is a key advanced intermediate in the synthesis of  $\alpha$ GalDAG. The target glycoside **BbGL-IIc** was obtained in three steps from this intermediate, however **BbGL-IIf** that possesses a sensitive-to-oxidation fatty acid—linoleic acid—could not be obtained with high purity in the same way. After various purification attempts we proposed that these targets can be achieved from the precursor **106** employing other orthogonal ester protecting groups or different acylation conditions. Unfortunately under the time restrictions we did not have time to explore these possibilities.

### 5.3. Future Work.

In the future, our group will focus on the synthesis of Alexa Fluor® fluorophore labelled  $\alpha$ GalCer and ThrCer for *in vivo* immunological assays. Our syntheses of  $^{14}\text{C}$  radiolabelled ThrCer and biotin-labelled ThrCer described here will provide valuable knowledge for the retrosynthetic analysis and forward syntheses of these expensive labels. In particular, we identified an attachment point next to the amide on the acyl chain, which is remote from the hydroxyl functional groups that are known to be important for the recognition of CD1d-lipid complex by the TCRs,<sup>[50]</sup> and at which attachment point our results demonstrated that a triazole can effectively attach a PEG spacer for elaborating the label.

The stereoselective synthesis of  $\alpha$ GalDAGs is an ongoing project in our lab and future work will capitalise on our findings and will probably focus on the orthogonal protection of  $\alpha$ -Galactosyl glycerol; for example, protecting the galactose moiety with levulinic protecting groups, or the identification of a mild acylation strategy of **109** that is compatible with the chloroacetate protecting groups on the galactose moiety to suppress the loss of material in side-reactions.

## **EXPERIMENTAL SECTION**

## VI. EXPERIMENTAL SECTION

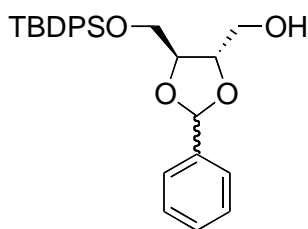
### 6.1. General Experimental.

Optical rotations were measured using an Optical Activity PolAAR2001 automatic polarimeter. Melting points were determined using open capillaries on a Gallenkamp MPD350 melting point apparatus and are uncorrected. Infrared spectra were recorded either neat as thin films between NaCl discs, on a Perkin Elmer 1600 FTIR spectrometer, or neat on a Perkin Elmer Spectrum 100 fitted with a universal ATR accessory. The intensity of each band is described as s (strong), m (medium) or w (weak), and with the prefix v (very) and suffix br (broad) where appropriate. <sup>1</sup>H-NMR spectra were recorded at 500 MHz, 400 MHz, or 300 MHz, using Bruker DRX 500, Bruker AMX 400, Bruker AV 400, Bruker AV 300 and Bruker AC 300 spectrometers. <sup>13</sup>C-NMR spectra were recorded at 125 MHz, 100 MHz, or 75 MHz, respectively, using Bruker DRX 500, Bruker AMX 400, Bruker AV 400, Bruker AV 300 and Bruker AC 300 spectrometers. Chemical shifts are reported as values (ppm) referenced to the following solvent signals: CHCl<sub>3</sub>,  $\delta_H$  7.26; CDCl<sub>3</sub>,  $\delta_C$  77.0; CH<sub>3</sub>OH,  $\delta_H$  3.34; CD<sub>3</sub>OD,  $\delta_C$  49.9. The term “stack” is used to describe a region where resonances arising from non-equivalent nuclei are coincident, and multiplet, m, to describe a region where resonances arising from a single nucleus (or equivalent nuclei) are coincident but coupling constants cannot be readily assigned. Mass spectra were recorded on a Micromass LCT spectrometer utilising electrospray ionisation (and a MeOH mobile phase), and are reported as (*m/z* (%)). HRMS were recorded on a Micromass LCT spectrometer using a lock mass incorporated into the mobile phase.

## Experimental Section

All reagents were obtained from commercial sources and used without further purification unless stated otherwise. Anhydrous solvents were purchased from Sigma-Aldrich UK, stored over 4 Å molecular sieves and under an Ar atmosphere. All solutions are aqueous and saturated unless stated otherwise.

Reactions were monitored by TLC using pre-coated aluminium-backed ICN silica plates (60A F<sub>254</sub>) and visualised by UV detection (at 254 nm) and staining with 5% phosphomolybdic acid in EtOH (MPA spray). Column chromatography was performed on Merck silica gel (particle size 40-63 m mesh) or Fluka 60 (40-60 m mesh) silica gel. Radiograms were produced by 2.5 minutes' exposure of Kodak X-Omat AR films to the TLC plates in the dark.

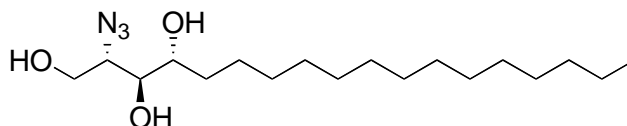
6.2. 1-O-(*tert*-Butyldiphenylsilyl)-2,3-O-benzylidene-L-threitol **53**

Chemical Formula: C<sub>27</sub>H<sub>32</sub>O<sub>4</sub>Si  
Molecular Weight: 448.63

A solution of (-)-2,3-O-benzylidene-L-threitol (1.00 g, 2.23 mmol) in THF (7 mL) was added dropwise over 5 min to a suspension of NaH (60% dispersion in mineral oil, 98 mg, 2.45 mmol) in THF (10 mL) at 0 °C. After 30 min, a solution of TBDPSCI (674 mg, 2.45 mmol) in THF (7 mL) was added dropwise over 15 min. After stirring at r.t. for 12 h, the reaction was quenched by the sequential addition of MeOH (2 mL) and NaHCO<sub>3</sub> solution (20 mL). The phases were separated and the aqueous phase was washed with CH<sub>2</sub>Cl<sub>2</sub> (3 × 20 mL). The combined organic phases were washed with brine (20 mL), dried (MgSO<sub>4</sub>), filtered and the solvent was evaporated under reduced pressure. The residue was purified by silica gel flash column chromatography (eluent: 20% EtOAc in hexanes) to provide silyl ether **53** as a colourless oil (1:1 mixture of diastereoisomers, 919 mg, 71%). Data on diastereoisomeric mixture: *R*<sub>f</sub> = 0.25 (20% EtOAc in hexanes); *v*<sub>max</sub> (film)/cm<sup>-1</sup> 3432br (OH), 3070m, 2930s, 2858s, 1654w, 1589w, 1471m, 1427m, 1390m, 1361m, 1310m, 1218m, 1112s, 1027m, 998m, 917m; *δ*<sub>H</sub> (300 MHz, CDCl<sub>3</sub>) 1.07 (4.5H, s, (CH<sub>3</sub>)<sub>3</sub>CSi), 1.09 (4.5H, s, (CH<sub>3</sub>)<sub>3</sub>CSi), 1.96-2.05 (1H, stack, CH<sub>2</sub>OH), 3.70-3.96 (4H, stack), 4.11-4.25 (1.5H, stack), 4.32-4.37 (0.5H, m), 5.96 (0.5H, s, PhCH), 5.99 (0.5H, s, PhCH), 7.35-7.50

(11H, stack, Ph), 7.65-7.72 (4H, stack, Ph);  $\delta_C$  (75 MHz,  $\text{CDCl}_3$ ) [19.1 (quat. C,  $(\text{CH}_3)_3\text{CSi}$ ), 19.2 (quat. C,  $(\text{CH}_3)_3\text{CSi}$ )], [26.72 ( $\text{CH}_3$ ,  $(\text{CH}_3)_3\text{C}$ ), 26.75 ( $\text{CH}_3$ ,  $(\text{CH}_3)_3\text{C}$ )], [62.7 ( $\text{CH}_2$ ,  $\text{CH}_2\text{O}$ ), 62.8 ( $\text{CH}_2$ ,  $\text{CH}_2\text{O}$ )], [63.9 ( $\text{CH}_2$ ,  $\text{CH}_2\text{O}$ ), 64.0 ( $\text{CH}_2$ ,  $\text{CH}_2\text{O}$ )], [77.8 ( $\text{CH}$ ,  $\text{CHO}$ ), 78.7 ( $\text{CH}$ ,  $\text{CHO}$ ), 79.6 ( $\text{CH}$ ,  $\text{CHO}$ ), 79.9 ( $\text{CH}$ ,  $\text{CHO}$ )], [103.7 ( $\text{CH}$ ,  $\text{PhCH}$ ), 104.1 ( $\text{CH}$ ,  $\text{PhCH}$ )], [126.52 ( $\text{CH}$ ,  $\text{Ph}$ ), 126.58 ( $\text{CH}$ ,  $\text{Ph}$ ), 127.73 ( $\text{CH}$ ,  $\text{Ph}$ ), 127.77 ( $\text{CH}$ ,  $\text{Ph}$ ), 128.26 ( $\text{CH}$ ,  $\text{Ph}$ ), 128.37 ( $\text{CH}$ ,  $\text{Ph}$ ), 129.3 ( $\text{CH}$ ,  $\text{Ph}$ ), 129.5 ( $\text{CH}$ ,  $\text{Ph}$ ), 129.79 ( $\text{CH}$ ,  $\text{Ph}$ ), 129.81 ( $\text{CH}$ ,  $\text{Ph}$ ), 129.82 ( $\text{CH}$ ,  $\text{Ph}$ ), 129.85 ( $\text{CH}$ ,  $\text{Ph}$ )], [132.81 (quat. C, *ipsoPh*), 132.85 (quat. C, *ipsoPh*)], [135.49 ( $\text{CH}$ ,  $\text{Ph}$ ), 135.53 ( $\text{CH}$ ,  $\text{Ph}$ )], [137.2 (quat. C, *ipsoPh*), 137.4 (quat. C, *ipsoPh*)], some resonances overlapped in the aromatic region;  $m/z$  (TOF ES<sup>+</sup>) 471.6 ([ $\text{M}+\text{Na}$ ]<sup>+</sup>, 100%); HRMS  $m/z$  (TOF ES<sup>+</sup>) 471.1972 ([ $\text{M}+\text{Na}$ ]<sup>+</sup>.  $\text{C}_{27}\text{H}_{32}\text{O}_4\text{SiNa}$  requires 471.1968).

### 6.3. (2S, 3S, 4R)-2-Azido-1,3,4-octadecanetriol **54**<sup>[46, 149]</sup>

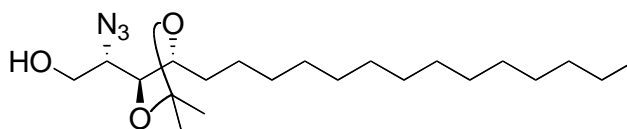


Chemical Formula:  $\text{C}_{18}\text{H}_{37}\text{N}_3\text{O}_3$   
Molecular Weight: 343.505

$\text{TfN}_3$  was freshly prepared prior to the reaction as follows:  $\text{NaN}_3$  (12.5 g, 192 mmol) was dissolved in a minimum volume of  $\text{H}_2\text{O}$  (35 mL, solubility of  $\text{NaN}_3$  in  $\text{H}_2\text{O}$  is  $\sim 0.4 \text{ g mL}^{-1}$ ) and cooled to  $0 \text{ }^\circ\text{C}$ .  $\text{CH}_2\text{Cl}_2$  (35 mL) was added, followed by dropwise addition over 15 min of  $\text{Tf}_2\text{O}$  (15.92 mL, 96 mmol) with vigorous stirring of the solution. The flask was stoppered and stirring continued at  $0 \text{ }^\circ\text{C}$ . After 2 h,  $\text{NaHCO}_3$  solution (30 mL) was carefully added while stirring was continued until gas evolution

had ceased. The reaction contents were then transferred to a separating funnel and the phases were separated. The aqueous phase was washed with  $\text{CH}_2\text{Cl}_2$  (2 × 25 mL). The combined organic phases were washed with a  $\text{NaHCO}_3$  solution (1 × 30 mL). The resulting solution of  $\text{TfN}_3$  in  $\text{CH}_2\text{Cl}_2$  was used in the azidation step without further purification as follows: Amine **52** (10.0 g, 31.5 mmol) and  $\text{CuSO}_4 \cdot 5\text{H}_2\text{O}$  (32 mg, 0.13 mmol) were dissolved in water (85 mL). The  $\text{CH}_2\text{Cl}_2$  solution of  $\text{TfN}_3$  (85 mL) was then added with vigorous stirring. MeOH (570 mL) was then added over 5 min. After 18 h, the reaction mixture was diluted with  $\text{H}_2\text{O}$  (260 mL) and extracted with EtOAc (3 × 260 mL). The combined organic phases were filtered through a silica plug and washed with EtOAc until complete elution of the product. Removal of the solvent under reduced pressure afforded azide **54** as a white solid (10.6 g, 98%).

Data:  $R_f = 0.7$  (eluent: EtOAc); mp 92 – 94 °C [lit. 91 - 92 °C];<sup>[46]</sup>  $[\alpha]_D^{25} + 9.6$  ( $c = 1.0$ ,  $\text{CHCl}_3$ ) [lit.  $[\alpha]_D^{25} + 10$  ( $c = 1$ ,  $\text{CHCl}_3$ )];<sup>[149]</sup>  $\nu_{\text{max}}(\text{film})/\text{cm}^{-1}$  3683m (OH), 3390m (OH) 3328m (OH), 3020s, 2918m, 2847m, 2108m ( $\text{N}_3$ ), 1602w, 1521m, 1462w, 1410m, 1355m, 1215s, 1148m, 1071w, 1014w, 929m, 849w;  $\delta_H$  (300 MHz,  $\text{CDCl}_3/\text{CD}_3\text{OD}$ , 2:1) 0.66 (3H, t,  $J$  6.5,  $\text{CH}_3\text{CH}_2$ ), 0.95-1.22 (24H, stack,  $\text{CH}_2$ ), 1.37-1.42 (2H, stack,  $\text{CH}(\text{OH})\text{CH}_2\text{CH}_2$ ), 3.34-3.39 (3H, stack), 3.58 (1H, dd,  $J$  6.1, 5.7), 3.72 (1H, dd,  $J$  3.9, 3.7);  $\delta_C$  (75 MHz, MeOD) 14.4 ( $\text{CH}_3$ ,  $\text{CH}_2\text{CH}_3$ ), 23.7 ( $\text{CH}_2$ ), 26.7 ( $\text{CH}_2$ ), 30.5 ( $\text{CH}_2$ ), 30.7 ( $\text{CH}_2$ ), 30.8 ( $\text{CH}_2$ ), 33.1 ( $\text{CH}_2$ ), 33.9 ( $\text{CH}_2$ ), 62.5 ( $\text{CH}_2$ ,  $\text{CH}_2\text{OH}$ ), 66.6 (CH,  $\text{CHN}_3$ ), 72.9 (CH,  $\text{CHOH}$ ), 76.0 (CH,  $\text{CHOH}$ ), some resonances overlapped in the alkyl region;<sup>[149]</sup>  $m/z$  (TOF ES<sup>+</sup>) 366.2 ( $[\text{M}+\text{Na}]^+$ , 100%); HRMS  $m/z$  (TOF ES<sup>+</sup>) 366.2728 ( $[\text{M}+\text{Na}]^+$ .  $\text{C}_{18}\text{H}_{37}\text{N}_3\text{O}_3\text{Na}$  requires 366.2733).

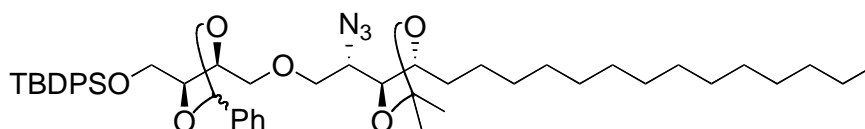
6.4. (2*S*, 3*S*, 4*R*)-2-Azido-3,4-*O*-isopropylidene-1,3,4-octadecanetriol **56**<sup>[47]</sup>

Chemical Formula: C<sub>21</sub>H<sub>41</sub>N<sub>3</sub>O<sub>3</sub>  
Molecular Weight: 383.569

Sc(OTf)<sub>3</sub> (286 mg, 0.58 mmol) was added to a suspension of triol **54** (2.0 g, 5.82 mmol) in a 1:1 mixture of acetone and 2,2-dimethoxypropane (50 mL) at 0 °C resulting in complete dissolution of the solid. The reaction mixture was stirred at this temperature for 20 min and then neutralised with Et<sub>3</sub>N. The solvent was removed under reduced pressure and the residue was dissolved in CH<sub>2</sub>Cl<sub>2</sub> (50 mL). The solution was washed with NaHCO<sub>3</sub> solution (20 mL) and the aqueous phase was extracted with CH<sub>2</sub>Cl<sub>2</sub> (3 × 20 mL). The organic fractions were combined, dried (Na<sub>2</sub>SO<sub>4</sub>), filtered and the solvent was evaporated under reduced pressure to provide a mixture of acetals **55** and **56**, which was dissolved in CH<sub>2</sub>Cl<sub>2</sub>/H<sub>2</sub>O (40 mL, 10:1) and treated with 50% TFA in H<sub>2</sub>O (432 μL, 5.82 mmol). After 10 min, TLC analysis showed that the acyclic acetal in **55** had been chemoselectively hydrolysed. The reaction mixture was neutralised with Et<sub>3</sub>N and diluted with NaHCO<sub>3</sub> solution (20 mL). The phases were separated and the aqueous phase was extracted with CH<sub>2</sub>Cl<sub>2</sub> (2 × 20 mL). The combined organic phases were dried (MgSO<sub>4</sub>), filtered and the solvent removed under reduced pressure. Purification of the residue by flash column chromatography (eluent: 20% EtOAc in hexanes) afforded the acetone **56** as a white, low-melting-point, amorphous solid (1.95 g, 87%). Data: *R*<sub>f</sub> = 0.3 (eluent: 25% EtOAc in hexanes); [α]<sub>D</sub><sup>25</sup> + 23 (*c* = 1.0, CHCl<sub>3</sub>); ν<sub>max</sub> (film)/cm<sup>-1</sup> 3440br (OH), 2925s,

2854s, 2100s (N<sub>3</sub>), 1465m, 1370m, 1247m, 1217m, 1169m, 1063br, 870w, 758s;  $\delta_H$  (300 MHz, CDCl<sub>3</sub>) 0.88 (3H, t, *J* 6.0, CH<sub>3</sub>CH<sub>2</sub>), 1.26-1.30 (23H, stack), 1.34 (3H, s, 1 × C(CH<sub>3</sub>)<sub>2</sub>), 1.43 (3H, s, 1 × C(CH<sub>3</sub>)<sub>2</sub>), 1.50-1.63 (3H, stack), 2.08 (1H, t, *J* 6.0, CH<sub>2</sub>OH), 3.44-3.50 (1H, m), 3.83-3.91 (1H, m), 3.94-4.03 (2H, stack), 4.15-4.21 (1H, m);  $\delta_C$  (75 MHz, CDCl<sub>3</sub>) 14.1 (CH<sub>3</sub>, CH<sub>3</sub>CH<sub>2</sub>), 25.5 (CH<sub>3</sub>, 1 × C(CH<sub>3</sub>)<sub>2</sub>), 26.5 (CH<sub>2</sub>), 28.0 (CH<sub>3</sub>, 1 × C(CH<sub>3</sub>)<sub>2</sub>), 29.35 (CH<sub>2</sub>), 29.41 (CH<sub>2</sub>), 29.53 (CH<sub>2</sub>), 29.58 (CH<sub>2</sub>), 29.59 (CH<sub>2</sub>), 29.65 (CH<sub>2</sub>), 29.68 (CH<sub>2</sub>), 29.69 (CH<sub>2</sub>), 31.9 (CH<sub>2</sub>), 61.2 (CH, CHN<sub>3</sub>), 63.9 (CH<sub>2</sub>, CH<sub>2</sub>OH), 76.6 (CH, CHO), 77.7 (CH, CHO), 108.7 (quat. C, C(CH<sub>3</sub>)<sub>2</sub>), some resonances overlapped in the alkyl region, the spectroscopic data agree with those of the lit.;<sup>[47]</sup> *m/z* (TOF ES<sup>+</sup>) 406.2 ([M+Na]<sup>+</sup>, 100%); HRMS *m/z* (TOF ES<sup>+</sup>) 406.3033 ([M+Na]<sup>+</sup>. C<sub>21</sub>H<sub>41</sub>N<sub>3</sub>O<sub>3</sub>Na requires 406.3046).

**6.5. 1-O-[1-O-(*tert*-Butyldiphenylsilyl)-2,3-O-benzylidene-L-threitol]-2-azido-3,4-O-isopropylidene-1,3,4-D-ribo-octadecantriol 46**



Chemical Formula: C<sub>48</sub>H<sub>71</sub>N<sub>3</sub>O<sub>6</sub>Si  
Molecular Weight: 814.179

Tf<sub>2</sub>O (329  $\mu$ L, 1.96 mmol) was added dropwise over 10 min to a solution of alcohol **53** (1:1 mixture of diastereoisomers, 878 mg, 1.96 mmol) and 2,6-di-*tert*-butylpyridine (484  $\mu$ L, 2.16 mmol) in CH<sub>2</sub>Cl<sub>2</sub> (20 mL) at 0 °C. After 1 h, the reaction mixture was diluted with CH<sub>2</sub>Cl<sub>2</sub> (20 mL) and the resulting solution washed sequentially with cold

## Experimental Section

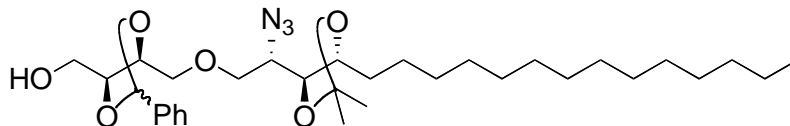
H<sub>2</sub>O (2 × 50 mL) and brine (10 mL), dried (MgSO<sub>4</sub>) and filtered. Removal of the solvent under reduced pressure and purification of the residue by flash column chromatography (eluent: 5% EtOAc in hexanes containing drops of Et<sub>3</sub>N) yielded triflate **49** as a colourless oil (1:1 mixture of diastereoisomers, 870 mg, 85%). The triflate was unstable and used immediately. Selected data on diastereoisomeric mixture: *R*<sub>f</sub> = 0.3 (5% EtOAc in hexanes); δ<sub>H</sub> (300 MHz, CDCl<sub>3</sub>) 1.07 (4.5H, s, (CH<sub>3</sub>)<sub>3</sub>CSi), 1.09 (4.5H, s, (CH<sub>3</sub>)<sub>3</sub>CSi), 3.81-3.99 (2H, stack), 4.11-4.17 (1H, stack), 4.41-4.45 (0.5H, m), 4.52-4.61 (1.5H, stack), 4.69-4.75 (1H, stack), 5.95 (0.5H, s, PhCH), 6.03 (0.5H, s, PhCH), 7.36-7.48 (11H, stack, Ph), 7.63-7.70 (4H, stack, Ph).

A solution of Alcohol **56** (575 mg, 1.5 mmol) in THF (10 mL) was treated with NaH (60% in mineral oil, 64 mg, 1.6 mmol) at 0 °C. After 1 h, a solution of triflate **49** (870 mg, 1.5 mmol) in THF (5 mL) was added dropwise over 5 min. The resulting solution was stirred at this temperature for 1 h and then at r.t. for 12 h. The reaction was then quenched by the addition of MeOH (2 mL) followed by NaHCO<sub>3</sub> solution (10 mL). The phases were separated and the aqueous phase was extracted with CH<sub>2</sub>Cl<sub>2</sub> (3 × 20 mL). The combined organic fractions were washed with brine (15 mL) and dried (MgSO<sub>4</sub>), filtered and the solvent was removed under reduced pressure. The residue was purified by flash column chromatography (eluent: 5% EtOAc in hexanes) to provide ether **46** as a colourless oil (1:1 mixture of diastereoisomers, 1.13 g, 92%). Data on diastereoisomeric mixture: *R*<sub>f</sub> = 0.35 (5% EtOAc in hexanes); ν<sub>max</sub>(film)/cm<sup>-1</sup> 3071w, 2926s, 2855s, 2098s (N<sub>3</sub>), 1589w, 1461m, 1427m, 1379m, 1220m, 1112s, 874w; δ<sub>H</sub> (300 MHz, CDCl<sub>3</sub>) 0.85 (3H, t, *J* 6.6, CH<sub>3</sub>CH<sub>2</sub>), 1.06 (4.5H, s, (CH<sub>3</sub>)<sub>3</sub>CSi), 1.09 (4.5H, s, (CH<sub>3</sub>)<sub>3</sub>CSi), 1.24-1.41 (32H, stack), 3.55-3.63 (1H, stack), 3.67-4.01

## Experimental Section

(7H, stack), 4.09-4.17 (1.5H, stack), 4.23-4.33 (1H, stack), 4.42-4.46 (0.5H, m), 5.99 (0.5H, s, PhCH), 6.00 (0.5H, s, PhCH), 7.33-7.51 (11H, stack, Ph), 7.66-7.73 (4H, stack, Ph);  $\delta_C$  (75 MHz, CDCl<sub>3</sub>) 14.1 (CH<sub>3</sub>, CH<sub>3</sub>CH<sub>2</sub>), 19.2 (quat. C, (CH<sub>3</sub>)<sub>3</sub>CSi), 22.7 (CH<sub>2</sub>), [25.6 (CH<sub>3</sub>, 1 × C(CH<sub>3</sub>)<sub>2</sub>), 25.7 (CH<sub>3</sub>, 1 × C(CH<sub>3</sub>)<sub>2</sub>), 26.4 (CH<sub>2</sub>), [26.82 (CH<sub>3</sub>, C(CH<sub>3</sub>)<sub>3</sub>, 26.86 (CH<sub>3</sub>, C(CH<sub>3</sub>)<sub>3</sub>), [28.1 (CH<sub>3</sub>, 1 × C(CH<sub>3</sub>)<sub>2</sub>, 28.2 (CH<sub>3</sub>, 1 × C(CH<sub>3</sub>)<sub>2</sub>), 29.3 (CH<sub>2</sub>), 29.41 (CH<sub>2</sub>), 29.45 (CH<sub>2</sub>), 29.53 (CH<sub>2</sub>), 29.57 (CH<sub>2</sub>), 29.59 (CH<sub>2</sub>), 29.6 (CH<sub>2</sub>), 29.7 (CH<sub>2</sub>), 31.9 (CH<sub>2</sub>), [59.8 (CH, CHN<sub>3</sub>), 59.9 (CH, CHN<sub>3</sub>)], [64.2 (CH<sub>2</sub>, CH<sub>2</sub>O), 64.3 (CH<sub>2</sub>, CH<sub>2</sub>O)], [72.0 (CH<sub>2</sub>, CH<sub>2</sub>O), 72.2 (CH<sub>2</sub>, CH<sub>2</sub>O)], [72.89 (CH<sub>2</sub>, CH<sub>2</sub>O), 72.94 (CH<sub>2</sub>, CH<sub>2</sub>O)], 75.6 (CH, CHO), [77.7 (CH, CHO), 77.8 (CH, CHO)], [77.9 (CH, CHO), 78.0 (CH, CHO)], [78.7 (CH, CHO), 78.8 (CH, CHO)], [104.0 (CH, PhCH), 104.3 (CH, PhCH)], [108.2 (quat. C, C(CH<sub>3</sub>)<sub>2</sub>), 108.3 (quat. C, C(CH<sub>3</sub>)<sub>2</sub>)], [126.7 (CH, Ph), 126.8 (CH, Ph)], [127.70 (CH, Ph), 127.74 (CH, Ph)], [128.2 (CH, Ph), 128.3 (CH, Ph)], [129.25 (CH, Ph), 129.34 (CH, Ph)], 129.73 (CH, Ph), 129.74 (CH, Ph), 129.77 (CH, Ph), 133.02 (quat. C, *ipso*Ph), 133.05 (quat. C, *ipso*Ph), 133.06 (quat. C, *ipso*Ph), 133.09 (quat. C, *ipso*Ph), 135.6 (CH, Ph), [137.4 (quat. C, *ipso*Ph), 137.5 (quat. C, *ipso*Ph), some resonances overlapped in the alkyl region; *m/z* (TOF ES<sup>+</sup>) 836.3 ([M+Na]<sup>+</sup>, 100%); HRMS *m/z* (TOF ES<sup>+</sup>) 836.5041 ([M+Na]<sup>+</sup>, C<sub>48</sub>H<sub>71</sub>N<sub>3</sub>O<sub>6</sub>SiNa requires 836.5010).

**6.6. 1-O-[2,3-O-benzylidene-L-threitol]-2-azido-3,4-O-isopropylidene-1,3,4-D-ribo-octadecantriol **48****

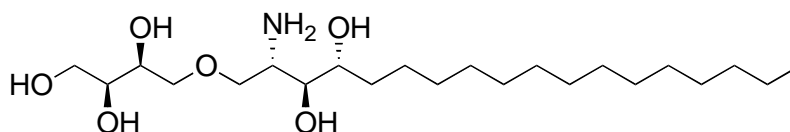


Chemical Formula: C<sub>32</sub>H<sub>53</sub>N<sub>3</sub>O<sub>6</sub>  
Molecular Weight: 575.780

TBAF (1 M solution in THF, 1.4 mL, 1.4 mmol) was added to a solution of silyl ether **46** (1.10 g, 1.35 mmol) in THF (15 mL) at r.t. After 4 h, NH<sub>4</sub>Cl solution (10 mL) was added. The phases were separated and the aqueous phase was extracted with CH<sub>2</sub>Cl<sub>2</sub> (3 × 10 mL). The solvent was removed under reduced pressure and the residue purified by flash column chromatography (eluent: 25% EtOAc in hexanes) to provide alcohol **48** as a colourless oil (1:1 mixture of diastereoisomers, 740 mg, 95%). Data on diastereoisomeric mixture:  $R_f = 0.35$  (30% EtOAc in hexanes);  $\nu_{\max}$  (film)/cm<sup>-1</sup> 3463br (OH), 2924s, 2853s, 2099s (N<sub>3</sub>), 1459m, 1379m, 1246m, 1220m, 1092m, 1065m, 1027m, 869w;  $\delta_H$  (300 MHz, CDCl<sub>3</sub>) 0.88 (3H, t,  $J$  6.6, CH<sub>3</sub>CH<sub>2</sub>), 1.23-1.31 (28H, stack), 1.35-1.41 (3H, stack), 1.45-1.60 (1H, stack), 1.96-2.04 (1H, stack, OH), 3.53-3.60 (1H, stack), 3.67-3.98 (7H, stack), 4.08-4.31 (3H, stack), 5.97 (0.5H, s, PhCH), 6.00 (0.5H, s, PhCH), 7.37-7.40 (3H, stack, Ph), 7.48-7.51 (2H, stack, Ph);  $\delta_C$  (75 MHz, CDCl<sub>3</sub>) 14.0 (CH<sub>3</sub>, CH<sub>2</sub>CH<sub>3</sub>), 22.6 (CH<sub>2</sub>), [25.5 (CH<sub>3</sub>, 1 × C(CH<sub>3</sub>)<sub>2</sub>), 25.6 (CH<sub>3</sub>, 1 × C(CH<sub>3</sub>)<sub>2</sub>), 26.3 (CH<sub>2</sub>), [28.0 (CH<sub>3</sub>, 1 × C(CH<sub>3</sub>)<sub>2</sub>), 28.1 (CH<sub>3</sub>, 1 × C(CH<sub>3</sub>)<sub>2</sub>), 29.27 (CH<sub>2</sub>), 29.33 (CH<sub>2</sub>), 29.35 (CH<sub>2</sub>), 29.46 (CH<sub>2</sub>), 29.51 (CH<sub>2</sub>), 29.57 (CH<sub>2</sub>), 29.6 (CH<sub>2</sub>), 31.8 (CH<sub>2</sub>), [59.8 (CH, CHN<sub>3</sub>), 59.9 (CH, CHN<sub>3</sub>)], 62.5 (CH<sub>2</sub>,

CH<sub>2</sub>O), [71.5 (CH<sub>2</sub>, CH<sub>2</sub>O), 71.6 (CH<sub>2</sub>, CH<sub>2</sub>O)], [72.78 (CH<sub>2</sub>, CH<sub>2</sub>O), 72.84 (CH<sub>2</sub>, CH<sub>2</sub>O)], [75.5 (CH, CHO), 76.4 (CH, CHO), 77.2 (CH, CHO), [77.68 (CH, CHO), 77.70 (CH, CHO)], [79.7 (CH, CHO), 79.9 (CH, CHO)], [103.8 (CH, PhCH), 104.0 (CH, PhCH)], [108.20 (quat. C, (CH<sub>3</sub>)<sub>2</sub>C), 108.23 (quat. C, (CH<sub>3</sub>)<sub>2</sub>C)], 126.6 (CH, Ph), [128.2 (CH, Ph), 128.3 (CH, Ph)], [129.3 (CH, Ph), 129.4 (CH, Ph)], [137.2 (quat. C, *ipso*Ph), 137.4 (quat. C, *ipso*Ph), some resonances overlapped in alkyl region; *m/z* (TOF ES<sup>+</sup>) 598.2 ([M+Na]<sup>+</sup>, 100%); HRMS *m/z* (TOF ES<sup>+</sup>) 598.3805 ([M+Na]<sup>+</sup>. C<sub>32</sub>H<sub>53</sub>N<sub>3</sub>O<sub>6</sub>Na requires 598.3832).

#### 6.7. 1-O-[L-Threitol]-2-amino-1,3,4-D-ribo-octadecantriol **47**

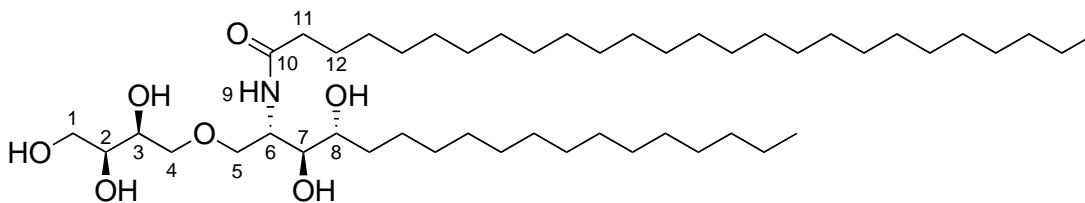


Chemical Formula: C<sub>22</sub>H<sub>47</sub>NO<sub>6</sub>  
Molecular Weight: 421.61

Ce(OTf)<sub>3</sub> (117 mg, 0.20 mmol) was added to a vigorously stirred solution of acetal **48** (200 mg, 0.32 mmol) in MeNO<sub>2</sub> (saturated with H<sub>2</sub>O, 3 mL) and CH<sub>2</sub>Cl<sub>2</sub> (2 mL). After 4 h at r.t., the reaction mixture was diluted with CH<sub>2</sub>Cl<sub>2</sub> (5 mL) and NaHCO<sub>3</sub> solution (10 mL) was added. The aqueous phase was extracted with CH<sub>2</sub>Cl<sub>2</sub> (10 mL) and the organic phases were combined and washed with brine (5 mL) and then dried (Na<sub>2</sub>SO<sub>4</sub>). The solvent was removed under reduced pressure. The residue (yellowish paste) was dissolved in MeOH (5 mL) and Pd/C (30 mg, 32 mol) and AcOH (40 μL, 0.65 mmol) were added. The reaction vessel was evacuated and then placed under an atmosphere of H<sub>2</sub>. The suspension was stirred overnight. The reaction mixture

was filtered and the filtrate was concentrated under reduced pressure. The residue was purified by column chromatography (eluent: 10% MeOH in CHCl<sub>3</sub> to 50% MeOH in CHCl<sub>3</sub>) to afford amine **47** as a white foam (72 mg, 50%). Data:  $R_f = 0.1$  (20% MeOH in CHCl<sub>3</sub>);  $\delta_H$  (300 MHz, CDCl<sub>3</sub>) 0.79 (3H, t,  $J$  6.7, CH<sub>2</sub>CH<sub>3</sub>), 1.08-1.32 (23H, stack, alkyl chain), 1.38-1.50 (1H, m), 1.55-1.69 (2H, m), 3.14-3.21 (1H, m), 3.25-3.65 (9H, stack), 3.68-3.75 (1H, m), exchangeable protons were exchanged with deuterium from CD<sub>3</sub>OD for clarity prior to running the <sup>1</sup>H-NMR spectrum;  $\delta_C$  (75 MHz, CDCl<sub>3</sub>) 13.9 (CH<sub>3</sub>, CH<sub>2</sub>CH<sub>3</sub>), 22.5 (CH<sub>2</sub>), 25.6 (CH<sub>2</sub>), 29.2 (CH<sub>2</sub>), 29.6 (CH<sub>2</sub>), 31.8 (CH<sub>2</sub>), 33.5 (CH<sub>2</sub>), 52.9 (CH), 63.4 (CH<sub>2</sub>), 70.1 (CH), 71.0 (CH<sub>2</sub>), 71.6 (CH), 72.5 (CH<sub>2</sub>), 73.2 (CH), 73.9 (CH), some resonances overlapped in alkyl region;  $m/z$  (TOF ES<sup>+</sup>) 422.3 ([M+H]<sup>+</sup>, 100%); HRMS  $m/z$  (TOF ES<sup>+</sup>) 422.3489 ([M+H]<sup>+</sup>. C<sub>22</sub>H<sub>48</sub>NO<sub>6</sub>, requires 422.3482).

### 6.8. 1-O-[L-Threitol]-2-hexacosanoylamino-1,3,4-D-ribo-octadecantriol **39**<sup>[51]</sup>



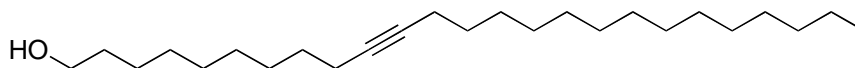
Chemical Formula: C<sub>48</sub>H<sub>97</sub>NO<sub>7</sub>  
Molecular Weight: 800.29

Hexacosanoic acid (37.6 mg, 94.9 mol) was placed in (COCl)<sub>2</sub> (1.0 mL) and the resulting solution stirred at 70 °C for 2 h, after which time, the solution was cooled to r.t. and the (COCl)<sub>2</sub> was removed under a stream of dry argon. The residual volatiles

were removed under reduced pressure. The resulting crude acyl chloride was dissolved in THF (500  $\mu\text{L}$ ) and added with vigorous stirring to a solution of amine **47** (20 mg, 47  $\mu\text{mol}$ ) in THF/NaOAc<sub>(aq)</sub> (8 M, 800  $\mu\text{L}$ , 1:1). Vigorous stirring was maintained for 2 h, after which time, the mixture was left to stand and the phases were separated. The aqueous phase was extracted with THF (2  $\times$  1 mL) and the combined organic phases were evaporated under reduced pressure. Purification of the residue by column chromatography (gradient from CHCl<sub>3</sub> to 15% MeOH in CHCl<sub>3</sub>) afforded threitol ceramide **39** as a white solid (23 mg, 60%). Data:  $R_f$  = 0.3 (8% MeOH in CHCl<sub>3</sub>); mp 107 - 109  $^\circ\text{C}$ ;  $[\alpha]_D$  (the insolubility of this amphiphilic compound at r.t. prevented us from obtaining reliable optical rotation data);  $\nu_{\text{max}}$  (neat disc)/ $\text{cm}^{-1}$  3308br m (OH, NH), 2915s, 2849s, 2098w, 1634m (C=O), 1540m, 1471m, 1108m, 1070m, 1026m, 718m;  $\delta_H$  (500 MHz, d<sub>8</sub>-THF, 45  $^\circ\text{C}$ ) 0.89 (6H, app t,  $J$  6.7, 2  $\times$  CH<sub>2</sub>CH<sub>3</sub>), 1.25-1.63 (72H, stack, alkyl chain), 2.12 (2H, t,  $J$  7.7, C(O)CH<sub>2</sub>), 3.40-3.47 (2H, stack, C(7)H, C(8)H), 3.47-3.57 (5H, stack, C(4)H<sub>2</sub>, C(1)H<sub>2</sub>, C(3)H or C(2)H), 3.59-3.63 (1H, m, C(5)H<sub>a</sub>H<sub>b</sub>), 3.67-3.72 (2H, stack, C(5)H<sub>a</sub>H<sub>b</sub>, C(2)H or C(3)H), 4.14-4.18 (1H, m, C(6)H), 6.93-6.96 (1H, m, NH);  $\delta_C$  (125 MHz, d<sub>8</sub>-THF, 45  $^\circ\text{C}$ ) 14.3 (CH<sub>3</sub>, 2  $\times$  CH<sub>2</sub>CH<sub>3</sub>), [23.5 (CH<sub>2</sub>), 26.6 (CH<sub>2</sub>), 26.8 (CH<sub>2</sub>), 29.3 (CH<sub>2</sub>), 30.3 (CH<sub>2</sub>), 30.5 (CH<sub>2</sub>), 30.59 (CH<sub>2</sub>), 30.64 (CH<sub>2</sub>), 30.7 (CH<sub>2</sub>), 30.8 (CH<sub>2</sub>), 32.8 (CH<sub>2</sub>), 34.1 (CH<sub>2</sub>), some alkyl resonances overlapped], 36.9 (CH<sub>2</sub>, C(O)CH<sub>2</sub>), 51.8 (CH, C(6)), 64.6 (CH<sub>2</sub>, C(1)), 71.3 (CH, C(2) or C(3)), 71.5 (CH<sub>2</sub>, C(5)), 73.0 (CH, C(8)), 73.1 (CH, C(3) or C(2)), 74.1 (CH<sub>2</sub>, C(4)), 76.7 (CH, C(7)), 173.0 (quat. C, C=O), the spectroscopic data were not directly comparable with those of the lit. as those were

measured in deuterated pyridine;<sup>[51]</sup>  $m/z$  (TOF ES<sup>+</sup>) 822.7 ([M+Na]<sup>+</sup>, 100%); HRMS  $m/z$  (TOF ES<sup>+</sup>) 822.7175 ([M+Na]<sup>+</sup>. C<sub>48</sub>H<sub>97</sub>NO<sub>7</sub>Na requires 822.7163).

### 6.9. Pentacos-10-yn-1-ol **59**

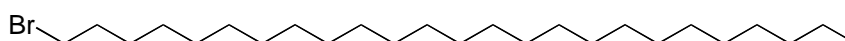


Chemical Formula: C<sub>25</sub>H<sub>48</sub>O  
Molecular Weight: 364.65

<sup>n</sup>BuLi (2.5 M solution in hexanes, 8.72 mL, 21.8 mmol) was added dropwise over 40 min to a solution of 10-undecyn-1-ol **57** (1.75 g, 10.4 mmol) in THF (21 mL) containing HMPA (7.68 mL, 41.6 mmol) at -78 °C. After 15 min, a solution of 1-bromotetradecane **58** (3.17 g, 11.4 mmol) in THF (2 mL) was added. The reaction mixture was stirred at -78 °C for 1 h and then left to warm to r.t. overnight. The reaction mixture was then diluted with Et<sub>2</sub>O (20 mL) and quenched by slow addition of H<sub>2</sub>O (20 mL). The phases were separated and the aqueous phase was extracted with Et<sub>2</sub>O (2 × 20 mL). The combined organic phases were dried with MgSO<sub>4</sub> and the volatiles were removed under reduced pressure. The residue was purified by column chromatography (eluent: 20% Et<sub>2</sub>O in hexanes) to afford the alkyne **59** as a white solid (1.57 g, 40%). Data:  $R_f$  = 0.15 (5% EtOAc in hexanes);  $\nu_{\max}$  (neat)/cm<sup>-1</sup> 3357w (OH), 2919s, 2848s, 1459m, 1130w, 1057m, 1036m, 1013m, 975w, 725s;  $\delta_H$  (300 MHz, CDCl<sub>3</sub>) 0.86 (3H, t,  $J$  6.8, CH<sub>3</sub>CH<sub>2</sub>), 1.15-1.60 (38H, stack, alkyl chain), 2.12 (4H, app. t,  $J$  7.1, CH<sub>2</sub>CCCH<sub>2</sub>), 6.63 (2H, app. q,  $J$  5.5, CH<sub>2</sub>OH), resonance for OH not visible;  $\delta_C$  (75 MHz, CDCl<sub>3</sub>) 14.1 (CH<sub>3</sub>, CH<sub>3</sub>CH<sub>2</sub>), 18.8 (CH<sub>2</sub>), 22.7 (CH<sub>2</sub>), 25.7

(CH<sub>2</sub>), 28.9 (CH<sub>2</sub>), 29.2 (CH<sub>2</sub>), 29.4 (CH<sub>2</sub>), 29.5 (CH<sub>2</sub>), 29.6 (CH<sub>2</sub>), 29.7 (CH<sub>2</sub>), 32.0 (CH<sub>2</sub>), 32.8 (CH<sub>2</sub>), 63.1 (CH<sub>2</sub>, CH<sub>2</sub>OH), 80.2 (quat. C, CC), 80.3 (quat. C, CC), some resonances overlapped in the alkyl region; *m/z* (TOF ES<sup>+</sup>) 471.3 ([M+Ag]<sup>+</sup>, 100%); HRMS *m/z* (TOF ES<sup>+</sup>) 471.2745 ([M+Ag]<sup>+</sup>, C<sub>25</sub>H<sub>48</sub>OAg requires 471.2756).

### 6.10. 1-Bromo-pentacosane 61

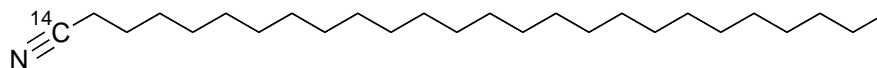


Chemical Formula: C<sub>25</sub>H<sub>51</sub>Br  
Molecular Weight: 431.58

Pd/C (29 mg, 0.27 mmol) was added to a solution of alkyne **59** (1.0 g, 2.74 mmol) in Et<sub>2</sub>O (10 mL). The reaction vessel was evacuated and replaced with a H<sub>2</sub> atmosphere and then the mixture was stirred overnight. The slurry was then filtered, washing the residue with hot THF (2 × 5 mL). The solvent was evaporated under reduced pressure to afford alcohol **60** as a white paste (943 mg, 95%). Data: *R<sub>f</sub>* = 0.15 (5% EtOAc in hexanes); *v*<sub>max</sub> (neat)/cm<sup>-1</sup> 3278br (OH), 2917s, 2849s, 1473m, 1452m, 1062m, 731m, 719m; *δ<sub>H</sub>* (300 MHz, CDCl<sub>3</sub>) 0.87 (3H, t, *J* 6.5, CH<sub>3</sub>CH<sub>2</sub>), 1.20-1.37 (44H, stack, alkyl chain), 1.50-1.60 (2H, m, CH<sub>2</sub>CH<sub>2</sub>OH), 3.63 (2H, t, *J* 6.4, CH<sub>2</sub>OH); *δ<sub>C</sub>* (75 MHz, CDCl<sub>3</sub>) 14.1 (CH<sub>3</sub>, CH<sub>2</sub>CH<sub>3</sub>), 22.7 (CH<sub>2</sub>), 25.7 (CH<sub>2</sub>), 29.38 (CH<sub>2</sub>), 29.45 (CH<sub>2</sub>), 29.7 (CH<sub>2</sub>), 31.9 (CH<sub>2</sub>), 32.8 (CH<sub>2</sub>), 63.1 (CH<sub>2</sub>, CH<sub>2</sub>OH), some resonances overlapped in alkyl region. Satisfactory mass spectral analysis could not be obtained on alcohol **60** and was then used without further purification in the next step. PPh<sub>3</sub> (531 mg, 2.02 mmol) and CBr<sub>4</sub> (492 mg, 1.48 mmol) were added sequentially to a solution of alcohol **60** (500 mg, 1.35 mmol) in CH<sub>2</sub>Cl<sub>2</sub> (10 mL) at 0

°C. After 1 h, hexanes (10 mL) were added slowly and the resulting precipitate was filtered off. The filtrate was diluted with CH<sub>2</sub>Cl<sub>2</sub> (20 mL) and washed with H<sub>2</sub>O (10 mL). The phases were separated and the organic phase was dried (Na<sub>2</sub>SO<sub>4</sub>). The volatiles were evaporated under reduced pressure to afford a residue, which was purified by column chromatography (eluent: 2% Et<sub>2</sub>O in hexanes) to afford alkyl bromide **61** as a white solid (378 mg, 65%). Data: *R*<sub>f</sub> = 0.4 (eluent: hexanes); δ<sub>H</sub> (300 MHz, CDCl<sub>3</sub>) 0.88 (3H, t, *J* 6.6, CH<sub>2</sub>CH<sub>3</sub>), 1.20-1.31 (43H, stack, alkyl chain), 1.39-1.48 (1H, m), 1.79-1.87 (2H, m), 3.40 (2H, t, *J* 6.9, CH<sub>2</sub>Br); δ<sub>C</sub> (75 MHz, CDCl<sub>3</sub>) 14.1 (CH<sub>3</sub>, CH<sub>2</sub>CH<sub>3</sub>), 22.7 (CH<sub>2</sub>), 28.2 (CH<sub>2</sub>), 28.8 (CH<sub>2</sub>), 29.4 (CH<sub>2</sub>), 29.5 (CH<sub>2</sub>), 29.7 (CH<sub>2</sub>), 31.9 (CH<sub>2</sub>), 32.8 (CH<sub>2</sub>), 34.0 (CH<sub>2</sub>), some resonances overlapped in alkyl region; satisfactory mass spectral analysis could not be obtained for bromide **61**.

### 6.11. [<sup>14</sup>C]Hexacosan-1-nitrile **62**

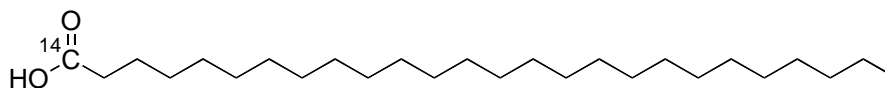


Chemical Formula: C<sub>26</sub>H<sub>51</sub>N  
Molecular Weight: 377.69

Alkyl bromide **61** (13 mg, 30 μmol) was added to a solution of Na<sup>14</sup>CN (1 mg, 20 μmol, 53 mCi mmol<sup>-1</sup> (1.961 GBq mmol<sup>-1</sup>)) in DMSO (1 mL). The mixture was heated at 85 °C for 72 h and then cooled to r.t. Et<sub>2</sub>O (1 mL) was added to the mixture followed by H<sub>2</sub>O (1 mL). The phases were separated and the aqueous phase was extracted with Et<sub>2</sub>O (3 × 1 mL). The combined organic phases were dried with MgSO<sub>4</sub> and the volatiles were removed under reduced pressure. The residue was

purified by column chromatography (eluent: 5% EtOAc in hexanes) to provide nitrile **62** (7 mg, 95%). Data:  $R_f = 0.35$  (5% EtOAc in hexanes);  $\nu_{\max}$  (film)/ $\text{cm}^{-1}$  2914s (br), 2848s, 2241w (CN), 1633w, 1471s, 1424w, 1377w, 730w, 716s;  $\delta_H$  (300 MHz,  $\text{CDCl}_3$ ) 0.86 (3H, t,  $J$  7.0,  $\text{CH}_2\text{CH}_3$ ), 1.90-1.32 (42H, stack, alkyl chain), 1.35-1.49 (2H, m), 1.60-1.72 (2H, m), 2.31 (2H, t,  $J$  6.7,  $\text{CH}_2\text{CN}$ );  $\delta_C$  (75 MHz,  $\text{CDCl}_3$ ) 14.1 ( $\text{CH}_3$ ,  $\text{CH}_2\text{CH}_3$ ), 17.1 ( $\text{CH}_2$ ), 22.7 ( $\text{CH}_2$ ), 25.4 ( $\text{CH}_2$ ), 28.7 ( $\text{CH}_2$ ), 28.8 ( $\text{CH}_2$ ), 29.3 ( $\text{CH}_2$ ), 29.4 ( $\text{CH}_2$ ), 29.5 ( $\text{CH}_2$ ), 29.7 ( $\text{CH}_2$ ), 30.0 ( $\text{CH}_2$ ), 31.9 ( $\text{CH}_2$ ), some resonances overlapped in the alkyl region; the nitrile resonance not observed;  $m/z$  (TOF  $\text{ES}^+$ ) 400.3 ( $[\text{M}+\text{Na}]^+$ , 100%); HRMS  $m/z$  (TOF  $\text{ES}^+$ ) 400.3932 ( $[\text{M}+\text{Na}]^+$ .  $\text{C}_{26}\text{H}_{51}\text{NNa}$  requires 400.3919); spectroscopic data and mass spectral analyses were taken of the nonradiolabelled nitrile; TLC and radiogram that compared radiolabelled with nonradiolabelled product provided confirmation of the radiolabelled nitrile **62**.

### 6.12. [ $^{14}\text{C}$ ]Hexacosanoic acid **63**

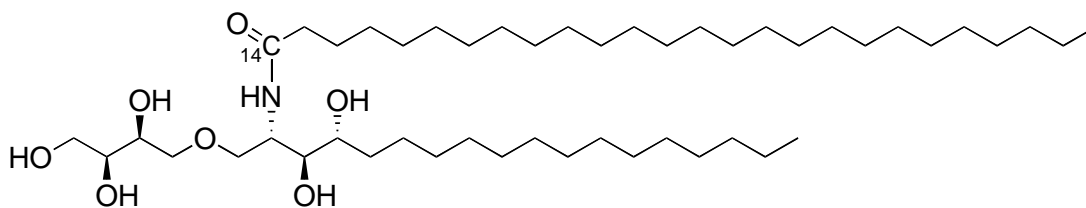


Chemical Formula:  $\text{C}_{26}\text{H}_{52}\text{O}_2$   
Molecular Weight: 396.69

A solution of NaOH (220 mg, 5.5 mmol) in a mixture of EtOH (2.4 mL) and  $\text{H}_2\text{O}$  (0.3 mL) was prepared. [ $^{14}\text{C}$ ]Nitrile **62** (7 mg, 20 mol) was placed in 1 mL of this solution and the mixture was heated at 70 °C for 6 d, after which time, TLC indicated that the alkyl nitrile had been consumed. The mixture was diluted with  $\text{H}_2\text{O}$  (2 mL) and the pH reduced to pH = 3 with conc. hydrochloric acid. The solution was extracted with  $\text{Et}_2\text{O}$

(3 × 2 mL). The phases were separated and the organic fraction was dried (MgSO<sub>4</sub>). The volatiles were evaporated under reduced pressure to afford the fatty acid **63** as a white solid (7.0 mg, 95%). Data: *R*<sub>f</sub> = 0.25 (eluent: 30% EtOAc in hexanes); δ<sub>H</sub> (300 MHz, CDCl<sub>3</sub>) 0.88 (3H, t, *J* 6.7, CH<sub>2</sub>CH<sub>3</sub>), 1.25-1.35 (44H, stack, alkyl chain), 1.60-1.69 (2H, m), 2.35 (2H, t, *J* 6.9, CH<sub>2</sub>CO<sub>2</sub>H), carboxylic acid resonance not visible; spectroscopic data agree with that from commercially available material; *m/z* (TOF ES-) 395.3 ([M-H]<sup>-</sup>, 100%); HRMS *m/z* (TOF ES-) 395.3908 ([M-H]<sup>-</sup>. C<sub>26</sub>H<sub>51</sub>O<sub>2</sub> requires 395.3905); spectroscopic data and mass spectral analyses were taken of the nonradiolabelled cerotic acid; TLC and radiogram that compared radiolabelled with nonradiolabelled product provided confirmation of the radiolabelled cerotic acid **63**.

**6.13. [<sup>14</sup>C]-1-O-[L-Threitol]-2-hexacosanoylamino-1,3,4-D-ribo-octadecantriol  
[<sup>14</sup>C]-39**

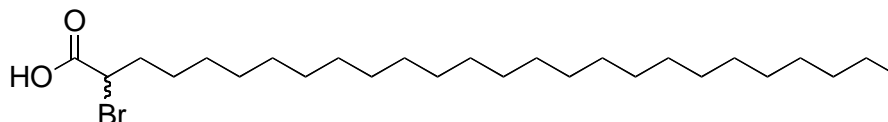


Chemical Formula: C<sub>48</sub>H<sub>97</sub>NO<sub>7</sub>  
Molecular Weight: 800.29

A solution of [<sup>14</sup>C]hexacosanoic acid [<sup>14</sup>C]-**63** (7.0 mg, 20 μmol) in (COCl)<sub>2</sub> (0.5 mL) was stirred at 70 °C for 2 h, after which time, the solution was cooled to r.t. and the (COCl)<sub>2</sub> was removed under a stream of dry Ar. The residual volatiles were removed under reduced pressure. The resulting crude acyl chloride (20 μmol, assuming 100%

conversion) was dissolved in THF (0.5 mL) and added with vigorous stirring to a solution of amine **47** (16.8 mg, 40  $\mu$ mol) in THF/NaOAc<sub>(aq)</sub> (8 M, 0.8 mL, 1:1). Vigorous stirring was maintained for 2 h, after which time, TLC showed that the fatty acid had been consumed. The mixture was left to stand and the phases were separated. The aqueous phase was extracted with THF (2  $\times$  1.0 mL) and the combined organic phases were evaporated under reduced pressure. Purification of the residue by column chromatography (eluting a gradient from CHCl<sub>3</sub> to 15% MeOH in CHCl<sub>3</sub>) afforded threitol ceramide [<sup>14</sup>C]-**39** as a white solid (13.6 mg, 85%). The product characterisation was inferred after TLC and radiogram of radiolabelled and nonradiolabelled products. We could not obtain the data directly from the radiolabel compound because of health and safety policies and health concerns.

#### 6.14. $\alpha$ -Bromo cerotic acid **74**

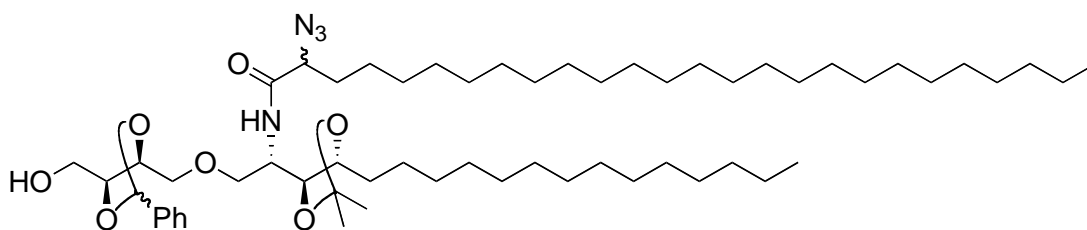


Chemical Formula: C<sub>26</sub>H<sub>51</sub>BrO<sub>2</sub>  
Molecular Weight: 475.586

A mixture of cerotic acid (200 mg, 0.5 mmol) and red phosphorus (16 mg, 0.5 mmol) was heated to 95 °C and Br<sub>2</sub> (90  $\mu$ L, 1.75 mmol) was added dropwise over 1 min at this temperature with stirring. The reaction mixture was stirred for 6 h after which time the heat was removed and the mixture allowed to cool to r.t. The reaction mixture was diluted with Et<sub>2</sub>O (10 mL) and washed with H<sub>2</sub>O (10 mL). The aqueous phase was extracted with Et<sub>2</sub>O (2  $\times$  10 mL), and the combined organic fractions were

washed with brine (10 mL), dried with  $\text{MgSO}_4$ , filtered and the solvent was removed under reduced pressure. The solid residue was re-crystallised from hexanes to yield  $\alpha$ -bromo acid **74** as a white solid (160 mg, 67%). Data:  $R_f = 0.35$  (eluent: 30% EtOAc in hexanes); mp. = 73 - 74 °C;  $\nu_{\text{max}}(\text{film})/\text{cm}^{-1}$  2915s, 2849s, 1715m (C=O), 1697s (C=O), 1476.5w, 1462m, 1429w, 1241w (br), 1164w, 1120w, 906w, 725m, 662m;  $\delta_H$  (300 MHz,  $\text{CDCl}_3$ ) 0.88 (3H, t,  $J$  6.8,  $\text{CH}_2\text{CH}_3$ ), 1.21-1.33 (44H, stack,  $(\text{CH}_2)$ acyl chain), 1.95-2.21 (2H, m,  $\text{CH}_2\text{CHBr}$ ), 4.24 (1H, t,  $J$  7.6,  $\text{CH}_2\text{CHBr}$ );  $\delta_C$  (75 MHz,  $\text{CDCl}_3$ ): 14.1 ( $\text{CH}_3$ ,  $\text{CH}_2\text{CH}_3$ ), 22.7 ( $\text{CH}_2$ ), 27.2 ( $\text{CH}_2$ ), 28.8 ( $\text{CH}_2$ ), 29.3 ( $\text{CH}_2$ ), 29.4 ( $\text{CH}_2$ ), 29.5 ( $\text{CH}_2$ ), 29.7 ( $\text{CH}_2$ ), 29.8 ( $\text{CH}_2$ ), 32.0 ( $\text{CH}_2$ ), 34.7 ( $\text{CH}_2$ ,  $\text{CH}_2\text{CHBr}$ ), 45.4 ( $\text{CH}$ ,  $\text{CH}_2\text{CHBr}$ ), 176.0 (quat. C, C=O), some resonance overlapped on the alkyl region;  $m/z$  (TOF ES-) 473.3, 475.3 ( $[\text{M}-\text{H}]^-$ , 100%); HRMS  $m/z$  (TOF ES-) 473.2989 ( $[\text{M}-\text{H}]^-$ .  $\text{C}_{26}\text{H}_{50}\text{BrO}_2$  requires 473.2994).

**6.15. 1-O-[2,3-O-benzylidene-L-threitol]-2-( $\alpha$ -azido-hexacosanoyl)amino-3,4-O-isopropylidene-1,3,4-D-ribo-octadecantriol **70****



Chemical Formula:  $\text{C}_{58}\text{H}_{104}\text{N}_4\text{O}_7$   
Molecular Weight: 969.469

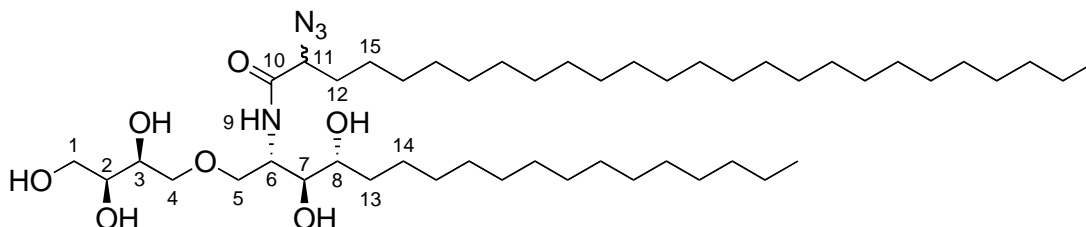
Me<sub>3</sub>P (1 M solution in THF, 1.25 mL, 1.25 mmol) was added to a solution of azide **48** (700 mg, 1.21 mmol) in THF (10 mL) at r.t. The reaction mixture was stirred for 3 h, after which time, TLC showed complete consumption of the starting material. H<sub>2</sub>O (1 mL, 55.55 mmol) was added and the reaction mixture was stirred for a further 1 h. The volatiles were then removed under reduced pressure and the resulting mixture was azeotroped with dry toluene (3 × 5 mL) to remove any residual H<sub>2</sub>O. The crude amine **72** was used in the next step without further purification as a stock solution 0.1 M in CH<sub>2</sub>Cl<sub>2</sub>.

Bromide **74** (0.18 mmol, 85 mg) was dissolved in THF (1.8 mL) and treated with 2 equivalents of TMSN<sub>3</sub> (1 M, 0.36 mmol, 360 μL) followed by the addition of 1.5 equiv of Py.xHF (70 wt. % HF, 0.27 mmol, 5 μL). The reaction mixture was stirred at r.t. for 15 min after which time the temperature was brought up to 45 °C. After 24 h, mass spectral analysis of the reaction mixture showed that the reaction was complete. The volatiles were removed under reduced pressure and the crude α-azido carboxylic acid **73** (80 mg, 0.18 mmol) was dissolved in CH<sub>2</sub>Cl<sub>2</sub> (1.5 mL). EDC.HCl (35 mg, 0.18 mmol) was added to the solution at r.t. and the resulting reaction mixture was stirred for 10 min. A solution of the crude amine **72** (0.1 M, 0.20 mmol, 200 μL) was then added. The mixture was stirred for 6 h. Silica gel (500 mg) was added to the reaction mixture and the suspension was stirred for 10 min, after which time, the resulting slurry was applied directly on to a silica gel column and eluted with 20% EtOAc in hexanes yielding the amide **71** as a white solid (105 mg, 60% from **48**, approx. 1:1:1:1 mixture of four diastereoisomers). Data on the diastereoisomeric mixture: *R*<sub>f</sub> = 0.2 (20% EtOAc in hexanes); *v*<sub>max</sub> (film)/cm<sup>-1</sup> 3583w, 3299br (NH), 2921s (CH), 2852s

## Experimental Section

(CH), 2105m (N<sub>3</sub>), 1652m (C=O), 1545w, 1465s, 1377m, 1246w, 1220w, 1068w, 758w, 721w, 698w, 665w;  $\delta_H$  (300 MHz) 0.88 (6H, app. t,  $J$  6.9, 2 × CH<sub>2</sub>CH<sub>3</sub>), 1.16-1.56 (76H, stack), 1.73-1.92 (2H, stack), 2.08-2.16 (1H, stack), 3.55-4.00 (8H, stack), 4.04-4.26 (4H, stack), 5.96-5.97 (1H, stack, PhCH), 6.42- 6.54 (1H, stack, CHNHCO), 7.37-7.43 (3H, stack, Ph), 7.46-7.50 (2H, stack, Ph);  $\delta_C$  (75 MHz) 14.1 (CH<sub>3</sub>, CH<sub>2</sub>CH<sub>3</sub>), 22.7 (CH<sub>2</sub>), 25.3 (CH<sub>2</sub>), 25.4 (CH<sub>2</sub>), [25.6 (CH<sub>3</sub>, CCH<sub>3</sub>), 25.7 (CH<sub>3</sub>, CCH<sub>3</sub>)], 26.5 (CH<sub>2</sub>), 26.6 (CH<sub>2</sub>), [27.9 (CH<sub>3</sub>, CCH<sub>3</sub>), 28.0 (CH<sub>3</sub>, CCH<sub>3</sub>)], 29.0 (CH<sub>2</sub>), 29.1 (CH<sub>2</sub>), 29.2 (CH<sub>2</sub>), 29.27 (CH<sub>2</sub>), 29.34 (CH<sub>2</sub>), 29.4 (CH<sub>2</sub>), 29.6 (CH<sub>2</sub>), 29.7 (CH<sub>2</sub>), 31.9 (CH<sub>2</sub>), 32.0 (CH<sub>2</sub>), 32.1 (CH<sub>2</sub>), 32.2 (CH<sub>2</sub>), 48.27 (CH), 48.33 (CH), 48.48 (CH), 48.54 (CH), 56.4 (CH), 62.50 (CH<sub>2</sub>), 62.55 (CH<sub>2</sub>), 62.58 (CH<sub>2</sub>), 62.64 (CH<sub>2</sub>), 64.1 (CH), 64.2 (CH), 64.4 (CH), 64.5 (CH), 71.3 (CH<sub>2</sub>), 71.4 (CH<sub>2</sub>), 75.8 (CH), 75.9 (CH), 76.0 (CH), 76.87 (CH), 76.92 (CH), 77.0 (CH), 77.4 (CH), 77.57 (CH), 77.67 (CH), 77.75 (CH), 77.82 (CH), 79.3 (CH), 79.4 (CH), 79.8 (CH), 79.9 (CH), 103.84 (CH, PhCH), 103.87 (CH, PhCH), 103.89 (CH, PhCH), 108.07 (quat. C, C(CH<sub>3</sub>)<sub>2</sub>), 108.00 (quat. C, C(CH<sub>3</sub>)<sub>2</sub>), 108.16 (quat. C, C(CH<sub>3</sub>)<sub>2</sub>), 108.19 (quat. C, C(CH<sub>3</sub>)<sub>2</sub>), 126.5 (CH, Ph), 128.35 (CH, Ph), 128.41 (CH, Ph), 129.45 (CH, Ph), 129.52 (CH, Ph), 137.2 (quat. C, *ipso*Ph), 168.85 (quat. C, NHCO), 168.89 (quat. C, NHCO), 169.0 (quat. C, NHCO), 170.2 (quat. C, NHCO); some resonance overlap;  $m/z$  (TOF ES<sup>+</sup>) 991.7 ([M +Na]<sup>+</sup>, 100%); HRMS  $m/z$  (TOF ES<sup>+</sup>) 991.7795 ([M+Na]<sup>+</sup>. C<sub>58</sub>H<sub>104</sub>N<sub>4</sub>O<sub>7</sub>Na requires 991.7803).

**6.16. 1-O-[L-threitol]-2-( $\alpha$ -azido-hexacosanoyl)amino-1,3,4-D-ribo-octadecantriol **70****

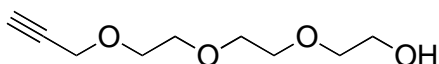


Chemical Formula:  $C_{48}H_{96}N_4O_7$   
Molecular Weight: 841.30

$Ce(OTf)_3$  (36.4 mg, 0.062 mmol) was added to a solution of bis-acetal **71** (100 mg, 0.103 mmol) in 4:1  $CH_2Cl_2/MeNO_2$  (1 mL). The resulting mixture was stirred for 2 h after which time, TLC showed complete disappearance of the starting material. The mixture was applied directly on to a silica column and eluted with a solvent gradient from  $CH_2Cl_2$  to 9:1  $CHCl_3/MeOH$  to provide the pentaol **70** as a white solid (69 mg, 80%, 1:1 mixture of diastereoisomers). Data on the mixture:  $R_f = 0.35$  (10% MeOH in  $CHCl_3$ ); mp. 109-110 °C;  $\nu_{max}(\text{neat disc})/cm^{-1}$ : 3303br w (OH, NH), 2914s, 2849s, 2450br w, 2101m ( $N_3$ ), 1655m (C=O), 1470m, 1446m, 1271w, 1115m, 1073m, 942m, 719m;  $\delta_H$  ( $CDCl_3/CD_3OD$  2:1, 300 MHz) 0.82 (6H, app. t,  $J$  6.8,  $CH_2CH_3$ ), 1.19-1.61 (72H, stack), 1.69-1.85 (1H, stack,  $N_3CHCO$ ), 3.50-3.85 (11H, stack), 4.14 (1H, stack);  $\delta_C$  (75 MHz) 13.9 ( $CH_3, CH_2CH_3$ ), 22.5 ( $CH_2$ ), 25.4 ( $CH_2$ ), 25.77 ( $CH_2$ ), 25.82 ( $CH_2$ ), 29.1 ( $CH_2$ ), 29.2 ( $CH_2$ ), 29.3 ( $CH_2$ ), 29.5 ( $CH_2$ ), 29.6 ( $CH_2$ ), 31.78 ( $CH_2$ ), 31.84 ( $CH_2$ ), 31.9 ( $CH_2$ ), 32.3 ( $CH_2$ ), 32.4 ( $CH_2$ ), 49.8 (CH,  $CHN_3$ ), 55.6 (CH, CHOH), 63.6 ( $CH_2, CH_2OH$ ), 63.8 (CH, CHOH), 70.1 ( $CH_2, CH_2OH$ ), 71.6 (CH, CHOH), 72.3 (CH, CHOH), [72.6 ( $CH_2, CH_2OH$ ), 72.7 ( $CH_2, CH_2OH$ )], 74.5 (CH, CHOH), [169.97 (quat.

C, NHCO), 170.00 (quat. C, NHCO)], some resonance overlap;  $m/z$  (TOF ES-) 841.0 ( $[M]^-$ , 100%), 812.0 (70); HRMS  $m/z$  (TOF ES-) 839.7195 ( $[M]^-$ .  $C_{48}H_{95}N_4O_7$  requires 839.7201).

### 6.17. 2-(2-(2-(Prop-2-ynoxy)ethoxy)ethoxy)ethanol **87**<sup>[150]</sup>

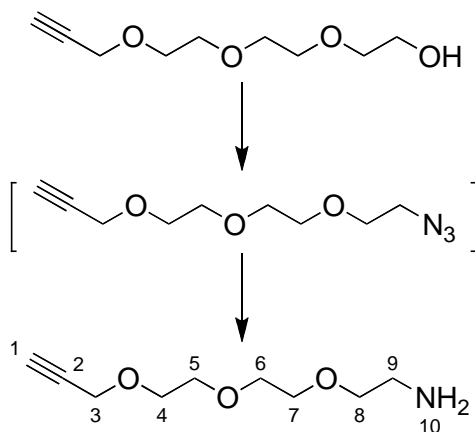


Chemical Formula:  $C_9H_{16}O_4$   
Molecular Weight: 188.22

$n$ BuLi (2.5 M in hexanes, 5.33 mL, 13.33 mmol) was added dropwise over 30 min to a cooled (0 °C) solution of triethylene glycol (2.00 g, 13.3 mmol) in THF (100 mL). The solution was stirred for 30 min before adding propargyl bromide (80% v/w in toluene, 1.78 mL, 15.9 mmol) over 15 min. The reaction mixture was allowed to warm to r.t. and stirred for 12 h and then quenched by the addition of  $H_2O$  (100 mL) and  $Et_2O$  (200 mL). The phases were separated. The aqueous phase was extracted with  $CHCl_3$  (3 × 200 mL). The  $CHCl_3$  extracts were combined and the volatiles were removed under reduced pressure to provide alcohol **87** as a colourless oil (630 mg, 25%). Data:  $R_f$  = 0.35 (eluent: 35% EtOAc in hexanes);  $\nu_{max}$  (film)/ $cm^{-1}$  3415br (OH), 3281br (-CC-H), 2876s, 2116m ( $C\equiv C$ ), 1719m, 1642m, 1457m, 1350m, 1299m, 1248m, 1094br, 935m, 885m, 838m;  $\delta_H$  (300 MHz) 2.37 (1H, t,  $J$  6.0, OH), 2.43 (1H, t,  $J$  2.3,  $CH_2CCH$ ), 3.60-3.79 (12H, stack), 4.21 (2H, d,  $J$  2.3,  $CH_2CCH$ ),  $\delta_C$  (75 MHz) 57.9 ( $CH_2$ ), 61.1 ( $CH_2$ ), 68.6 ( $CH_2$ ), 69.83 ( $CH_2$ ), 69.86 ( $CH_2$ ), 70.1 ( $CH_2$ ), 72.1 ( $CH_2$ ),

74.1 (CH, CH<sub>2</sub>CCH), 79.2 (quat. C, CH<sub>2</sub>CCH), the spectroscopic data agree with those of the lit.;<sup>[150]</sup> attempts to obtain mass spectral data (ES, EI) were unsuccessful.

### 6.18. 3-(2-(2-(2-Aminoethoxy)ethoxy)ethoxy)pro-1-yne **86**<sup>[151]</sup>

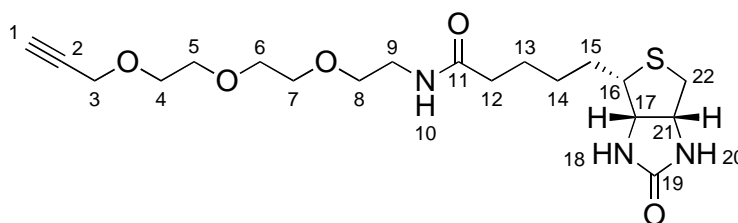


Chemical Formula: C<sub>9</sub>H<sub>17</sub>NO<sub>3</sub>  
Molecular Weight: 187.24

DBU (873  $\mu$ L, 5.84 mmol) was added dropwise over 10 min to a stirred solution of BNPPA (2.13 g, 5.84 mmol) and alcohol **87** (1.00 g, 5.33 mmol) in toluene (5.3 mL). The mixture was stirred at r.t. for 12 h after which time TLC showed complete consumption of starting material. The reaction mixture was diluted with EtOAc (20 mL) and quenched with NaHCO<sub>3</sub> solution (20 mL). The phases were separated and the aqueous layer was extracted with EtOAc (2  $\times$  40 mL). The combined organic fractions were washed with NaHCO<sub>3</sub> solution (2  $\times$  20 mL), then with brine (20 mL) and dried with MgSO<sub>4</sub>, filtered and the solvent was removed under reduced pressure. The residue was partially purified by flash column chromatography. The azide product was contaminated with *para*-nitrophenol (yellowish-green oil) and was used in the next reaction without further purification.

The crude azide **88** from the previous step was dissolved in THF/H<sub>2</sub>O (10 mL, 20:1) and treated with Me<sub>3</sub>P (1 M in THF, 584  $\mu$ L, 5.84 mmol). The mixture was stirred for 4 h, after which time, the volatiles were removed under reduced pressure. The residue was dissolved in CH<sub>2</sub>Cl<sub>2</sub> (10 mL) and washed with hydrochloric acid (0.1 N, 2  $\times$  10 mL). The aqueous phase was extracted with CH<sub>2</sub>Cl<sub>2</sub> (2  $\times$  10 mL) and then basified to pH = 11 with 1 M NaOH solution. The basic aqueous phase was then back extracted with CH<sub>2</sub>Cl<sub>2</sub> (3  $\times$  10 mL). The volatiles were evaporated under reduced pressure to provide amine **86** as a colourless oil (550 mg, 55%). Data:  $\nu_{\max}$  (film)/cm<sup>-1</sup> 3376br (NH<sub>2</sub>), 3251br (-CC-H), 2871s, 2112m (C $\equiv$ C), 1578s, 1474s, 1351s, 1309m, 1098br, 1032m, 838w;  $\delta_H$  (300 MHz) 2.41 (1H, t, *J* 2.4, C(1)*H*), 2.85 (2H, t, *J* 5.2, C(10)*H*), 3.50 (2H, t, *J* 5.3, C(9)*H*), 3.60-3.72 (10H, stack), 4.20 (2H, d, *J* 2.4, C(3)*H*);  $\delta_C$  (75 MHz) 41.3 (CH<sub>2</sub>), 58.1 (CH<sub>2</sub>), 68.8 (CH<sub>2</sub>), 69.9 (CH<sub>2</sub>), 70.1 (CH<sub>2</sub>), 70.3 (CH<sub>2</sub>), 72.8 (CH<sub>2</sub>), 74.4 (CH, CH<sub>2</sub>CCH), 79.3 (quat. C, CH<sub>2</sub>CCH), the spectroscopic data agree with those of the lit.;<sup>[151]</sup> attempts to obtain mass spectral data (ES, EI) were unsuccessful.

### 6.19. 3-(2-(2-(2-Amide-D-biotin-ethoxy)ethoxy)ethoxy)pro-1-yne **85**

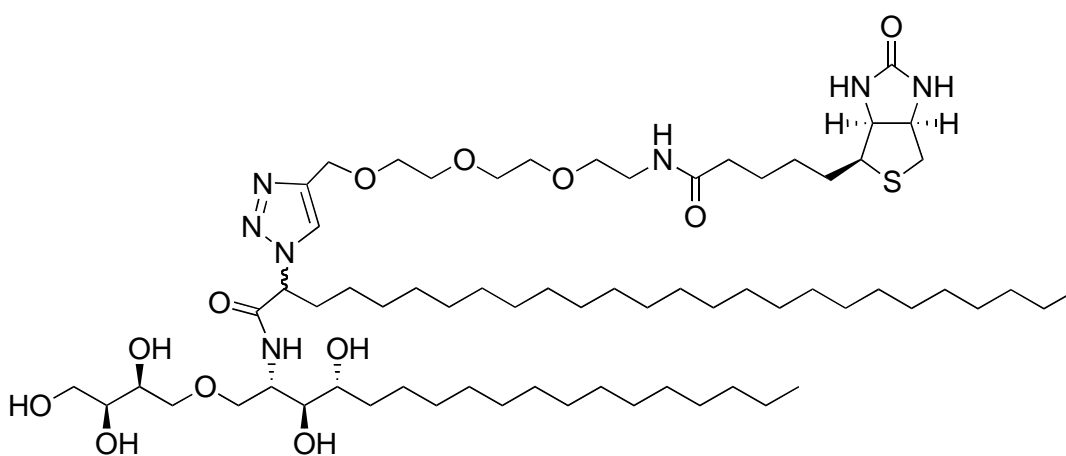


Chemical Formula: C<sub>19</sub>H<sub>31</sub>N<sub>3</sub>O<sub>5</sub>S  
Molecular Weight: 413.532

Et<sub>3</sub>N (438  $\mu$ L, 3.68 mmol) was added to a suspension of D-(+)-biotin (300 mg, 1.23 mmol) in DMF (10 mL) at 0 °C and the mixture was stirred until the suspension became a clear solution. At this time, pentafluorophenol trifluoroacetate (344 mg, 1.23 mmol) was added via syringe. The mixture was stirred for 4 h after which time TLC showed complete formation of the ester. The reaction vessel was cooled to 0 °C and a solution of amine **86** (230 mg, 1.23 mmol) in DMF (2 mL) was added. The resulting solution was stirred for 12 h. The solvent and pentafluorophenol were evaporated under reduced pressure (40 °C at 0.1 mbar). The resulting amorphous solid was dissolved in CHCl<sub>3</sub> / MeOH (20:1, 5 mL) and applied directly on to a silica column (eluent: gradient from 20:1 to 9:1 CHCl<sub>3</sub>/CH<sub>3</sub>OH) to provide the amide **85** as a colourless paste (356 mg, 70%). Data:  $R_f$  = 0.4 (eluent: 5% MeOH in CHCl<sub>3</sub>);  $\nu_{\max}$  (film)/cm<sup>-1</sup> 3306s, 3017s, 2928s, 2251w (C $\equiv$ C), 1701s (C=O), 1654m (C=O), 1524m, 1459m, 1349w, 1331w, 1215s, 1096m, 1032w, 909s, 758s, 668s;  $\delta_H$  (300 MHz, CDCl<sub>3</sub>) 1.38 (2H, app. quintet,  $J$  7.2, C(14)H), 1.57-1.73 (4H, stack, C(15)H, C(13)H), 2.17 (2H, t,  $J$  7.6, C(12)H), 2.43 (1H, t,  $J$  2.2, C(1)H), 2.68 (1H, app. d,  $J$  12.7, C(22)H<sub>a</sub>), 2.84 (1H, dd,  $J$  12.7, 4.8, C(22)H<sub>b</sub>), 3.08-3.15 (1H, m, C(16)H), 3.37-3.41 (2H, m, C(9)H), 3.51 (2H, t,  $J$  5.1, C(8)H), 3.56-3.59 (4H, stack, C(6)H, C(7)H), 3.60-3.65 (4H, stack, C(5)H, C(4)H), 4.14 (2H, d,  $J$  2.2, C(3)H), 4.24-4.26 (1H, m, C(17)H), 4.43-4.46 (1H, m, C(21)H), 6.05 (1H, s, C(20)H), 6.81 (1H, s, C(18)H), 6.85 (1H, t,  $J$  5.4, C(10)H);  $\delta_C$  (CDCl<sub>3</sub>, 125 MHz) 25.5 (CH<sub>2</sub>, C(13)), 27.97 (CH<sub>2</sub>, C(15)), 28.20 (CH<sub>2</sub>, C(14)), 35.8 (CH<sub>2</sub>, C(12)), 39.0 (CH<sub>2</sub>, C(9)), 40.40 (CH<sub>2</sub>, C(22)), 55.6 (CH, C(16)), 58.2 (CH<sub>2</sub>, C(3)), 60.1 (CH, C(21)), 61.6 (CH, C(17)), 68.9 (CH<sub>2</sub>, C(4)), 69.80 (CH<sub>2</sub>, C(8)), 69.87 (CH<sub>2</sub>, C(7)), 70.10 (CH<sub>2</sub>, C(5)), 70.21 (CH<sub>2</sub>, C(6)), 74.6 (CH, C(1)), 79.4 (quat. C, C(2)), 164.2 (quat. C, C(19)), 173.3 (quat. C, C(11));  $m/z$  (TOF

ES<sup>+</sup>) 436.1 ([M+Na]<sup>+</sup>, 100%); HRMS m/z (TOF ES<sup>+</sup>) 436.1869 ([M+Na]<sup>+</sup>. C<sub>19</sub>H<sub>31</sub>N<sub>3</sub>O<sub>5</sub>NaS requires 436.1882).

**6.20. 1-O-[L-Threitol]-2-(25-[4-(1-methylene-10-N-amide-D-biotin-triethyleneglycol)-1,2,3-triazole]-hexacosanoyl)amino-1,3,4-D-ribo-octadecantriol **84****

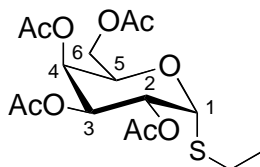


Chemical Formula: C<sub>67</sub>H<sub>127</sub>N<sub>7</sub>O<sub>12</sub>S  
Molecular Weight: 1254.83

CuSO<sub>4</sub>·5H<sub>2</sub>O (296 μg, 1.2 μmol) and ascorbic acid (405 μg, 2.3 μmol) were added to a solution of alkyne **85** (4.87 mg, 11.8 μmol) and azide **70** (10 mg, 11.8 μmol) in THF/H<sub>2</sub>O/MeOH (1 mL, 5:5:2). The mixture was stirred vigorously for 12 h at r.t and a further 12 h at 40 °C. H<sub>2</sub>O (5 mL) was added to the mixture and the precipitate was collected by filtration and purified by chromatography on silica gel (eluent: 10% MeOH in CHCl<sub>3</sub>) to provide triazole **84** as a white solid (11 mg, 74%). Data: *R*<sub>f</sub> = 0.3 (eluent: 15% MeOH in CHCl<sub>3</sub>); δ<sub>H</sub> (500 MHz, CDCl<sub>3</sub>/CD<sub>3</sub>OD 2:1) 0.76 (6H, t, *J* 6.5, CH<sub>2</sub>CH<sub>3</sub>), 1.05-1.20 (72H, stack), 1.31-1.35 (2H, stack), 1.45-1.63 (6H, stack), 2.62 (1H, d, *J* 12.8, SCH<sub>a</sub>H<sub>b</sub>), 2.81-2.86 (1H, m, SCH<sub>a</sub>H<sub>b</sub>), 3.05-3.11 (1H, m, SCH),

3.35-3.69 (2H, stack), 4.03-4.07 (1H, m), 4.19-4.23 (1H, m, NHCHCH), 3.37-4.39 (1H, m, NHCHCH<sub>2</sub>), 4.55-4.56 (2H, m, CCH<sub>2</sub>O), 5.18 (1H, app. q, *J* 8.2, COCHN), 7.84 (0.5H, s, NCHC), 7.85 (0.5H, s, NCHC); <sup>13</sup>C NMR were measured but the signal to noise ratio was too poor to allow accurate reporting of the <sup>13</sup>C resonances; HRMS *m/z* (TOF ES<sup>+</sup>) 1276.8325 ([M+Na]<sup>+</sup>. C<sub>67</sub>H<sub>127</sub>N<sub>7</sub>O<sub>12</sub>SNa) requires 1276.8305).

### 6.21. Ethyl 2,3,4,6-tetra-*O*-acetyl-1-thio- $\alpha$ -D-galactopyranoside **102**<sup>[152, 153]</sup>

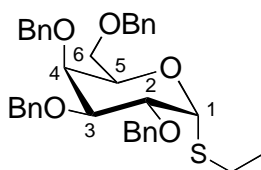


Chemical Formula: C<sub>16</sub>H<sub>24</sub>O<sub>9</sub>S  
Molecular Weight: 392.42

To a solution of peracetylated galactose (10.0 g, 25.60 mmol) and ethanethiol (2 mL, 26.90 mmol) in CH<sub>2</sub>Cl<sub>2</sub> (250 mL) was added BF<sub>3</sub>·OEt<sub>2</sub> (3.8 mL, 30.70 mmol) at 0 °C dropwise over 10 min with stirring. The reaction mixture was allowed to warm to r.t. and then stirred for 12 h, after which time, when TLC analysis showed the disappearance of the starting material. The reaction mixture was then diluted with CH<sub>2</sub>Cl<sub>2</sub> (250 mL) and washed with NaOH solution (1 M, 2 × 250 mL). The organic extracts were then washed with hydrochloric acid (1 M, 1 × 100 mL). The combined organic phases were evaporated under reduced pressure to afford thiogalactoside **102** as a 1:1 mixture of anomers (9.2 g, 91%). Pure  $\alpha$ -anomer was obtained by recrystallisation from a mixture of hexanes and EtOAc (4.1 g, 45% based on crude). Data: *R*<sub>f</sub> = 0.45 (eluent: 50% ethyl acetate in hexanes); mp 106 – 107 °C; [ $\alpha$ ]<sub>D</sub><sup>24</sup> + 216

( $c = 1.0$ ,  $\text{CHCl}_3$ ) [lit.  $[\alpha]_D^{24} + 210$  ( $c = 1.0$ ,  $\text{CHCl}_3$ )];<sup>[152]</sup>  $\nu_{\text{max}}$  (film)/ $\text{cm}^{-1}$  2966w (br), 1750s (C=O), 1740s (C=O), 1367w 1209s, 1116w, 1078m, 1048s, 1007m, 974m, 911s, 836w, 792w;  $\delta_H$  (300 MHz,  $\text{CDCl}_3$ ) 1.28 (3H, t,  $J$  6.5,  $\text{SCH}_2\text{CH}_3$ ), 2.00 (3H, s,  $\text{CH}_3\text{CO}$ ), 2.05 (3H, s,  $\text{CH}_3\text{CO}$ ), 2.08 (3H, s,  $\text{CH}_3\text{CO}$ ), 2.15 (3H, s,  $\text{CH}_3\text{CO}$ ), 2.56 (2H, m,  $\text{SCH}_2$ ), 4.11 (2H, d,  $J$  6.6, (C6) $H$ ), 4.60 (1H, app. t,  $J$  6.6, (C5) $H$ ), 5.22 (1H, dd,  $J$  10.9, 3.1, (C3) $H$ ), 5.28 (1H, dd,  $J$  10.9, 5.4, (C2) $H$ ), 5.46 (1H, d,  $J$  3.1, (C4) $H$ ), 5.76 (1H, d,  $J$  5.4, (C1) $H$ );  $\delta_C$  (75 MHz,  $\text{CDCl}_3$ ) 14.7 ( $\text{CH}_3$ ,  $\text{SCH}_2\text{CH}_3$ ), 20.6 ( $\text{CH}_3$ ), 20.8 ( $\text{CH}_3$ ), 24.0 ( $\text{SCH}_2\text{CH}_3$ ), 61.7 ( $\text{CH}_2$ , C6), 66.4 (CH), 67.9 (CH), 68.2 (CH), 81.9 (CH, C1), 169.8 (quat. C,  $\text{CH}_3\text{CO}$ ), 170.1 (quat. C,  $\text{CH}_3\text{CO}$ ), 170.3 (quat. C,  $\text{CH}_3\text{CO}$ ), some resonance overlap for the acetate signals and for CHs in galactose;  $m/z$  (TOF ES<sup>+</sup>) 415.0 ( $[\text{M}+\text{Na}]^+$ , 100%); HRMS  $m/z$  (TOF ES<sup>+</sup>) 415.1042 ( $[\text{M}+\text{Na}]^+$ .  $\text{C}_{16}\text{H}_{24}\text{O}_9\text{NaS}$  requires 415.1042); the spectroscopic data could not be directly compared to those of the lit. as they were measured in DMSO.<sup>[152, 153]</sup>

## 6.22. Ethyl 2,3,4,6-tetra-*O*-benzyl-1-thio- $\alpha$ -D-galactopyranoside **104**<sup>[152, 153]</sup>



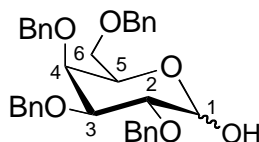
Chemical Formula:  $\text{C}_{36}\text{H}_{40}\text{O}_5\text{S}$   
Molecular Weight: 584.76

To a solution of thiogalactoside **102** (4.0 g, 10.20 mmol) in MeOH (50 mL) was added NaOMe (25 wt. % in MeOH, 114  $\mu\text{L}$ , 0.5 mmol) at r.t. The reaction mixture was stirred for 2 h, after which time, TLC showed that all of the starting material had been

consumed. The appearance of a single more polar spot ( $R_f = 0.15$  (eluent: 25% MeOH in  $\text{CHCl}_3$ )) indicated the successful formation of the tetraol. Dowex® 50WX8 ( $\text{H}^+$ , 100-200 mesh, 2.0 g) was then added until the pH of the reaction mixture was neutral. The resin was filtered and the filtrate was evaporated under reduced pressure to afford the crude tetraol **103**. To a solution of the crude tetraol **103** in DMF (50 mL) was added NaH (60% in mineral oil, 1.8 g, 44.90 mmol) in 3 portions at 0 °C. The resulting mixture was stirred for 30 min, allowing the reaction mixture to warm to r.t. BnBr (5.33 mL, 44.90 mmol) was added dropwise over 5 min at 0 °C. The resulting mixture was then stirred for 4 h, after which time, TLC showed that the reaction was complete. The reaction mixture was diluted with  $\text{Et}_2\text{O}$  (50 mL) and quenched with  $\text{H}_2\text{O}$  (50 mL). The phases were separated and the aqueous phase was extracted with  $\text{Et}_2\text{O}$  (2 × 50 mL). The combined organic phases were evaporated under reduced pressure and the residue was purified by column chromatography to provide thiogalactoside **104** as a clear oil (5.10 g, 85%). Data:  $R_f = 0.25$  (eluent: 10% EtOAc in hexanes);  $\nu_{\text{max}}$  (film)/ $\text{cm}^{-1}$  3066w, 3030w, 2926w (br), 2865w (br), 1703w (br), 1496w, 1453m, 1359m, 1262w (br), 1207w, 1089s (br) 1027s, 910w;  $\delta_{\text{H}}$  (300 MHz,  $\text{CDCl}_3$ ) 1.31 (3H, t,  $J$  6.6,  $\text{SCH}_2\text{CH}_3$ ), 2.65-2.81 (2H, m,  $\text{SCH}_2\text{CH}_3$ ), 3.51-3.62 (4H, stack), 3.83 (1H, t,  $J$  9.6), 3.96 (1H, d,  $J$  2.7), 4.38-4.48 (3H, stack), 4.62 (1H, d,  $J$  11.7,  $\text{CH}_a\text{H}_b\text{Ph}$ ), 4.73 (2H, s,  $\text{CH}_2\text{Ph}$ ), 4.80 (1H, d,  $J$  9.8,  $\text{CH}_c\text{H}_d\text{Ph}$ ), 4.88 (1H, d,  $J$  9.8,  $\text{CH}_c\text{H}_d\text{Ph}$ ), 4.95 (1H, d,  $J$  11.7,  $\text{CH}_a\text{H}_b\text{Ph}$ ), 7.19-7.42 (20H, stack, Ph);  $\delta_{\text{C}}$  (75 MHz,  $\text{CDCl}_3$ ) 15.0 ( $\text{CH}_3$ ,  $\text{SCH}_2\text{CH}_3$ ), 24.6 ( $\text{CH}_2$ ,  $\text{SCH}_2\text{CH}_3$ ), 68.7 ( $\text{CH}_2$ ), 73.4 ( $\text{CH}_2$ ), 73.5 (CH), 74.3 ( $\text{CH}_2$ ), 75.6 ( $\text{CH}_2$ ), 77.3 (CH), 78.3 (CH), 84.0 (CH), 85.2 (CH), 126.4 (CH, Ph), 126.5 (CH, Ph), 126.6 (CH, Ph), 126.7 (CH, Ph), 126.8 (CH, Ph), 126.9

(CH, Ph), 127.0 (CH, Ph), 127.2 (CH, Ph), 127.3 (CH, Ph), 137.7 (quat. C, *ipso*Ph) 138.23 (quat. C, *ipso*Ph), 138.26 (quat. C, *ipso*Ph), 138.6 (quat. C, *ipso*Ph), some resonance overlap on the aromatic region;  $m/z$  (TOF ES<sup>+</sup>) 607.3 ([M+Na]<sup>+</sup>, 100%); HRMS  $m/z$  (TOF ES<sup>+</sup>) 607.2491 ([M+Na]<sup>+</sup>. C<sub>36</sub>H<sub>40</sub>O<sub>5</sub>NaS requires 607.2494); the spectroscopic data could not be compared to those of the lit. as they were measured in DMSO.<sup>[152, 153]</sup>

### 6.23. 2,3,4,6-Tetra-O-benzyl-( $\alpha,\beta$ )-D-galactopyranose **105**<sup>[143, 144]</sup>



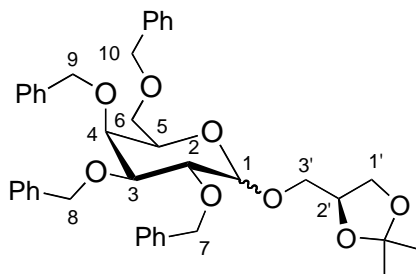
Chemical Formula: C<sub>34</sub>H<sub>36</sub>O<sub>6</sub>  
Molecular Weight: 540.65

To a solution of thiogalactoside **104** (5.0 g, 8.55 mmol) in acetone (50 mL) was added NIS (4.8 g, 21.37 mmol). The brownish-red reaction mixture was stirred for 30 min, after which time, TLC showed that all the starting material was consumed. CH<sub>2</sub>Cl<sub>2</sub> (100 mL) was added and Na<sub>2</sub>S<sub>2</sub>O<sub>3</sub>·5H<sub>2</sub>O (approx. 300 mg) was then added until the colouration disappeared H<sub>2</sub>O (50 mL) was then added. The phases were separated and the aqueous phase was extracted with CH<sub>2</sub>Cl<sub>2</sub> (2 × 50 mL). The combined organic phases were evaporated under reduced pressure and the residue was purified by column chromatography to provide the hemiacetal **105** as a colourless oil (3.5 g, 75%,  $\alpha/\beta$  ratio = 1:1). Data on the diastereomeric mixture:  $R_f$  = 0.15 (eluent: 25% EtOAc in hexanes);  $\nu_{\max}$  (film)/cm<sup>-1</sup> 3414w (br), 3030w, 2920w (br), 2867w (br),

## Experimental Section

2248w (br), 1496w (s), 1453m (s), 1363w (br), 1208w, 1092s (br), 1060s (br), 1027m, 908s (s), 730s (s);  $\delta_H$  (300 MHz,  $CDCl_3$ ) 2.93 (0.5H, d,  $J$  2.0,  $CHOH$ ), 3.15 (0.5H, d,  $J$  6.2,  $CHOH$ ), 3.45-3.61 (3H, stack), 3.76 (0.5H, dd,  $J$  9.5, 7.4), 3.88-4.06 (2H, stack), 4.38-4.50 (2H, stack), 4.56-4.85 (5.5H, stack), 4.90-4.96 (1.5H, stack), 5.27-5.29 (0.5H, stack), 7.23-7.39 (20H, stack, Ph);  $\delta_C$  (75 MHz,  $CDCl_3$ ) 69.0 ( $CH_2$ ), 69.2 ( $CH_2$ ), 69.5 (CH), 73.1 ( $CH_2$ ), 73.4 ( $CH_2$ ), 73.5 ( $CH_2$ ), 73.6 ( $CH_2$ ), 73.7 (CH), 74.6 ( $CH_2$ ), 74.7 ( $CH_2$ ), 74.9 (CH), 75.2 ( $CH_2$ ), 76.6 (CH), 78.8 (CH), 80.8 (CH), 82.3 (CH), 91.9 (CH), 97.8 (CH), 127.62 (CH, Ph), 127.67 (CH, Ph), 127.71 (CH, Ph), 127.78 (CH, Ph), 127.83 (CH, Ph), 127.88 (CH, Ph), 127.9 (CH, Ph), 128.11 (CH, Ph), 128.17 (CH, Ph), 128.2 (CH, Ph), 128.34 (CH, Ph), 128.38 (CH, Ph), 128.42 (CH, Ph), 128.47 (CH, Ph), 128.53 (CH, Ph), 128.59 (CH, Ph), 137.8 (quat. C, *ipsoPh*), 137.9 (quat. C, *ipsoPh*), 138.4 (quat. C, *ipsoPh*), 138.5 (quat. C, *ipsoPh*), 138.63 (quat. C, *ipsoPh*), 138.68 (quat. C, *ipsoPh*), 138.8 (quat. C, *ipsoPh*), some resonance overlap in the aromatic region, and in the  $CHOH$  and  $CH_2OH$  region;  $m/z$  (TOF  $ES^+$ ) 563.3 ( $[M+Na]^+$ , 100%); HRMS  $m/z$  (TOF  $ES^+$ ) 563.2396 ( $[M+Na]^+$ .  $C_{34}H_{36}O_6Na$  requires 563.2410); the spectroscopic data agree with that of commercially available material and lit.<sup>[143, 144]</sup>

**6.24. 3-O-[2,3,4,6-Tetra-O-benzyl-( $\alpha,\beta$ )-D-galactopyranoside]-1,2-O-isopropylidene-*syn*-glycerol **106ii****

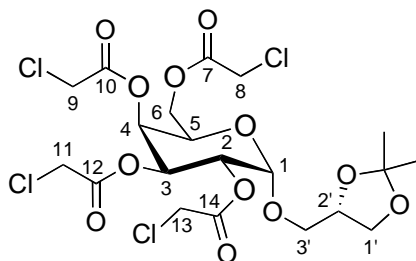


Chemical Formula:  $C_{40}H_{46}O_8$   
Molecular Weight: 654.79

To a solution of hemiacetal **105** (400 mg, 0.74 mmol) in  $CH_2Cl_2$  (6.4 mL) was added  $Ph_3P$  (582 mg, 2.22 mmol) and  $CBr_4$  (736 mg, 2.22 mmol). The reaction mixture was stirred for 3 h after which time, TLC showed that most of the starting hemiacetal was converted to the glycosyl bromide. Activated 4Å MS (200 mg) were added to the reaction mixture and stirring was continued for 5 min followed by the sequential addition of  $iPr_2EtN$  (322  $\mu L$ , 1.85 mmol), TMU (533  $\mu L$ , 4.44 mmol) and  $Et_4NBr$  (466 mg, 2.22 mmol). The reaction mixture was stirred for 5 min before a solution of alcohol **93** (293 mg, 276  $\mu L$ , 2.22 mmol) in  $CH_2Cl_2$  (1.0 mL) was added dropwise over 10 min. The reaction mixture was then stirred for 12 h after which time, TLC showed the reaction was complete. The reaction mixture was diluted with toluene (10 mL), which caused the precipitation of  $Ph_3PO$ . The precipitate was filtered and the  $Ph_3PO$  rinsed with toluene (10 mL). The filtrate was washed with water ( $2 \times 10$  mL) and the aqueous phase was extracted with toluene ( $2 \times 10$  mL). The combined organic phases were evaporated under reduced pressure and the residue was purified by column chromatography to provide the glycoside **106ii** as a colourless oil

(considerable resonance overlap in the  $^1\text{H}$  NMR spectrum of both crude and purified products prevented an accurate measurement of the  $\alpha/\beta$  ratio; therefore an estimate was obtained from the crude  $^{13}\text{C}$  NMR spectrum,  $\alpha/\beta$  ratio = 10:1) (412 mg, 85%). Data for the  $\alpha$ -anomer:  $R_f$  = 0.35 (eluent: 25% EtOAc in hexanes);  $\nu_{\text{max}}$  (film)/ $\text{cm}^{-1}$  3030w, 2985w, 2871w (br), 1497w, 1454w, 1254w, 1210w, 1156w, 1095s, 1052s, 1028s, 911w, 841w;  $\delta_H$  (500 MHz,  $\text{CDCl}_3$ ) 1.41 (3H, s,  $\text{C}(\text{CH}_3)_2$ ), 1.46 (3H, s,  $\text{C}(\text{CH}_3)_2$ ), 3.60 (2H, app. d,  $J$  6.3,  $\text{C}(6)\text{H}$ ), 3.64 (1H, dd,  $J$  10.7 and 5.7,  $\text{C}(3')\text{H}_a$ ), 3.68 (1H, dd,  $J$  10.7, 5.8,  $\text{C}(3')\text{H}_b$ ), 3.79 (1H, dd,  $J$  8.3, 6.3,  $\text{C}(1')\text{H}_a$ ), 3.99 (1H, dd,  $J$  9.4, 2.7,  $\text{C}(3)\text{H}$ ), 4.02-4.04 (2H, stack,  $\text{C}(4)\text{H}$ ,  $\text{C}(5)\text{H}$ ), 4.10 (1H, dd,  $J$  8.2, 6.3,  $\text{C}(1')\text{H}_b$ ), 4.12 (1H, dd,  $J$  9.4, 3.6,  $\text{C}(2)\text{H}$ ), 4.41 (1H, app. t,  $J$  5.9,  $\text{C}(2')\text{H}$ ), 4.46 (1H, d,  $J$  11.8,  $\text{C}(10)\text{H}_a$ ), 4.53 (1H, d,  $J$  11.8,  $\text{C}(10)\text{H}_b$ ), 4.65 (1H, d,  $J$  11.5,  $\text{C}(9)\text{H}_a$ ), 4.74 (1H, d,  $J$  12.0,  $\text{C}(7)\text{H}_a$ ), 4.79 (1H, d,  $J$  11.7,  $\text{C}(8)\text{H}_a$ ), 4.87 (1H, d,  $J$  12.0,  $\text{C}(7)\text{H}_b$ ), 4.90 (1H, d,  $J$  11.7,  $\text{C}(8)\text{H}_b$ ), 4.99 (1H, d,  $J$  3.6,  $\text{C}(1)\text{H}$ ), 5.02 (1H, d,  $J$  11.5,  $\text{C}(9)\text{H}_b$ ), 7.29-7.45 (20H, stack, Ph);  $\delta_C$  (125 MHz,  $\text{CDCl}_3$ ) 25.4 ( $\text{CH}_3$ ,  $\text{C}(\text{CH}_3)_2$ ), 26.6 ( $\text{CH}_3$ ,  $\text{C}(\text{CH}_3)_2$ ), 66.8 ( $\text{CH}_2$ ,  $\text{C}(1')$ ), 68.88 ( $\text{CH}_2$ ,  $\text{C}(6)$ ), 68.96 ( $\text{CH}_2$ ,  $\text{C}(3')$ ), 69.4 ( $\text{CH}$ ,  $\text{C}(5)$ ), 73.0 ( $\text{CH}_2$ ,  $\text{C}(7)$ ,  $\text{C}(8)$ ), 73.3 ( $\text{CH}_2$ ,  $\text{C}(10)$ ), 74.5 ( $\text{CH}$ ,  $\text{C}(2')$ ), 74.6 ( $\text{CH}_2$ ,  $\text{C}(9)$ ), 74.9 ( $\text{CH}$ ,  $\text{C}(4)$ ), 76.4 ( $\text{CH}$ ,  $\text{C}(2)$ ), 78.7 ( $\text{CH}$ ,  $\text{C}(3)$ ), 98.0 ( $\text{CH}$ ,  $\text{C}(1)$ ), 109.2 (quat. C,  $\text{C}(\text{CH}_3)_2$ ), 127.3 ( $\text{CH}$ , Ph), 127.40 ( $\text{CH}$ , Ph), 127.46 ( $\text{CH}$ , Ph), 127.53 (C, Ph), 127.6 ( $\text{CH}$ , Ph), 127.7 ( $\text{CH}$ , Ph), 128.06 ( $\text{CH}$ , Ph), 128.07 ( $\text{CH}$ , Ph), 128.15 ( $\text{CH}$ , Ph), 128.18 ( $\text{CH}$ , Ph), 128.22 ( $\text{CH}$ , Ph), 137.8 (quat. C, *ipso*Ph), 138.51 (quat. C, *ipso*Ph), 138.53 (quat. C, *ipso*Ph), 138.7 (quat. C, *ipso*Ph), some resonance overlap in the aromatic region;  $m/z$  (TOF ES $^+$ ) 677.2 ( $[\text{M}+\text{Na}]^+$ , 100%); HRMS  $m/z$  (TOF ES $^+$ ) 677.3087 ( $[\text{M}+\text{Na}]^+$ .  $\text{C}_{40}\text{H}_{46}\text{O}_8\text{Na}$  requires 677.3090).

**6.25. 3-O-[2,3,4,6-Tetra-O-(chloroacetyl)- $\alpha$ -D-galactopyranoside]-1,2-O-isopropylidene-*syn*-glycerol **108****



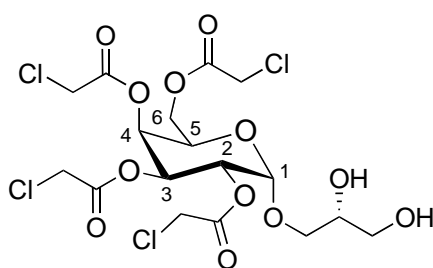
Chemical Formula:  $C_{20}H_{26}Cl_4O_{12}$   
Molecular Weight: 600.23

To a solution of the benzyl ether-protected galactoside **106ii** (650 mg, 0.99 mmol) in DMF (10 mL) was added Pd/C (10 wt. %, 105 mg, 99  $\mu$ mol). The reaction vessel was flushed twice with  $H_2$  before being filled with  $H_2$  and stoppered. The progress of the reaction was monitored by TLC until the disappearance of the starting material and formation of a new product indicating that the tetraol **107** was formed,  $R_f = 0.15$  (eluent: 10% MeOH in  $CHCl_3$ ). The charcoal was filtered and the filtrate was evaporated under reduced pressure. The residue was purified by flash column chromatography to provide the tetraol **107** as a syrup, which was dissolved in pyridine (10 mL). The resulting solution was treated with chloroacetic anhydride (745 mg, 4.36 mmol). After 10 min, TLC showed that the starting tetra-ol was consumed and a single new product formed. The reaction mixture was diluted with  $CH_2Cl_2$  (20 mL) and quenched with  $H_2O$  (20 mL). The phases were separated and the aqueous phase was extracted with  $CH_2Cl_2$  (2  $\times$  10 mL). The combined organic phases were evaporated under reduced pressure and the residue was purified by column chromatography to provide chloroacetylated galactoside **108** as a colourless oil (356

mg, 60%). Data:  $R_f = 0.35$  (eluent: 50% EtOAc in hexanes);  $\delta_H$  (500 MHz,  $CDCl_3$ ) 1.36 (3H, s,  $C(CH_3)_2$ ), 1.41 (3H, s,  $C(CH_3)_2$ ), 3.52 (1H, dd,  $J$  11.1, 6.3,  $C(3')H_a$ ), 3.68 (1H, dd,  $J$  8.5, 6.0,  $C(1')H_a$ ), 3.75 (1H, dd,  $J$  11.1, 4.1,  $C(3')H_b$ ), 3.97 (2H, s,  $C(11)H$ ), 4.043 (1H, app. t,  $J$  6.8,  $C(1')H_b$ ), 4.046 (2H, s,  $C(8)H$  or  $C(13)H$ ), 4.07 (2H, d,  $J$  3.5,  $C(8)H$  or  $C(13)H$ ), 4.14 (2H, s,  $C(9)H$ ), 4.23-4.28 (3H, stack,  $C(6)H$ ,  $C(2')H$ ), 4.38 (1H, t,  $J$  6.9,  $C(5)H$ ), 5.17 (1H, dd,  $J$  10.6, 3.7,  $C(2)H$ ), 5.27 (1H, d,  $J$  3.7,  $C(1)H$ ), 5.48 (1H, dd,  $J$  10.6, 3.4,  $C(3)H$ ), 5.51 (1H, app. d,  $J$  3.4,  $C(4)H$ );  $\delta_C$  (125 MHz,  $CDCl_3$ ) 25.3 ( $CH_3$ ,  $CCH_3$ ), 26.7 ( $CH_3$ ,  $CCH_3$ ), 40.26 ( $CH_2$ ,  $C(11)$ ), 40.33 ( $CH_2$ ,  $C(9)$ ), 40.38 ( $CH_2$ ,  $C(8)$  or  $C(13)$ ), 40.46 ( $CH_2$ ,  $C(8)$  or  $C(13)$ ), 62.7 ( $CH_2$ ,  $C(6)$ ), 65.89 ( $CH_2$ ,  $C(1')$ ), 65.98 ( $CH$ ,  $C(5)$ ), 68.8 ( $CH$ ,  $C(3)$ ), 69.1 ( $CH$ ,  $C(2)$ ), 69.6 ( $CH$ ,  $C(4)$ ), 69.7 ( $CH_2$ ,  $C(3')$ ), 74.6 ( $CH$ ,  $C(2')$ ), 96.3 ( $CH$ ,  $C(1)$ ), 109.8 (quat. C,  $C(CH_3)_2$ ), 166.3 (quat. C,  $C(12)$ ), 166.7 (quat. C,  $C(14)$  and  $C(7)$ ), 17.1 (quat. C,  $C(10)$ );  $m/z$  (TOF ES<sup>+</sup>) 621.0 ( $[M+Na]^+$ , 100%); HRMS  $m/z$  (TOF ES<sup>+</sup>) 621.0070 ( $[M+Na]^+$ .  $C_{20}H_{26}O_{12}Na^{35}Cl_4$  requires 621.0076).

## 6.26. 3-O-[2,3,4,6-Tetra-O-(chloroacetyl)- $\alpha$ -D-galactopyranoside]-*syn*-glycerol

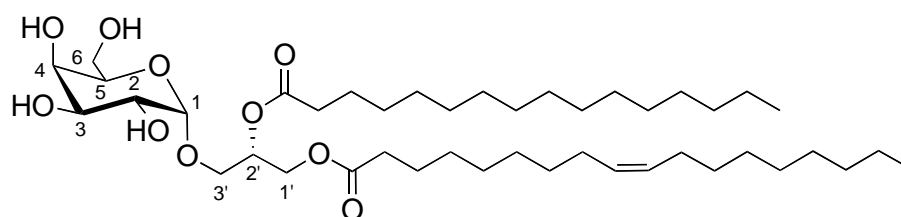
109



Chemical Formula:  $C_{17}H_{22}Cl_4O_{12}$   
Molecular Weight: 560.16

To a solution of acetal **108** (250 mg, 0.42 mmol) in MeNO<sub>2</sub> saturated with H<sub>2</sub>O (4.2 mL) was added Ce(OTf)<sub>3</sub> (75 mg, 0.13 mmol). The reaction mixture was stirred for 2 h, after which time, TLC showed the disappearance of the starting material. The reaction mixture was diluted with CH<sub>2</sub>Cl<sub>2</sub> (5 mL) and quenched with H<sub>2</sub>O (5 mL). The phases were separated and the aqueous phase was extracted with CH<sub>2</sub>Cl<sub>2</sub> (2 × 5 mL). The combined organic phases were evaporated under reduced pressure. The residue was purified by column chromatography to provide diol **109** (172 mg, 75%) as a colourless oil. Data: *R*<sub>f</sub> = 0.20 (eluent: 80% EtOAc in hexanes); δ<sub>H</sub> (300 MHz, CDCl<sub>3</sub>) 1.95-2.01 (1H, m, OH), 2.54 (1H, d, *J* 4.4, OH), 3.56 (1H, dd, *J* 10.3, 6.7), 3.60-3.79 (1H, m), 3.85 (1H, dd, *J* 10.3, 3.8), 3.90-3.97 (1H, m), 3.99 (2H, s, ClCH<sub>2</sub>), 4.08 (4H, s, 2 × ClCH<sub>2</sub>), 4.16 (2H, s, ClCH<sub>2</sub>), 4.25-4.33 (3H, stack), 4.42 (1H, t, *J* 6.1), 5.20-5.27 (2H, stack), 5.46-5.54 (2H, stack); δ<sub>C</sub> (75 MHz, CDCl<sub>3</sub>) 40.3 (CH<sub>2</sub>, ClCH<sub>2</sub>), 40.43 (CH<sub>2</sub>, ClCH<sub>2</sub>), 40.45 (CH<sub>2</sub>, ClCH<sub>2</sub>), 63.0 (CH<sub>2</sub>), 63.4 (CH<sub>2</sub>), 66.0 (CH), 68.9 (CH), 69.1 (CH), 69.7 (CH), 70.0 (CH<sub>2</sub>), 70.5 (CH), 96.2 (CH, C1), 166.6 (quat. C, CH<sub>2</sub>CO), 166.8 (quat. C, CH<sub>2</sub>CO), 167.1 (quat. C, CH<sub>2</sub>CO), 167.2 (quat. C, CH<sub>2</sub>CO); *m/z* (TOF ES<sup>+</sup>) 580.0 ([M+Na]<sup>+</sup>, 100%); HRMS *m/z* (TOF ES<sup>+</sup>) 580.9769 ([M+Na]<sup>+</sup>. C<sub>17</sub>H<sub>22</sub>O<sub>12</sub>Na<sup>35</sup>Cl<sub>4</sub> requires 580.9763).

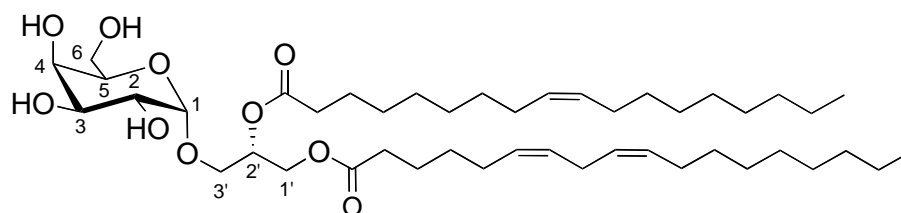
### 6.27. Preparation of BbGL-IIc<sup>[52, 154]</sup>



Chemical Formula: C<sub>43</sub>H<sub>80</sub>O<sub>10</sub>  
Molecular Weight: 757.09

## Experimental Section

To a solution of diol **10** (25.0 mg, 44.6  $\mu\text{mol}$ ) and oleic acid (12.6 mg, 44.6  $\mu\text{mol}$ ) in  $\text{CH}_2\text{Cl}_2$  (1 mL) was added DCC in  $\text{CH}_2\text{Cl}_2$  (1.00 M, 44.6  $\mu\text{mol}$ , 44.6  $\mu\text{L}$ ) and DMAP in  $\text{CH}_2\text{Cl}_2$  (0.5 mg, 4  $\mu\text{mol}$ , 25  $\mu\text{L}$ ). The solution was stirred for 2 h after which time TLC showed that all the starting diol had been consumed. Palmitic acid in  $\text{CH}_2\text{Cl}_2$  (11.4 mg, 44.6  $\mu\text{mol}$ , 50  $\mu\text{L}$ ), DCC in  $\text{CH}_2\text{Cl}_2$  (1.00 M, 44.6  $\mu\text{mol}$ , 44.6  $\mu\text{L}$ ) and DMAP in  $\text{CH}_2\text{Cl}_2$  (0.5 mg, 4  $\mu\text{mol}$ , 25  $\mu\text{L}$ ) were then added and stirring was continued for 12 h. The reaction mixture was diluted with  $\text{CH}_2\text{Cl}_2$  (5 mL) and quenched with  $\text{H}_2\text{O}$  (5 mL). The phases were separated and the aqueous phase was extracted with  $\text{CH}_2\text{Cl}_2$  (3  $\times$  5 mL). The combined organic phases were evaporated under reduced pressure. The residue was dissolved in  $\text{CH}_2\text{Cl}_2/\text{MeOH}$  (1:1, 1 mL) and the solution was treated with  $\text{Et}_3\text{N}$  (1.00 M in  $\text{H}_2\text{O}$ , 446  $\mu\text{mol}$ , 446  $\mu\text{L}$ ). The reaction mixture was stirred for 2 h after which time TLC showed that the starting material was consumed. The reaction mixture was diluted with  $\text{H}_2\text{O}$  (5 mL) and the aqueous phase was extracted with  $\text{CHCl}_3$  (3  $\times$  5 mL). The combined organic extracts were evaporated under reduced pressure and the residue was purified by column chromatography (eluent: gradient from  $\text{CHCl}_3$  to 10% MeOH in  $\text{CHCl}_3$ ) to provide **BbGL-Ilc** (15 mg, 44%) as a colourless oil. Data:  $R_f$  = 0.45 (eluent: 10% MeOH in  $\text{CHCl}_3$ );  $\delta_H$  (300 MHz,  $\text{CDCl}_3$ ) 0.85 (6H, app. t,  $J$  6.4, 2  $\times$   $\text{CH}_2\text{CH}_3$ ), 1.18-1.27 (44H, stack), 1.55-1.62 (4H, m), 1.95-2.01 (4H, m, 2  $\times$   $\text{CH}_2\text{CH}=\text{CH}$ ), 2.29 (4H, app. t, 2  $\times$   $\text{CH}_2\text{CO}$ ), 3.57-3.63 (1H, m), 3.72-3.84 (6H, stack), 4.07-4.13 (2H, stack), 4.35 (1H, dd,  $J$  11.9, 3.9), 4.91 (1H, d,  $J$  3.6, C(1) $H$ ), 5.20-5.26 (1H, m, C(2') $H$ ), 5.30-5.34 (2H, stack,  $\text{CH}=\text{CH}$ );  $m/z$  (TOF ES<sup>+</sup>) 780.0 ( $[\text{M}+\text{Na}]^+$ , 100%); HRMS  $m/z$  (TOF ES<sup>+</sup>) 779.5636 ( $[\text{M}+\text{Na}]^+$ .  $\text{C}_{43}\text{H}_{80}\text{O}_{10}\text{Na}$  requires 779.5649).

**6.28. Preparation of BbGL-IIlf**<sup>[52, 154]</sup>

Chemical Formula: C<sub>45</sub>H<sub>80</sub>O<sub>10</sub>  
 Molecular Weight: 781.11

To a solution of diol **109** (20.0 mg, 35.7  $\mu$ mol) and linoleic acid (10.0 mg, 35.7  $\mu$ mol) in CH<sub>2</sub>Cl<sub>2</sub> (1 mL) was added DCC in CH<sub>2</sub>Cl<sub>2</sub> (1.00 M, 35.7  $\mu$ mol, 35.7  $\mu$ L) and DMAP in CH<sub>2</sub>Cl<sub>2</sub> (0.4 mg, 3  $\mu$ mol, 25  $\mu$ L). The solution was stirred for 2 h after which time TLC showed that all the starting diol had been consumed. Oleic acid in CH<sub>2</sub>Cl<sub>2</sub> (10.2 mg, 35.7  $\mu$ mol, 50  $\mu$ L), DCC in CH<sub>2</sub>Cl<sub>2</sub> (1.00 M, 35.7  $\mu$ mol, 35.7  $\mu$ L) and DMAP in CH<sub>2</sub>Cl<sub>2</sub> (0.4 mg, 3  $\mu$ mol, 25  $\mu$ L) were then added and the stirring was continued for 12 h. The reaction mixture was diluted with CH<sub>2</sub>Cl<sub>2</sub> (5 mL) and quenched with H<sub>2</sub>O (5 mL). The phases were separated and the aqueous phase was extracted with CH<sub>2</sub>Cl<sub>2</sub> (3  $\times$  5 mL). The combined organic phases were evaporated under reduced pressure. The residue was dissolved in CH<sub>2</sub>Cl<sub>2</sub>/MeOH (1:1, 1 mL) and the solution was treated with Et<sub>3</sub>N (1.00 M in H<sub>2</sub>O, 357  $\mu$ mol, 357  $\mu$ L). The reaction mixture was stirred for 2 h after which time TLC showed that the starting material was consumed. The reaction mixture was diluted with H<sub>2</sub>O (5 mL) and the aqueous phase was extracted with CHCl<sub>3</sub> (3  $\times$  5 mL). The combined organic extracts were evaporated under reduced pressure and the residue was purified by column chromatography (eluent: gradient from CHCl<sub>3</sub> to 10% MeOH in CHCl<sub>3</sub>) to provide **BbGL-IIlf** (11.8 mg, 33%) as a colourless oil. Data:  $R_f$  = 0.45 (eluent: 10% MeOH in CHCl<sub>3</sub>);  $\delta_H$  (500 MHz, CDCl<sub>3</sub>)

## Experimental Section

0.84 (6H, stack, 2 × CH<sub>2</sub>CH<sub>3</sub>), 1.25-1.36 (34H, stack), 1.58-1.67 (4H, stack), 1.98-2.05 (8H, stack), 2.29-2.32 (4H, stack), 2.76 (2H, t, *J* 6.8), 3.62 (1H, dd, *J* 10.9, 6.1), 3.73 (1H, dd, *J* 9.8, 3.2), 3.79-3.85 (4H, stack), 3.89-3.93 (1H, m), 4.05 (1H, d, *J* 2.9), 4.11 (1H, dd, *J* 11.9, 5.8), 4.36 (1H, dd, *J* 11.9, 4), 4.93 (1H, d, *J* 3.7), 5.22-5.26 (1H, m), 5.28-5.40 (6H, stack); *m/z* (TOF ES<sup>+</sup>) 803.6 ([M+Na]<sup>+</sup>, 100%); HRMS *m/z* (TOF ES<sup>+</sup>) 803.5635 ([M+Na]<sup>+</sup>. C<sub>45</sub>H<sub>80</sub>O<sub>10</sub>Na requires 803.5649).

## **REFERENCES**

## VII. REFERENCES

- [1] C. A. Janeway, P. Travers, S. Hunt, M. Walport, *Immunobiology*, 6th ed., Garland Science, **1997**.
- [2] H. O. Mcdevitt, *Annu. Rev. Immunol.* **2000**, 18, 1.
- [3] C. Alfonso, L. Karlsson, *Annu. Rev. Immunol.* **2000**, 18, 113.
- [4] L. H. Martin, F. Calabi, C. Milstein, *Proc. Natl. Acad. Sci. USA* **1986**, 83, 9154.
- [5] J. L. Matsuda, T. Mallevaey, J. Scott-Browne, L. Gapin, *Curr. Opin. Immunol.* **2008**, 20, 358.
- [6] C. R. Berkers, H. Ovaa, *Trends Pharmacol. Sci.* **2005**, 26, 252.
- [7] V. S. Stronge, M. Salio, E. Y. Jones, V. Cerundolo, *Trends Immunol.* **2007**, 28, 455.
- [8] R. R. Brutkiewicz, *J. Immunol.* **2006**, 177, 769.
- [9] T. I. Prigozy, O. Naidenko, P. Qasba, D. Elewaut, L. Brossay, A. Khurana, T. Natori, Y. Koezuka, A. Kulkarni, M. Kronenberg, *Science* **2001**, 291, 664.
- [10] D. I. Godfrey, J. Rossjohn, J. McCluskey, *Immunity* **2008**, 28, 304.
- [11] E. Kobayashi, K. Motoki, T. Uchida, H. Fukushima, Y. Koezuka, *Oncol. Res.* **1995**, 7, 529.
- [12] M. Morita, K. Motoki, K. Akimoto, T. Natori, T. Sakai, E. Sawa, K. Yamaji, Y. Koezuka, E. Kobayashi, H. Fukushima, *J. Med. Chem.* **1995**, 38, 2176.
- [13] K. Motoki, K. Maeda, H. Ueno, E. Kobayashi, T. Uchida, H. Fukushima, Y. Koezuka, *Oncol. Res.* **1996**, 8, 155.
- [14] F. M. Spada, Y. Koezuka, S. A. Porcelli, *J. Exp. Med.* **1998**, 188, 1529.
- [15] O. V. Naidenko, Y. Koezuka, M. Kronenberg, *Microbes Infect.* **2000**, 2, 621.

- [16] N. Burdin, L. Brossay, M. Degano, H. Iijima, M. Gui, I. A. Wilson, M. Kronenberg, *Proc. Natl. Acad. Sci. USA* **2000**, *97*, 10156.
- [17] D. B. Moody, G. S. Besra, I. A. Wilson, S. A. Porcelli, *Immunol. Rev.* **1999**, *172*, 285.
- [18] D. B. Moody, B. B. Reinhold, M. R. Guy, E. M. Beckman, D. E. Frederique, S. T. Furlong, S. Ye, V. N. Reinhold, P. A. Sieling, R. L. Modlin, G. S. Besra, S. A. Porcelli, *Science* **1997**, *278*, 283.
- [19] C. Angenieux, J. Salamero, D. Fricker, J. P. Cazenave, B. Goud, D. Hanau, H. De La Salle, *J. Biol. Chem.* **2000**, *275*, 37757.
- [20] H. De La Salle, S. Mariotti, C. Angenieux, M. Gilleron, L. F. Garcia-Alles, D. Malm, T. Berg, S. Paoletti, B. Maitre, L. Mourey, J. Salamero, J. P. Cazenave, D. Hanau, L. Mori, G. Puzo, G. De Libero, *Science* **2005**, *310*, 1321.
- [21] B. Sullivan, N. Nagarajan, M. Kronenberg, *Trends Immunol.* **2005**, *26*, 282.
- [22] Z. Zeng, A. R. Castano, B. W. Segelke, E. A. Stura, P. A. Peterson, I. A. Wilson, *Science* **1997**, *277*, 339.
- [23] L. H. Martin, F. Calabi, F. A. Lefebvre, C. A. Bilsland, C. Milstein, *Proc. Natl. Acad. Sci. USA* **1987**, *84*, 9189.
- [24] R. S. Blumberg, D. Gerdes, A. Chott, S. A. Porcelli, S. P. Balk, *Immunol. Rev.* **1995**, *147*, 5.
- [25] W. A. Ernst, J. Maher, S. Cho, K. R. Niazi, D. Chatterjee, D. B. Moody, G. S. Besra, Y. Watanabe, P. E. Jensen, S. A. Porcelli, M. Kronenberg, R. L. Modlin, *Immunity* **1998**, *8*, 331.

- [26] A. Giuliani, S. A. Porcelli, L. Tentori, G. Graziani, C. Testorelli, S. P. Prete, S. Bussini, D. Cappelletti, M. B. Brenner, E. Bonmassar, A. Aquino, *Life Sci.* **1998**, *63*, 985.
- [27] F. Winau, V. Schwierzeck, R. Hurwitz, N. Remmel, P. Sieling, R. Modlin, S. Porcelli, V. Brinkmann, M. Sugita, K. Sandhoff, S. Kaufmann, U. Schaible, *Nat. Immunol.* **2004**, *5*, 169.
- [28] M. Exley, S. Porcelli, M. Furman, J. Garcia, S. P. Balk, *J. Exp. Med.* **1998**, *188*, 867.
- [29] M. Koch, V. S. Stronge, D. Shepherd, S. D. Gadola, B. Mathew, G. Ritter, A. R. Fersht, G. S. Besra, R. R. Schmidt, E. Y. Jones, V. Cerundolo, *Nat. Immunol.* **2005**, *6*, 819.
- [30] D. Wu, G. W. Xing, M. A. Poles, A. Horowitz, Y. Kinjo, B. Sullivan, V. Bodmer-Narkevitch, O. Plettenburg, M. Kronenberg, M. Tsuji, D. D. Ho, C. H. Wong, *Proc. Natl. Acad. Sci. USA* **2005**, *102*, 1351.
- [31] T. Kawano, J. Cui, Y. Koezuka, I. Toura, Y. Kaneko, K. Motoki, H. Ueno, R. Nakagawa, H. Sato, E. Kondo, H. Koseki, M. Taniguchi, *Science* **1997**, *278*, 1626.
- [32] K. Miyamoto, S. Miyake, T. Yamamura, *Nature* **2001**, *413*, 531.
- [33] B. A. Sullivan, M. Kronenberg, *J. Clin. Invest.* **2005**, *115*, 2328.
- [34] S. Oki, A. Chiba, T. Yamamura, S. Miyake, *J. Clin. Invest.* **2004**, *113*, 1631.
- [35] T. Toba, K. Murata, K. Nakanishi, B. Takahashi, N. Takemoto, M. Akabane, T. Nakatsuka, S. Imajo, T. Yamamura, S. Miyake, H. Annoura, *Bioorg. Med. Chem. Lett.* **2007**, *17*, 2781.

- [36] M. Fujio, D. Wu, R. Garcia-Navarro, D. D. Ho, M. Tsuji, C. Wong, *J. Am. Chem. Soc.* **2006**, *128*, 9022.
- [37] K. O. Yu, J. S. Im, A. Molano, Y. Dutronc, P. A. Illarionov, C. Forestier, N. Fujiwara, I. Arias, S. Miyake, T. Yamamura, Y. T. Chang, G. S. Besra, S. A. Porcelli, *Proc. Natl. Acad. Sci. USA* **2005**, *102*, 3383.
- [38] J. Schmieg, G. Yang, R. W. Franck, M. Tsuji, *J. Exp. Med.* **2003**, *198*, 1631.
- [39] G. Yang, J. Schmieg, M. Tsuji, R. W. Franck, *Angew. Chem., Int. Ed.* **2004**, *43*, 3818.
- [40] S. Fujii, K. Shimizu, H. Hemmi, M. Fukui, A. J. Bonito, G. Chen, R. W. Franck, M. Tsuji, R. M. Steinman, *Proc. Natl. Acad. Sci. USA* **2006**, *103*, 11252.
- [41] X. Chen, X. Wang, J. M. Keaton, F. Reddington, P. A. Illarionov, G. S. Besra, J. E. Gumperz, *J. Immunol.* **2007**, *178*, 6181.
- [42] C. Paduraru, L. Spiridon, W. Yuan, G. Bricard, X. Valencia, S. A. Porcelli, P. A. Illarionov, G. S. Besra, S. M. Petrescu, A. J. Petrescu, P. Cresswell, *J. Biol. Chem.* **2006**, *281*, 40369.
- [43] T. Natori, Y. Koezuka, T. Higa, *Tetrahedron Lett.* **1993**, *34*, 5591.
- [44] K. Akimoto, T. Natori, M. Morita, *Tetrahedron Lett.* **1993**, *34*, 5593.
- [45] T. Mukaiyama, Y. Murai, S.-I. Shoda, *Chem. Lett.* **1981**, *10*, 431.
- [46] S. Figueroa-Perez, R. R. Schmidt, *Carbohydr. Res.* **2000**, *328*, 95.
- [47] R. R. Schmidt, T. Maier, *Carbohydr. Res.* **1988**, *174*, 169.
- [48] W. J. Du, J. Gervay-Hague, *Org. Lett.* **2005**, *7*, 2063.
- [49] J. D. Silk, M. Salio, B. G. Reddy, D. Shepherd, U. Gileadi, J. Brown, S. H. Masri, P. Polzella, G. Ritter, G. S. Besra, E. Y. Jones, R. R. Schmidt, V. Cerundolo, *J. Immunol.* **2008**, *180*, 6452.

- [50] N. A. Borg, K. S. Wun, L. Kjer-Nielsen, M. C. Wilce, D. G. Pellicci, R. Koh, G. S. Besra, M. Bharadwaj, D. I. Godfrey, J. Mccluskey, J. Rossjohn, *Nature* **2007**, *448*, 44.
- [51] B. G. Reddy, J. D. Silk, M. Salio, R. Balamurugan, D. Shepherd, G. Ritter, V. Cerundolo, R. R. Schmidt, *ChemMedChem* **2009**, *4*, 171.
- [52] Y. Kinjo, E. Tupin, D. Wu, M. Fujio, R. Garcia-Navarro, M. R. Benhnia, D. M. Zajonc, G. Ben-Menachem, G. D. Ainge, G. F. Painter, A. Khurana, K. Hoebe, S. M. Behar, B. Beutler, I. A. Wilson, M. Tsuji, T. J. Sellati, C. H. Wong, M. Kronenberg, *Nat. Immunol.* **2006**, *7*, 978.
- [53] Y. Oikawa, T. Tanaka, K. Horita, O. Yonemitsu, *Tetrahedron Lett.* **1984**, *25*, 5397.
- [54] M. N. Galbrait, D. H. S. Horn, E. J. Middleton, R. J. Hackney, *J. Chem. Soc., Chem. Commun.* **1968**, 466.
- [55] E. E. Dueno, F. X. Chu, S. I. Kim, K. W. Jung, *Tetrahedron Lett.* **1999**, *40*, 1843.
- [56] A. R. Katritzky, A. Bieniek, L. Chiang, *Org. Prep. Proced. Int.* **1989**, *21*, 129.
- [57] T. Hegmann, B. Neumann, R. Wolf, C. Tschierske, *J. Mater. Chem.* **2005**, *15*, 1025.
- [58] S. Takahashi, A. Kubota, T. Nakata, *Tetrahedron Lett.* **2002**, *43*, 8661.
- [59] A. Yazbak, S. C. Sinha, E. Keinan, *J. Org. Chem.* **1998**, *63*, 5863.
- [60] R. D. Howells, J. D. Mc Cown, *Chem. Rev.* **1977**, *77*, 69.
- [61] S. A. Ross, M. Pitie, B. Meunier, *J. Chem. Soc., Perkin Trans. 1* **2000**, 571.
- [62] A. El Nemr, T. Tsuchiya, *Carbohydr. Res.* **2001**, *330*, 205.
- [63] P. B. Alper, S. C. Hung, C. H. Wong, *Tetrahedron Lett.* **1996**, *37*, 6029.

- [64] P. T. Nyffeler, C. H. Liang, K. M. Koeller, C. H. Wong, *J. Am. Chem. Soc.* **2002**, *124*, 10773.
- [65] A. Isidro-Llobet, M. Alvarez, F. Albericio, *Chem. Rev.* **2009**, *109*, 2455.
- [66] S. Muller, R. R. Schmidt, *Pract. Applic. Appl. Chem.* **2000**, *342*, 779.
- [67] V. Pozsgay, *Tetrahedron: Asymmetry* **2000**, *11*, 151.
- [68] R. Dalpozzo, A. De Nino, L. Maiuolo, A. Procopio, A. Tagarelli, G. Sindona, G. Bartoli, *J. Org. Chem.* **2002**, *67*, 9093.
- [69] H. H. Bosshard, R. Mory, M. Schmid, H. Zollinger, *Helv. Chim. Acta* **1959**, *42*, 1653.
- [70] R. Busch, H.-J. Kneuper, T. Weber, W. Muller, A. Stamm, J. Henkelmann, in *US Patent* **2004**, 6770783.
- [71] G. S. Besra, *PhD Thesis*, University of Newcastle Upon Tyne (Newcastle Upon Tyne), **1990**.
- [72] S. C. Wu, S. L. Wong, *J. Biol. Chem.* **2005**, *280*, 23225.
- [73] M. Howarth, D. J. Chinnapen, K. Gerrow, P. C. Dorrestein, M. R. Grandy, N. L. Kelleher, A. El-Husseini, A. Y. Ting, *Nat. Methods* **2006**, *3*, 267.
- [74] W. A. Hendrickson, A. Pähler, J. L. Smith, Y. Satow, E. A. Merritt, R. P. Phizackerley, *Proc. Natl. Acad. Sci. USA* **1989**, *86*, 2190.
- [75] S. A. Kalovidouris, C. I. Gama, L. W. Lee, L. C. Hsieh-Wilson, *J. Am. Chem. Soc.* **2005**, *127*, 1340.
- [76] X. T. Zhou, C. Forestier, R. D. Goff, C. Li, L. Teyton, A. Bendelac, P. B. Savage, *Org. Lett.* **2002**, *4*, 1267.
- [77] H. Klein, A. Schmidt, U. Flörke, H. Haupt, *Inorg. Chim. Acta* **2003**, *342*, 171.
- [78] C. Hell, *Ber.* **1881**, *14*, 891.

- [79] J. Volhard, *Ann.* **1887**, 242, 141.
- [80] N. Zelinsky, *Ber.* **1887**, 20, 2026.
- [81] N. O. V. Sonntag, *Chem. Rev.* **1953**, 52, 237.
- [82] J. C. Little, A. R. Sexton, Y. L. C. Tong, T. E. Zurawic, *J. Am. Chem. Soc.* **1969**, 91, 7098.
- [83] F. A. Taylor, P. A. Levene, *J. Biol. Chem.* **1928**, 609.
- [84] R. Ashton, R. Robinson, J. C. Smith, *J. Chem. Soc.* **1936**, 283.
- [85] P. Patnaik, *Handbook of inorganic chemicals*, McGraw-Hill, **2002**.
- [86] C. Grison, S. Dumarcay, P. Coutrot, *Tetrahedron Lett.* **2003**, 44, 2489.
- [87] J. Baldwin, M. Spyvee, R. Whitehead, *Tetrahedron Lett.* **1994**, 35, 6575.
- [88] J. Otera, K. Nakazawa, K. Sekoguchi, A. Orita, *Tetrahedron* **1997**, 53, 13633.
- [89] D. Amantini, R. Beleggia, F. Fringuelli, F. Pizzo, L. Vaccaro, *J. Org. Chem.* **2004**, 69, 2896.
- [90] F. Cheng, A. Hector, W. Levason, G. Reid, M. Webster, W. Zhang, *Chem. Commun.* **2009**, 1334.
- [91] E. A. Losey, M. D. Smith, M. Meng, M. D. Best, *Bioconjug. Chem.* **2009**, 20, 376.
- [92] V. O. Rodionov, V. V. Fokin, M. G. Finn, *Angew. Chem., Int. Ed.* **2005**, 44, 2210.
- [93] C. Gurcel, A.-S. Vercoutter-Edouart, C. Fonbonne, M. Mortuaire, A. Salvador, J.-C. Michalski, J. Lemoine, *Anal. Bioanal. Chem.* **2008**, 390, 2089.
- [94] Q. Wang, T. R. Chan, R. Hilgraf, V. V. Fokin, K. B. Sharpless, M. G. Finn, *J. Am. Chem. Soc.* **2003**, 125, 3192.

- [95] J. I. Gavriilyuk, U. Wuellner, C. F. Barbas, *Bioorg. Med. Chem. Lett.* **2009**, *19*, 1421.
- [96] F. Himo, T. Lovell, R. Hilgraf, V. V. Rostovtsev, L. Noodleman, K. B. Sharpless, V. V. Fokin, *J. Am. Chem. Soc.* **2005**, *127*, 210.
- [97] H. Orgueira, D. Fokas, Y. Isome, P. Chan, C. Baldino, *Tetrahedron Lett.* **2005**, *46*, 2911.
- [98] D. S. Wilbur, D. K. Hamlin, M. K. Chyan, B. B. Kegley, P. M. Pathare, *Bioconjug. Chem.* **2001**, *12*, 616.
- [99] I. Bell, S. Gallicchio, M. Abrams, L. Beese, D. Beshore, H. Bhimnathwala, M. Bogusky, C. Buser, J. Culberson, J. Davide, *J. Med. Chem.* **2002**, *45*, 2388.
- [100] M. Mizuno, T. Shioiri, *Chem. Commun.* **1997**, *1997*, 2165.
- [101] K. D. McCreynolds, A. Bhat, J. C. Conboy, S. S. Saavedra, J. Gervay-Hague, *Bioorg. Med. Chem.* **2002**, *10*, 625.
- [102] F. Roleira, F. Borges, L. Andrade, J. Paixão, M. Almeida, R. Carvalho, E. Tavares Da Silva, *J. Fluorine Chem.* **2009**, *130*, 169.
- [103] M. Green, J. Berman, *Tetrahedron Lett.* **1990**, *31*, 5851.
- [104] R. Huisgen, *1,3-dipolar cycloaddition chemistry*, Wiley, New York, **1984**.
- [105] S. J. Howell, N. Spencer, D. Philp, *Tetrahedron* **2001**, *57*, 4945.
- [106] J. Wijner, R. A. Steiner, J. B. F. N. Engberts, *Tetrahedron Lett.* **1995**, *36*, 5389.
- [107] D. Hlasta, J. Ackerman, *J. Org. Chem.* **1994**, *59*, 6184.
- [108] C. W. Tornøe, C. Christensen, M. Meldal, *J. Org. Chem.* **2002**, *67*, 3057.
- [109] V. V. Rostovtsev, L. G. Green, V. V. Fokin, K. B. Sharpless, *Angew. Chem., Int. Ed.* **2002**, *41*, 2596.

- [110] P. Wu, A. K. Feldman, A. K. Nugent, C. J. Hawker, A. Scheel, B. Voit, J. Pyun, J. M. Fréchet, K. B. Sharpless, V. V. Fokin, *Angew. Chem., Int. Ed.* **2004**, *43*, 3928.
- [111] I. Van Rhijn, D. C. Young, J. S. Im, S. B. Levery, P. A. Illarionov, G. S. Besra, S. A. Porcelli, J. Gumperz, T. Y. Cheng, D. B. Moody, *Proc. Natl. Acad. Sci. USA* **2004**, *101*, 13578.
- [112] Y. Hayakawa, D. I. Godfrey, M. J. Smyth, *Curr. Med. Chem.* **2004**, *11*, 241.
- [113] J. L. Amprey, J. S. Im, S. J. Turco, H. W. Murray, P. A. Illarionov, G. S. Besra, S. A. Porcelli, G. F. Späth, *J. Exp. Med.* **2004**, *200*, 895.
- [114] C. Forestier, A. Molano, J. S. Im, Y. Dutronc, B. Diamond, A. Davidson, P. A. Illarionov, G. S. Besra, S. A. Porcelli, *J. Immunol.* **2005**, *175*, 763.
- [115] J. Mattner, K. L. Debord, N. Ismail, R. D. Goff, C. Cantu, D. Zhou, P. Saint-Mezard, V. Wang, Y. Gao, N. Yin, K. Hoebe, O. Schneewind, D. Walker, B. Beutler, L. Teyton, P. B. Savage, A. Bendelac, *Nature* **2005**, *434*, 525.
- [116] C. Xia, D. Zhou, C. Liu, Y. Lou, Q. Yao, W. Zhang, P. G. Wang, *Org. Lett.* **2006**, *8*, 5493.
- [117] A. O. Speak, M. Salio, D. C. Neville, J. Fontaine, D. A. Priestman, N. Platt, T. Heare, T. D. Butters, R. A. Dwek, F. Trottein, M. A. Exley, V. Cerundolo, F. M. Platt, *Proc. Natl. Acad. Sci. USA* **2007**, *104*, 5971.
- [118] V. Sriram, W. Du, J. Gervay-Hague, R. R. Brutkiewicz, *Eur. J. Immunol.* **2005**, *35*, 1692.
- [119] D. Mootoo, P. Konradsson, U. Udodong, B. Fraser-Reid, *J. Am. Chem. Soc.* **1988**, *110*, 5583.

- [120] S. Hashimoto, H. Sakamoto, T. Honda, H. Abe, S. Nakamura, S. Ikegami, *Tetrahedron Lett.* **1997**, *38*, 8969.
- [121] D. Crich, M. Li, *Org. Lett.* **2007**, *9*, 4115.
- [122] K. Adachi, Y. Yamada, H. Wada, A. Kameyama, H. Ishida, M. Kiso, *J. Carbohydr. Chem.* **1998**, *17*, 595.
- [123] K. B. Hendriks, R. V. Stick, K. James, R. U. Lemieux, *J. Am. Chem. Soc.* **1975**, *97*, 4056.
- [124] A. I. Zinin, N. N. Malysheva, A. M. Shpirt, V. I. Torgov, L. O. Kononov, *Carbohydr. Res.* **2007**, *342*, 627.
- [125] K. Tanaka, K. Fukase, *Synlett* **2007**, 164.
- [126] K. Suzuki, H. Nonaka, M. Yamaura, *Tetrahedron Lett.* **2003**, *44*, 1975.
- [127] M. Mogemark, M. Eloffsson, J. Kihlberg, *J. Org. Chem.* **2003**, *68*, 7281.
- [128] C. R. Shie, Z. H. Tzeng, S. S. Kulkarni, B. J. Uang, C. Y. Hsu, S. C. Hung, *Angew. Chem., Int. Ed.* **2005**, *44*, 1665.
- [129] D. Crich, W. Cai, Z. Dai, *J. Org. Chem.* **2000**, *65*, 1291.
- [130] D. Crich, M. De La Mora, A. U. Vinod, *J. Org. Chem.* **2003**, *68*, 8142.
- [131] D. Crich, O. Vinogradova, *J. Org. Chem.* **2006**, *71*, 8473.
- [132] A. V. Demchenko, E. Rousson, G. J. Boons, *Tetrahedron Lett.* **1999**, *40*, 6523.
- [133] D. Crich, T. Hu, F. Cai, *J. Org. Chem.* **2008**, *73*, 8942.
- [134] M. Bols, *J. Chem. Soc., Chem. Commun.* **1992**, 913.
- [135] M. Bols, *J. Chem. Soc., Chem. Commun.* **1993**, 791.
- [136] G. Stork, J. J. Laclair, *J. Am. Chem. Soc.* **1996**, *118*, 247.
- [137] Y. Ito, Y. Ohnishi, T. Ogawa, Y. Nakahara, *Synlett* **1998**, 1102.
- [138] Y. Ito, T. Ogawa, *J. Am. Chem. Soc.* **1997**, *119*, 5562.

- [139] A. Dan, Y. Ito, T. Ogawa, *J. Org. Chem.* **1995**, *60*, 4680.
- [140] Y. Shingu, Y. Nishida, H. Dohi, K. Kobayashi, *Org. Biomol. Chem.* **2003**, *1*, 2518.
- [141] Y. Shingu, A. Miyachi, Y. Miura, K. Kobayashi, Y. Nishida, *Carbohydr. Res.* **2005**, *340*, 2236.
- [142] J. J. Gridley, A. J. Hacking, H. M. I. Osborn, D. G. Spackman, *Tetrahedron* **1998**, *54*, 14925.
- [143] J. Dinkelaar, M. D. Witte, L. J. Van Den Bos, H. S. Overkleeft, G. A. Van Der Marel, *Carbohydr. Res.* **2006**, *341*, 1723.
- [144] T. Oshitari, M. Shibasaki, T. Yoshizawa, M. Tomita, K. Takao, S. Kobayashi, *Tetrahedron* **1997**, *53*, 10993.
- [145] D. Colombo, L. Franchini, L. Toma, F. Ronchetti, N. Nakabe, T. Konoshima, H. Nishino, H. Tokuda, *Eur. J. Med. Chem.* **2005**, *40*, 69.
- [146] D. Kodali, A. Tercyak, D. Fahey, D. Small, *Chem. Phys. Lipids* **1990**, *52*, 163.
- [147] S. Stamatov, J. Stawinski, *Org. Biomol. Chem.* **2007**, *5*, 3787.
- [148] F. Paltauf, A. Hermetter, *Prog. Lipid Res.* **1994**, *33*, 239.
- [149] T. Maier, R. R. Schmidt, *Carbohydr. Res.* **1991**, *216*, 483.
- [150] G. Lu, S. Lam, K. Burgess, *Chem. Commun.* **2006**, 1652.
- [151] A. Natarajan, W. Du, C. Xiong, G. L. Denardo, S. J. Denardo, J. Gervay-Hague, *Chem. Commun.* **2007**, 695.
- [152] L. Kasbeck, H. Kessler, *Liebigs Ann.* **1997**, 169.
- [153] R. Lemieux, *Can. J. Chem.* **1951**, *29*, 1079.
- [154] G. Ben-Menachem, J. Kubler-Kielb, B. Coxon, A. Yergey, R. Schneerson, *Proc. Natl. Acad. Sci. USA* **2003**, *100*, 7913.